INVESTIGATING NOVEL PROGENITOR CELL POPULATIONS IN THE FISH HEART



ABIGAIL C KILLEN-DEVINE

ST CROSS COLLEGE

UNIVERSITY OF OXFORD

A thesis submitted for the degree of

Doctor of Philosophy

Michaelmas 2018

ACKNOWLEDGEMENTS

I would struggle to fully express my gratitude to my supervisor, Professor Tilly Mommersteeg, for everything she has done over the last four years, and before. She is an inspirational scientist who supervises with perfect levels of enthusiasm, patience and encouragement. Any student is lucky to have her as a supervisor. I'd also like to thank my second supervisor Professor Paul Riley for his invaluable input into this work.

My thanks also go to the British Heart Foundation, who funded my studentship and the majority of this work.

I am very grateful to Susann, Will, Zhilian and Mala for their invaluable support and encouragement in the laboratory. Jana Koth deserves a special thank you for her excellent teaching, wise words and for always thinking of me.

To the OUWBC squads of 2017 and 2018, thank you for your friendship and support over the course of my DPhil and for ensuring that part of each day was always filled with laughter despite the rain, injuries, floods and the Beast from the East. To Stef, Laura, Olivia, Shari and Jill F Betts, thank you for being the most amazing friends and to Ellie Watts for enduring us.

A huge thank you goes to the Devine family for always offering me hugs, Irish charm and the perfect words when needed.

Jack, Grandma, Grandad, Debbie, Franck, George and Joseph – thank you for always supplying terrible puns and jokes, impromptu discos, loud support from the river bank, Oxford day trips and fun get-togethers always, but particularly when most needed.

Mum and Dad, thank you for all of the above and more. You have always been so supportive of me and I am so lucky to have parents as wonderful as you.

Lastly, I would like to thank my husband, Matt, for always backing me and, on my trickiest days, being ready with a slab of chocolate and a reminder that I once said my greatest ambition in life was to own two golden retrievers, so none of this matters anyway.

ABSTRACT

After cardiac injury, most mammals, including humans, cannot regenerate lost heart muscle with new, functioning cardiomyocytes. The cave-dwelling variant of *A mexicanus,* a species of teleost fish, is similar to humans and also cannot regenerate. Remarkably, the surface-dwelling variant of the same species can regrow damaged heart muscle, like its fellow teleost fish the zebrafish. Comparison of the surface and cave-dwelling *A mexicanus* fish is, therefore, a powerful method to identify new mechanisms behind the ability to regenerate, which could lead to therapeutic interventions for humans who have suffered a cardiac injury. Using this model system, comparison of cave and surface variants showed that there are variations in the levels of epicardial fat before and after cardiac injury between the fish, suggesting differential activity of a mesenchymal fat progenitor. Fat has been found to have a positive effect on injury outcome, but fatty fibrotic scar tissue is a symptom of a non-regenerative environment. Such a progenitor has not been found in the fish before, therefore efforts were made to identify it. Investigations using a mesenchymal stem cell marker, Pdgfrα, identified previously unknown populations positive for this marker in the fish heart, including one in the epicardium and another in the endocardium. Lineage tracing experiments showed that the epicardium, likely Pdgfrα-positive epicardial cells, is the source of the epicardial fat that arises during development and after injury, a process that has been previously reported in the mouse. Investigation of the identity of the endocardial population showed that some of these endocardial cells begin to express Runx1, a hematopoietic progenitor marker, after injury. The expression of hematopoietic markers in endothelial cells has been previously shown during development, where endocardial cells undergo an endothelial-to-hematopoietic transition (EHT) and detach, forming hematopoietic stem cells that give rise to the blood lineages. Transcriptomic analyses showed that the injured endocardium has upregulated expression of many key hematopoietic development genes. Live imaging experiments in cultured heart slices, a novel experimental method, show endocardial cells detaching from the myocardium after injury in a way that recapitulates the developmental EHT. These results strongly suggest that the injured fish endocardium produces hematopoietic stem cells after injury. In summary, through analysis of fish hearts, two novel injury-responsive progenitors have been identified: an epicardial fat progenitor and hematopoietic progenitors derived from the injured endocardium. These progenitors offer an exciting new avenue for investigations into the mechanisms behind the ability to repair damaged hearts.

Abstract: 400 words

Total word count (excluding figure legends, references and appendix): approximately 48,000.

TABLE OF ABBREVIATIONS

(s)gRNA	Guide RNA
AFOG	Acid Fuchsin Orange G
BZ	Border zone
CRISPR	Clustered regularly interspaced short palindromic repeats
DPA	Days post amputation (resection injury)
DPF	Days post fertilisation
DPI	Days post injury (cryoinjury)
ECM	Extracellular matrix
eCPC	Endogenous cardiac progenitor cell
EHT	Endothelial-to-hematopoietic transition
EMT	Epicardial-to-mesenchymal transition
FACS	Fluorescence-activated cell sorting
HDR	Homology directed repair
HE	Hemogenic endothelium
HPF	Hours post fertilisation

HSC	Hematopoietic stem cell
KO	Knockout
MMEJ	Microhomology-mediated end joining
MMP	Matrix metalloproteinase
MSC	Mesenchymal stem cell
NHEJ	Non-homologous end joining
P	Postnatal day
PAM	Protospacer adjacent motif
TALEN	Transcription activator-like effector nuclease
TLR	Toll-like receptor
WT	Wild-type
MI	Myocardial infarction

TABLE OF CONTENTS

ACKNOWLEDGEMENTS **2**

ABSTRACT **3**

TABLE OF ABBREVIATIONS **4**

CHAPTER 1 - INTRODUCTION **10**

1.1 WHY STUDY HEART REGENERATION? 10

1.2 WHAT IS CURRENTLY KNOWN ABOUT THE INJURY RESPONSE IN THE HEART? 11

1.2.1 Cardiomyocytes and heart regeneration *11*

1.2.3 Permanent scar vs scar resolution *14*

1.2.4 Epicardium and endocardium *18*

1.2.5 Immune cells *21*

1.2.6 Other cell types *24*

1.2.7 Progenitor cells *26*

1.3 AIM OF THE STUDY: LOOKING FOR NOVEL PROGENITORS IN THE FISH HEART 28

1.4 *ASTYANAX MEXICANUS*: A POWERFUL TOOL FOR INTERROGATING THE MECHANISMS BEHIND HEART REGENERATION 28

1.4.1 An introduction to Astyanax mexicanus *28*

1.4.2 Why use A. mexicanus to study heart regeneration? *32*

1.5 OUTLINE OF THE THESIS 34

CHAPTER 2 - METHODS **36**

2.1 FISH HUSBANDRY 36

2.2 FISH INJURY 36

2.3 PARAFFIN EMBEDDING 37

2.4 SEMIQUANTITIVE ANALYSIS OF FAT ON THE *ASTYANAX* HEART 37

2.5 OIL-RED O STAINING ON CAVEFISH AND ZEBRAFISH WHOLE HEARTS 38

2.6 IMMUNOHISTOCHEMISTRY 38

2.7 SGRNA DESIGN AND PRODUCTION 41

2.8 CAS9 MRNA PRODUCTION 42

2.9 MICROINJECTIONS OF CAS9 MRNA, SGRNAS AND INSERT CASSETTES 43

2.10 T7E1 TEST 43

2.11 INJECTED EMBRYO AND GERMLINE TRANSITION SCREENING 44

2.12 TAMOXIFEN ADMINISTRATION 44

2.13 CELL COUNTS OF PDGFRA-POSITIVE CELLS 45

2.14 CELL COUNTS OF RUNX1/KDRL DOUBLE-POSITIVE CELLS 45

2.15 SLICE CULTURES 46

2.16 DIGESTION OF HEARTS FOR SINGLE CELL SUSPENSIONS 48

2.17 FACS 48

2.18 RNA ISOLATION AND CDNA PREPARATION FROM FAC SORTED CELLS 48

2.19 QPCR 49

2.20 Single cell sequencing 49
2.21 RNAscope 50
2.22 AFOG Staining and *runx1* mutant phenotype analysis 51
2.23 PCNA proliferation analysis 52
2.24 Microscopy 52
2.25 Statistics 53
CHAPTER 3 – IDENTIFYING AN EPICARDIAL PROGENITOR THAT FORMS FAT IN THE FISH HEART 54
Chapter 3 – Introduction 54
3.1.1 Summary of the chapter 54
3.1.2 Background information – why study cardiac fat? 54
Chapter 3 results 56
3.2 *Astyanax* ecotypes have different fat populations on the heart 56
3.3 Cavefish and zebrafish form fat on their hearts after injury 59
3.4 Potential origins of developmental and injury-related fat 61
3.5 Investigating epicardial mesenchymal progenitors in the fish heart 63
3.5.1 Expression of Pdgfrα in A. mexicanus hearts 64
3.5.2 Expression of Pdgfrα in the epicardium 66
3.5.3 Expression of Pdgfrα in scar tissue 74
3.5.4 Investigating Pdgfrβ as a mesenchymal stem cell marker 77
3.6 Developing novel fish lines to investigate Pdgfra-positive populations in injury response . 78
3.7 The epicardium forms epicardial fat during development in the zebrafish 86
3.8 The epicardium forms fat on the wound site 88
3.9 Discussion 90
3.10 Conclusion 94
CHAPTER 4 – INVESTIGATING OTHER PDGFRA PROGENITOR POPULATIONS 95
Chapter 4 – introduction 95
4.1.1 Summary of the chapter 95
4.1.2 background information 96
Chapter 4 – Results 97
4.2 Investigating other Pdgfra-positive cells after injury 97
4.3 Identifying Pdgfra-positive cells resident in the ventricle 104
4.4 Investigating the Runx1 and Arg1 Pdgfra-positive populations after injury 108
4.5 Investigating Runx1-positive cells in *A. mexicanus* hearts after injury 113
4.6 Developmental Runx1 expression in endothelial cells 115
4.7 Using zebrafish to investigate whether a hemogenic endothelium is formed In the fish heart after injury 121
4.8 The Runx1-P2:citrine transgene recapitulates Runx1 mRNA expression and is found in multiple cell types after injury 122

4.9 The zebrafish heart also contains Pdgfra-positive Runx1-positive and Erg1-positive Runx1-positive cells after injury 124
4.10 Runx1 Kdrl double positive cells appear in response to wounding 127
4.11 Runx1 Kdrl double positive cells appear to have multiple morphologies that represent the stages of EHT 132
4.12 Discussion 133
4.13 Conclusion 136
CHAPTER 5 – INVESTIGATING INJURY INDUCED HEMOGENIC ENDOTHELIUM 138
Chapter 5 – Introduction 138
5.1.1 Summary of the chapter 138
5.1.2 background information 140
Chapter 5 - Results 141
5.2 Developing a novel slice culture technique to image EHT after injury in real time 141
5.2.1 Optimisation of the sectioning process 143
5.2.2 Culture conditions for fish heart slices 147
5.2.3 Optimisation of the imaging process 148
5.2.4 Exploring the uses of zebrafish heart slice culture experiments 149
5.2.5 Adapting the protocol specifically for investigating EHT 152
5.3 Runx1 positive cells are highly active after injury 152
5.4 Endothelial cells appear to round and detatch after injury 155
5.5 Analysing cells with endothelial and hematopoietic identity 157
5.5.1 Fluorescence activated cell sorting can isolate Runx1/Kdrl double positive cells from zebrafish hearts 157
5.5.2 Gene expression analysis of endothelial and hematopoietic cells by qPCR 159
5.6 Removing Runx1 function improves regeneration 161
5.7 Loss of Runx1 has a protective and pro-proliferative effect on injured myocardium 166
5.8 Loss of Runx1 does not appear to AFFECT the appearance of runx1-positive endocardium 170
5.9 Gene expression analysis of endothelial and hematopoietic cells by single cell sequencing 173
5.9.1 Some cell types are only present in injured hearts or are drastically increased in injured fish 176
5.9.2 The Runx1 mutant has a different cell complement to WT fish 179
5.9.3 Comparing cardiomyocytes from injured WT and KO fish 181
5.9.4 Analysing double positive cells 183
5.10 RNAscope marker genes 187
5.11 Discussion 195
5.12 Conclusion 199
CHAPTER 6 – DISCUSSION AND CONCLUSION OF THE TOTAL WORK 200
6.1 A summary of the findings of the study 200

6.2 Limitations of the study 201
6.2.1 identification of the epicardial fat progenitor 201
6.2.2 Identification of a hemogenic endothelium after injury 202
6.3 What do these progenitors tell us about regenerative capacity? 205
6.4 Further work 209
6.4.1 further identification of the epicardial fat progenitor and its function 209
6.4.2 Functional analysis of post-injury eht 210
6.5 final conclusion 211
APPENDIX 212
Publications 212
Publications from work performed during the DPhil 212
Previous publications 212
Table A.1 – Antibodies 212
TABLE A.2 – Primers 213
TABLE A.3 – sgRNAs 213
TABLE A.4 – RNAscope probes 214
Supplementary information 214
References 215

CHAPTER 1 - INTRODUCTION

1.1 WHY STUDY HEART REGENERATION?

When heart muscle is damaged, for example after myocardial infarction where a blocked blood vessel starves cardiomyocytes of oxygen, it cannot currently be repaired. Instead of forming new muscle in the damaged area, the dead heart muscle is replaced by rigid scar tissue. This scar tissue cannot contract, meaning cardiac function is reduced. The remaining heart tissue becomes hypertrophic and dilation of the scar tissue results in an increase in chamber volume, reducing efficiency (Pfeffer & Braunwald 1990). These changes can result in a high risk of arrhythmias and heart failure (Goldstein et al. 1984; Minicucci et al. 2011). Currently, the only cure for heart failure is a heart transplant but, unfortunately demand far outstrips supply. Even if a transplant is obtained, there are risks such as organ rejection (Toyoda et al. 2013). In the face of these difficulties, a new solution must be sought. Encouraging the heart to grow new muscle *in situ* or replacement of cardiomyocytes by cell transplantation would offer a more readily available and sustainable treatment. However, the mechanisms behind the growth of endogenous cardiomyocytes are not yet understood to the extent that their formation can be forced in living humans. Additionally, transplantation of cardiomyocytes or progenitor cells has yet to offer much success, with problems such as irregular heartbeats in engrafted cells, poor engraftment, teratomas, among others, seen or predicted (Lin & Pu 2014; Shiba et al. 2016; Chong et al. 2014; Tzahor & Poss 2017; Laflamme & Murry 2011).

Therefore, there is a huge drive to investigate how the heart responds to injury, how new cardiomyocytes are formed and what cell types play a part in injury response. Work in the last 20 years in particular has done much to illuminate the factors involved in the heart's

ability to regenerate. Through this work it has become clear that successful heart regeneration is multifactorial and delicately balanced, involving spatio-temporally restricted activities of all major cardiac cell types and a carefully choreographed immune response.

1.2 WHAT IS CURRENTLY KNOWN ABOUT THE INJURY RESPONSE IN THE HEART?

1.2.1 CARDIOMYOCYTES AND HEART REGENERATION

Experiments in adult mice and rats have shown that their hearts respond to cardiac injury in much the same way as human hearts do, with the formation of a permanent fibrotic scar rather than the generation of new muscle. Studies have shown that some new cardiomyocytes are formed after injury, but these are insufficient in number to replace what was lost (Senyo et al. 2013; Hsieh et al. 2007; though these finding have been heavily questioned recently in Lee 2018). By contrast, the zebrafish and neonatal mouse have been found to regenerate lost muscle after injury (Jopling et al. 2010; Porrello et al. 2011; Poss et al. 2002). In these animals, the scar that is formed initially after injury is resolved and replaced by new cardiomyocytes.

In both the zebrafish and the neonatal mouse, these new cardiomyocytes are not formed by a progenitor cell, but rather through robust proliferation of existing cardiomyocytes. They achieve this through an intermediary stage of de-differentiation, leading to partial disassembly of sarcomeres and loss of mature cardiomyocyte characteristics, as well as upregulation of embryonic myosins (Sallin & Jaźwińska 2016; Wu et al. 2015). These de-differentiated cardiomyocytes then proliferate and replace the scar concomitant with its degradation. It is thought that de-differentiation occurs when cardiomyocytes lose contact with their neighbours after injury and might be a survival mechanism, with the loss of mature

cardiomyocyte functions helping them save energy (Wang et al. 2017; Poling et al. 2012; Thijssen et al. 2001). Exactly how this process is triggered and how it is controlled is currently under intense scientific scrutiny, to the extent that many contributing factors have been discovered.

After injury, the cardiomyocytes adjacent to the site of injury come into contact with multiple signals released by the damaged tissues and other reacting cells. Examples of these signals include inflammatory cytokines and also other signals: BMP, TGFβ ligands, Nrg1, retinoic acid, Igf, Shh, NF-κB and Hif1, amongst others. These are all thought to play a role in regulation of cardiomyocyte proliferation after injury (Sharma & Wu 2015; Nakada et al. 2016; Wu et al. n.d.; Chablais & Jaźwińska 2012; Kikuchi et al. 2011; Y. Huang et al. 2013; Wang et al. 2015; Karra et al. 2015; W.-C. Huang et al. 2013; Gemberling et al. 2015). As the cardiomyocytes strive to achieve a more de-differentiated, developmental state after injury, it is interesting to note that many of these play a role in developmental cardiomyocyte proliferation as well. For example, IGF induces proliferation during heart development and the developmental cardiac transcription factor Gata4, which is switched off after development, is found to be reactivated and marks proliferating cells in both mice and zebrafish after injury (Gupta et al. 2013; Malek Mohammadi et al. 2017). This shows that regeneration is in some way dependent on re-activation of multiple developmental pathways.

It is important to note that, whilst it appears that re-activation of a pro-proliferative developmental state in cardiomyocytes is vital for successful regeneration, the extent to which this can be achieved likely varies in each animal due to the different environments and inherent features of cardiomyocytes. Adult rodents and humans have poly-nucleated or polyploid cardiomyocytes, whilst their neonatal and zebrafish counterparts are only mono-

nucleated and diploid. Cell division events in adult mammals appear to be exceedingly rare, with most cycling being endoreplication associated with hypertrophy. These changes should not be barriers to proliferation, as polyploid cells are seen to divide in other systems, but conditions in adult mammals appear to be such that cell division is not preferred over hypertrophy (Tzahor & Poss 2017). As well as the fact that the nature of the cardiomyocytes themselves differ, embryonic and zebrafish environments are also very unlike those of adult mammals. In zebrafish and the neonatal mouse, blood pressure is much lower than in adult mammals and the loss of contractility that occurs when cardiomyocytes dedifferentiate to proliferate therefore likely has less serious consequences (Le et al. 2012). Indeed, in mice, a rise to adult blood pressure levels coincides with loss of regenerative potential at P5-7. Additionally, the oxygen environment in neonatal mice is different to adults, with the increase in oxygen availability after birth inducing a switch from glycolysis to oxidative phosphorylation (Lalowski et al. 2018). Besides the physical environment, the genetic environment is also markedly different in neonatal mice compared to adults; many of the genes involved in heart development and maturation become methylated by P7, preventing their transcription, and many of these changes are retained until adulthood. It is possible that these pathways are helpful to regeneration and simply cannot be re-activated in the adult, due to this epigenetic regulation (Górnikiewicz et al. 2016). Therefore, whilst cardiomyocyte dedifferentiation and proliferation is key to successful regeneration in lower vertebrates and neonatal mammals, the question still remains whether it would be possible or even safe to completely recapitulate this process in adult mice and humans.

At the moment, these are questions for the future. For most factors yet found to regulate cardiomyocyte proliferation, removing their action in regenerative models inhibits

regeneration, whilst forcing it in adult rodents, for example through application of mitogenic signals and miRNAs or induction of hypoxia, is insufficient to trigger complete regeneration of lost muscle and resolution of scar tissue (Bersell et al. 2009; Nakada et al. 2017; Tian et al. 2015). This suggests that, whilst the formation of new cardiomyocytes through cell division is obviously necessary to complete heart regeneration, the actions of other cell types and factors must be similarly important and studied with similar intensity.

1.2.3 PERMANENT SCAR VS SCAR RESOLUTION

After injury, all model organisms, whether they regenerate or not, form a scar. Initial formation of a scar is useful, as the dead tissue would be highly fragile under the pressure of contraction and blood flow. The scar therefore provides structure, protecting against potential cardiac rupture (Talman & Ruskoaho 2016). However, beyond this, a permanent scar impedes full regeneration of heart function and presents a physical barrier to growth of new heart muscle. For successful regeneration to occur, the scar must be removed as new muscle grows. Uncovering the different mechanisms behind scar permanence and resolution to allow their manipulation would overcome a major barrier to regeneration. However, the origin of scar forming cells and pathways involved in scar resolution are under debate or comparatively unknown, meaning that current tools targeting the scar are relatively blunt and seem to focus on minimising scar deposition. Beyond the risk of heart rupture with this approach, it appears that even in models where regeneration occurs, preventing scar deposition abrogates the regenerative response; in zebrafish it has recently been seen that genetically removing collagen 1α2–expressing cells prevented proliferation of cardiomyocytes (Sánchez-Iranzo et al. 2018). It has also been noted that the extent and

composition of scar deposition has an effect on injury resolution time: when zebrafish heart tissue is injured by cryo-injury, where a cold probe is placed onto the heart, scar deposition is much greater than when tissue is removed by apical resection (Chablais et al. 2011; González-Rosa et al. 2011). As well as the difference in amounts of ECM, it also differs in composition between the models. In zebrafish, apical resection injury results in fibrin deposition with minimal collagen laid down. After cryo-injury, the scar tissue formed is overwhelmingly collagen-based (González-Rosa et al. 2011; Chablais et al. 2011; Poss et al. 2002). The relatively small amounts of mostly fibrinous scar tissue from the resection injury model is resolved much more quickly than that in cryo-injured fish. This suggests that the extent of ECM deposition has an effect on timeline, but not overall outcome, after injury. In addition, injection of ECM from regenerative zebrafish, and also specifically Agrin from neonatal mice, into adult mice significantly improves heart function after MI, suggesting that initial scar deposition can be beneficial beyond simple mechanics (Chen et al. 2016; Bassat et al. 2017). Indeed, particular ECM genes, such as Tenascin-C and Fibronectin, and ECM remodelling genes appear to be highly enriched in regenerative models such as the newt and zebrafish but not mice and humans, suggesting the existence of a 'regenerative matrix' (Mercer et al. 2013). These results are perhaps unsurprising considering that the scar ECM components can interact and induce signalling in adjacent cells, including cardiomyocytes, affecting cell migration/motility, apoptosis and proliferation (reviewed in Valiente-Alandi et al. 2016).

Research into the origin of scar-expressing cells has been extensive, if thus far inconclusive. Recent results have shown that macrophages may contribute ECM proteins to the scar (Mouton et al. 2018). However, it is believed that the scar is predominantly formed by

fibroblasts that become activated after injury, causing them to proliferate, migrate to the wound area and subsequently differentiate into myofibroblasts. Myofibroblasts are a specialised cell type that expresses smooth muscle alpha-actin and secretes large amounts of ECM proteins into the injury area (Chistiakov et al. 2016). The activation of fibroblasts is thought to be mediated by the necrotic tissue environment, changes in the mechanical structure of the heart and signals from infiltrating immune cells (Chistiakov et al. 2016; Turner 2016). The origin of myofibroblasts is currently under debate, with some studies indicating that resident fibroblasts are the main source, while others suggest the epicardium, endocardium, or bone marrow (reviewed in Chistiakov et al. 2016). Once deposited, the scar then matures through cross-linking of the collagen fibres and then remains indefinitely. In adult mice, some myofibroblasts remain in the scar, with some evidence that they differentiate further into specialised scar-maintaining cells (Fu et al. 2018). By contrast, in the zebrafish, the myofibroblasts become inactivated and enter a quiescent state more like baseline fibroblasts found in uninjured cells (Sánchez-Iranzo et al. 2018). Unpicking the mechanisms behind these different fibroblast fates may prove useful to disentangling control of initial scar deposition versus its permanent maintenance.

Less research has been done into the physical dissolution of the collagenous scar, with little known about the pathways involved in its direct clearance. In zebrafish, the progression of the scar has been well described, however, even though the processes behind its progression have yet to be found. By 4 days post cryo-injury (dpi), fibrin is deposited and scar formation begins. At 7 dpi, the fibrin matrix is mostly removed, along with the dead cells and other debris and replaced by collagen with a fibrin border, particularly along the outside edge of the wound. By 14 dpi there is extensive collagen deposition and the fibrin outside edge is

beginning to be replaced by a new compact myocardium. Collagen is gradually replaced with new muscle by 60 dpi, however, how the collagen is lysed and removed is relatively unknown. In the regenerative zebrafish and neonatal mouse hearts, there is evidence of collagenolytic activity in the injury site, potentially through the activity of matrix-metalloproteases (MMPs) 2 and 14a (Gamba et al. 2017). However, beyond this nothing is known about the cell types and triggers that begin and control this process. Other MMPs active in the wound site from as early as 1 dpi in the zebrafish may act to digest basement membranes and enhance chemotactic cytokines through cleavage, attracting and allowing the infiltration of inflammatory cells into the wound to pick-up cell and lysis debris (Xu et al. 2018). It is likely that a similar mechanism acts later in the injury timeline when the scar is removed.

Whilst successful removal of the scar is one aim, how to time the resolution of the scar with new myocardial growth is another matter. It appears that the scar, scar forming cells and adjacent myocardium can 'talk' to each other. For example, the expression of the intermediate filament Tenascin-C along the border of the scar immediately adjacent to the re-growing myocardium in zebrafish and regenerative newts might help the proliferation, migration and orientation of newly-formed myocytes (Mercer et al. 2013). Besides the guidance of regenerated muscle, it also appears that, to some extent, the generation of new muscle is dependent on lysis of the scar tissue. In zebrafish, inhibition of MMPs with an inhibitor reduced cardiomyocyte proliferation and leukocyte infiltration, and resulted in increased scar size (Xu et al. 2018). In cultured rodent neonatal cardiomyocytes, less stiff matrices induced de-differentiation and proliferation (Yahalom-Ronen et al. 2015). In addition, reducing scar rigidity through inhibition of ECM cross-linking rescued regeneration in non-regenerative postnatal day 3 (P3) mice (Notari et al. 2018). Could it be that peri-injury

cardiomyocytes can sense scar lysis, resulting in decreasing stiffness, and be stimulated to proliferate? If true it seems that it is only part of the story, as scar lysis alone arguably appears insufficient to stimulate new muscle growth. Some scar lysis is seen in a non-regenerative injury model in the neonatal mouse where massive scar deposition is thought to prevent regeneration (Gamba et al. 2017). However, this lysis appears to be initiated to a lesser degree than in the zebrafish and it remains to be seen whether the forced widespread lysis/softening of scar tissue after injury in adult rodents could enhance myocardial proliferation and regeneration.

To summarise, there is much to be learned about the scar and how its dual nature of being helpful and harmful is regulated. The regulation behind differences in myofibroblast end fate in mice and zebrafish needs to be further explored, as does the cross-talk between the scar, scar-related cells, such as myofibroblasts and leukocytes, and cardiomyocytes. The scar is not a passive player in injury and therefore offers much to the study of regeneration.

1.2.4 EPICARDIUM AND ENDOCARDIUM

Endothelial cells make up a large percentage of the cellular component of the heart, whether as parts of coronary vessels or as the endocardium, the lining of the heart. Estimates vary, but they are often present in roughly an equivalent or greater number to cardiomyocytes in both zebrafish and mammals and constitute approximately one third of the cellular complement of the heart (Zhou & Pu 2016; Pinto et al. 2016; Patra et al. 2017). Epicardial cells cover the outside of the heart. Whilst they are disparate in type and position, endothelial and epicardial cells share similar responses to injury.

Upon injury, both cell types become activated, and this activation allows them to contribute signals and cells to the wound. For zebrafish endocardial cells, this involves their rounding up and partial detachment from cardiomyocytes almost immediately after injury. Endocardial cells around the wound proliferate relatively early, a couple of days before peak cardiomyocyte proliferation. They subsequently migrate to cover the wound area and then form an organised wound lining (Kikuchi et al. 2011; Münch et al. 2017). Besides forming this lining, activated endothelial and/or endocardial cells can form new vessels in the wound site after injury in fish and mice, as they do during development (Zhao et al. 2014; He et al. 2017; Kobayashi et al. 2017; Harrison et al. 2015). New vessels begin to be formed in the first 2 days after injury in the zebrafish and blocking this initial vessel formation prevents successful regeneration (Marín-Juez et al. 2016). Therefore, the importance of the endocardium in injury response cannot be underestimated. Besides new vessel formation, there is also some evidence that the endocardium can produce cells that contribute to fibrosis, but this is still debated and requires further experimentation (Sánchez-Iranzo et al. 2018; Gamba et al. 2017).

In addition to producing cells, the endocardium is also a source of signals that are necessary for heart regeneration. One of these is IGF and IGF signalling is required for *gata4*-positive cardiomyocyte proliferation in development and in regeneration, as mentioned previously (Y. Huang et al. 2013). Notch receptors are activated in endocardial cells after injury and Notch signalling is necessary for cardiomyocyte proliferation, with blockage of Notch signalling causing permanent scar formation in the zebrafish (Zhao et al. 2014). In addition, the endocardium is a source of retinoic acid signals that are also necessary for efficient

regeneration (Kikuchi et al. 2011) as well as a source of chemokines (Harrison et al. 2015). The endocardium therefore is a potent source of pro-regenerative signals.

Interestingly, despite being comprised of diverse cell types, the epicardium also acts as a source of these signals after injury. The epicardium has been better studied in regeneration and been shown to produce a variety of cell types and signals after injury in mice and zebrafish (Cao & Poss 2018; Simoes & Riley 2018). Beyond the signalling it shares with the endocardium, the epicardium is also involved in BMP, TGFβ, NF-κB, Nrg1, FGF and hedgehog signalling with the myocardium. Epicardial activation occurs within 1 to 2 days of wounding and involves the re-expression of developmental genes, such as *Wt1*, *Tbx18*, *Raldh2* and *Fn1a* (Guadix et al. 2011; Rudat et al. 2013; Cao & Poss 2018; Zhou et al. 2011; Masters & Riley 2014; Smart & Riley 2012; Simoes & Riley 2018). In both mice and zebrafish, some of these activated cells undergo epithelial-to-mesenchymal transition and migrate towards the wound, where they differentiate to form cells such as fibroblasts, pericytes and smooth muscle cells in another recapitulation of development (Smith et al. 2011; Smart et al. 2007; Simoes & Riley 2018; Gonzalez-Rosa et al. 2012). The fibroblasts formed in this process are thought to be a major contributor to scar formation. Ablation of the epicardium itself or its activation results in defective regeneration in the zebrafish, meaning the contribution of the cells and signals from the epicardium are necessary for full recovery.

There is some evidence that the epicardium and endocardium produce cardiomyocytes after injury, but in such low numbers as to be negligible and insufficient for regeneration (reviewed in Masters & Riley 2014; Cao & Poss 2018; Simoes & Riley 2018). However, their other cellular and signal contributions to wound healing, cardiomyocyte proliferation and angiogenesis are absolutely necessary. As the less studied of the two, further work investigating the

endocardium and its response to injury might highlight as yet unknown mechanisms behind regenerative capacity. Further interrogation of the epicardial and endocardial processes after injury might highlight areas for pharmacological intervention.

1.2.5 IMMUNE CELLS

The immune system is one of the first responders to cardiac injury and also one of the main mediators of wound progression. Most studies on the subject have been done looking at leukocyte recruitment, focussing heavily on neutrophils, monocytes and macrophages.

Immediately after injury, damage-associated molecular patterns (DAMPs) and reactive oxygen species are released from dying cells. These bind toll-like receptors (TLRs), resulting in activation and recruitment of immune cells and also fibroblasts. The response of immune cells can broadly be split into 3 phases: acute inflammation, pro-inflammatory maintenance and inflammation resolution.

The acute inflammatory stage is marked by the infiltration of neutrophils and monocytes and the upregulation of pro-inflammatory genes such as TNFα and IL-6 (Forte et al. 2018; Zlatanova et al. 2016). Preventing IL6 expression at this stage completely prevents regeneration in neonatal mice and reduces the number of proliferating cardiomyocytes, whilst depleting neutrophils in adult mice significantly worsens outcome (Han et al. 2015; Horckmans et al. 2017). This initial reaction to injury appears to be conserved in regenerating and non-regenerating models, however, after this initial phase, differences begin to appear.

In adult mice, this initial wave of neutrophils is succeeded by the invasion of pro-inflammatory ly6^{hi} (Ly6 is a membrane bound marker of murine monocytes) monocytes and macrophages, that maintain the pro-inflammatory environment and degrade the ECM around the injured

cells, helping to activate fibroblasts and engulf debris. Neutrophils that are undergoing apoptosis after engulfing initial debris are hoovered up by these macrophages. This inflammatory wave gradually transitions, via a period of macrophage proliferation and phagocytosis, to an anti-inflammatory ly6^{lo} wave, the inflammation resolution phase. This can also be termed a reparatory phase, where anti-inflammatory and reparative cytokines, and potentially also ECM components, are released that aid myofibroblasts in accumulating and laying down the scar and promote angiogenesis (Mouton et al. 2018). In adult mice, depleting leukocytes either in number or activity has been found to both help and hinder outcome after MI, no doubt reflecting the fact that scarring is both helpful and harmful.

In contrast to their aged counterparts, in regenerative neonatal mice, depletion of macrophages abrogates regeneration (Aurora et al. 2014). It has been seen that neonates too have a ly6^{hi} followed by ly6^{lo} biphasic monocyte recruitment, but gene expression analysis shows that leukocytes in these mice have a pro-regenerative and pro-angiogenic expression pattern, distinct from that in cells isolated from non-regenerative mice (Aurora et al. 2014). It has been suggested, though, that the main cells that constitute the non-neutrophil leukocyte response are, in fact, tissue resident macrophages, rather than recruited monocytes, which are embryonic-derived and non-inflammatory, pro-regenerative and pro-angiogenic (Lavine et al. 2014). Therefore, it seems that there is a fundamental difference in the nature of invading immune cells, rather than differences in their invasion and departure times.

In the zebrafish, the initial accumulation of neutrophils beginning at 6 hours post injury and peaking at 5 dpi is accompanied by an initially small accumulation of macrophages that increases and peaks at 7 dpi. Delaying macrophage accumulation results in failed

regeneration, with issues occurring in neutrophil clearance, angiogenesis, cardiomyocyte proliferation and scar resolution. When compared to another fish, the medaka, which cannot regenerate its heart, the zebrafish more strongly activates pathways involved in macrophages and phagocytosis, whereas in the medaka the more strongly activated genes are involved in neutrophil and monocyte chemotaxis (Lai et al. 2017). The medaka and adult mouse seem to share a reliance on monocytes over macrophages in their immune response, based on this gene activation comparison. In another similarity between fish and mammal, in familiarity with the neonatal mice, depleting phagocyte recruitment in zebrafish prevents regeneration, resulting in a permanent scar (W.-C. Huang et al. 2013).

The research done to date has shown that the immune response is a key component of the injury response and a mediator of outcome. It would seem that initial inflammation is common to non-regenerative and regeneration models and is also required for regeneration. In regenerative models, neutrophil recruitment is followed by recruitment or activation of phagocytic, pro-regenerative macrophages and interference with these macrophages inhibits regeneration, as seen in the neonatal mouse and zebrafish. By contrast, the later immune cells in adult mice and medaka appear to contribute to scar permanence. It could be that this difference in regenerative potential is linked to the pro-inflammatory versus non-inflammatory nature of macrophages recruited to the wound in the different models. The initial wave of inflammation is necessary for debris removal and initial scar formation, but the maintenance of inflammation seen in the adult mouse for an extended period with the inflammatory monocyte/macrophage could lead to or be a contributing factor to excessive fibrosis. As the active immune cells after initial inflammation in the neonatal mouse are non-inflammatory macrophages, this therefore reduces the inflammatory period to little longer

than the acute inflammatory response immediately after injury. Another example of a lengthened inflammatory period in a non-regenerative response is seen in the medaka, where inflammatory neutrophils are maintained in the wound for longer than in the zebrafish. It would be interesting to compare the profile of the phagocytic macrophages seen in the zebrafish to those of the neonatal mouse, to see if they share a similar non-inflammatory nature. Regardless of the current unknowns, there appear to be intriguing differences in the immune responses between regenerative and non-regenerative models and their relation to permanent scar formation. Further investigation should prove very interesting and provide much to the understanding of regenerative capacity.

1.2.6 OTHER CELL TYPES

Much of the research done on heart regeneration has focussed on the most numerous cells of the heart, such as cardiomyocytes and endothelial cells, and those involved heavily in the initial injury response. However, some of the less usual suspects have also been shown to have profound effects on regenerative capacity.

Lymphatic vessels are formed from specialised lymphatic endothelial cells and are involved in tissue fluid homeostasis and immune cell invasion and clearance, amongst other processes. After injury in the mouse, the lymphatic vasculature responds to form new vessels through reactivation of a developmental angiogenic program to form new vessels at a number significantly above the baseline level of the uninjured heart (Klotz et al. 2015). Disrupting functional lymphangiogenesis after injury adversely affects injury (Tatin et al. 2017). It seems that lymphatic vessels are required due to their role in clearing leukocytes after injury. In a mouse model where lymphangiogenesis is unaffected but the transition of leukocytes into

the vessels is blocked, there is a significant accumulation of leukocytes by 7 dpi, adversely affecting injury response through attenuation of fibrosis and pathological remodelling (Vieira et al. 2018).

Cardiac innervation has also been shown to be crucial for a successful regenerative response, with both pre-existing nerves and the formation of new nerves in the injury area being necessary (Mahmoud et al. 2015; White et al. 2015). Adult zebrafish hearts with reduced developmental innervation show a reduction in cardiomyocyte proliferation after injury, whilst pharmacological inhibition of cholinergic nerve transmission in wild-type (WT) zebrafish and neonatal mice after injury reduced regeneration. However, cholinergic stimulation in non-regenerative mice was insufficient to recapitulate complete regeneration. Mice that had had their vagus nerve removed before injury also showed reduced regeneration, but cardiomyocyte proliferation could be rescued by the application of Nrg1 and Ngf, potent cardiomyocyte mitogens (Mahmoud et al. 2015). In neonatal mice, sympathetic nerves grow into the injury zone and inhibiting this re-growth abrogates regeneration, with a huge increase in scar size (White et al. 2015). Conversely, over-activation of the sympathetic nervous system through stress adversely affects regeneration through IGF-related cardiomyocyte proliferation in zebrafish (Sallin & Jaźwińska 2016). This suggests that nerves play a profound and potentially direct role in regulating cardiomyocyte proliferation. However, this may not be the only pathway that they act through: in other injury contexts, nerves have been found to regulate stem cell niche maintenance and patterning of the regenerate (Farkas & Monaghan 2017; Satoh et al. 2018). Further investigation of nerves in control of cardiomyocyte patterning after injury and in regulation of cardiac resident progenitors could provide useful insights into regenerative capacity.

1.2.7 PROGENITOR CELLS

Progenitor cells that have been found residing within the heart may broadly be divided into two categories, myogenic and non-myogenic. The latter has been described above in the epicardial and endocardial cellular contributions to injury and, for the most part, have been discovered whilst on the hunt for the former. Both epicardial and endocardial cells have been posited to form cardiomyocytes in mice and fish, though not in great numbers (Masters & Riley 2014; Cao & Poss 2018). The existence of myogenic progenitor cells in the heart is highly controversial and dogged by lack of reproducibility.

It was originally though that the mammalian heart is terminally differentiated and that the number of cardiomyocytes slowly diminishes across a lifetime. However, studies have shown that the heart is capable of myocardial renewal during homeostasis and after injury (Bergmann et al. 2009; Anversa & Nadal-Ginard 2002; Hsieh et al. 2007; Senyo et al. 2013)). Once this was realised, the search was on for the cardiac stem cell responsible for the formation of new myocytes in adult rodents and humans. Initial experiments looked outside the heart, with injected c-Kit^{+}Lin^{-} bone marrow-derived stem cells claimed to form a large percentage of myocytes and smooth muscle cells after infarction in adult mice (Orlic et al. 2001). The labelling c-Kit^{+}Lin^{-} means that the cells were lineage negative (not positively stained for any markers of mature, lineage committed cells) and positive for c-Kit, a cell-surface receptor expressed on hematopoietic stem cells. However, controversy began almost immediately, with other groups unable to reproduce these results (Balsam et al. 2004; Murry et al. 2004). The disparity was blamed on the high rate of non-specific antibody uptake in cardiomyocytes, as the latter studies used genetic markers rather than immunohistochemistry to mark cardiomyocytes (Chien 2004). As further studies indicated that new cardiomyocytes formed after injury in adult mice derived from stem cells (Hsieh et

al. 2007) the search then turned to stem cells resident in the heart, so called endogenous cardiac progenitor cells or eCPCs. Again c-Kit was used most commonly as a marker, and niches in the apex and atria containing rare eCPCs were discovered. These cells were seen to adopt myogenic and vascular fates after infarction in the mouse, but in some work this ability appeared to be limited to the neonate (Jesty et al. 2012; Zaruba et al. 2010; Beltrami et al. 2003; Ellison et al. 2013). However, again reproducibility has been an issue, with other work being unable to show the cardiomyogenic potential of eCPCs (van Berlo et al. 2014; Keith & Bolli 2015; Sultana et al. 2015). It has been suggested that previous lineage tracing results that showed c-Kit-derived cardiomyocytes were due to labelling of pre-existing c-Kit-positive cardiomyocytes, or due to c-Kit-positive (due to their hematopoietic lineage) leukocyte fusion with cardiomyocytes (Liu et al. 2015; Fu et al. 2018; Maliken et al. 2018).

Along with c-Kit, other markers such as Sca1 and Isl1 have been used to find eCPCs, with similar controversy (Tzahor & Poss 2017). With the many types and markers of eCPCs and the surrounding dispute about their myogenic capacity, it is fortunate that a stem cell marker-independent method of assessing the origin of cardiomyocyte production in the adult mouse has been recently developed (Yan et al. 2018). Yan Li and colleagues used a novel and stringent method of marking all non-myocytes prior to injury to assess their contribution to new cardiomyocytes. This study found that new myocytes formed in adult mice were derived only from pre-existing myocytes, whilst only in the embryo, during initial formation of the heart, could non-myocytes form myocytes. Combined with the multitude of reproducible evidence in the neonatal mouse and zebrafish that proliferation of existing cardiomyocytes is responsible for new myocardium growth after injury, this suggests that pursuing a eCPC solution to the problem of non-regeneration could be fruitless.

1.3 AIM OF THE STUDY: LOOKING FOR NOVEL PROGENITORS IN THE FISH HEART

In light of the lack of conclusive evidence of a cardiac stem cell, why look for progenitors in the fish heart?

The aims of this study are to identify novel progenitor populations in the fish heart that are responsible for the formation not of cardiomyocytes, but of other cells that might be involved in a regenerative response. The work summarised above indicates that enhancing proliferation of cardiomyocytes alone is insufficient to stimulate complete regeneration of the heart, which is the aim of the field. As new heart muscle is the aim, other cell types that are important for regeneration are often overlooked or under-studied, for example the endocardium and also processes involved in scar formation and dissolution. This study aims to identify overlooked progenitor cell populations by using a new model to the field of heart regeneration, the Mexican cavefish. These fish exist as two ecotypes of the same species, where one ecotype can regenerate its heart and the other cannot. By observing differences in the cell types seen after injury in these fish, it is hoped that novel progenitor populations can be identified.

1.4 *ASTYANAX MEXICANUS*: A POWERFUL TOOL FOR INTERROGATING THE MECHANISMS BEHIND HEART REGENERATION

1.4.1 AN INTRODUCTION TO *ASTYANAX MEXICANUS*

Astyanax mexicanus, also known as the Mexican cavefish, is a species of teleost fish, like the zebrafish, that has been used in evolutionary developmental biology for decades. Its use comes from the fact that it exists as a single species that can be separated into two broad ecotypes: the surface-dwelling fish and the cave-dwelling fish. It is thought that cavefish

evolved from surface fish due to flooding events that stranded surface fish in caves, where the subsequent nutrient-deficient conditions necessitated the adaption of the stranded fish to cave life for survival. The timeline of this conversion is under debate, with the formation of cavefish being described as occurring anywhere from 20,000 to 8 million years ago depending on the experimental method used (Fumey et al. 2018; Herman et al. 2018; Gross 2012; Jeffery 2009).

Regardless of the debatable timeline of their origin, many of the underlying mechanisms behind the acquisition of 'cave-like' traits have been well studied. It seems that the acquisition of 'cave-like' traits is geared towards one or both of two things: an increase in energy efficiency and the specialisation of food-finding behaviour. In the broadest terms, this is increasing energy uptake and reducing energy expenditure. In cavefish, the most obviously observable examples of cave-trait acquisition are that the cavefish have lost their eyes and their pigment (Fig. 1.1 A, B). Seeing in the dark is actually more energy-draining than seeing in the light, so losing their eyes and reducing the energetically-expensive region of the brain that computes sight is thought to be highly beneficial (Soares et al. 2004; Moran et al. 2015). New research points to the idea that eye loss might drive other changes beneficial to cave live, for example sight loss in cavefish/surface fish progeny has been associated with hypermelanation, which is very energetically expensive and would be selected against in the nutrient-poor cave (Gross et al. 2016). Loss of pigmentation appears to also affect behaviours such as feeding and sleep, presenting another avenue for selection pressure (Bilandzija et al. 2018; Bilandzija et al. 2013). As well as a potential effect on pigment formation, eye loss appears to also influence adaptations to feeding in the cavefish. The changes in gene expression patterns associated with eye loss have profound influence on the craniofacial

structure of the fish, widening their jaws and increasing the numbers of taste buds (Yamamoto et al. 2009; Yamamoto et al. 2003). Additionally, eye-loss is associated with enhanced olfactory senses that increase sensory range, aiding foraging (Blin et al. 2018; Lloyd et al. 2018). Eye regression has also been linked to a specialised feeding behaviour in cave fish, vibration-attraction behaviour (VAB), through an increase in specialised vibration sensors in the eye orbit (Yoshizawa et al. 2012). This behaviour allows them to sense specific prey, such as small shrimp, through the oscillations of the prey's movement.

As well as vibration-attraction behaviour, other specialised behaviours cavefish exhibit are an altered feeding posture that aids bottom feeding, sleep loss and a bias towards solo food-finding over hierarchical schooling and the accompanying aggression (Kowalko et al. 2013; Elipot et al. 2013; Elipot et al. 2014; Duboué et al. 2011; Yoshizawa et al. 2015). Sleep loss is found in independently evolved cave morphs, suggesting convergent evolution, and it is thought that this means the cavefish is awake for longer periods to take full advantage of food when it is available, as such an event may be rare in the cave. When the nutritional environment is poor and the cavefish is starving, sleep is promoted to save energy. This behaviour is thought to be driven by increased sensory input from the sensors involved in VAB, which promotes wakefulness. Ablating these sensors promotes sleep in the cavefish by reducing activity of a particular population of neurons in the cavefish hypothalamus. These neurons promote hyperactivity and are present in larger numbers in the cavefish hypothalamus, which is increased in size compared to the surface fish (Jaggard et al. 2018; Jaggard et al. 2017; Alié et al. 2018). Similarly, the reduction in aggression and social behaviours in the cavefish is also thought to be due to changes in the transmitter composition in the brain, for example with increases in serotonin levels (Elipot et al. 2013; Elipot et al.

2014). This behavioural change promotes solo foraging, which is likely a more efficient method of finding food in cave conditions.

Changes to the cavefish are not just on the outside but also within. They possess a mutation in the *melanocortin 4 receptor* gene, which leads them to have an insatiable appetite, increased growth and to lose weight more slowly when starving, all properties that would encourage survival in a poor nutrient environment (Aspiras et al. 2015). The ability to eat more is accompanied by insulin resistance, resulting in increased weight and hyperglycaemia without adverse effects, another adaptation to low nutrient conditions (Riddle et al. 2018). Less easily perceptible is the change in the molecular circadian rhythm; the cavefish molecularly look as though they are constantly in the 'light' phase of the surface fish. Their molecular clock does oscillate, but only minimally and out of phase with the surface fish. It is thought that this helps them as it enables continual expression of light-related genes in the dark and, importantly, there is also evidence that this makes their metabolism more efficient, by preventing the large energy expenditure oscillations seen in the surface fish depending on day or night (Beale et al. 2013; Moran et al. 2014; Frøland Steindal et al. 2018).

Due to these energy-saving and behaviour-modifying adaptions to cave life, the cave fish has been used to look at many conditions affecting humans. Their altered energy storage and metabolism has been compared to human obesity and diabetes related genes and their asocial stereotypic behaviour has been compared to human autism-spectrum disorders, showing both possess alterations in many of the same associated genes (Riddle et al. 2018; Aspiras et al. 2015; Yoshizawa et al. 2018). Now, the cavefish is to be used to study another human ailment: the inability to regenerate lost heart muscle.

1.4.2 WHY USE *A. MEXICANUS* TO STUDY HEART REGENERATION?

Astyanax mexicanus are teleost fish, like the zebrafish, so it might be expected that they can regenerate their hearts in a similar manner. However, this is only partially the case: only the surface fish shows the ability to regenerate after apical resection injury (removal of the apex of the heart). The cavefish instead forms a permanent fibrotic scar and, like humans and higher vertebrates, this scar undergoes remodelling and even dilation (Fig. 1.1 C-F).

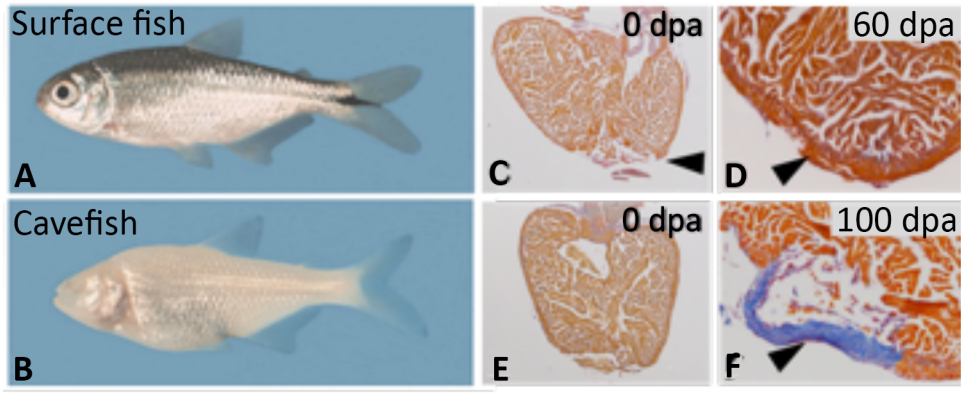


Fig. 1.1 *Astyanax mexicanus* ecotypes have different regenerative capacities. A and B show images of whole surface fish and cavefish, respectively. **C** and **D** show Acid Fuchsin Orange G (AFOG) staining of surface heart sections at 0 and 60 days after injury respectively. Orange/red indicates myocardium, pink is fibrin and blue is collagen. **E** and **F** shows AFOG staining in the cavefish heart at 0 days after injury and 100 days after injury, respectively, showing that the scar remains in the cavefish long after regeneration has occurred in the surface fish. Images reconstituted from data collected for Stockdale et al. 2018.

Recent work in this laboratory has shown that, surprisingly, cardiomyocytes proliferate in both the surface and cavefish in the same robust manner as seen in the zebrafish. However, in the cavefish, these proliferating cardiomyocytes fail to produce new myocardium. In fact, there appears even to be an additional stage of myocardial proliferation in the cavefish at 30 dpa (days post amputation), that also fails to add to new muscle growth. This adds further

credence to the idea that stimulation of myocardial proliferation alone is insufficient to drive complete regeneration (Stockdale et al. 2018).

Comparison of another key determinate in regenerative capacity, the immune response, showed an upregulation in inflammation, concomitant with an increase in ECM synthesis and turnover in the cavefish compared to the surface fish. Additionally, cavefish alter their metabolism compared to surface fish, with down-regulation of mitochondrial and glycolytic pathways after injury, which more mirrors the metabolic environment of the human heart than the neonatal mouse (Lalowski et al. 2018; Puente et al. 2014). The fact that cavefish and surface fish are the same species allows analysis that can map regenerative capacity to specific genomic loci (Quantitative Trait Locus analysis). This identified potential roles for the ECM proteins Ncam1a and Itgam, which, given the altered scarring response in the two fish, are key targets for more investigation (Stockdale et al. 2018).

This work done in the cavefish and surface fish again highlights the importance of cell types and processes other than the proliferation of cardiomyocytes to the ability to renew the heart. The fact the two fish are the same species allows the performance of unique experimental processes, like the QTL analysis, and also means it is more likely that any differences seen in the heart after injury are due to, or causative of, differing regenerative capacity rather than unrelated fundamental differences between species. *A mexicanus* can therefore be a powerful tool to identify novel processes behind the capacity to renew.

Here, the difference in cell type production after injury between surface and cavefish is analysed to help identify progenitors that are either present in only one fish, or are affected by the different regenerative environments of the fish. This approach has allowed

identification of two progenitor cells, one of which is produced by a transition process that has not been identified after injury in any animal before.

1.5 OUTLINE OF THE THESIS

This thesis describes the work undertaken to identify novel stem cells in the fish heart. *A. mexicanus* hearts of both ecotypes were observed before and after injury to look for obvious differences in cell types formed that would indicate differential activity of a perhaps unknown progenitor.

The work performed indicates that the cavefish heart produces fat on the heart after injury by apical resection, whilst the regenerative surface fish does not. This suggests the residence of a fat-producing mesenchymal stem cell (MSC) in the *Astyanax* heart. Labelling using Pdgfrα, a marker of MSCs, indicates the presence of potential progenitors within the epicardium. The zebrafish also produces fat on the wound after cryoinjury, allowing lineage tracing to identify the progenitor cell in existing transgenic zebrafish labelling lines. Lineage tracing using an epicardial tamoxifen-inducible Cre line indicates that the epicardium does indeed form fat after injury, consistent with work done in the mouse. This progenitor has not previously been identified in fish and the fact it appears to be active in the cavefish but not the surface fish may offer information on their different regenerative capacities.

Other cells labelled with Pdgfrα are present in the endocardial region of the heart and in the blood of the surface fish and cavefish. The number of these cells fluctuates markedly in response to injury, suggesting a highly injury responsive population. After injury, large numbers of these cells are present in the border zone of the wound, and identification of

these cells with other markers shows these cells to be of a dual endothelial/hematopoietic nature, similar to that of the hemogenic endothelium (HE) that forms hematopoietic stem cells (HSCs) during development. Further analysis in zebrafish, where a transgenic line marking these cells was available, indicates that the endocardium activates a developmental pathway, becoming a specialised HE that undergoes endothelial-to-hematopoietic transition (EHT) after injury, forming new HSCs. Runx1, a key regulator of EHT and marker of HSCs, is expressed in the hemogenic endothelium and also the epicardium and border zone myocardial cells. These are all cells that undergo activation to more developmental-type states. Given this, it is perhaps an unexpected result that examination of *runx1* knockout (KO) fish shows that they regenerate much better than WT fish, with increased myocardial proliferation at early stages and an initial reduction in scarring. They also exhibit increased myocardial survival in the initial stages, indicating a protective effect in addition to increased proliferative capacity.

Single cell sequencing of Runx1-positive and Runx1/Kdrl (a marker of endothelium) double-positive and Kdrl-positive positive cells isolated from uninjured and injured hearts, indicates that cells positive for both of these markers also exhibit increased expression of other hemogenic endothelium genes identified in published developmental studies. These results lend more credence to the idea that endothelial cells within the wound become hemogenic and produce hematopoietic progenitors within the wound area.

To summarise, this thesis describes the finding of 2 novel progenitor activities in the fish heart after injury: the formation of fat in the scar by an epicardial progenitor and the transition of the endocardium into HSCs. These cells may play an important and as yet undiscovered role in the ability to regenerate heart muscle after loss of cardiomyocytes.

CHAPTER 2 - METHODS

2.1 FISH HUSBANDRY

All the experimental procedures were performed in accordance with the UK Animals (Scientific Procedures) Act 1986 and institutional guidelines. Zebrafish embryos and fish are kept at 28 °C on a 12/12h light cycle. *Astyanax mexicanus* are kept on a 14/10h photoperiod at 22-25 °C, where 25 °C is used to induce spawning. *A mexicanus* breeding was performed by raising the temperature and placing tubs containing marbles into the tanks for the fish to breed over. The marbles provide a spawning surface and prevents the fish from reaching the eggs. Fish breeding in zebrafish was performed in 3 ways: a tub full of marbles was placed in a corner of a pre-existing tank in the evening and the tray with embryos was removed the next morning, in the evening groups of fish were placed in a separate tank outside of the flow system that had an insert with holes in, allowing eggs to drop to the bottom of the tank separated from the fish when they spawn in the morning , or, lastly, fish couples were isolated and put into two fish tanks outside the main flow system, again with an insert with holes in and also another insert separating the two fish. In the morning, the divider was removed allowing the male and female to make contact and spawn.

2.2 FISH INJURY

Fish cryoinjuries were performed in the following manner: the fish was anaesthetised in 250 mg/L tricaine dissolved in fish water and brought to pH 7. Once anaesthetised, the fish was moved to a sterile sponge and placed ventral side up under a dissecting microscope. The chest wall above the heart was then opened with surgical scissors and the pericardial sac was carefully opened with fine-tipped forceps. Once the heart was exposed, gentle pressure was placed on the side of the sponge to encourage the apex of the heart to protrude from the

incision in the chest wall. The heart surface was dried with sterile tissue. After this, a cryoprobe made of a small circle of copper wire that had been dipped in liquid nitrogen was pressed onto the exposed apex until the probe thawed, approximately 5s. Once the probe thawed, it was then refrozen and applied again. Afterwards, the fish was removed from the sponge and placed into a tank by itself to recover. Sterile procedures and maintenance of sterile equipment was observed throughout.

2.3 PARAFFIN EMBEDDING

After isolation, hearts were placed into 4% paraformaldehyde (PFA) and left at 4°C overnight. The next morning, the hearts were briefly washed in PBS before being placed through an alcohol series to dehydrate them. The series consists of 1 hour in each of 70%, 80%, 90% and 96% EtOH before spending half an hour each in 100% EtOH. After dehydration, the hearts were left in butanol overnight. The hearts were then washed in hot paraffin (Paraplast Plus, Sigma Aldrich) to remove the butanol, before undergoing 3 repeats of washes in fresh paraffin in an oven at 62 C for 2 hours each, to ensure paraffin invasion into the tissue. After the washes, the hearts were mounted into a block of paraffin which was left to solidify. The blocks were all sectioned on a microtome at a thickness of 7 μm.

2.4 SEMIQUANTITIVE ANALYSIS OF FAT ON THE *ASTYANAX* HEART

Whole mount fish hearts isolated from fish of 6 or 30 months of age were observed for the approximate number of fat cells present on the heart. Hearts were placed in 0.1% agarose w/v in PBS to keep them still, before images were taken at various angles so all of the heart was captured for visual analysis. Fat was determined to be the opaque white cells present on the surface of the heart. Fat cells are normally clear, but the hearts had been in storage for an extended period and this had turned the fat opaque. The hearts were grouped into 4

different categories: 0-50 adipocytes, 51-100 adipocytes, 101-200 and 201+. The number of hearts of each type per category was then plotted and analysed.

2.5 OIL-RED O STAINING ON CAVEFISH AND ZEBRAFISH WHOLE HEARTS

Oil-Red O staining was performed on fish hearts that had been isolated and fixed in 4% PFA at 4°C overnight. Following fixation, the hearts were stored in 1X PBS at 4°C until use for Oil Red O staining. The whole mount Oil Red O staining protocol used was adapted from (Kim et al. 2015). The staining solution was made by dissolving Oil Red O (Sigma-Aldrich) in 100% 2-propanol to 0.5% w/v. This is then mixed with distilled water to a ratio of 3 Oil Red O:2 water and filtered using a 45 micron syringe filter (Fisher scientific) to remove particulates. Hearts were rinsed in 1x PBST (1X PBS with 0.5% Tween-20 (Sigma-Aldrich) 3 times for 5 minutes each. Hearts were then briefly washed in 60% 2-propanol. Following this, hearts were placed into an Eppendorf containing the Oil Red O staining solution for 15 minutes. Hearts were then washed 3 times for 5 minutes each in 1X PBST, before washing in 60% isopropanol until Oil Red O wasn't released into the wash solution. Then the hearts were washed in 1X PBS and fixed again in 4% PFA for 2h at RT before being placed in PBS. Before imaging, hearts were placed in 0.1% w/v agarose in 1X PBS to keep them still whilst images were taken.

2.6 IMMUNOHISTOCHEMISTRY

Immunohistochemistry was performed on paraffin-embedded sections. The paraffin was removed from the section by placing the slides into xylene for 10 minutes, then this was repeated with fresh xylene to ensure complete removal of the paraffin. The sections were rehydrated in a descending alcohol series from 100% to 70% with ddH_2O. The slides were initially placed in 100% ethanol for 2 mins, then repeated with fresh ethanol. After, the slides were placed in 96%, 90%, 80% and 70% alcohol in that order for 1 minute each. Following

this, the slides were placed in 1X PBS. After, the slides were put under an antigen retrieval protocol. Concentrated Antigen Unmasking Solution (Vector Laboratories) was diluted 100X in ddH_2O then placed in a pressure cooker over a heat source and heated to boiling point. The slides, in a metal slide rack, were placed into the pressure cooker and the lid was closed. Once the cooker was pressurised and steam was escaping, 4 minutes was allowed to elapse before the cooker was removed from the heat. The slides were then removed from the solution and placed in 1X PBS.

Once cooled, one by one the glass around the sections was briefly dried, taking care not to dry the sections themselves. An ImmEdge pen (Vector Laboratories) was used to draw a line of wax around the sections, creating miniature wells for staining liquid. Each section was then covered with TNB blocking solution (0.5% TSA Blocking reagent (PerkinElmer), 0.15 M NaCl, 0.1 M TRIS-HCl, pH 7.5) and left for a minimum of 30 minutes at room temperature. The slides were placed into a slide box with moistened tissue paper in the bottom, to prevent the slides from drying out.

Following the blocking step, the primary antibody or antibodies were added to the sections diluted in TNB blocking buffer. The antibodies used and their working dilutions can be found in Table A1. The sections were left in the primary antibody solution overnight, in a humid slide box at room temperature.

The following morning, the slides were washed 3X for 5 minutes each in 1X PBS, to wash off any primary antibody solution. Following this, secondary antibodies were added. For some primary antibodies, AlexaFluor antibodies (Invitrogen) of the desired wavelength were diluted 1 in 200 in blocking buffer and added to the sections for 2 hours at room temperature. However, some primary antibodies are not very efficient at binding to fish tissue and must

undergo additional steps to develop a visible signal. For which primary antibodies require which method, see Table A.1 marked with E after the name. For these antibodies, instead of a fluorescent-conjugated secondary, a biotinylated secondary antibody must be added. These antibodies are diluted 1 in 200 in TNB blocking buffer and left for 2 hours at room temperature. Following this, slides were washed 3X 5 minutes in 1X PBS and conjugated Streptavidin-Horse Radish Peroxidase (PerkinElmer) was added to slides in a 1 in 200 dilution (see Table A.1 for exceptions to this) in TNB blocking buffer. The slides were left for 30 minutes to allow binding of the biotin to the streptavidin. The slides were then washed in 1X PBS 3X for 5 minutes and afterwards the amplification step was done. This was performed using the TSA amplification kit (PerkinElmer). The fluorophore of the desired colour (either Fluorescein or Tetramethylrhodamine), dissolved in DMSO, was diluted 1 in 100 in Amplification Diluent and added to the sections. For Fluorescein, this was left on the sections for 3 minutes and for TMR it was left on for 10 minutes, as the Fluorescein appears much brighter than the Tetramethylrhodamine. After amplification, the slides were washed in 1X PBS 3X for 5 minutes, stained with DAPI.

Special situations: occasionally, two primary antibodies that had been raised in the same species were used on the same sections. This necessitated extra steps to prevent aberrant staining of both primaries with both colours. The times this problem arose, both primary antibodies required the enhanced secondary staining and therefore aberrant overlap of staining could be prevented by doing each stain sequentially, completing the staining for one primary before adding the second primary. In between the stains, after the amplification step for the first primary and before adding the second primary, the HRP was quenched by the addition of 10% H_2O_2 diluted in PBS for 10 minutes. Using this method, complete aberrant

overlap of colours was never seen. Primaries in the same species where one was enhance and one was not enhanced were not required.

After staining was complete the stained slides were dried, without drying out the sections, then Mowiol (made according to Cold Harbor Springs protocol) was added to each section. A coverslip was then lowered slowly to prevent air bubbles forming, then the slides were placed in an incubator at 37˚C in the dark to dry overnight.

2.7 sgRNA DESIGN AND PRODUCTION

To design the sgRNAs, the 600-200 bp region of the 5' UTR of *pdgfrα* from the zebrafish and cavefish was entered into both ChopChop and ZiFiT (or just ChopChop in the case of the cavefish, ZiFiT did not have the cavefish genome at the time) to identify target sequences in that region of the genome, with the caveat that one or both of the first two in the sequence should be a G, to ensure compatibility with a T7 promoter for later *in vitro* transcription. If only one of the first two in the sequence is a G, the other letter is altered to be a G. The top 4 target sequences with the smallest predicted off-target sequences were selected. The sequences were then modified and positioned into a guide oligo, containing a 5' clamp sequence, T7 promoter, the aforementioned target sequence and the Cas9 binding scaffold (Talbot & Amacher 2014) (see Table A.3 for target sequences). This total sequence was then reverse transcribed and ordered as a long oligo.

The oligo was then amplified using PCR (see Table A.2 for primer sequences) and the resulting PCR product was then run on a gel to ensure amplification of the correct sequence. The correct band was then excised and the DNA purified using the QIAquick Gel Extraction Kit (Qiagen). Approximately 30ng of the amplified oligo was then used for *in vitro* transcription using the MAXIscript T7 kit (Life Tech). The kit was used according to manufacturer's

instructions, though the transcription reaction was left to run overnight, due to initial low yields. The RNA was precipitated using 8M LiCl, as in (Talbot & Amacher 2014) as column purification dramatically reduced the amount of sgRNA produced. The sgRNAs were then checked for correct length by gel electrophoresis.

2.8 CAS9 mRNA PRODUCTION

Plasmid MLM3613 was transferred into DH5a cells (Invitrogen) and the bacteria were then spread onto plates containing LB agar with ampicillin. Positive colonies were then picked and grown overnight in 500 mls LB broth in a shaking incubator at 37 C. Plasmids were then isolated from the bacteria using the Qiagen MAXIprep kit. 20 µg of plasmid was then linearised using PmeI restriction enzyme (NEB), according to the manufacturer's instructions over 3 hours. The resulting linearised fragments were then cleaned using the QIAquick PCR purification kit, splitting across two columns to avoid overloading them with DNA. Correct digestion was checked by running some of the digested sample on a gel, with one clear band only seen.

The resulting linearised plasmid was transcribed using the T7 mMessage mMachine kit (Ambion, Life Technologies), according to the manufacturer's instructions. 1 µg of linearised plasmid was transcribed over a period of 2 hours, the longest period recommended by the manufacturer. This was done to maximise yield. The RNA was then capped with a polyA tail to allow translation within the cells. The completed mRNA was then recovered using the LiCl method suggested by the manufacture of the mMessage mMachine kit, using the reagents supplied in the kit. To check the correct mRNA had been produced, it was run on a gel to check the length of the transcript.

2.9 MICROINJECTIONS OF CAS9 mRNA, sgRNAS AND INSERT CASSETTES

1 nanolitre of the mixture of Cas9 mRNA, sgRNAs and insert cassettes was injected into single cell-stage embryos, whilst the cell was very flat, immediately after fertilisation. This was done to try and ensure integration before too many cell divisions, increasing the likelihood of integration into the germline. Embryos were discarded when the cell became very pronounced from the yolk, indicating imminent division, and refreshed with newly fertilised embryos. The injection mixture was kept cold in between injection rounds on dry ice to prevent degradation of the RNAs.

After injection, embryos were placed into E3 medium and immediately incubated to aid survival. Dead embryos were removed 3-4 hours after injections, as survival rate is reduced by the injection process, both through the mechanical intervention of the needle and the injection components themselves. The removal ensures the dead embryos do not impact the survival of the remaining embryos by affecting water quality.

After some optimisation, the final injection mixture contained 2 µl of 750 ng/µl Cas9 mRNA, 2 µl of 35 ng/µl genomic sgRNA, 2 µl of 35 ng/µl eGFPbait sgRNA (to linearise the insert cassette) and 1 µl of 70 ng/µl of the insert cassette, this was then made up to 10 µl with ddH2O and 1 µl Phenol red, to allow visualisation of the injection.

2.10 T7E1 TEST

To detect heteroduplex DNA formed after Cas9 mediated cuts in the genome and thus detect if the sgRNAs cut efficiently, a T7E1 assay was performed. Briefly, genomic DNA was isolated from larvae that had been injected with Cas9 mRNA and genomic sgRNA, without insert cassette, and fish that weren't injected. The DNeasy Blood and Tissue kit (Qiagen) was used to extract DNA from 10-20 pooled embryos of each group. A PCR amplifying the target region

of the sgRNA was then performed and run on a gel, the correct band was then excised and purified using the QIAquick Gel Extraction kit (Qiagen). The PCR product was then hybridised and digested with the T7E1 endonuclease (NEB). The resulting digestion was loaded onto a gel for electrophoresis, with positive Cas9 activity being seen in the presence of more than 1 band in the gel.

2.11 INJECTED EMBRYO AND GERMLINE TRANSITION SCREENING

Injected embryos were checked for the expected fluorescence (cerulean expression in the lens or red Pdgfrα-positive cells) at 4 dpf in E2 fish water without methylene blue. Positive embryos were kept and transferred to the nursery for growth and negative embryos were culled.

Once the positive fish reached sexual maturity, they were bred with Wildtype fish with the aim of identifying founders with germline transgene integration. The offspring of these matings were checked for the desired fluorescence. As no fluorescent offspring were detected, the supposed transgenic parents were genotyped. This was performed by PCR analysis on genomic DNA extracted from fin clippings. Unexpectedly, given the positive fluorescence screening when they were embryos, the adult fish failed to show any integration of the desired transgene in the tissue.

2.12 TAMOXIFEN ADMINISTRATION

For zebrafish larvae, 10 mM 4-hydroxytamoxifen in ethanol was dissolved in 40 ml E3 medium to a final concentration of 10µM. Larvae were placed in this water at 12 hours post fertilisation (hpf) overnight, then again at 2dpf overnight, in the dark. In between treatments, they were in regular E3 medium in a regular light cycle. The double exposure was to increase the amount of labelling.

Adult zebrafish were placed in system water at a density of 3 fish per 150 ml, then 10mM 4-hydroxytamoxifen in EtOH was added to a final concentration of 10µM. The fish were bathed in the tamoxifen for 12 hours in the dark, before being returned to normal circulating water for 2 days before cryosurgery was performed on them.

2.13 CELL COUNTS OF PDGFRα-POSITIVE CELLS

Immunohistochemistry for Pdgfrα was performed on paraffin sections from 4 hearts per ecotype per time point. The number of Pdgfrα-positive cells was then counted as follows: the area of the ventricle away from the injured region was measured using Photoshop and the numbers of blood-borne and endothelial type cells were counted. Blood borne cells were determined as fully spherical cells, normally not in contact with the trabecular myocardium. Endocardial-type cells were defined as those in close apposition to the myocardium with a squashed, flattened morphology. For counts in the border zone, the area of the regenerated myocardium was measured using Photoshop. The number of Pdgfrα-positive cells per time point was then counted. All counts were normalised by the count area, to ensure no skewing by differences in ventricle and/or injury size.

2.14 CELL COUNTS OF RUNX1/KDRL DOUBLE-POSITIVE CELLS

Immunohistochemistry for GFP/Citrine and mCherry was done on sections from zebrafish hearts that were uninjured, sham injured and 1, 3, 7 and 14 dpi (n=4 per time-point). For each section, the uninjured ventricle area and the injury area was measured using Photoshop and the number of dim and bright double positive cells in each was counted and normalised to the count area. Bright cells were defined as cells as bright as the Citrine in the round, blood borne cells. All cells with brightness below this were classed as ‘dim’.

2.15 SLICE CULTURES

Briefly, hearts were isolated from fish at a set time-point after injury. The hearts were dried, then embedded in 4% LMP-agarose in PBS. The blocks were then sectioned on a vibratome, with slices being collected with fine-tipped forceps and kept in culture medium (DMEM, 10% fetal bovine serum, 1% MEM-NEAA, antibiotics/anti-contaminants (100U/ml penicillin, 100µg/ml streptomycin, primocin) and 50uM beta-mercaptoethanol). Sections were then placed onto 1% LMP agarose in PBS in a coverslip with culture wells (see main body of text for further description). After solidification the wells were filled with culture medium and covered with a glass microscope slide. The sections were then imaged on a confocal microscope (Zeiss LSM 880 Airy Scan), with images taken at intervals for periods as described.

Detailed protocol:

1. Perform cryoinjury on the appropriate transgenic fish line.
2. Cull the fish at 3 dpi in 5g/L tricaine solution (buffered to pH 7).
3. Isolate the heart.
4. Put the heart into chilled PBS on ice.
5. Remove any excess blood and tissue from the outside of the heart.
6. Dry the heart gently with tissue paper.
7. Put heart into the middle of a square mould.
8. Add 4% low-melting-point agarose to the heart in the mould. 4% agarose should be kept in a water bath at 42 C and pipetted into the mould using a plastic Pasteur pipette. Pipette the heart and agarose up and down 2-3 times to ensure heart is fully surrounded by the agarose.
9. Place mounted tissue onto ice for the agarose to solidify.

10. Section the heart into 75 µm slices into a bath of chilled PBS. If using a Leica VT 1000S then use the settings of 1.1mm/s 600Hz for blade (Astonics, INC, 89-0015) speed and frequency.
11. Capture slices as they appear using a pair of fine-tipped forceps. It may be necessary to pause the blade movement whilst catching the tissue, as the sections are very small and can be easily moved around by blade movement. Caution: be careful not to damage tissue with the forceps.
12. Place the slices into a dish containing chilled PBS on ice.
13. If not imaging immediately, transfer to culture medium (DMEM, 10% fetal bovine serum, 1% MEM-NEAA, antibiotics/anti-contaminants (100U/ml penicillin, 100ug/ml streptomycin, primocin) and 50uM beta-mercaptoethanol) and place in an incubator at 28 C.
14. When ready to image, place the welled coverslip onto a hot plate at 42 °C and transfer molten LMP agarose to the wells.
15. With a pair of fine-tipped forceps, carefully pick up sections of heart tissue and float on top of the agarose.
16. Remove excess agarose from the well, leaving a thin layer on the bottom.
17. Remove coverslip from hot plate and wait for agarose to solidify (approximately 30s).
18. Cover the wells with culture medium and place microscope slide over the top. Remove excess medium from the sides of the slide.
19. Image the slice every 2 mins 30 sec – 5 mins over 15 h under a confocal microscope. Image multiple focal planes/ areas if possible.

2.16 DIGESTION OF HEARTS FOR SINGLE CELL SUSPENSIONS

The protocol used for the production of single cell suspensions from isolated hearts was broadly adapted from (Cao et al. 2015). Hearts were isolated from fish and placed into cold HBSS. The bulbus arteriosus and atria were then removed and the remaining ventricles cut into at least 4 pieces using surgical scissors. The pieces of ventricle were then collated and placed into the digestion mixture (0.13 U/ml Liberase DH (Roche) and 1% sheep serum in HBSS). Up to 10 hearts could be digested in 1 ml digestion mixture in a 2 ml Eppendorf tube. The digests were then placed into a rotating incubator at 32˚C and 80-100 rpm, to prevent aggregation. The temperature is a compromise between the optimum temperature for zebrafish tissue (28˚C) and the enzyme optimum temperature (37˚C), reducing enzyme efficiency but maintaining cell viability. Every 10-15 minutes, the supernatant was collected and placed on ice and fresh digestion mixture was added to the remaining undigested tissue. The mixture was then pipetted up and down, gently, approximately 5-8 times before being replaced back into the incubator to break up aggregates. Once fully digested (1 hour to 1 hour 30 minutes), all collected suspensions were spun down at 300 g for 10 minutes. The supernatants were removed and HBSS with 1% FBS was added.

2.17 FACS

FAC sorting was performed by Michal Maj and Line Eriksen from the Flow Cytometry facility at the Dunn School of Pathology. It was done using the MoFlo Astrios cell sorter from Beckman Coulter, with gates set to select for Citrine and/or mCherry positive. Dead cells were excluded by selecting for DAPI-negative cells after DAPI addition.

2.18 RNA ISOLATION AND CDNA PREPARATION FROM FAC SORTED CELLS

After FACS, RNA was isolated using the PureLink RNA Micro Scale kit (Invitrogen) according to the manufacturer's instructions for the number of cells to isolate RNA from. The purified RNA was then used to make cDNA using the QuantiTect Whole Transcriptome Kit (Qiagen). The whole transcriptome kit was used as low yields of RNA were isolated from the sorted cells, due to the small numbers of cells isolated. The kit was used according to the manufacturer's instructions and, where possible, the longest incubation/reaction periods were used to enhance cDNA yield.

2.19 qPCR

qPCR was performed cDNA prepared from RNA isolated from FAC sorted cells. The cDNA was used for quantitative real-time PCR using SYBR green and was performed on the Applied Biosystems ViiA 7 Real-Time PCR system and analysed using QuantStudio software. Data were normalised to housekeeping gene eef1a1 and relative expression was then calculated using the $-2\Delta\Delta C_t$ method (Livak & Schmittgen 2001).

2.20 SINGLE CELL SEQUENCING

The single cell sequencing experiment was performed on single cells isolated from uninjured wildtype and 3 dpi injured WT and Runx1 mutant hearts. 20 hearts were pooled per sample and the hearts digested as discussed previously. The single cell suspensions were then sorted via FACs and populations of single and double positive cells were isolated separately. The single and double positive cells were then mixed, so that the samples were 1/3 Citrine positive, 1/3 double positive and 1/3 mCherry positive. These samples were then transferred to the Oxford Genomics Centre at the Wellcome Trust Centre for Human Genetics for processing using the 10X Genomics Chromium system. Once library preparation and sequencing had been completed and compared to the Grzc11 reference genome for zebrafish

(see chapter 5 for more details), the raw data was sent to Xiaonan Wang, in Professor Göttgens group at Cambridge University.

Xiaonan Wang performed the analyses as follows: quality control was performed by removing cells that had fewer than 4000 highly detectable genes and the percentage of these genes that were mitochondrial were less than 0.4. The data were normalised for sequencing depth, or counts of genes, so that after normalisation each cell has a total count equal to the median of total counts before normalisation. The selection of highly variable genes was done using the Seurat method, with min_mean set to 0.0125, max_mean as 4 and min_disp as 0.5. From this 2070 highly variable genes were selected. Noise from the effect of total count per cell and mitochondrial genes were regressed out and the data was scaled to unit variance and zero mean. Louvain clustering was then performed with a resolution of 0.4. Differential expression between populations was analysed for statistical significance using edgeR.

2.21 RNASCOPE

RNAscope (acdbio) was performed according to the manufacturer's instructions. Briefly, paraffin sections were mounted onto slides and left to dry overnight, before being baked at 60°C for an hour. The sections were then deparaffinised in fresh Xylene for 2X 5 minutes and washed in fresh 100% EtOH for 2 minutes, twice. The sections were then air-dried, before the hydrogen peroxide in the kit was added for 10 minutes. The slides were then briefly washed in ddH2O before being placed into the supplied target retrieval solution for 15 mins at 98-102 °C. Following this the slides were thoroughly dried overnight. The next morning the slides were prepared for hybridisation through addition of supplied Protease III. The probes were then mixed, added and amplified according to the manufacturer's instructions, with the slides

being washed in ddH2O in between each step. After the amplification steps, each probe was then developed one by one, with a conjugated-HRP responding to the 'channel' of each probe being added before developers of the correct colour were added. The HRP for the preceding probe was quenched with hydrogen peroxide before the new one was added. These steps were all performed as directed by the manufacturer of the probe. The sequence of the probes used is described in Table A.4.

2.22 AFOG STAINING AND *RUNX1* MUTANT PHENOTYPE ANALYSIS

Acid fuchsin orange g (AFOG) staining was performed as follows. Paraffin sections were mounted onto slides, then deparaffinised and rehydrated as described in the immunohistochemistry section (2. 5). The sections were then placed into distilled water before being placed into Bouin fixative for 3 hours at 60°C, before being left to cool to room temperature. The sections were then washed in distilled water until the yellow colour of the Bouin was not visible to the naked eye. The slides were then rinsed in tap water before being placed in Phosphomolibidic acid for 10 minutes. The slides were then washed in distilled water before being submerged in AFOG for 5 minutes. The slides were then briefly washed in distilled water, before being dehydrated quickly through an alcohol series. The slides are then mounted and cover-slipped using DPX mounting medium.

The analysis of myocardial regeneration was quantified by measuring the perimeter of the ventricle of each heart section of AFOG-stained hearts from *runx1* mutant and WT fish and the length of open compact myocardium. The biggest open myocardium length and ventricle perimeter measurement from each fish was then taken and the open myocardium length was divided by the ventricle perimeter and multiplied by 100 to give the percentage of the myocardium that was still open. Scar area and ventricle area were also measured for each

section and again the biggest measurement of each for each fish was used to calculate the size of the scar. This was done by dividing the scar area by the ventricle size, then multiplying by 100 to give a percentage. This was performed for 5 of each fish type at 3, 7, 14, 30 and 70 dpi and the measurements were analysed for statistically significant variance by 2-way ANOVA.

2.23 PCNA PROLIFERATION ANALYSIS

To analyse the myocardial proliferation in the *runx1* loss of function mutant compared to the wildtype, immunohistochemistry from Mef2, a nuclear myocardial marker, and proliferating cell nuclear antigen (PCNA), a nuclear marker of proliferation, was performed in paraffin sections of 3 dpi injured hearts. The border zone region was established as the cardiomyocytes closest to the wound in the healthy myocardial tissue. The number of Mef2-positive nuclei was then counted and the number of PCNA Mef2 double-positive nuclei counted. The percentage of Mef2 nuclei that were also PCNA was then calculated. This process was repeated for at least 3 sections per fish, for four fish per condition. The average percentage per fish was then calculated and these were compared by an unpaired t-test for statistical significance at $p \leq 0.05$.

2.24 MICROSCOPY

Brightfield microscopy was performed using the Nikon Digital Sight stereo microscope (SMZ1500, Nikon). Fluorescence imaging of fixed paraffin sections was done using either the Leica DM6000 fluorescence microscope or the Olympus FluoView3000 confocal microscope. Time-lapse imaging of the live heart slice cultures was performed using the Zeiss LSM 880 Airy Scan confocal microscope.

2.25 STATISTICS

Statistical differences between groups was calculated using the unpaired t-test, Chi-square test or two-way ANOVA, as indicated by the text in the figure legend. Post hoc tests in ANOVA were performed using Tukey's test. Statistical significance was deemed to be when the P value was less than 0.05. All error bars on graphs represent the standard error of the mean (SEM) *=P<0.05 **=P<0.001.

CHAPTER 3 – IDENTIFYING AN EPICARDIAL PROGENITOR THAT FORMS FAT IN THE FISH HEART

CHAPTER 3 – INTRODUCTION

3.1.1 SUMMARY OF THE CHAPTER

Astyanax mexicanus is a powerful tool that can be used to identify the mechanisms behind the capacity to regenerate lost heart muscle. As this model has never been used to study heart regeneration before, observation of gross morphological differences between the two ecotypes before and after injury were explored. This chapter describes the identification of a cell type, namely adipocytes, that differs markedly between ecotypes. Observations show that the surface fish possess large amounts of epicardial fat on uninjured hearts, whilst the cavefish do not. The regenerative zebrafish more closely resembles the surface fish, with large amounts of epicardial fat. After injury, cavefish and the cryoinjured zebrafish, where scarring is extensive, form fat in the wound site, mirroring humans and adult rodents.

Lineage tracing in the zebrafish identifies a novel mesenchymal progenitor that resides in the epicardium, producing the fat that arises during normal development and after injury. The formation of fat by the epicardium is a novel finding in fish. This chapter also explores attempts to create transgenic *Astyanax mexicanus* fish for lineage tracing using a novel CRISPR approach and explains why it was not used.

3.1.2 BACKGROUND INFORMATION – WHY STUDY CARDIAC FAT?

Fat is found on the hearts of most studied animals, including humans, and has been found to have a profound, if duplicitous, role in outcome after injury. In the adult mouse and in humans, epicardial fat resides in the atrioventricular grooves (Yamaguchi et al. 2015; Liu et

al. 2014) with humans possessing extra fat in the inter-ventricular grooves and around major coronary vessels (Sacks & Fain 2007).

On the one hand, it has been found that increased cardiac fat correlates with improved outcome after myocardial infarction (MI) in humans (Biere et al. 2017; Gohbara et al. 2016). Additionally, fat and adipose tissue-resident progenitors have been found to have a beneficial effect on outcome after MI in multiple animal models (Kim et al. 2016; Bayes-Genis et al. 2013; Nagata et al. 2016). The positive effects have been linked to the contribution of adipose-resident progenitors to the wound and pro-angiogenic paracrine signals from the fat tissue. On the other hand, whilst fat can be beneficial, it can also be a symptom of unsuccessful regeneration. Fat deposition and scarring are common to non-regenerating tissues, including in arrhythmogenic right ventricular cardiomyopathy and after MI in the human heart, and Duchenne muscular dystrophy in skeletal muscle (Farup et al. 2015; Murphy et al. 2010; Goldfarb et al. 2009; Ichikawa et al. 2009). *De novo* cardiac fat formation after injury has also been seen in the non-regenerative mouse heart after MI, with the epicardium as a source (Liu et al. 2014).

Whilst fat has not been explored in the hearts of *A mexicanus* previously, it has been shown that, putatively to aid in energy storage, cavefish possess greater amounts of fat in their bodies generally and that these cells are also larger (Xiong et al. 2018; Aspiras et al. 2015).

Given the importance of cardiac fat in injury outcome and the differences in fat stores between *A mexicanus* ecotypes, a difference in adipocytes on the heart between cavefish and surface fish is an intriguing finding.

3.2 *ASTYANAX* ECOTYPES HAVE DIFFERENT FAT POPULATIONS ON THE HEART

Observing morphological variances between ecotypes of *A. mexicanus* would give an indication of the difference in cell types, and perhaps underlying stem cells, present in the heart. One striking difference, clearly observable to the naked eye when isolating hearts from the fish, is the difference in levels of fat present on the heart.

Laboratory-resident cavefish tend to have a greater fat content within the body in comparison to surface fish and this is thought to be an adaptation to the nutrient-poor conditions in caves (Aspiras et al. 2015). However, this trend appears to be completely reversed when it comes to fat present on the surface of the heart. In general, surface fish hearts tend to have a greater number of fat cells and larger collections of fat than cavefish (Fig. 3.1 A). A semi-quantitative analysis performed on fish hearts isolated at 6 months and 30 months of age, where hearts were grouped into categories based on the estimated number of adipocytes, shows that all cavefish studied, regardless of age, have 100 or fewer fat cells, whilst for the surface fish just over half have 200+ and all but one have 100+ (Fig. 3.1 B). Despite the contrast in amounts of fat, the distribution of adipose tissue in the fish was not dissimilar, with the greatest concentrations of fat found between the bulbus arteriosus and the ventricle, and the atrium and the ventricle (Fig. 3.1 A) (this work has been reported in Tang et al. 2018). This is not a dissimilar location to epicardial adipose tissue found in mice, which sits in the groove between the atrial and ventricular chambers (Yamaguchi et al. 2015).

In addition to the differences in amount of fat, the nature of the fat cells appears to be distinctive in the fish. In line with recently published data suggesting that cavefish fat cells are

hypertrophic (Xiong et al. 2018), cavefish heart fat cells seem to be larger, whilst the surface fish fat cells are smaller and more compact (fig 3.1 A, arrowheads indicate the outlines of individual fat cells). These observations suggest a fundamental difference in the formation of adipose tissue in the two fish, both in the number of cells formed and the morphology of those cells. For an unknown reason, fat progenitors in cavefish form fewer fat cells than in the surface fish, but these cells seem driven to store much more per cell.

As these results suggest differential activity of a fat progenitor during homeostasis, it was decided that fat formation after injury should be investigated to discern if similar differences apply.

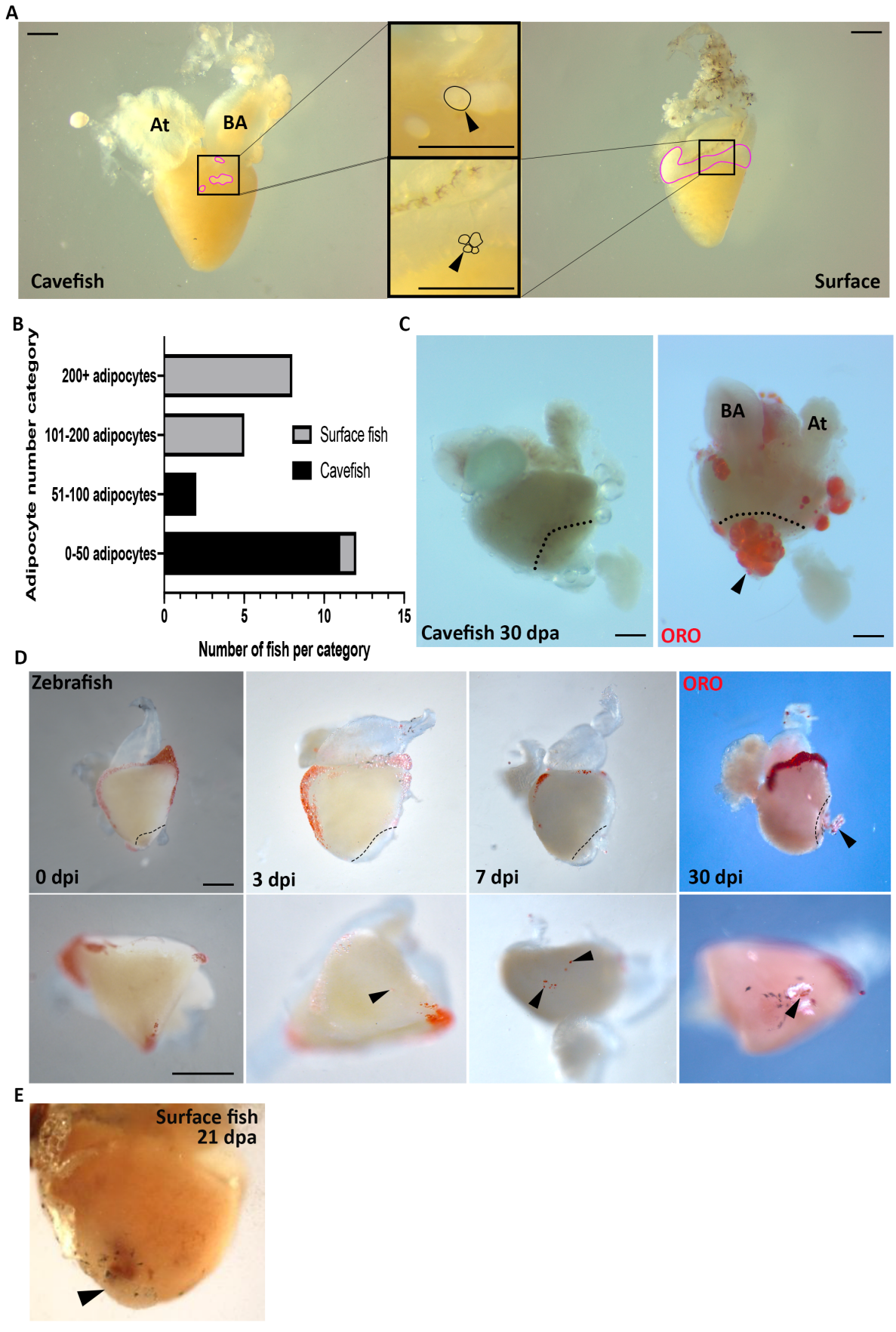


Fig. 3.1 Fat levels in *A mexicanus* differ between ecotype before and after injury. The zebrafish shows

trends of both. **A** shows images of whole hearts isolate from cavefish and surface fish and zooms in on areas of fat, N≥6. N.B. surface fish heart is smaller by chance and does not show average surface fish heart size, the image was chosen as the clearest and most indicative of general fat levels. Pink lines outline the fat areas and in the magnified boxes, the fat cells are outlined in black, indicated by arrowheads. **B** is a chart showing the differences in numbers of adipocytes on the hearts of the two ecotypes, N≥6. Chi-square test P value <0.001. **C** shows a cavefish heart after injury. ORO=oil red O, a lipid stain. **D** shows zebrafish hearts at set time points after injury. Top panel shows overview of the zebrafish hearts at the time points, bottom panel is a view of the injury on the apex, black arrowheads indicate Oil Red O positive cells. **E** shows a surface fish heart after apical resection, arrowhead indicates wound site and lack of fat cells. N=4. All scale bars indicate 100 µm.

3.3 CAVEFISH AND ZEBRAFISH FORM FAT ON THEIR HEARTS AFTER INJURY

As the previous results show that fat deposition is fundamentally different in the ecotypes and with the literature demonstrating the importance of fat in the wound response, the difference in fat formation after injury was explored.

Observations of whole-mount images of isolated hearts indicate that *A mexicanus* ecotypes show a disparity in their fat formation after injury by apical resection, but in reverse to the difference seen in uninjured hearts. On the site of injury in the cavefish, many exceptionally large, fluid-filled cells are formed (Fig. 3.1 C, left panel). Oil Red O lipid stains of cavefish hearts isolated 30 days after injury by apical resection were performed to confirm that these are indeed lipid filled cells (Fig. 3.1 C, right panel). Oil Red O is a basic lipid stain that labels all fat red. The surface fish by comparison does not form these cells (Fig. 3.1 E) and so Oil Red O staining was not performed to save valuable fish for other experiments. The response after injury, therefore, is a reverse to the uninjured situation, where the surface fish have more fat

present on the heart, in comparison to the cavefish. The only similarity that remains to the pre-injury heart is that the cavefish again produces very large fat cells after injury.

The formation of fat was also explored in zebrafish, as there was a limited supply of *A mexicanus* fish for further study, whilst zebrafish have a rapid generational time and many transgenic lines are readily available. In uninjured hearts, the zebrafish appears to mirror its fellow regenerative, the surface fish. It likewise has large aggregates of small fat cells present in the grooves between the bulbus arteriosus, atrium and ventricle (Fig. 3.1 D). However, after injury, it behaves more like cavefish, with the formation of fat on the wound site seen. This is perhaps unusual, as it could be expected to follow the surface fish, as both can regenerate after cardiac injury. The appearance of fat after injury in both the regenerative zebrafish and non-regenerative cavefish could be due to a change in injury type, with the surgeries in *A. mexicanus* performed via apical resection and those in the zebrafish via cryoinjury. It is well understood that cryo-injury produces a greater scarring response than in apical resection, in a manner that more follows non-regenerative mammalian MI and also the cavefish response (González-Rosa et al. 2011; Chablais et al. 2011). This fat deposition begins with a few, very small cells at 3 dpi, that appear to gradually increase in size until around 7 dpi (Fig. 3.1 D). However, it produces them in much smaller numbers than the cavefish and they do not reach the same large cell size. At 30 dpi, they are still present but appear to be removed from the wound surface, now present in scar tissue that is hanging off the heart. As myocardial overgrowth is achieved and the compact wall becomes contiguous once again, this scar tissue is presumably resolved or extruded, and the fat along with it.

As fat is formed after injury in both the cavefish and, to a lesser extent, the zebrafish, it appears that the fish heart contains a mesenchymal progenitor that responds to injury in an

environmentally-sensitive manner. Where extensive scar formation is present, such as in the cavefish and cryo-injured zebrafish, it can form fat, whereas in the surface fish it does not. It also appears to form less fat in a regenerative environment like the zebrafish than it does in the cavefish. Such an injury-responsive progenitor could play a role in the ability to regenerate the heart. Given this suggestion, the next step was to investigate this progenitor, to discern its identity and location and analyse its activity after injury.

3.4 POTENTIAL ORIGINS OF DEVELOPMENTAL AND INJURY-RELATED FAT

The existence of an injury-sensitive fat progenitor in the fish heart has not previously been posited or investigated. Given the different amounts of fat depending on the experimental model, it is interesting to speculate that this progenitor contributes negatively to the regenerative environment. Clearing large amounts of large, lipid filled cells from the wound would likely take a long time – meaning that reducing adipogenesis from this progenitor could aid regeneration.

Studies looking at the origins of epicardial fat in the mouse both developmentally and after injury have identified the epicardium as a source (Liu et al. 2014; Yamaguchi et al. 2015). During both development and after injury, a subpopulation of the epicardium undergoes EMT, forming mesenchymal progenitors that give rise to fatty tissue deposited either into the atrio-ventricular grooves or around the wound. The same process is also one of the likely methods of production of myofibroblasts that contribute to fibrosis (Gonzalez-Rosa et al. 2012; Talman & Ruskoaho 2016), therefore it seems that the epicardium produces both fibrogenic and adipogenic progenitors after injury. Fibro-adipogenic mesenchymal progenitors that play a role in injury response are not unheard of; they have long been recognised in skeletal muscle. These progenitors can aid new muscle growth in regenerative

environments (healthy muscle) and form fatty-fibrotic scar tissue in non-regenerative settings (diseased muscle) (Joe et al. 2010; Uezumi et al. 2010). They do this by either controlling the correct proliferation and differentiation of muscle stem cells, or themselves proliferating and then differentiating into fatty-fibrotic scar tissue, respectively. Progenitors showing this type of activity have been found in multiple muscle tissues and have multiple origins (Paylor et al. 2014; Stuelsatz et al. 2014). Their activities are thought to be regulated by inflammatory cues and Notch signalling, mediated primarily by immune cells and the activity of these cells is necessary for skeletal muscle regeneration (Marinkovic et al. 2017; Fiore et al. 2016).

Another option is that these lipid-filled cells are not adipocytes, but macrophages. In mammals, foam cells are a malfunctioning type of macrophage that arise in areas of atherosclerosis, formed from monocytes attracted to the lipid rich area that differentiate into macrophages capable of taking up toxically-modified lipoproteins (Maguire et al. 2018). This is nominally a helpful process done to remove harmful lipids, where the lipid is taken up, rendered less harmful and effluxed. However, foam cells are cells where this process has gone awry and they maintain increasing lipid levels within. The attraction of monocytes to these areas is due to signals released by damaged endothelial cells, including IL-8, which are likely similar signals to those released after cardiac injury (Maguire et al. 2018). Zebrafish are capable of producing foam cells in a manner similar to mammals (Johansen et al. 2018; Miller et al. 2009) and so if modified lipids are found in the cardiac wound, then it is possible that macrophages could form foam cells after injury. The lipid modifications necessary could be made by free radicals and reactive oxygen species, glycoxidation and perhaps free metal ions, such as iron (Hamilton 1997).

Therefore, it could be that the epicardium of the fish contains a mesenchymal fibro-adipogenic progenitor that forms fat and fibroblasts during development and also after injury, where it produces its progeny to a different extent depending on the regenerative environment. If this progenitor behaves as similar populations do in skeletal muscle, it could also aid regeneration in regenerative environments through stimulation of myocyte proliferation.

3.5 INVESTIGATING EPICARDIAL MESENCHYMAL PROGENITORS IN THE FISH HEART

Identifying mesenchymal stem cells in the fish heart required use of a cell type specific marker. Mesenchymal stem cells have been well studied in mammalian biology and cell surface markers for this population are well established. One of the most frequently used is platelet-derived growth factor receptor alpha (Pdgfrα), a cell-surface receptor that has been used to isolate defined MSCs from murine and human tissues (Farahani & Xaymardan 2015a). It is also the marker used to identify fibro-adipogenic progenitors in mammalian muscle (Joe et al. 2010; Uezumi et al. 2010). Therefore, Pdgfrα is a good marker to use to locate mesenchymal fibro-adipogenic progenitors in the fish heart. However little is currently known about its expression in this system and how restricted to MSCs the marker is in teleost fish. Analysis of known expression patterns in mammalian systems, and other better studied higher vertebrates, gives an indication of expected expression in *A. mexicanus*.

During development in many higher vertebrates, Pdgfrα is found in most cells until gastrulation, where it becomes largely restricted to the mesoderm and some mesenchymal neural crest-derived cells. In adult mammalian tissue, including the heart, Pdgfrα expression is not limited to MSCs, being expressed in perivascular stromal cells, fibroblasts and smooth muscle, with only a subsection of these cells displaying MSC characteristics (Chong et al.

2011). Mammalian Pdgfrα-positive progenitor populations have been identified in multiple tissues, including bone marrow, skin, skeletal muscle and, importantly, the heart (Chong et al. 2013; Paylor et al. 2014; Noseda et al. 2015; Farahani & Xaymardan 2015b; Joe et al. 2010; Uezumi et al. 2010). Sca1/Pdgfrα double-positive cells with vascular and cardiogenic potential have been isolated from mammalian hearts and Pdgfrα-positive fibroblast smooth muscle progenitors are formed when the epicardium undergoes EMT during development (Noseda et al. 2015; Chong et al. 2011). Therefore, in fish hearts it seems likely to expect Pdgfrα-positive cells to be fibroblast, smooth muscle or epicardial in nature and have a broad range of potency. As the epicardium in mouse has been shown to be the source of epicardial fat produced during development and after injury, it is more probable that epicardial Pdgfrα-positive cells are the population of interest.

3.5.1 EXPRESSION OF PDGFRα IN *A. MEXICANUS* HEARTS

To look for mesenchymal stem cells in the fish heart, immunohistochemistry for Pdgfrα was performed in fixed sections of both ecotypes. Images of Pdgfrα expression in *A mexicanus* show relatively broad presence of Pdgfrα throughout the heart (Fig. 3.2). Surprisingly, it is found in cells residing around the edges of the trabecular myocardium that resemble endocardial cells, which is a novel expression pattern that appears to be restricted to fish, as it has not been reported in the mammalian literature (Fig. 3.2 white arrowheads in magnified boxes in upper panel).

In both the surface and the cavefish, Pdgfrα expression is found in cells surrounding vessels. These cells are particularly visible in the vessels running through the compact myocardium (Fig. 3.2 yellow arrowheads) and appear to fully or partially enclose the vessel. This closely follows the Pdgfrα-positive perivascular stromal cells seen in mammals and, more specifically,

the Pdgfrα-positive smooth muscle and fibroblast cells previously identified in the mammalian heart (Bax et al. 2010; Zhou et al. 2015; Chong et al. 2013; Chen et al. 2015; Bax et al. 2011) Likewise, expression of Pdgfrα is seen in the epicardial region of both ecotypes, suggesting the presence of Pdgfrα-positive epicardial cells (Fig. 3.2 lower panel, white arrowheads). Strong expression is also seen in the valves (Fig. 3.2 magenta arrowheads).

In conclusion, Pdgfrα expression in the fish heart is more widespread than in the mammalian heart, with expected expression around vessels and in the epicardium, but with added expression around the endocardium. There also appears to be no significant difference in the patterns of expression between the two ecotypes.

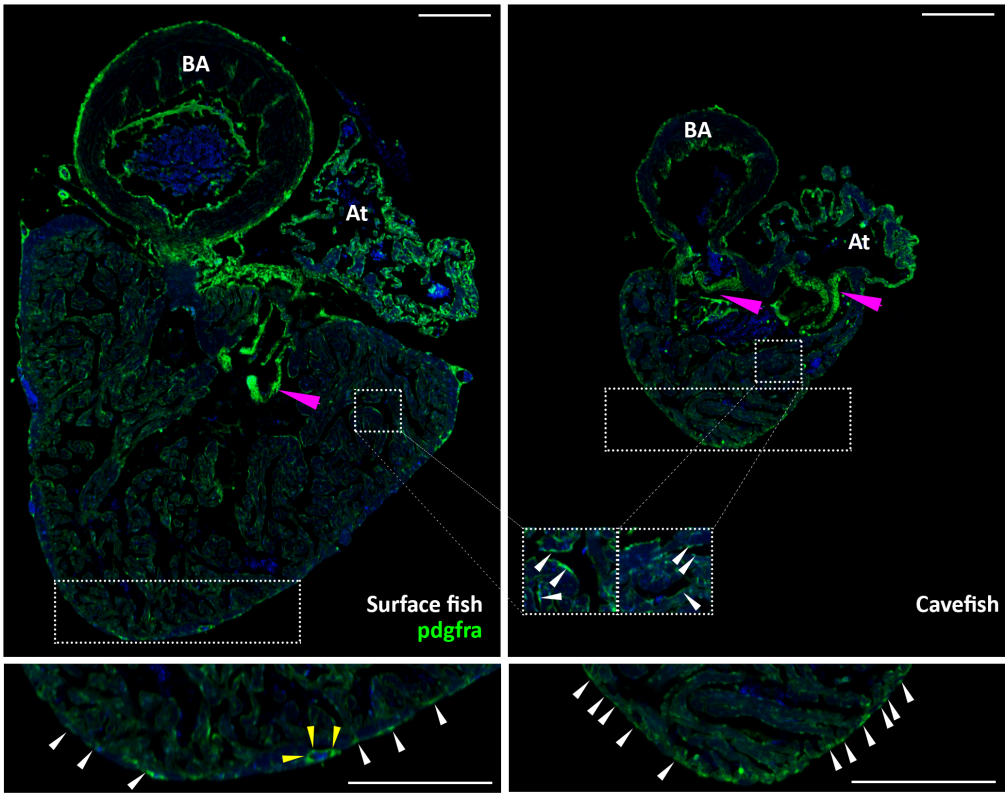


Fig. 3.2 An overview of Pdgfrα expression in uninjured *A mexicanus* ecotypes. Upper panel: magenta arrowheads indicate the valves and white arrowheads in magnified panel indicate endocardial-type

cells. Lower panel: white arrowheads indicate epicardial Pdgfrα-positive cells, yellow arrowheads indicate Pdgfrα-positive perivascular cells. N=3. The DAPI nuclear stain is in blue. Scale bar = 100 µm.

3.5.2 EXPRESSION OF PDGFRα IN THE EPICARDIUM

As epicardial cells are likely the origin of the injury-responsive progenitor cells responsible for fat formation after injury and during development, further analysis of the epicardial Pdgfrα-positive population was performed through immunohistochemistry for other markers. Staining using the Wt1 antibody, an established epicardial marker, shows that Pdgfrα expression is within the same cells as those expressing Wt1 in *A. mexicanus* (Fig. 3.3). Wt1 is a transcription factor that is expressed in epicardial cells and is highly upregulated in the epicardium during development and after injury in mammals and fish, where it plays a role in regulating EMT (Bax et al. 2010; Bax et al. 2011; Ceci et al. 2018). In adult mammals, its expression is restricted to approximately 25% of the epicardium (Zhou et al. 2011). Co-expression of Pdgfrα and an injury-responsive transcription factor involved in regulating EMT, suggests that cells with the potential to become mesenchymal progenitors could reside in the epicardium.

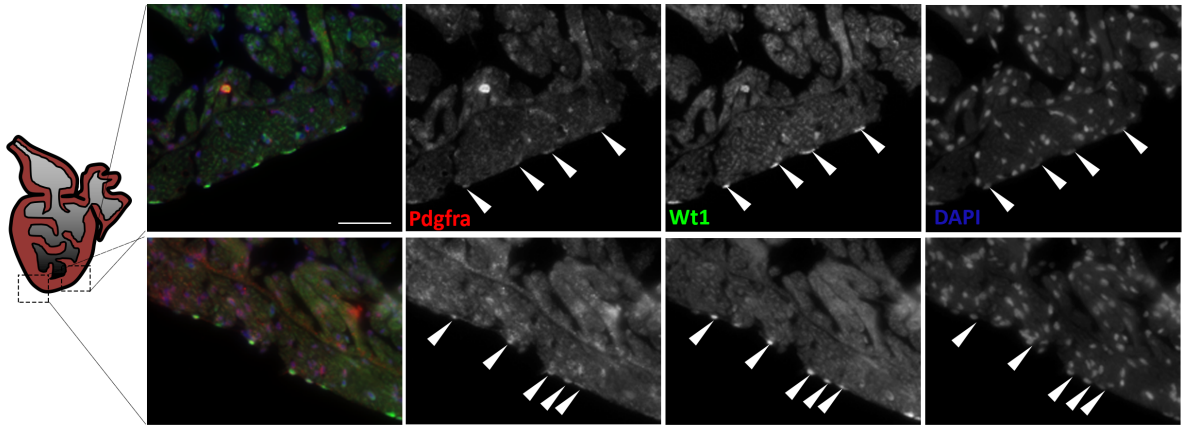


Fig. 3.3 Co-expression of Pdgfrα and Wt1 in the epicardium of uninjured *A. mexicanus* hearts. Boxes on the heart schematic shows the approximate regions of the images. Arrowheads indicate double-positive cells. N=3. Scale bar indicates 10 µm.

Wt1 is highly upregulated after injury in the zebrafish, with many epicardial cells switching on Wt1 as they begin to undergo EMT (Peralta et al. 2014). Therefore, the co-expression of Wt1 and Pdgfrα in injured *Astyanax* hearts was analysed at two time-points after injury by apical resection, to see if epicardial cells continue to express both markers and, if so, to investigate where these cells reside within the wound tissue.

Immunohistochemistry of Wt1 and Pdgfrα at 3 dpa, before the formation of the collagen scar, shows no double-positive cells within the blood clot at the site of injury, indicating that Pdgfrα-positive epicardial cells have not migrated there (Fig. 3.4, left hand side of the magnified panels for both fish). Double-positive cells are found, however, in the area adjacent to damaged heart tissue at the approximate position of the regenerating epicardium (Fig. 3.4 white arrowheads). There appears to be much more Pdgfrα staining in the wound site of the surface fish compared to the cavefish at this time-point, but the levels of double positive cells appear to be broadly similar, with no striking differences observed. The bright expression of Pdgfrα in the blood clot of the wound in the surface fish is likely to be expression in thrombocytes. The differences in other non-epicardial or Wt1-positive Pdgfrα cells will be discussed in Chapter 4.

Double-positive cells are also found away from the wound, indicating either migratory epicardial cells or another, unknown cell-type that is Wt1 and Pdgfrα-positive (Fig. 3.5 arrowheads). Images of Pdgfrα and Wt1 expression in injured fish at 7 days after apical resection show extensive presence of Wt1 and Pdgfrα within cells in and around the wound.

In both surface and cavefish, Wt1 Pdgfrα double-positive cells are present in the regenerating area next to the scar tissue, the border zone, with lots of clusters of aggregated, rounded double-positive cells (Fig. 3.5 A arrowheads). These rounded cells that are Pdgfrα and Wt1 positive could be migrating epicardial progenitors that have undergone EMT, or be another previously unidentified cell type. Some of the double-positive cells appear to be in the blood, which was unexpected. Wt1 is expressed in hematopoietic progenitor cells, so it seems likely that these cells are hematopoietic progenitors (Svedberg et al. 2001). However, hematopoietic progenitors expressing Pdgfrα have not been reported or characterised previously.

Pdgfrα appears to have slightly different expression patterns between the two fish at 7 dpa, like at 3 dpa. At this time point, both fish possess double-positive cells in the epicardium away from the wound, but in the wound Pdgfrα expression in the surface fish is much more distinct, with extensive expression in the border zone (BZ) of the wound, where the regenerating myocardium meets the wound tissue. In the cavefish, Pdgfrα is less spatially restricted and expressed to a lesser extent in the BZ.

Cavefish expression of Pdgfrα at 7 dpa extends further into the scar tissue, with lots of staining visible within the scar. In both fish, but more so in the cavefish, there are lots of double-positive cells present within the collagen scar tissue, with a more elongated, spindle-like fibroblast morphology (Fig. 3.5 arrowheads). The double-positive cells with a spindle-shaped morphology embedded within the collagen scar tissue, seem likely to be a product of these regenerating epicardial cells that have undergone EMT. It is likely they have formed fibroblasts that produce the collagen scar, giving the heart structure whilst it undergoes regeneration or repair, dependent on the ecotype. If correct, this follows the finding in

mammalian hearts that Pdgfrα is required for the formation of fibroblasts from epicardium during EMT (Smith et al. 2011). These results are, therefore, suggestive of a Pdgfrα-positive progenitor cell resident in the epicardium that is responsive to injury in both ecotypes.

Fig. 3.4

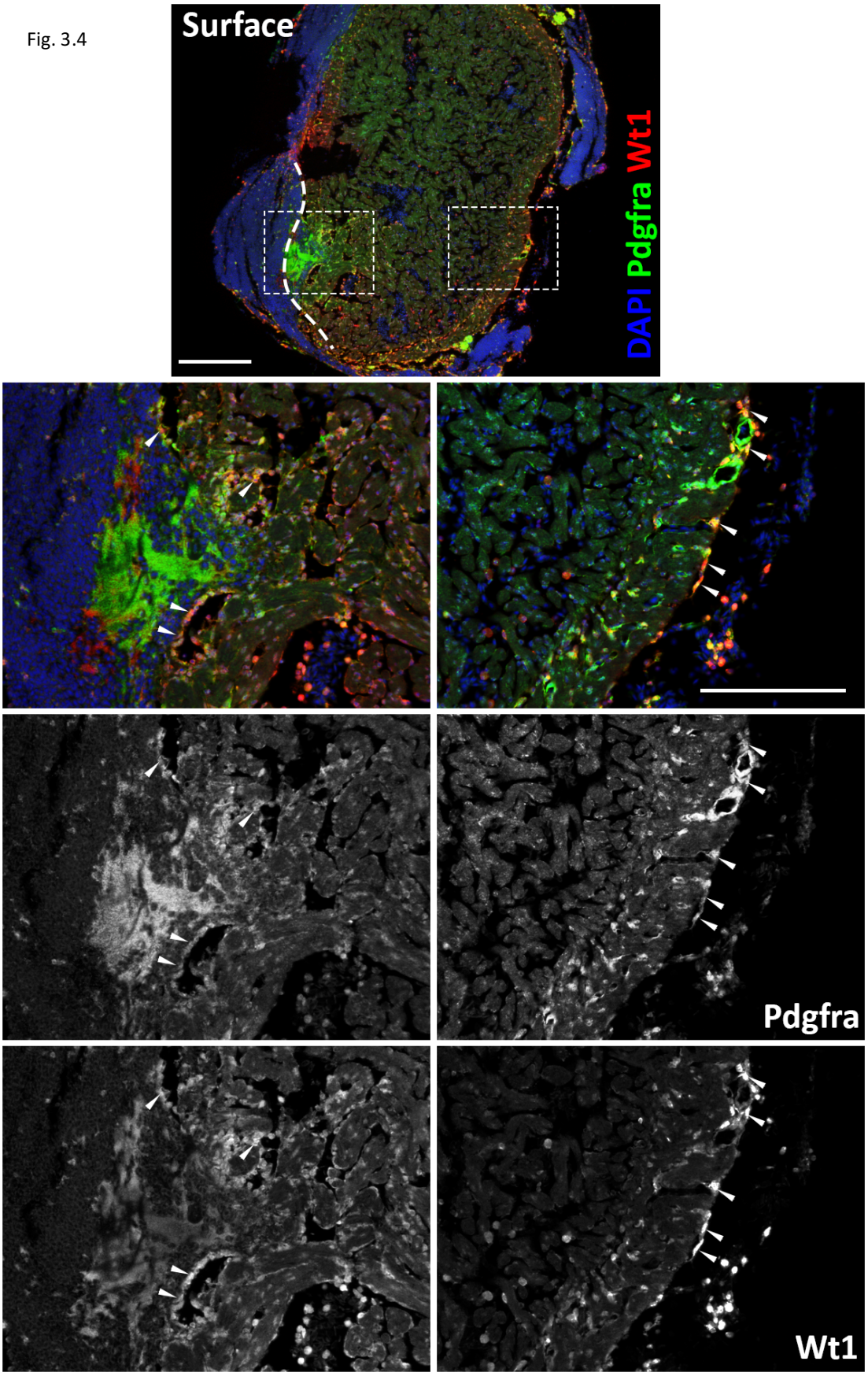


Fig. 3.4

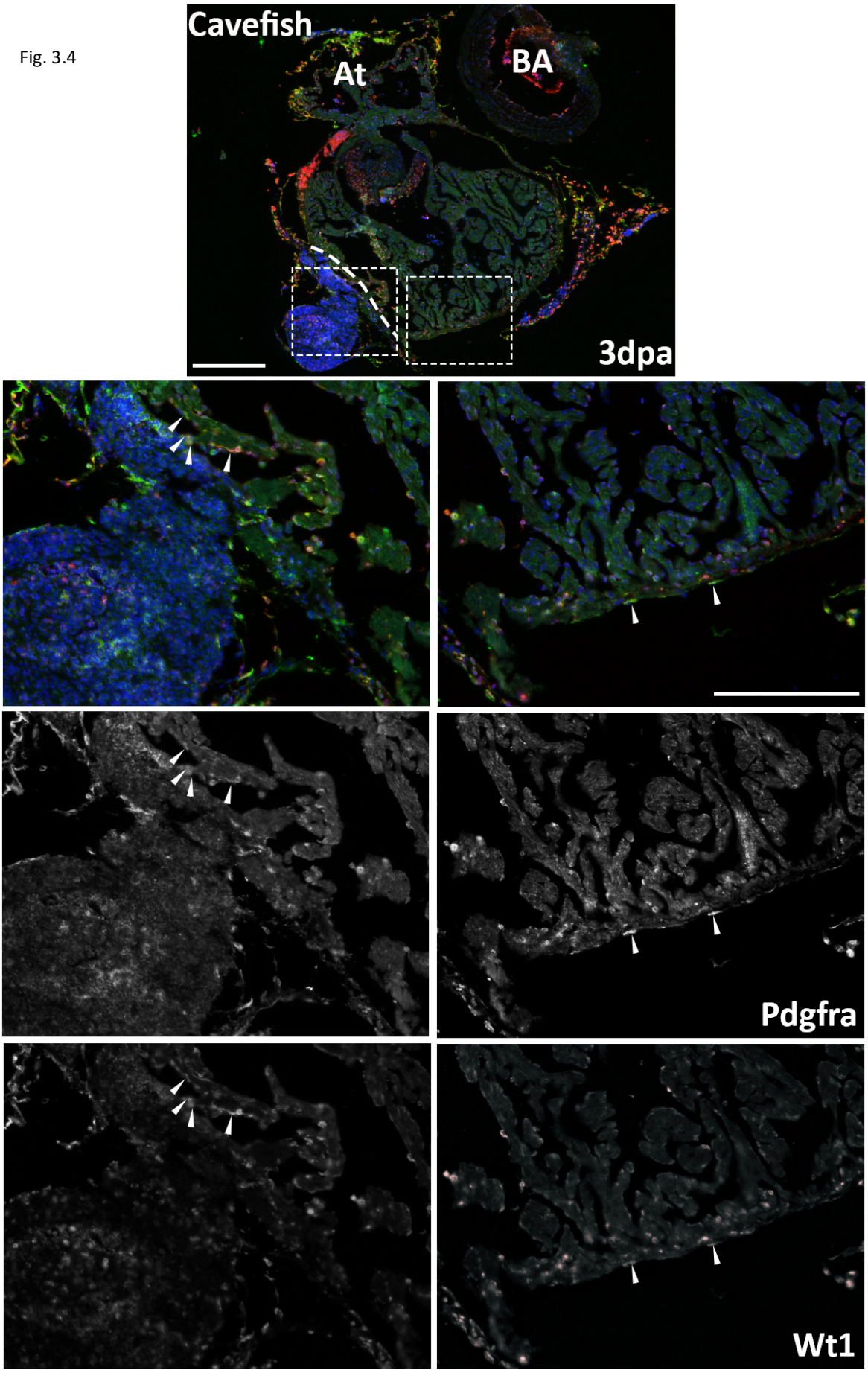


Fig. 3.4 Co-expression of Wt1 and Pdgfrα in *A. mexicanus* ecotypes 3 days after injury by apical resection. White arrowheads indicate co-expressing cells. Dashed line indicates approximate level of resection, dotted boxes indicate magnified areas in the panels below. The left hand magnified panels show the blood clot (marked by contiguous DAPI staining), the right panel indicates the epicardium with double-stained cells. N=3. Scale bar indicates 100 μm.

Fig. 3.5

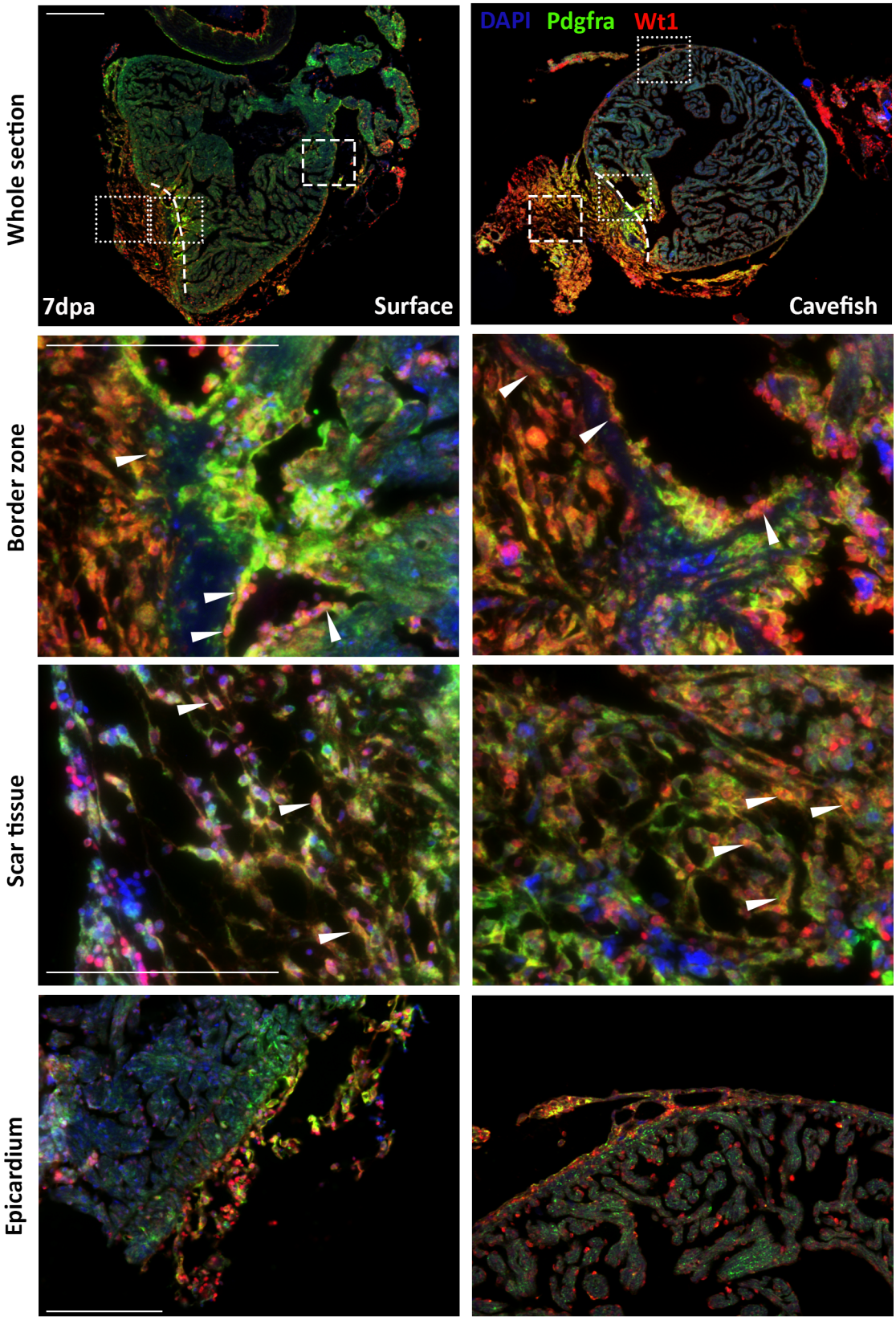

Whole section
Border zone
Scar tissue
Epicardium
7dpa
Surface
DAPI
Pdgfra
Wt1
Cavefish

Fig. 3.5 Co-expression of Wt1 in *A. mexicanus* ecotypes 7 days after injury by apical resection in areas of the heart and wound tissue. Dotted boxes show magnified regions of the top panels shown in the panels below, dashed boxes show approximate regions of the magnified boxes below, where representative images of magnified areas have been taken from other sections than the two shown in the upper panel. Arrowheads indicate double-positive cells. Dotted line indicates approximate level of apical resection. N=3. Scale bar denotes 100 µm.

3.5.3 EXPRESSION OF PDGFRα IN SCAR TISSUE

As the previous data indicates that there are many Pdgfrα-positive cells resident within the scar tissue, immunohistochemistry for collagen1, a major ECM component of the scar was performed on fish at 7 dpa, along with immunohistochemistry. This was done to allow better comparison of Pdgfrα-positive scar-based cells through analysis of their distribution and orientation within the scar.

In both fish ecotypes, Pdgfrα-positive cells of morphology consistent with fibroblasts are found lying along and surrounded by collagen fibres in the scar (Fig. 3.6 E-H, arrowheads in E, F). Additionally, there are clusters of Pdgfrα-positive cells in the scar tissue nearest the wound site, but in the cavefish the Pdgfrα-positive cells are spread throughout the scar tissue, whilst in the surface fish they are more restricted to the peri-wound area (Fig. 3.6 E-H). The peri-wound area scar-tissue Pdgfrα-positive cells appear to be similar, but the number of cells in the border zone appear by eye to be increased in the surface fish.

In the surface fish, the collagen mesh appears to be more densely packed throughout the scar, whereas in the cavefish the collagen mesh is much more spread out and disorganised-looking away from the wound area (Fig. 3.6 G-H).

In the surface fish and cavefish, Pdgfrα-positive cells are associated with areas that look to be consistent with fat tissue. The nature of the tissue processing for immunohistochemistry removes the fat, however, the round holes left in their place are identifiable. In the surface fish, where fat is normally found in the grooves between the bulbus arteriousus and the ventricle, Pdgfrα-positive cells are in close approximation to the holes left by the fat tissue. In the cavefish scar, large round spaces, potentially occupied by large wound fat cells, are surrounded by collagen scar and also surrounded by Pdgfrα-positive staining (Fig. 3.6 J, arrowheads). In the surface fish, Pdgfrα-positive cells are also present around the presumptive fat, but to a lesser extent (Fig. 3.6 I, arrowhead).

The finding of Pdgfrα-positive cells enmeshed within both the collagen scar tissue and in close approximation to areas of fat, whilst not conclusive, is indicative of Pdgfrα-positive cells being involved in the formation of fatty fibrotic scar tissue. There are some differences in the distribution of Pdgfrα-positive cells within the scar tissue between the two fish, indicating that Pdgfrα-positive cells might play a role in the difference in regenerative capacity between the two fish.

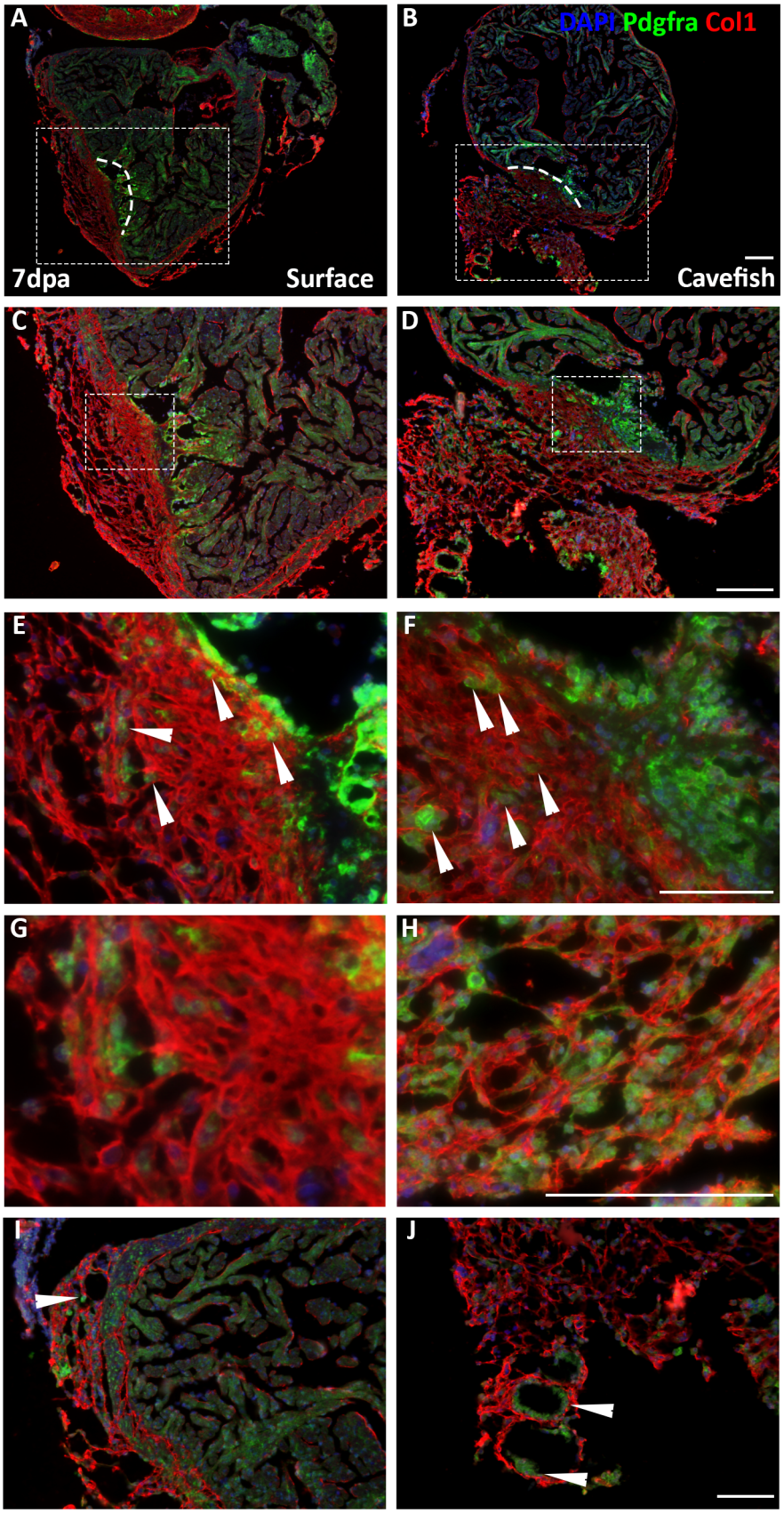


Fig. 3.6 Immunohistochemistry for Pdgfrα and Col1 in *A. mexicanus* at 7 dpa. **A** – **D** show overviews of expression patters in the whole and large regions of the heart and scar tissue. **E-H** shows the wound tissue in detail, arrowheads indicate Pdgfrα-positive cells surrounded by collagen. **I** and **J** show Pdgfrα-positive cells (arrowheads) in areas of fat formation, the wound in the cavefish (**J**) and the edge nearest the bulbus arteriosus in the surface fish (**I**). N=3. Scale bar indicates 50 µm.

3.5.4 INVESTIGATING PDGFRβ AS A MESENCHYMAL STEM CELL MARKER

Pdgfrβ is closely related to Pdgfrα and has been studied relatively extensively as a pre-adipocyte marker through its expression in pericytes, the adipocyte progenitors present in skeletal muscle and adipose tissue (Kim et al. 2017; Gao et al. 2018; Birbrair et al. 2013; Vishvanath et al. 2016). In addition, Pdgfrβ has been shown to be upregulated in the epicardium and wound of zebrafish hearts after apical resection (Kim et al. 2010). Consequently, Pdgfrβ expression in *Astyanax mexicanus* was also explored.

Analysis of its expression pattern at 7 dpa by immunohistochemistry showed that it is much more broadly expressed than Pdgfrα (Fig. 3.7). It is found strongly lining the trabeculae in both fish, to a greater extent than Pdgfrα. In the cavefish, it appears to be expressed in the wound, though at low levels, whilst in the surface fish it appears to be absent from the wound area. It is present in the scar tissue of both fish, but more so in the surface fish. It appears that Pdgfrα and β have very different expression patterns. Given that the fat seen after injury is found in areas that are here shown to be much more Pdgfrα-positive, namely the scar area of the cavefish, Pdgfrα was pursued as a marker.

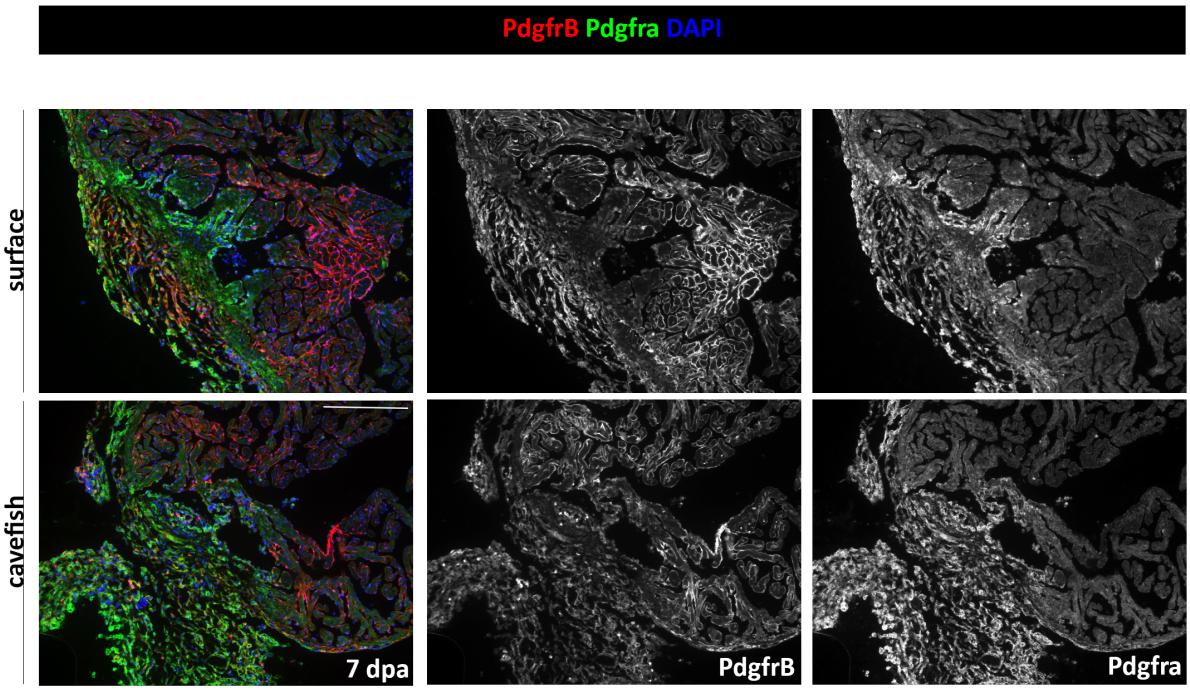


Fig. 3.7 Figure showing Pdgfrβ expression in *A mexicanus* ecotypes at 7 dpa compared to Pdgfrα. Scale bar shows 100 µm. N=3.

3.6 DEVELOPING NOVEL FISH LINES TO INVESTIGATE PDGFRα-POSITIVE POPULATIONS IN INJURY RESPONSE

The immunohistochemistry data suggests that Pdgfrα-positive cells reside within the epicardium and form a considerable number of the scar-based cells after injury. These cells are in close apposition to the collagen scar and fat tissue, presenting the interesting possibility that Pdgfrα-positive cells form both fat and fibroblasts after injury. To test this further, a strategy to create transgenic fish lines that allow fluorescent and lineage labelling of cells, as well as their specific destruction was devised. Pdgfrα lineage tracing using inducible Cre-lox technology offers the ability to mark Pdgfrα-positive cells before cardiac injury is performed, allowing the progeny of Pdgfrα-positive cells created during the injury response to be tracked, thus indicating the *in vivo* potential of the Pdgfrα-positive pluripotent cells and a putative role in the regenerative response. When tamoxifen is added, the Cre recombinase becomes

activated and induces recombination between a pair of loxP sites, allowing expression of a fluorescent marker in cells where recombination has taken place, for example. This change is passed down to subsequent progeny. The use of tamoxifen means this recombination can be used to mark a certain population of cells at a certain time, to distinguish developmental from injury-related progeny for example. The use of a diphtheria-toxin A line, where Cre activation causes expression of this toxin and subsequent cell death, allows specific destruction of Pdgfrα cells. Pdgfrα marker lines allow isolation of these cells for further functional analysis, for example isolation by fluorescence activated cell sorting (FACS) for culture. However, no such lines exist in the Mexican cavefish, where very few transgenic lines have been reported. The same is true in the zebrafish, despite the large number of transgenic lines available. Therefore, a strategy for developing novel transgenic *pdgfrα:creERT2* and *pdgfrα:mCherry* lines was created, with the aim of allowing lineage tracing and marking of Pdgfrα-positive cells in both *A. mexicanus* and zebrafish.

The most common method for fish transgenesis, and longest established, involves the use of I-SceI meganuclease or Tol2/Sleeping beauty transposon system, where the desired component (fluorescent marker, Cre etc.) is placed under the regulatory elements of the desired gene in a donor vector. The donor vector is often a bacterial artificial chromosome (BAC), as it has a large enough capacity to incorporate long range regulatory elements (Suster et al. 2011). The desired region of the BAC with the reporter gene is then transferred randomly into the fish genome, allowing expression of the inserted element in cells that endogenously express the gene of interest (Rafferty & Quinn 2018). However, whilst there exists a comprehensive BAC library for the zebrafish, the same is not true for the Mexican cavefish. As a direct comparison of the activity of Pdgfrα-positive cells between the surface

and cavefish was highly desirable, the creation of these lines in both ecotypes of *Astyanax mexicanus* as well as zebrafish was necessary. To this end, a strategy was devised that enabled easy cross-over between the types of fish with minimal change to the reagents and techniques used.

Whilst there may not be a BAC library or much known about regulatory elements for most genes in *A. mexicanus*, the genome of the Pachón cavefish ecotype had just been sequenced and available online at the time the strategy was designed. This therefore allowed use of genome editing technologies to create the desired transgenic fish, with the aim of adding reporter/Cre gene sequences directly into the genome and therefore under the control of endogenous regulatory elements. This is achieved by inducing double-stranded breaks in specific regions of the genome, into which an exogenous DNA sequence can be inserted. This can be done in one of three ways: homology directed repair (HDR), non-homologous end joining (NHEJ) or micro-homology mediated end joining (MMEJ) (For good reviews of genome editing techniques see Rafferty & Quinn 2018; Morita et al. 2017). HDR involves adding long sequences of DNA to either end of the sequence for insertion, which are homologous to the sequences at the site of the DSB. In this manner, exogenous sequences can be added accurately into the genome (Irion et al. 2014). NHEJ involves incorporation of inserted DNA into the genome by repair machinery simply joining the end of the genomic break to that of the exogenous sequence. This type of repair may induce insertion/deletion mutations into the break site, leading to mosaicism of the mutation. However, it does not require homologous arms, therefore allowing the donor DNA vector to be used for multiple break sites and in different species (Auer et al. 2014; Kimura et al. 2014). This is, therefore, ideal for the creation of multiple zebrafish and A. mexicanus fish lines. MMEJ involves the use of short

homology arms that are much easier to produce than the long arms required for HDR, but provide a similar accuracy in the type of mutation produced (Nakade et al. 2014; Hisano et al. 2015; Morita et al. 2017). However, with the genome of the surface fish still unknown at this point, generation of micro-homologous arms was difficult, due to the potential differences between the cavefish and surface genome. However, analysis suggests that homology between the two is very high.

In recent years, two main methods for creating breaks at targeted genomic loci have emerged - Clustered Regularly Interspaced Short Palindromic Repeats (CRISPR) and Transcription Activator-Like Effector Nuclease (TALEN). Both allow precise targeting of genomic regions and have been used previously to generate knock-in transgenic zebrafish and mutant *A. mexicanus* (Hwang et al. 2013; Kimura et al. 2014; Klaassen et al. 2018; Ma et al. 2015; Shin et al. 2014).

TALENs consist of a TALE domain, which is the part that can be engineered to recognise genomic DNA sequences, attached to a FokI nuclease. The TALE domain is formed from DNA recognition motifs, or units, of amino acid sequences that recognise specific nucleic acids. These units can be combined in any order to recognise genomic sequences, where they bind and dimerise with TALENs recognising the same region on the other strand and cut the genome, inducing a double-strand break (Bedell et al. 2012; Bitinaite et al. 1998; Boch et al. 2009; Moscou & Bogdanove 2009). This technology can be targeted to any region on the genome, with no specific DNA sequences required for activation of the FokI nuclease. This means TALENs are highly flexible in terms of targeting, as opposed to other gene editing technologies. This technology does have slight disadvantages, however, in ease of

preparation. The DNA recognition motifs are amino acid based, making them much harder to engineer than other methods.

CRISPR technology emerged in the early 2010s as a method to induce targeted breaks in genomic DNA (Cong et al. 2013; Mali et al. 2013; Cho et al. 2013; Jinek et al. 2012). It takes advantage of the prokaryotic immune system, where specific nucleases recognise and cut exogenous DNA acquired from viral infection (Hille & Charpentier 2016). The enzyme most commonly used for genome editing is an engineered form of an enzyme called Cas9 and it is guided to induce a double stranded break at a particular point in the genome by a synthetic sequence of RNA, called a guide RNA (gRNA), which is specifically targeted to the gene of interest (Mali et al. 2013). This sequence of RNA is complementary to a sequence of genomic DNA at the cut site and the choice of this sequence is determined by the nature of the edit required (e.g. interruption of a particular exon), as well as the availability of sequences suitable for enzyme activity and the uniqueness of this sequence within the whole genome. Cas9 requires the target sequence to have a certain nucleotide content and to be adjacent to a particular 3 base pair sequence called a Protospacer Adjacent Motif (PAM) (Hille & Charpentier 2016). Choosing a sequence that is highly dissimilar to any other sequence within the genome limits the chances the enzyme will mistakenly cut elsewhere, causing undesired mutations (Peng et al. 2015). Once the genomic DNA is broken, exogenous DNA can be incorporated into the break site, allowing targeted insertional transgenesis.

By designing different gRNAs that target Pdgfrα in all three fish types, double-stranded breaks can be introduced into the genome that can be repaired with the insertion of desired DNA, CRISPR technology can be used to edit the genomes of the different ecotypes and species with little change in experimental method and reagents. In recent years, multiple online

programs have been written that aid in gRNA design (https://zifit.partners.org/ZiFiT/, https://chopchop.cbu.uib.no/). Additionally, producing gRNA in the laboratory is a relatively short and simple process, meaning CRISPR presents as the most efficient method to produce multiple transgenic fish of different species/ecotypes. The technology has already been used to create multiple transgenic lines of model species, including mice and, importantly, zebrafish, meaning established protocols are readily available for adaptation (Shen et al. 2013; Wang et al. 2013; Gratz et al. 2013; Friedland et al. 2013).

To interrogate Pdgfrα-positive population activity and function it was necessary to insert exogenous DNA sequences under control of *pdgfrα* regulatory sequences, without altering gene function. In addition, for ease, it was required that the same exogenous DNA (fluorescent reporter or Cre) could be used for all fish. Therefore the work of (Kimura et al. 2014) and (Auer et al. 2014) was adapted for this purpose. Kimura et al designed their gRNAs to cut within the 600-200bp 5' upstream region of their gene of interest and they incorporated the promoter of *Heat Shock Protein 70 (Hsp70p)* into their donor DNA for insertion as a basal promoter. This enhancer trap-type approach allowed expression of their insert without abrogation of endogenous gene function. Auer et al incorporated their DNA for insertion into a plasmid that contained a portion of the sequence for GFP, against which they had designed a highly efficient gRNA. This allowed linearization of the plasmid ready for insertion within the cell by Cas9 with the addition of the GFP gRNA. By adapting the plasmid used by Auer et al by inserting Hsp70p and Cre or a fluorescent reporter and designing gRNAs against the 600-200bp upstream region, a protocol for producing transgenic *pdgfrα:creER*^{T2} and *pdgfrα:mCherry* fish was developed (Fig. 3.8). If the insert plasmid was not for the

creation of a transgenic reporter line, the *cryaa:cerulean* sequence was included so that embryos could be fluorescently genotyped by cerulean expression in the lens.

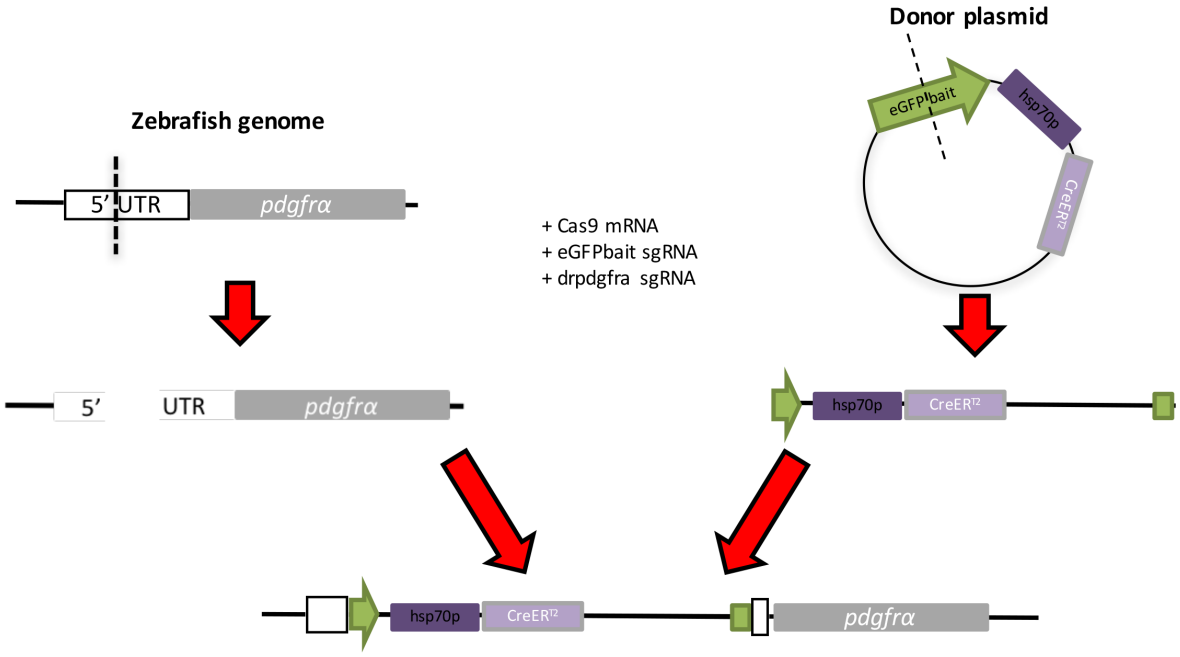


Fig. 3.8 A schematic showing the CRISPR strategy to generate transgenic fish. After injection of the *Cas9* mRNA and eGFPbait sgRNA that targets the donor plasmid and drPdgfrα sgRNA that targets the 5' UTR of *pdgfrα* in the genome, the *Cas9* mRNA is made into protein, which then is guided to make DSBs in the genome and donor plasmid. Following breakage, the linearised donor plasmid is then incorporated into the genome by NHEJ.

Cas9 mRNA, gRNA against the 600-200bp upstream region of *pdgfrα*, gRNA against GFP and the plasmid containing the Cre/fluorescent reporter were injected into one cell stage embryos, to allow Cas9 protein to be made and integration of the exogenous DNA to occur early, thus being present in as many cells of the resultant fish as possible. Injected fish were monitored and checked for incorporation of the DNA insert 4 days after fertilisation. In zebrafish, multiple rounds of injections were made and many fish looked to be positive for insertion of the transgene when screened as they expressed fluorescent proteins in the

correct regions of the larvae, for example cerulean expression in the lens. However, upon breeding of these fish when they reached adulthood, no germline transmission of the transgene was detected. Unfortunately, the *Astyanax mexicanus* housing facility was relatively new at the time these experiments were attempted and the fish would not breed, due to various husbandry issues occurring in the new system. This limited the attempts that could be made to inject embryos to just one and no evidence of integration of the transgene was seen, in contrast to the zebrafish where approximately 1-5% of injected embryos showed signs of integration at every injection round.

The reasons for this failure to create the transgenic fish lines could be multiple. Firstly, it could be that the method would have worked, but not enough attempts were made to find fish with germline transmission. However, the rates of transmission recorded in the work of Auer et al and Kimura et al were relatively high and would suggest that germline transmission should have readily occurred within the number of attempts made, though this construct was bigger in size and might have reduced the efficiency. In addition, the experiment was hugely time consuming and a cost-benefit analysis of continuing at the detriment of other experiments determined that other avenues should be explored to prevent the research from stalling. It is most likely that conditions were not optimised correctly for the experiment, with the concentration of sgRNAs, Cas9 and/or exogenous DNA incorrect for successful insertion.

As the required transgenic fish lines could not be generated, interrogating whether Pdgfrα-positive cells in the epicardium produce cardiac fat developmentally and after injury required the derivation of a new strategy.

3.7 THE EPICARDIUM FORMS EPICARDIAL FAT DURING DEVELOPMENT IN THE ZEBRAFISH

An epicardial transgenic fish line, where *CreERT2* is expressed under the control of the *tcf21* promoter, was crossed with a *ubi:Lox-GFP-Stop-Lox-mCherry* reporter line, allowing temporal control of reporter expression in epicardial cells. When tamoxifen is added, the Cre recombinase becomes activated and induces recombination between a pair of loxP sites, in this case removing the *GFP-Stop* portion of the transgene, ending GFP expression and beginning mCherry expression in the Cre-expressing cells. *Tcf21* is expressed in the majority of epicardial cells and is therefore used extensively as an epicardial marker gene (Cao et al. 2015). Therefore, using these fish, epicardial cells expressing *tcf21* should be labelled when tamoxifen is added and their subsequent progeny will be labelled also. *As* the immunohistochemistry data shows the presence of Pdgfrα-positive population in the epicardium, suggesting a mesenchymal progenitor within the epicardium, and tracing studies in the mouse suggest that the epicardium is a major contributor to epicardial fat and injury fat in the mouse, this line was used to trace the origin of developmental and injury-related epicardial fat in the zebrafish.

Whole-mount imaging of hearts isolated from adult fish that have undergone this lineage tracing during the early stages of development was performed that shows bright red mCherry fluorescence in and around the fat cells that reside in the groove between the bulbus arteriosus and atrium and the ventricle (Fig. 3.9 A). Magnification shows many small mCherry-positive regions within the fat, likely representing the cell portions of the fat cells outside the fat deposits (Fig. 3.9 B). Adipocyte cell mass is comprised mostly of the lipid filled fat reservoir, with the majority rest of the organelles and cytoplasm compressed to one side. mCherry

expression around the fat would be hard to see, but it would be quite concentrated in this compressed area, which could be the red dots seen within the fat tissue.

This data indicates that the epicardium forms the fat that develops normally over the life of a fish, like it does in the mouse. As the epicardium is also reported to produce fat after injury in the mouse, it seemed increasingly likely that this is the case in the fish too. Therefore, the next step was to identify the cellular contribution of the epicardium to injury-related fat.

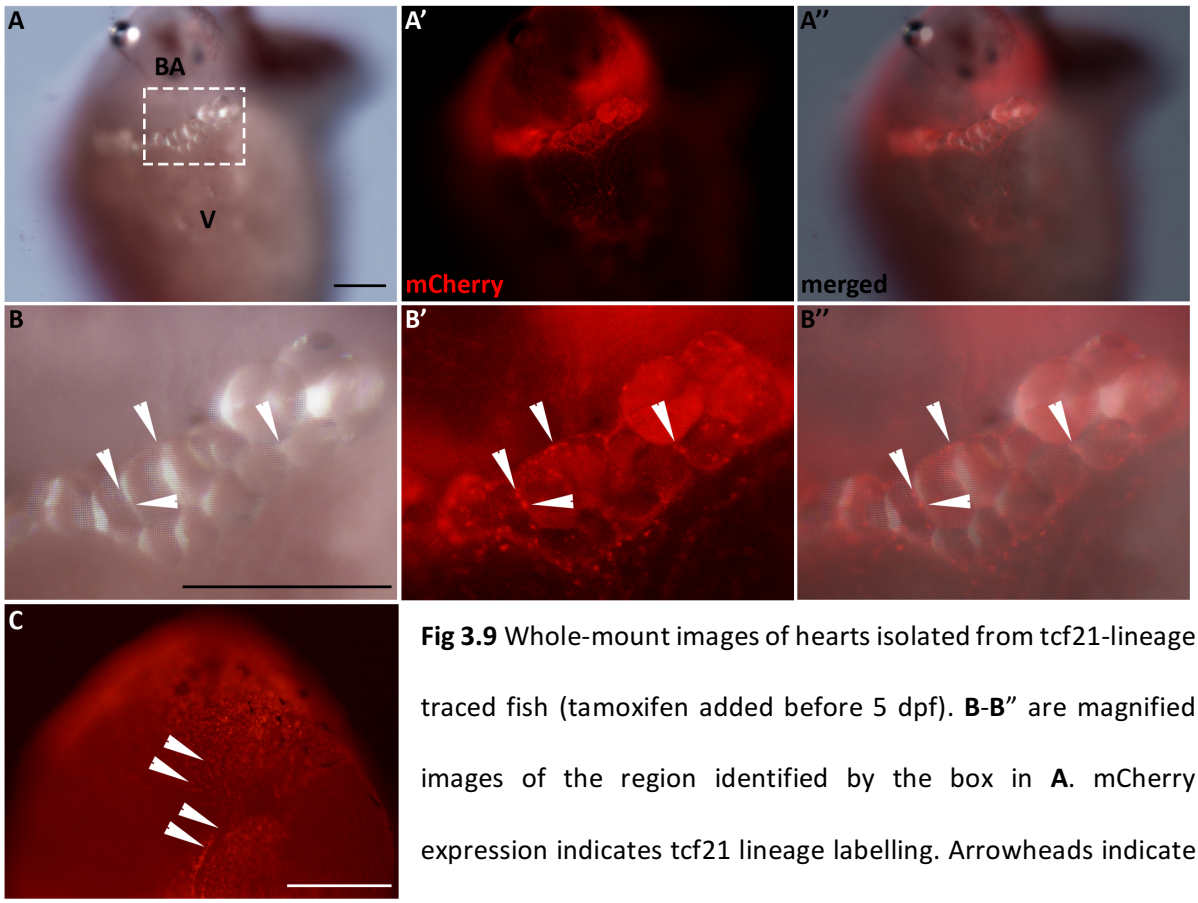


Fig 3.9 Whole-mount images of hearts isolated from tcf21-lineage traced fish (tamoxifen added before 5 dpf). **B**-**B**" are magnified images of the region identified by the box in **A**. mCherry expression indicates tcf21 lineage labelling. Arrowheads indicate mCherry positive cell bodies/ cells in the epicardial fat. BA = bulbus arteriosus. **C** shows epicardial labelling, where mCherry-positive cells can be seen as red dots on the heart surface. The arrowheads indicate a coronary vessel that is not labelled for contrast. BA = bulbus arteriosus, V = ventricle. Scale bar is 100 μm, N=4.

3.8 THE EPICARDIUM FORMS FAT ON THE WOUND SITE

Tamoxifen was dosed just before injury to *tcf21:CreER^{T2};ubi:LoxP-GFP-STOP-LoxP-mCherry* fish, causing *tcf21*-positive epicardial cells and their subsequent progeny post-injury to be labelled with mCherry. This experiment was performed to show the contribution of the injury-responsive adult epicardium to fat cells in the wound. The hearts were injured using cryo-injury and the hearts were isolated 14 days later.

Whole-mount imaging of hearts isolated from adult labelled fish at 14 dpi was done and this data shows that fat cells on the wound appear to derive from the injured epicardium (Fig. 3.10 B', C white arrowheads). It is important to note that the red cells around the bulbus arteriosus is blood, not an Oil Red O stain. Further investigation in paraffin sections was done, which shows that mCherry cells are in close apposition to the holes left behind in the scar tissue due to fat cell presence (Fig. 3.10 C). These cells are not positive for *tcf21* mRNA, as shown by RNAscope. RNAscope is a type of *in situ hybridisation* that involves the hybridisation of multiple small probes to the target RNA, followed by hybridisation of an amplifier molecule and then label probes. Each dot of staining represents 1 successfully identified RNA molecule, with multiple dots with in a cell indicating high levels of expression. As these cells aren't positive for *tcf21*, they were likely the progeny of epicardial cells and not epicardial cells themselves. This suggests that an epicardial cell has undergone a cellular transition, epicardial-to-mesenchymal transition (EMT) becoming a mesenchymal progenitor that forms fat, losing its epicardial identity.

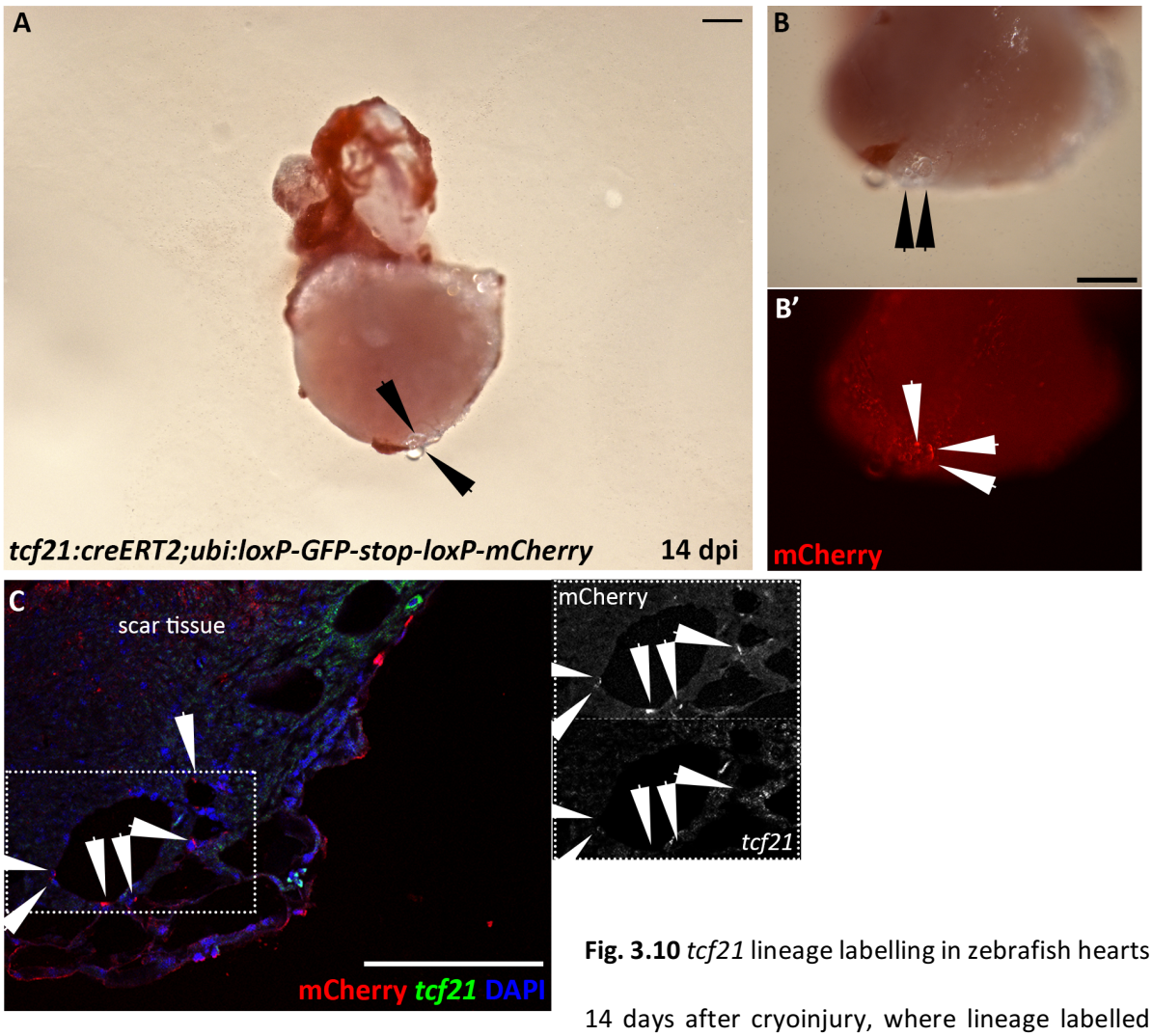


Fig. 3.10 *tcf21* lineage labelling in zebrafish hearts 14 days after cryoinjury, where lineage labelled cells are mCherry-positive. **A** shows an overview of an isolated whole heart, with fat on the injury site indicated by the arrowheads. **B** and **B'** show a magnified and angled view of the fat (black arrowheads in B) where mCherry positive fat is labelled by white arrowheads in B'. **C** shows immunohistochemistry for mCherry and *tcf21* RNAscope in a paraffin section from the same set of hearts. White arrowheads indicate mCherry positive cells in the fat region. N=4, scale bars = 100 µm.

In summary, this evidence suggests that the epicardium is a source of fat that is produced in the wound site after injury. This data is in line with previous findings in the mouse (Liu et al. 2014), where the epicardium has also previously been found to produce fat after injury.

3.9 DISCUSSION

The work above demonstrates that, like mice and humans, fish have fat that resides on the heart and are capable of forming fat in the wound site after injury. The *A. mexicanus* ecotypes show marked differences in the amount of fat present on the heart both before and after injury. The cavefish, despite having overall higher levels of body fat, have smaller deposits of larger fat cells on the heart than the surface fish and this trend is reversed after injury, with the cavefish forming large fat cells on the wound whilst the surface fish does not. The zebrafish appears somewhere between the two, with fat on the uninjured heart resembling the surface fish and fat produced after injury like the cavefish, though to a much lesser extent. This seeming discrepancy, that the regenerative zebrafish resembles the non-regenerative cavefish in this injury response rather than the surface fish could be due to the different injury approaches taken in the different species, with apical resection injury being performed in *A mexicanus* and cryoinjury in the zebrafish. Cryo-injury is known to produce more scarring and have an increased regeneration time compared to apical resection (Chablais et al. 2011; González-Rosa et al. 2011). Injury responses due to missing tissue are acknowledged to be different to those of damaged but present tissue in the context of missing and damaged appendages (Owlarn et al. 2017), so a similar phenomenon is likely in the heart. This data suggests the presence of a previously unidentified mesenchymal progenitor resident in the heart, which acts differently in different regenerative environments, seemingly producing many more adipocytes in non-regenerative hearts or those with extensive scarring.

Identification of the progenitor population that produces the fat is important, with a view to developing a future understanding of how it can sense the regenerative environment and then modulate its lineage potential or activity accordingly. Pdgfrα is a commonly used marker

of mesenchymal progenitors that can produce fat both during regular life and after injury. Pdgfrα-positive cells are seen in the epicardium of both fish, before and after injury, where fat progenitors are produced in mice. Additionally, Pdgfrα-positive cells are found in the scar tissue, where the fat is formed after injury. Further experiments using zebrafish to perform lineage tracing of epicardial cells show that the epicardium produces the fat that normally resides in the epicardial groove and that formed within the wound. Whether these epicardial cells that produce fat express Pdgfrα is unknown, due to the inability to produce transgenic lines capable of lineage-tracing Pdgfrα-positive cells. However, despite the incapability to identify more specifically the epicardial population responsible for fat formation, the finding that the epicardium produces fat in fish, like in the mouse (Yamaguchi et al. 2015; Liu et al. 2014), is a further exciting and novel example of a conserved developmental process, such as cardiomyocyte de-differentiation, and injury response between fish and mammals.

The role of fat in fish heart injury and homeostasis has not been studied before and presents a new avenue for investigation. The fat present in the atrioventricular groove of the surface and zebrafish is of unknown function, however, in humans it is suggested that it acts as a cushion to protect against distortion due to contraction, releases free fatty acids to sustain myocardial energy demands, generates heat in response to cold exposure and is a source of multiple bioactive cytokines that regulate the inflammatory state of the underlying tissue and vasculature and also endothelial function (Wu et al. 2017). The seemingly beneficial effect of increased epicardial fat in human MI reported in Gohbara et al. 2016 and Biere et al. 2017 is theorised by the authors to be due to the secretion of beneficial hormones, vascular regulators and/or the potential of epicardial adipose tissue as an energy store to be released to the injured myocardium. The correlation of epicardial adipose tissue presence in

regenerative zebrafish and surface fish versus its absence in non-regenerative cavefish, suggests that it could be similarly beneficial to injury outcome in fish as it is in humans. Whether these benefits manifest through similar mechanisms in the fish to in humans, for example through enhancement of angiogenesis, is unknown and would make an interesting further study. Also unknown is why the cavefish would lack epicardial adipocytes. The increase in size of cavefish adipocytes compared to surface fish is thought to be a mechanism to store extra energy in an efficient manner (Xiong et al. 2018). It could be that energy storage around the heart is not efficient in these fish and they store more energy in visceral adipose tissue, perhaps a more readily released energy store. Another possibility is that myocardial energy demands through free fatty acid oxidation is much reduced in the cavefish, due to the fact they are hyperglycaemic (Riddle et al. 2018). Experiments looking at the metabolic states of *Astyanax* hearts are ongoing in the laboratory currently.

The presence of large amounts of fat on the cavefish wound site after injury and the reduced deposition of fat by zebrafish likely relates to the large amounts of scarring seen in both injury models. The lack of fat production in the surface fish is possibly due to the regenerative environment of the fish coupled with the injury model used, which has lower levels of scarring compared to cryoinjury, which was used on the zebrafish. The role of this fat in the injury response is unknown; as it appears in both a regenerative and non-regenerative model, it seems unlikely to be a major determinant of regenerative potential. It seems likely that it is a symptom of an injury with an extensive scarring response, likely through the possibility that the epicardial progenitors responsible for producing the myofibroblasts that produce the scar are from the same pool that produce adipocytes. In this case, adipocytes are merely a by-product of scarring. However, there is a possibility that they play an active and positive role

in the injury response, through their aforementioned signalling or energy benefits. It could be that in the cavefish they are too large to remove and their beneficial effects are insufficient to enable complete regeneration and scar removal. As such, it seems likely that their beneficial effects are minimal in a non-regenerative environment. Further investigation of the exact identity of the adipogenic progenitors, allowing their specific isolation and assessment of their fibrogenic potential will indicate if the same progenitor involved in cell productions for scar formation is the same as that that produces fat.

Once the progenitor can be isolated, its activity during injury can be investigated. It has been shown that similar progenitors in skeletal muscle are influenced in their activity by inflammatory cues and Notch signalling (Marinkovic et al. 2017; Muñoz-Cánoves & Serrano 2015; Lemos et al. 2015), so investigating the same pathways in the heart may show how the epicardial progenitor can sense and react to the injury environment. The fibro-adipogenic progenitors in skeletal muscle aid the creation of new muscle in regenerative settings and form fatty-fibrotic scar tissue in non-regenerative settings (Joe et al. 2010; Uezumi et al. 2010), raising the exciting possibility that, whilst the fat itself may not play a major role in regenerative capacity, the epicardial progenitor might. In this context, it is interesting to note the differences in the Pdgfrα and Wt1 immunohistochemistry staining between the two ecotypes, with the extent to which they are expressed in the wound and scar tissue varying between ecotypes. Once the signals influencing the activity of this progenitor are identified, manipulation of these pathways may be possible, opening up avenues for therapeutic intervention.

Overall, this work adds to the body of existing literature showing that cardiac fat can be both a help and hindrance, with it being found in different forms in regenerative and non-

regenerative settings. As a conserved process in regenerative and non-regenerative organisms, investigation of this progenitor and its differences between organisms might provide novel insights into the capacity to renew.

3.10 CONCLUSION

This work has identified the epicardium as the source of fat progenitors in the fish heart that can produce fat that resides on the heart and is produced within the wound after injury. This is a mechanism that is conserved amongst species, being seen also in the mouse. Further work is required to identify the injury signals that promote fat production and regulate the extent to which fat deposition is stimulated. The effect of fat production on regenerative capacity would also make intriguing further investigation.

Stricter identification of these progenitors through further interrogation of their differentiation pathway is a priority. This will allow their isolated ablation after injury, which might help shed some light on their function. Monitoring the effect of regeneration on their loss should help identify the role of fat in wound response, whether it is merely a side effect of an environment where scar deposition is currently very high, or plays an active role in the injury reaction. Isolating the signals involved in promoting fat formation in the scar is a more challenging prospect. Harnessing the genetic power of the *A mexicanus* model and doing a QTL analysis based on degree of fat production in the scar might shed some light, but would likely only be worthwhile if fat production was shown to be linked to regenerative capacity.

CHAPTER 4 – INVESTIGATING OTHER PDGFRα PROGENITOR POPULATIONS

CHAPTER 4 – INTRODUCTION

4.1.1 SUMMARY OF THE CHAPTER

The previous chapter shows that epicardial Pdgfrα-positive populations are likely involved in the production of fat after injury. However, the immunohistochemistry shows that Pdgfrα-positive cells are also found resident in the blood and some endocardial cells also look to be Pdgfrα-positive (section 3.5.1). In addition, blood-borne Pdgfrα-positive Wt1-positive cells are present after injury. Wt1 has been shown to be expressed in hematopoietic progenitor cells, suggesting that these are Pdgfrα-positive hematopoietic progenitor cells (Svedberg et al. 2001). Cells like these have never been identified before in mice or fish and are of unknown type and function. In addition, when looking at epicardial Pdgfrα-positive populations after injury, it can be seen that cells other than epicardial cells express Pdgfrα within the wound (Fig. 3.4, 3.5). As Pdgfrα is used as a progenitor marker and the aim of the study was to identify novel progenitors in the fish heart, these populations were also studied to investigate whether they do indeed show a response to injury and, if so, what these cells are and what the nature of this response is. This chapter describes the work done to identify how these cells respond to injury and give them a preliminary identity.

Analysis of the reaction of these populations to injury shows that they fluctuate markedly in number after wounding, following grossly similar patterns over time in both the surface fish and cavefish. Identification of these cells using immunohistochemistry against common marker proteins suggests that they could be hematopoietic cells, likely hematopoietic

progenitor cells, through their expression of Runx1, a transcription factor found in hematopoietic stem cells.

The Runx1-positive cells appear to look like endothelial cells in some cases after injury, rather than blood-borne cells as expected for a hematopoietic cell. Further analysis using co-staining with endothelial markers showed that these cells do indeed have a dual endothelial/hematopoietic nature, a cell-identity state that mirrors that of the hemogenic endothelium that is seen during development. The developmental hemogenic endothelium is a specialised endothelium found in all investigated vertebrates that produces hematopoietic stem cells in the developing embryo/larvae that give rise to all blood lineages. This raises the exciting possibility that the injured endocardium produces hematopoietic stem cells *in situ* after injury, an injury-response phenomenon that has not been identified before in any organism.

4.1.2 BACKGROUND INFORMATION

As mentioned in the previous chapter, Pdgfrα-positive cells have not been well characterised in the fish heart. Whilst most commonly associated with mesenchymal stem cells, in the mammalian heart, Pdgfrα has also been found in perivascular stromal cells, fibroblasts and smooth muscle (Chong et al. 2011). However, the Pdgfrα-positive cells in the blood and what look to be endothelial Pdgfrα-positive populations in the fish heart found in the *A mexicanus* ecotypes do not resemble these established mammalian populations.

Peripheral blood mononuclear cells in mammals are reported to be a heterogeneous population of progenitor cells that can form multi-lineage progeny, including blood, endothelial, smooth muscle cells and myofibroblasts (reviewed in Zhang & Huang 2012).

These blood cells have not been reported on in the fish, but given the expression of Pdgfrα in occasional blood cells, it is intriguing to speculate that this could be a population of circulating mesenchymal progenitor cells or other multi-lineage progenitor similar to those seen in mammals. Given the overlap with Wt1 in the blood seen in the previous data, another interesting possibility is that these are circulating hematopoietic progenitors.

Expression of Pdgfrα has been noted in developing endocardium at early stages of cardiac development in the zebrafish and Pdgfrα loss has been noted to cause endocardial developmental defects (El-Rass et al. 2017). The expression of Pdgfrα in certain adult endocardial cells could identify a sub-population of endothelial cells that retain a developmental expression pattern. As discussed in the thesis introduction, the endocardium is known to contribute multiple cell types during development and after injury, raising the intriguing possibility that Pdgfrα could delineate a population of endothelial cells with specialised potential.

Given the unknown nature of these cells but the interesting possibilities raised by the established literature, the unidentified blood and endocardial Pdgfrα-positive cells were investigated further, leading to the discovery of a specialised endothelial population that can potentially form hematopoietic progenitors after injury.

4.2 INVESTIGATING OTHER PDGFRα-POSITIVE CELLS AFTER INJURY

To analyse the response of endocardial-type and blood-borne Pdgfrα-positive cells to injury, both surface and cavefish had cardiac injury by apical resection performed on them and the

hearts were collected at 0, 3, 7 or 30 days after injury and prepared for immunohistochemistry. The numbers of Pdgfrα-positive cells within the heart that were not present in the epicardium were then quantified at these time points, to discern if the numbers of these different cell types fluctuate in response to cardiac injury.

Non-epicardial Pdgfrα cells appear to be either blood-borne (Fig. 4.1 B), or endocardial (Fig. 4.1 C). These cells appear in both fish and have not been reported on in the fish previously. Therefore, these were treated as two separate populations, referred to from here as blood-borne and endocardial-like Pdgfrα-positive cells.

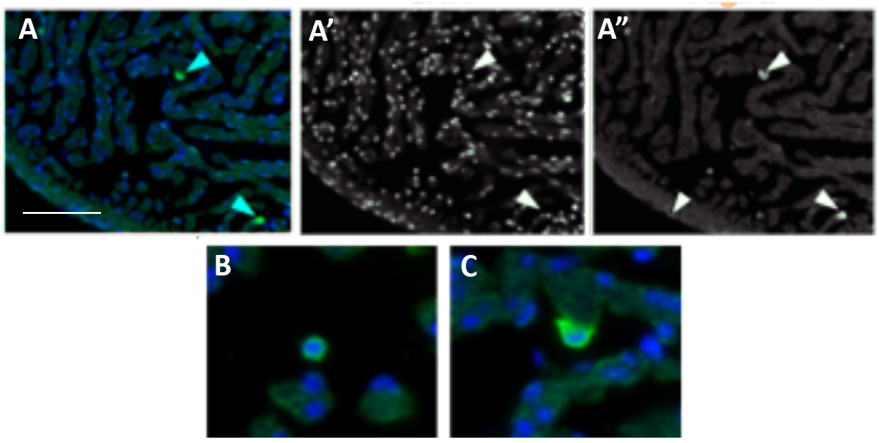


Fig. 4.1 Non-epicardial Pdgfrα-positive cells resident in the uninjured *A. mexicanus* heart. A-A shows an overview of the hearts, B and C show magnified blood-borne and endocardial-like cells, respectively. Scale bar indicates 100 µm.

Directly after injury, there are endocardial-like Pdgfrα-positive cells next to the site of amputation at 0 dpa (Fig. 4.2, white arrowheads). At this stage, in both fish, the concentration of Pdgfrα-positive endocardial-like cells along the wound edge looks to be similar to that in the rest of the myocardium, suggesting no accumulation of these cells at the wound edge in either fish. However, according to counts of the number of endocardial-like cells in the ventricle away from the wound, the cavefish appear to have many more Pdgfrα-positive

endocardial-like cells across the myocardium than the surface fish do (Fig. 4.2 A, graph in B, $p<0.001$).

It is important to note that in the majority of surface fish, the Pdgfrα antibody also stains a line around the edge of the trabeculae. This gives the impression of extra endocardial staining in comparison to the cavefish, however, stained endocardial cell bodies are rarer than this staining pattern would suggest. It could be that this is background staining of an ECM layer between the true endocardium and the myocytes, though why it is present more in the surface fish is unknown. It is not impossible that the ECM components of cavefish and surface fish hearts differ.

At 3 dpa, Pdgfrα-positive cells begin to accumulate in the border zone of the wound of both fish, in roughly equivalent numbers (Fig. 4.2 B). Most of these cells look to be endocardial (Fig. 4.2 A, white arrowheads) though some look to be blood-borne. For many cells, it was hard to distinguish if they were blood or endocardial-type as Pdgfrα-positive cells were packed in very tightly. Therefore, cell counts performed within the wound counted total Pdgfrα-positive cells.

At 7 dpa, both fish appear to have many endocardial-like Pdgfrα-positive cells in the border zone of the wound (Fig. 4.2 A, white arrowheads). These cells appear bobbled and some are relatively flat, whilst others look much rounder (Fig. 4.2 A, 7 dpa, compare the magnified boxes). Both fish appear to have roughly the same numbers within the border zone of the wound (Fig. 4.2 B). Cell counts that were performed show that surface fish have slightly more endocardial-like cells away from the wound at this time point (Fig. 4.2 B). It appears that both fish have reduced numbers of endocardial-type cells away from the wound in comparison to baseline, uninjured levels.

By 30 dpa, some of the harvested cavefish hearts still have a sizeable scar whilst most surface fish do not. In the cavefish, where the scar still remains, Pdgfrα-positive endocardial-like cells are still present in the scar tissue (Fig 4.2 A). One surface fish has a visible scar, where some ventricle had only been partially amputated, and an endocardial-type cell is visible. Due to the lack of extensive scar tissue and wound in surface fish at 30 dpa, counts within the wound were not performed, however counts in the rest of the ventricle show that the number of endocardial-like cells is similar in both ecotypes and minimal, appearing much reduced compared to uninjured fish (Fig. 4.2 B).

The general trend in endocardial-type cells, with some variation between ecotypes, is that the number away from the injury site decreases as injury time progresses. They appear in increased numbers in the border zone of the wound of both fish, with varying morphologies, with some being very round and others much flatter. This gives them the appearance of cells that are either about to depart, or have just attached to, the inner lining of the wound.

In uninjured fish, the cavefish appear to have more blood-borne Pdgfrα-positive cells than the surface fish (Fig. 4.2 B). Blood borne cells are not seen in any great concentration in the wound site at 0 dpa. Where the blood clot is present, it does contain some rare Pdgfrα-positive cells (Fig. 4.2 A, pink arrowheads). At 3 dpa, blood-borne cells are present in the wound area of both fish (Fig 4.2 A, pink arrowheads). They appear to be at a greater concentration in the wound area than within the clot and elsewhere in the ventricle, suggesting accumulation within the wound area. Counts comparing the number of blood cells away from the heart show no difference between ecotypes at 3 dpa, but suggest that both fish have increased numbers of circulating Pdgfrα-positive cells at this time-point, with normalised counts indicating an approximately 10-fold increase to those at 0 dpa. At 7 dpa,

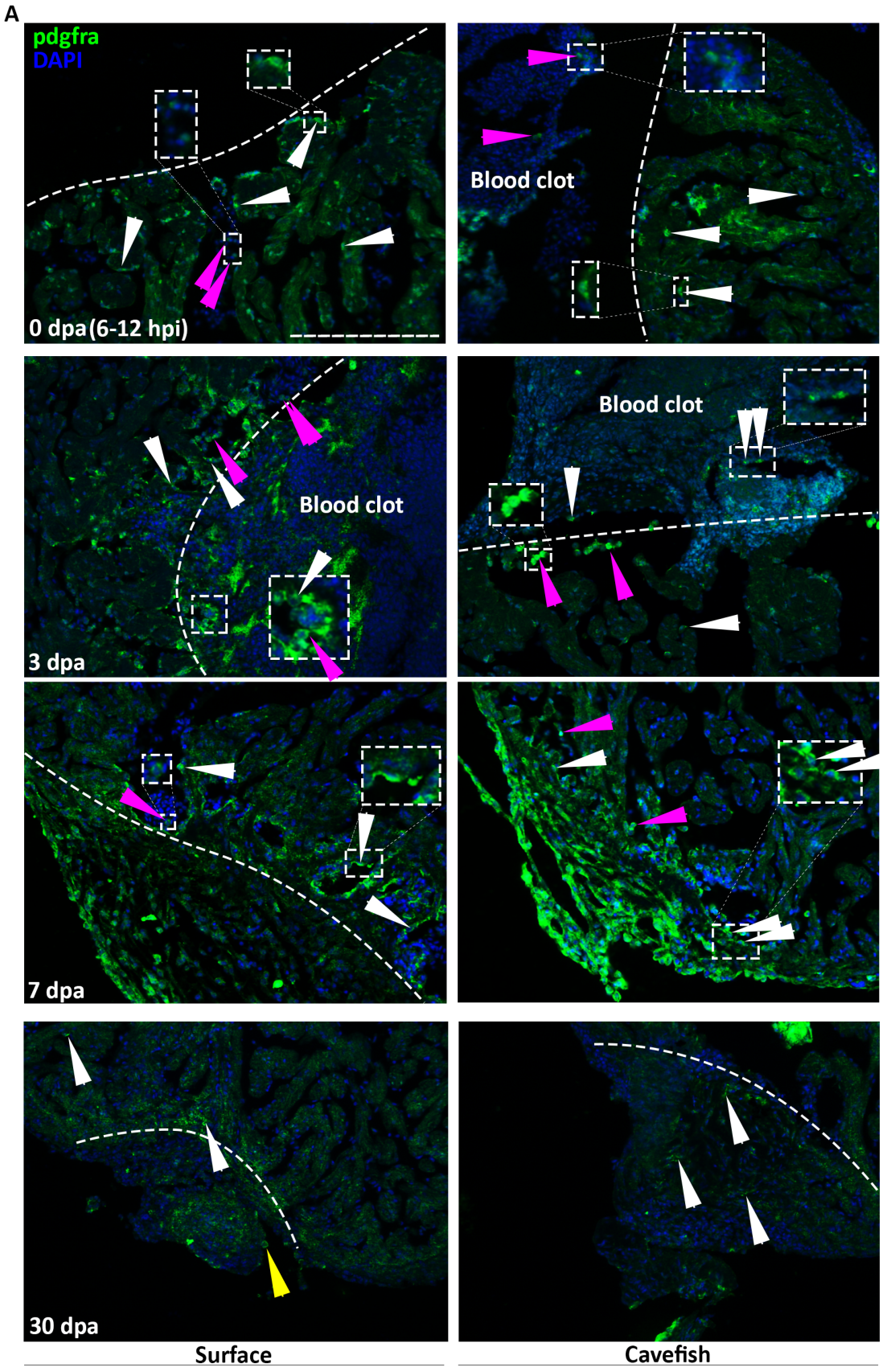
blood type cells appear within the wound site of both fish still (Fig. 4.2 A) though their numbers within the rest of the ventricle seem to be reduced after the peak at 3 dpa (Fig. 4.2 B).

The increase in blood-type cells at 3 dpa could represent an infiltrating leukocyte or other immune cell population, as it has been noted in the zebrafish that lots of neutrophils and many macrophages have normally accumulated by this point (Lai et al. 2017). The general decrease in endothelial-type cells (Fig. 4.2 B) is harder to decipher, but is nonetheless intriguing in that it is both marked and present in both fish. As the endocardium can form new blood vessels and potentially other cell types such as myofibroblasts after injury (Zhao et al. 2014; He et al. 2017; Kobayashi et al. 2017; Harrison et al. 2015; Sánchez-Iranzo et al. 2018; Gamba et al. 2017), it could be that these cells are true endocardium and their decrease represents endocardial trans-differentiation. This would mean the Pdgfrα-positive endocardial cells are becoming other cell types, thus reducing the number of these cells present in the heart across the injury timeline.

Overall, this data indicates further that epicardial cells are not the only Pdgfrα-positive cells that appear to respond to wounding in the heart. After wounding, the numbers of endothelial- and blood–type Pdgfrα-positive cells outside the wound fluctuate, with the blood cells showing a drastic increase at 3 days and the endothelial type cells decreasing hugely across the injury timeline. Within the wound border zone, there appears to be a large heterogeneous population of Pdgfrα-positive cells that increase in number between 3 and 7 days post amputation. Whilst not conclusive of a function in wound response, the fact that the number of Pdgfrα-positive cells of this type varies after injury in such a dynamic way is suggestive. Therefore, further work was done to identify these cell types, as a crucial

stepping-stone to understanding why these cells fluctuate in number so much in response to injury and elucidating a potential role for them in regeneration and wound healing.

Fig. 4.2


A
pdgfra
DAPI
0 dpa(6-12 hpi)
Blood clot
Blood clot
3 dpa
Blood clot
7 dpa
30 dpa
Surface
Cavefish

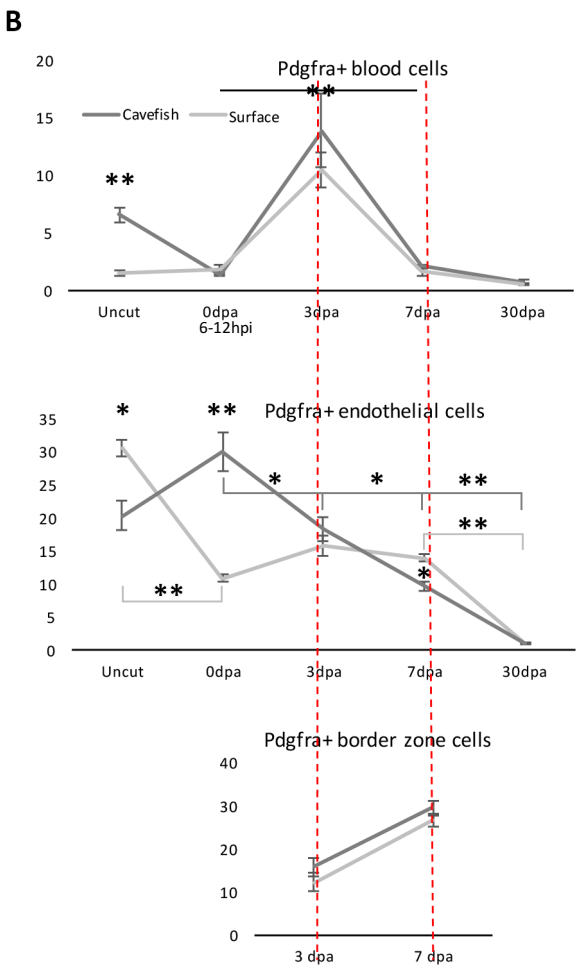


Fig. 4.2 Pdgfrα-positive blood-, endocardial-like and wound cells across the injury timeline in surface and cavefish. **A** Pdgfrα expression in sections from 0, 3, 7 and 30 days after injury by apical resection, Surface fish- left panel and Cavefish - right. 0 dpa denotes fish with hearts isolated at 6-12 hpa. Dotted line represents approximate level of amputation or remaining wound. White arrowheads indicate endocardial-like cells and pink arrowheads show blood-type cells **B** Quantitative analysis of Pdgfrα-positive cells of blood (upper panel) and endocardial-like (middle panel) type cells in the ventricle away from the wound and all Pdgfrα-positive (excluding epicardial) cells in the border zone of the wound (lower panel). Statistics performed by two-way ANOVA, * $p<0.05$ ** $p<0.001$. Horizontal bars light grey bars show comparisons between time-points in surface fish, dark grey for cavefish. Red dotted line indicates counts at the same time point after injury. N=4 for each time point and ecotype.

4.3 IDENTIFYING PDGFRα-POSITIVE CELLS RESIDENT IN THE VENTRICLE

To identify what the endocardial and blood type Pdgfrα-positive cells that reside in the ventricle are, immunohistochemistry was performed in heart tissue isolated from F1 fish, whose parents were a surface fish and a cavefish. These fish inherit half cavefish and half surface fish genes and all look identical. Therefore, F1 fish are ideal for identifying what these cell types could be as ecotype differences are eliminated.

The endocardial-type Pdgfrα-positive cells are relatively rare and certainly do not represent all endocardial cells in the ventricle. They could, therefore, be a small sub-population of endocardial cells or another, rarer cardiac-resident cell type attached to the trabecular myocardium. Cardiac-resident progenitor cells are certainly rare in the heart and have not been well characterised in fish (Zeng et al. 2017), but have been more so in the mouse. Various types have been isolated, with the majority being positive for the now controversial cell-surface marker c-Kit and some positive for the transcription factor Islet1 (reviewed in Le & Chong 2016). Therefore, antibodies for these markers were used in addition to Pdgfrα to see if these rare cells could be progenitor cells. Interestingly in the case of both Islet1 and c-Kit, some, but not all 'endothelial-type' Pdgfrα-positive cells are double positive, indicating that these cells may be progenitor cells of unknown type (Fig. 4.3 A, B – A'', B'').

As Pdgfrα-positive cells have been seen in the blood, to identify these cells, some blood markers that have working antibodies in fish were also used for immunohistochemistry. Arg1 is a marker of macrophages, whilst Runx1 is predominantly used as a marker of hematopoietic stem cells (HSCs) (Jablonski et al. 2015; Lacaud et al. 2002). Runx1 is particularly interesting, given that overlap with Wt1 in the blood-type Pdgfrα-positive cells was shown in Chapter 3, already indicating that these cells could be hematopoietic progenitors. Many, but not all, of the Pdgfrα-positive blood-type cells are also positive for Arg1, suggesting these cells are indeed blood cells. Overlap with Runx1 is also seen in the blood cells (Fig 4.3, lower panel, left white arrowhead). Most intriguingly, given that the endothelial-type cells can also be positive for other stem cell markers, Runx1 also stains some endothelial-type Pdgfrα-positive cells (Fig. 4.3).

It is important to note that the enhancement staining protocol was used with the Runx1 and Arg1 antibodies and that both antibodies using this protocol stain the trabecular lining, which is unexpected based on their use as blood cell markers. They are not present in all endocardial cells, yet the entire trabecular myocardium lining is labelled. This suggests that there are low levels of non-specific binding in the ECM with these antibodies, highlighted by the enhancement protocol. Runx1 works, but variably and extremely weakly, without enhancement and this potential ECM staining cannot be seen (Fig. 4.3 D, E).

It therefore appears that some, but not all, of the blood-type Pdgfrα-positive cells stain for Arginase1 and therefore are likely white blood cells. The previous count data shows that the number of Pdgfrα-positive blood cells peaks at 3 dpa, which tallies with previous studies in other fish species that have shown a peak in leukocyte accumulation around this period (Lai et al. 2017; de Preux Charles et al. 2016). This is a surprising finding, as Pdgfrα expression has not been noted in white blood cells previously.

Perhaps most interesting is the finding that the endothelial-type population can stain for the cardiac progenitor markers c-Kit and Islet1 and, perhaps unexpectedly, the hematopoietic progenitor marker Runx1. These results suggest that this population could represent a previously unidentified progenitor endocardial cell type that resides on the trabecular myocardium in the fish heart. Most intriguingly, the previous cell count data indicates that this population fluctuates markedly in number after injury in a manner that is suggestive of an active wound response, aside from cell damage. This novel cell population, therefore, could be contributing significantly to the wound and scar tissue, or to cells involved in the resolution of the wound.

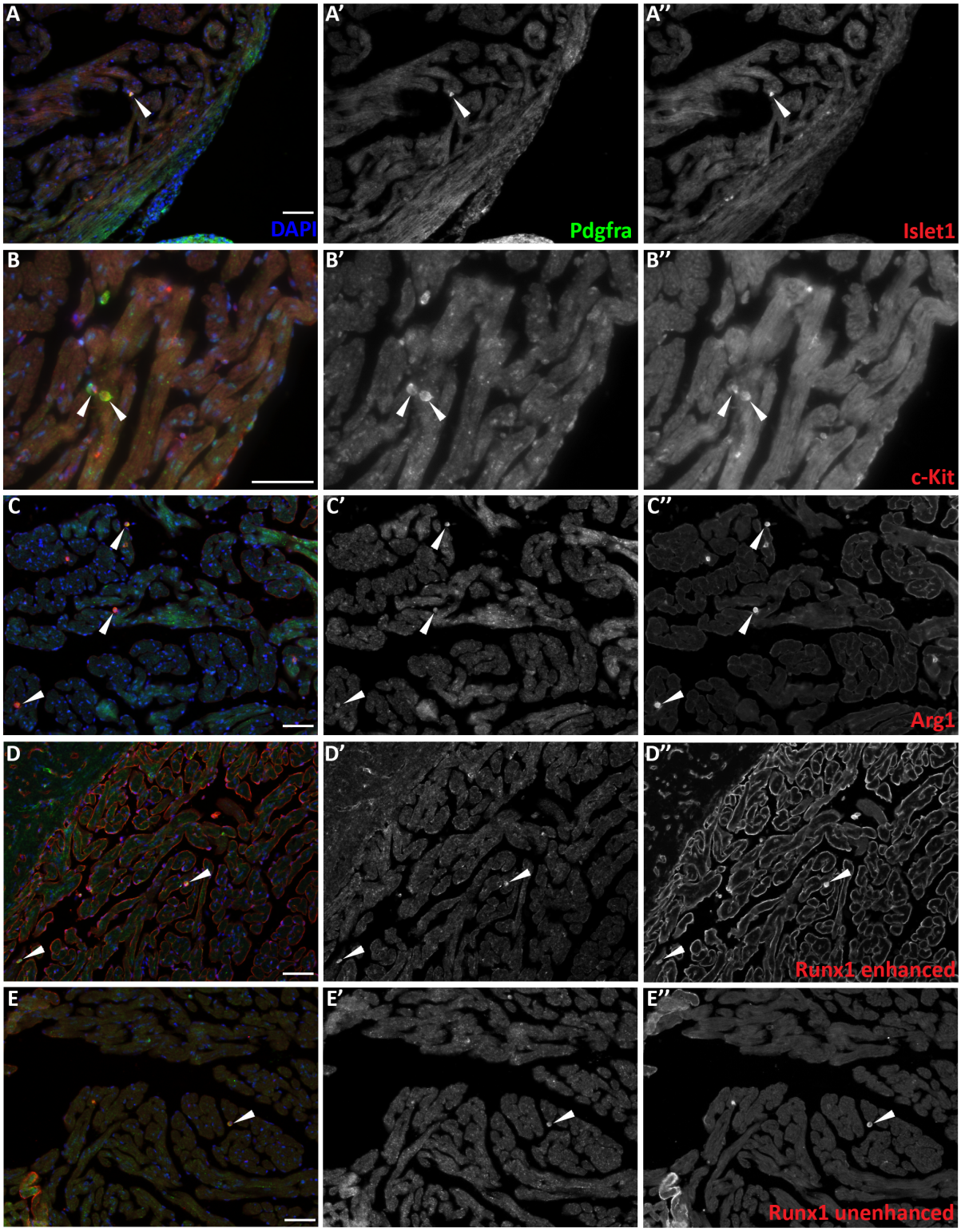


Fig. 4.3 Characterisation of Pdgfrα-positive blood and endothelial cells with stem cell and blood markers in F1 fish. **A-B"** are co-labelling with the stem cell markers Islet1 and c-Kit, respectively. **C-D"** are co-labelling with the blood markers Arg1, a macrophage marker, and Runx1, a HSC marker,

respectively. D shows the Runx1 antibody with the enhancement protocol and E shows it without. White arrows indicate double-positive cells. N=3. Scale bar shows 50 μm.

4.4 INVESTIGATING THE RUNX1 AND ARG1 PDGFRα-POSITIVE POPULATIONS AFTER INJURY

As Runx1 and Arg1 appear to demarcate novel Pdgfrα-positive cell types that could play a role in injury resolution, immunohistochemistry looking to identify these double-positive cells was performed on heart tissue isolated from injured hearts at 7 dpa.

At 7 dpa, there are plenty of Arg1 single-positive blood cells, but, unexpectedly, the Arg1 cells that are also positive for Pdgfrα are not found solely in the blood. In both ecotypes, most of the double Arg1 and Pdgfrα positive cells are in close apposition to the wound site, such that they look like they are part of the inside endothelium of the wound (Fig. 4.4 A', B' arrowheads) Indeed, some even appear to be very flat, looking more endothelial than white blood cell-like in nature (Fig. 4.4 A', B', magenta arrowheads). Arg1 is also seen lining all the trabeculae and in the scar tissue of the wound. The trabeculae lining staining could be staining due to the enhancement kit again, where low levels not normally picked up are shown brightly. The Arg1 within the scar tissue could be invading macrophages that have migrated to the wound tissue. However, it is also seen in what looks to be the ECM component of the scar tissue, particularly in the surface fish. In which case, as mentioned above, it could be that the enhancement kit with this antibody causes staining in the ECM of both the trabecular lining and the scar tissue. Perhaps some antibodies stick to the ECM more than others and differences in ECM components between surface and cavefish account for the differences.

Given the endothelial Runx1 staining seen in uninjured fish, it is less surprising that after injury there are also many cells that appear to be attached to the inside of the wound tissue and some that look very flat and endothelial (Fig. 4.4 C', D'). The density of these cells in the wound is much greater than that seen in the trabecular myocardium of uninjured fish, however. There are also some double positive cells present in the blood. To investigate this endothelial-type staining in the wound further, staining was done with Runx1 at 3 dpa to look at whether this type of cell appears in the border zone of the wound at an earlier time point and if they appear different to those at 7 dpa (Fig 4.5). Many Runx1 Pdgfrα double-positive cells can be seen at 3 dpa and, again, appear to be more endothelial in morphology, suggesting these cells exist for an extended period of the injury timeline (Fig. 4.5 A-A'', C-C''). Cells of varying morphologies exist at both time-points (Fig. 4.5, arrowheads). Some are very flat, and others are very rounded and look like they are about to detach. These endocardial cells likely comprise a considerable portion of the cells that account for the increase in number of Pdgfrα-positive cells found in the wound between 3 and 7 dpa.

It seems, therefore, that a cell type with a hematopoietic identity and endothelial-type morphology exists in *A. mexicanus* ecotypes after injury. These cells reside in relatively high numbers and density along the inside surface of the wound, in the border zone. That these cells are positive for Runx1 suggests that they have some degree of hematopoietic potency, thus indicating the exciting possibility of an injury-responsive hematopoietic progenitor in the fish heart. Such a population has not been reported before. The importance of hematopoietic-lineage cells in fish heart regeneration has been well documented, with the activities of immune cells being crucial to injury progression and regeneration (Lai et al. 2017; de Preux Charles et al. 2016; W.-C. Huang et al. 2013). Hematopoietic progenitors from the

bone marrow have been shown to contribute macrophage and monocyte populations crucial to regeneration in mammalian models, so the potential presence of *in situ* progenitors was therefore an exciting finding that was investigated further.

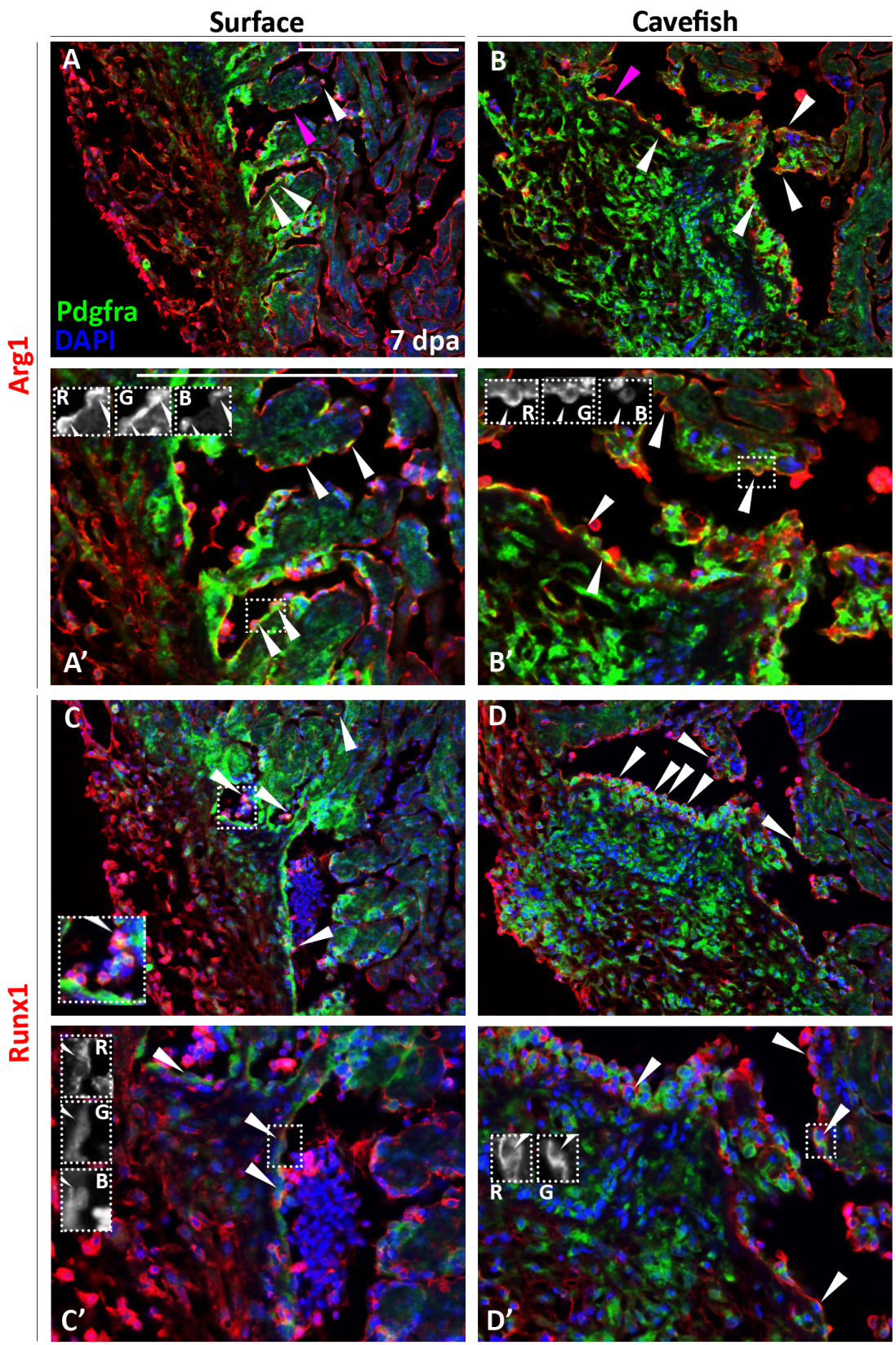


Fig. 4.4. Expression of Pdgfrα with Runx1 and Arg1 at 7 dpa in the cavefish and surface fish. **A-B'** show Pdgfrα with Arg1 and **C-D'** show Pdgfrα with Runx1. White arrowheads indicate double positive cells,

magenta arrowheads indicate flattened, endothelial-like double-positive cells. Scale bars indicate 100 µm. N=3.

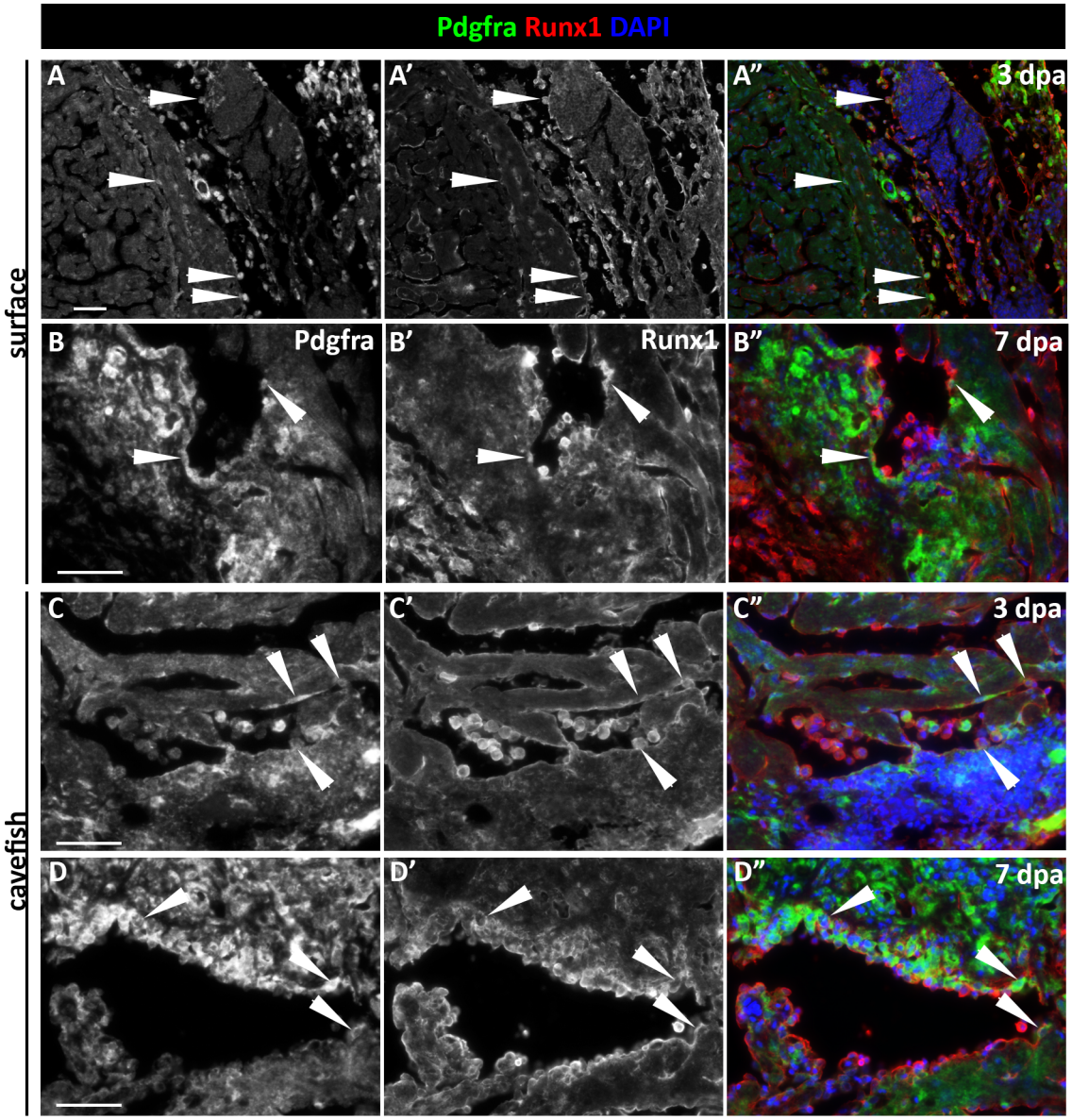


Fig. 4.5 Runx1 and Pdgfrα staining in injured *A mexicanus* hearts at 3 and 7 dpa, showing the different morphologies of endothelial-type double positive cells. **A** and **C** are at 3 dpa for surface and cavefish , respectively. **B** and **D** show staining at 7dpa. Arrowheads indicate double-positive cells of note. Scale bars indicate 100 µm.

4.5 INVESTIGATING RUNX1-POSITIVE CELLS IN *A. MEXICANUS* HEARTS AFTER INJURY

To understand the Runx1-positive population seen in the wound after injury, it needed to be further characterised. This was because it is highly unusual in its combination of marker expression and morphology, which presents two options: these really are endothelial cells that express Runx1, or they are Runx1 positive cells that simply have an endothelial morphology in the wound for an unknown reason. For example, the Runx1-positive cells could be infiltrating leukocytes that, captured in a snapshot of time, look to be endothelial as they attach to a gap on the inside of the wound. It was therefore important to establish which of these options is what is happening after injury.

To answer this question, immunohistochemistry for Runx1 and an endothelial cell marker, Erg1, was performed in injured fish at both 3 and 7 days after injury by apical resection, when this cell population has previously been seen in the wound. Images show that Runx1 expression coincides with Erg1 staining in both fish ecotypes at both 3 and 7 dpa, suggesting that these are indeed endothelial cells that also express Runx1 (Fig. 4.6).

These results suggest that there are many endothelial cells on the inside edge of the wound in the *A. mexicanus* heart that express Runx1. This is an exciting finding, as it suggests the formation of an endothelium with hematopoietic potential after cardiac injury, a response to injury that has not been identified before in any model organism.

However, there are some important caveats to note. The specificity of the Runx1 antibody in fish is unknown, as it was designed for use in mammalian tissue. Additionally, Erg is expressed in, and important to the function of, hematopoietic progenitors (Knudsen et al. 2015). In Fig. 4.6, Erg1 staining in the blood clot can be seen, showing that it is not endothelial-specific in

fish. Interestingly, this staining within the wound is seen more in the cavefish at 3 dpa than the surface fish.

On this basis, it is important to verify these findings through other means, to eliminate the possibility that non-specific staining or staining of non-endothelial cells is the case. *A. mexicanus,* unfortunately, offers limited opportunity for this, due to a combination of a lack of transgenic marker lines available and limited working antibodies for further immunohistochemistry. The zebrafish, on the other hand, with its high genetic amenability and popularity in many fields of research for decades, does offer such opportunities. Additionally, as no clear differences in this process are seen between cavefish and surface fish, it is more likely that this process is a conserved one to at least teleost fish. Therefore, the decision was made to study these cells further in the zebrafish, to try and verify their dual hematopoietic/endothelial identity and investigate how they arise in the fish heart.

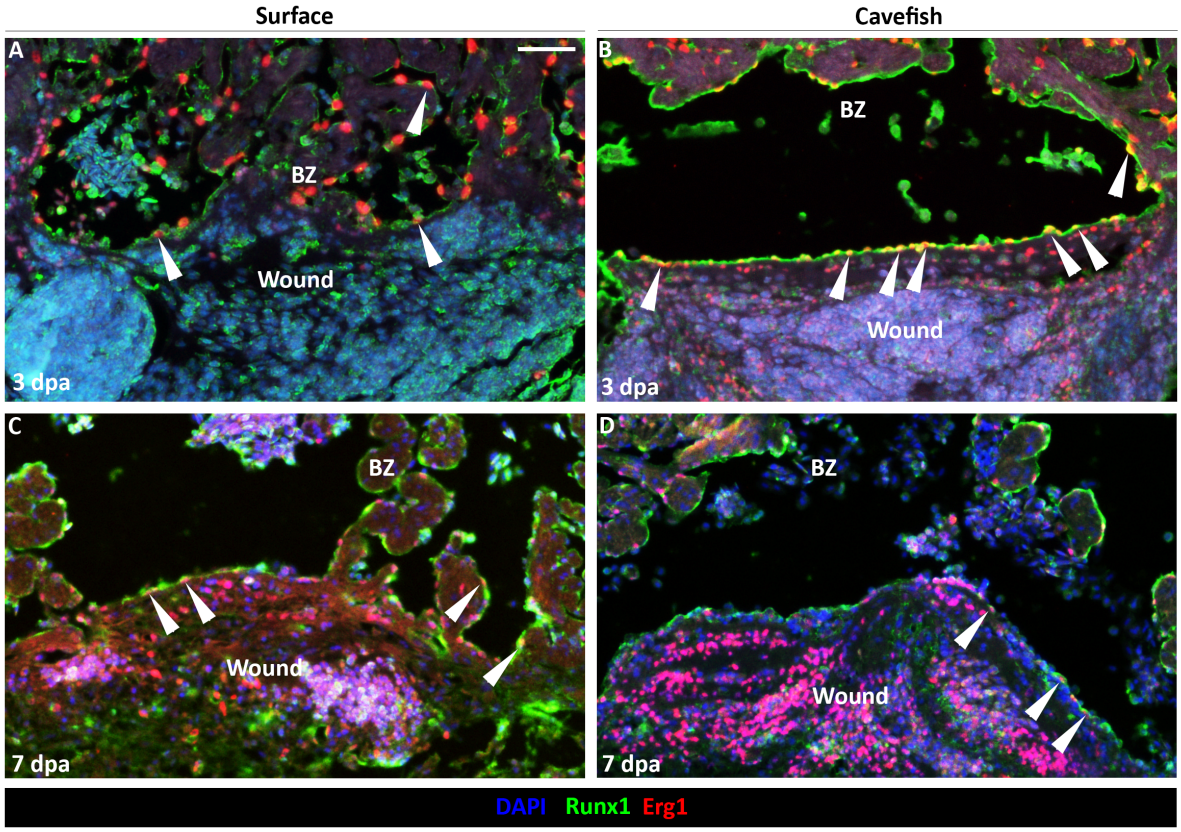


Fig. 4.6 Overlapping expression of runx1 and erg1 in surface and cavefish after injury at 3 (**A**, **B**) and 7 (**C**, **D**) dpa. White arrowheads indicate examples of double-positive cells. BZ= border zone. N=3. Scale bar is 50 μm.

4.6 DEVELOPMENTAL RUNX1 EXPRESSION IN ENDOTHELIAL CELLS

Finding expression of Runx1 in endothelial cells in the adult fish heart is an entirely novel finding. The expression of hematopoietic markers in endothelial cells has previously only been noted in a developmental setting in both mouse and fish and, even then, not in the developing fish heart. The finding of a developmental expression pattern in an injured adult heart is perhaps not unexpected, as it has been shown repeatedly that the injury response involves re-establishment of developmental pathways. This is likely because development is normally the period of most dramatic growth within an organism, and successful regrowth of damaged tissue is often desired after injury. Within the heart, for example, this is seen in the

upregulation of developmental growth factors that promote cardiomyocyte proliferation, reactivation of EMT and signalling from the epicardium, amongst others (well reviewed in (Porrello & Olson 2014), (Y. Huang et al. 2013; Masters & Riley 2014)).

Endothelial cells that express Runx1 are seen during developmental hematopoiesis, in a process that is repeated in all common laboratory vertebrates and also humans. Hematopoiesis is the process by which all cells that comprise the blood and their progenitors are formed. It occurs in two forms during development, the first of which is primitive hematopoiesis, an initial wave of short-lived, limited cell types that aid the growing embryo. These cells are then replaced by the products of the second form of hematopoiesis that occurs later in development, definitive hematopoiesis, which produces all the blood cells and long-lived progenitors that are required in the adult. Hematopoietic endothelial (HE) cells arise during the production of hematopoietic stem cells that happens during definitive hematopoiesis. HE cells are specialised cells that give rise to hematopoietic stem cells through a cellular transition (Sood & Liu 2012; Dzierzak & Speck 2008). Specifically, a subset of endothelial cells, termed the hemogenic endothelium, begin to downregulate endothelial genes and upregulate genes related to hematopoietic cells in a process known as endothelial-to-hematopoietic transition (EHT) (Swiers et al. 2013; Zovein et al. 2008; Eilken et al. 2009; Jaffredo et al. 1998; Lancrin et al. 2009; Bertrand, Chi, et al. 2010; Boisset et al. 2010; Kissa & Herbomel 2010; Lam et al. 2010). The traditional view is that this process occurs in a spatially and temporally restricted manner, with the primary site in zebrafish being in the dorsal aorta between 30-32 and 48 hpf (Kissa & Herbomel 2010; Bertrand, Chi, et al. 2010). Endothelial cells undergoing EHT in live zebrafish embryos and in cultured HE from mice can be followed by microscopy. These endothelial cells are seen to contract into the sub-aortic space,

becoming crescent shaped, before then bending enough that its endothelial neighbours attach to each other and the now-rounded cell is eventually released (Fig. 4.7) (Kissa & Herbomel 2010; Boisset et al. 2010; Lam et al. 2010). This change is concurrent with the upregulation of a hematopoietic gene program of which Runx1 is an essential part, with the loss of Runx1 abrogating or extensively diminishing EHT and the formation of HSCs during definitive hematopoiesis (Kissa & Herbomel 2010; Boisset et al. 2010; Lancrin et al. 2009; Lacaud et al. 2002; Lam et al. 2010; Tanaka et al. 2012; Chen et al. 2009). Runx1 acts to promote cell migration through the direct upregulation of genes involved in cell movement and adhesion, and also discontinues endothelial gene expression through control of downstream epigenetic silencers (Lie-A-Ling et al. 2014; Lancrin et al. 2012; Thambyrajah et al. 2016).

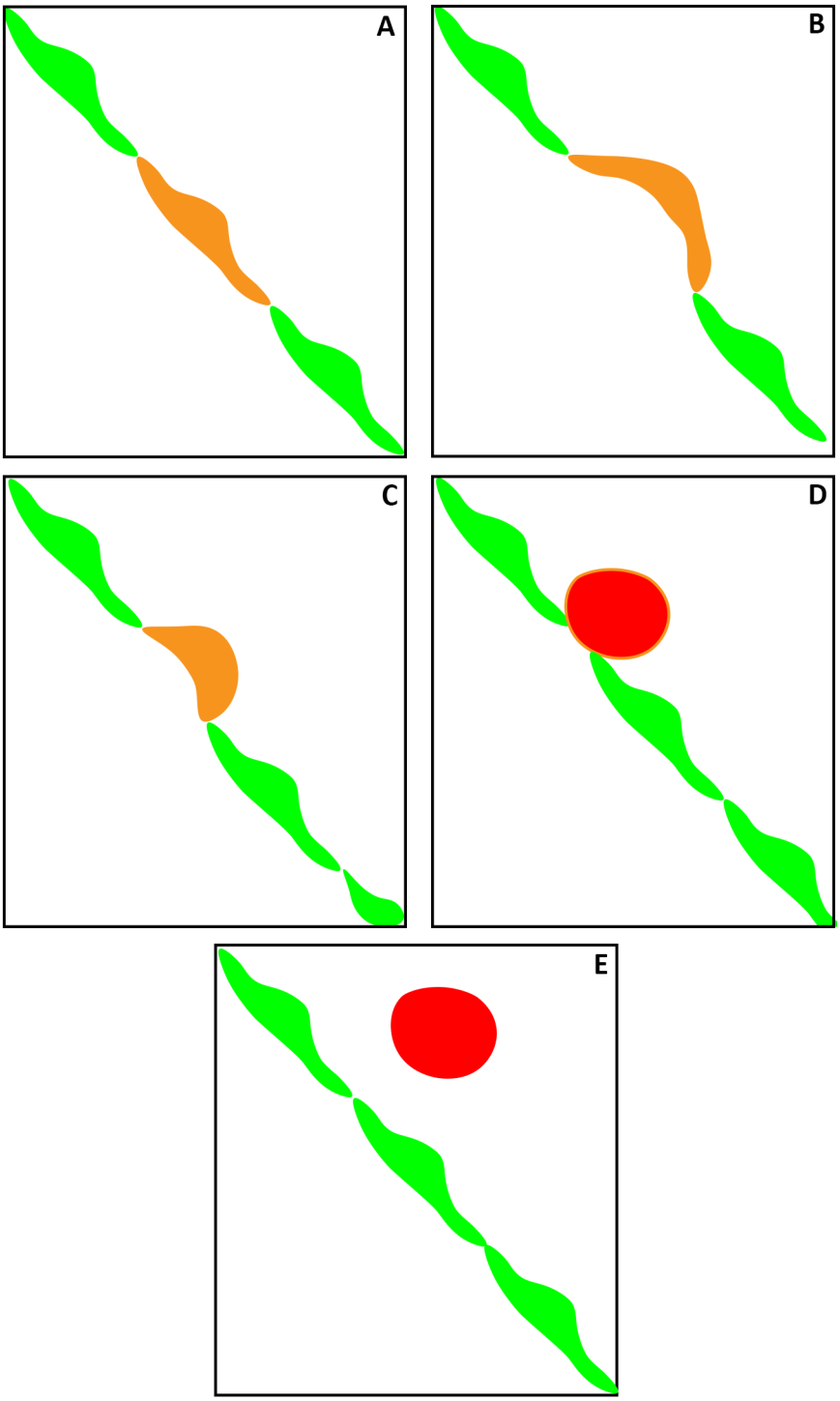


Fig. 4.7 Schematic showing the cell movements of an endothelial cell undergoing EHT. **A** shows a row of hemogenic endothelial cells (green) where one cell is about to undergo EHT (orange). **B** shows this cell bending outwards and becoming crescent-shaped. **C** shows this cell becoming increasingly rounded and pulling its neighbours inwards. **D** shows EHT nearly complete, with the cell undergoing EHT being rounded and more resembling a mature HSC (now red). **E** The cell then detaches completely and its former neighbours are in contact, leaving an unbroken endothelium.

The co-expression of Runx1 in endothelial cells in the injured fish hearts raises the possibility that EHT could be yet another developmental pathway that is re-activated after injury. This is

not as unexpected as it first appears; there is growing evidence that EHT is not as spatially restricted as first thought, with HSC emergence being posited from other organs, including the head and, most importantly here, the heart (Li et al. 2012; Yzaguirre & Speck 2016; Nakano et al. 2013). Yzaguirre & Speck advanced the theory that the heart gives rise to multiple waves of hematopoiesis, similar to those seen in the yolk sac during development, with the initial production of hematopoietic progenitors with myeloid and erythroid potential from Nkx2-5 and Isl1 positive endocardium, followed by the presence of Runx1-positive endocardial cells and clusters in the trabecular myocardium, ending with the formation of cardiac blood islands from the ventricular endocardium (Jankowska-Steifer et al. 2015; Yzaguirre & Speck 2016; Nakano et al. 2013; Ratajska et al. 2009). Additionally, cultured adult mouse endothelial cells have been shown to have the capacity to undergo EHT and form functional HSCs capable of clonal engraftment, whilst EHT in the lungs of adult humans has been proposed as a major player in pulmonary arterial hypertension (Lis et al. 2017; Liang et al. 2017). This evidence that EHT occurs in the developing heart and can occur in adult tissues, under certain conditions, suggests that injury-derived signals may be sufficient to permit EHT in the endocardium of the fish heart after injury.

The signals involved in initiating and regulating EHT during development are present in the heart after injury. Hedgehog signalling in the positioning of endothelial progenitors in the dorsal aorta and in arterial specification is necessary for HSC formation (Gering & Patient 2005; Kim et al. 2013). After injury, hedgehog signalling is required for epicardial cell migration and epicardial and myocardial proliferation (Choi et al. 2013; Wang et al. 2015). Downstream of hedgehog, VEGF signalling activates the Notch signalling pathway, which is crucial for the successful establishment of EHT (Burns et al. 2005; Nakagawa et al. 2006;

Gering & Patient 2005; Kim et al. 2013; Burns et al. 2009). In addition, TGFβ signalling has been implicated in both HE specification and EHT itself, acting through Notch signalling (Monteiro et al. 2016). Interestingly, Notch signalling pathway genes are strongly upregulated in the endocardium of the heart after injury in zebrafish, later becoming restricted to the endocardium nearest the wound. This upregulation is associated with drastic gene and morphology changes in the endocardial cells (Kikuchi et al. 2011; MacGrogan et al. 2018; Münch et al. 2017; Raya et al. 2003; Zhao et al. 2014). TGFβ signalling is also upregulated in the wound site after injury, where it is implicated in regulation of ECM deposition in the scar and cardiomyocyte proliferation (Chablais & Jaźwińska 2012; Choi et al. 2013). Relatively recently, it has been shown in the zebrafish that inflammatory signals can also play important roles in EHT, with the pro-inflammatory cytokine TNFα from embryonic neutrophils interacting with HE cells, leading to active NF-κB in nascent HSCs that is necessary for their development (Espín-Palazón et al. 2014). Another inflammatory response required for correct progression of EHT is the inflammation-responsive MMP2 in zebrafish, which is required to remodel the ECM during HSC budding in a CXCL12 dependent manner (Theodore et al. 2017). There is a dramatic and sustained increase in TNFα production almost immediately after injury and *mmp2* is also upregulated, both of these play an important role in scar dynamics (de Preux Charles et al. 2016; Gamba et al. 2017; W.-C. Huang et al. 2013). Therefore, to a certain extent the cocktail of ingredients required for HSC emergence from hemogenic endothelium has been shown to be present after injury in the zebrafish. However, whether the timing and positioning of these signals is suitable and whether the adult endocardium is responsive to these signals is unknown.

The co-expression of Runx1, a key marker of HSCs, and an endothelial marker in the injured *A. mexicanus* fish heart is tentatively suggestive of the formation of a hemogenic endothelium in the *A. mexicanus* heart after injury. The fact that the endocardium has been shown to potentially undergo EHT during development, and that developmental signals that activate EHT in hemogenic endothelium are once again found in the injured heart, lends more credence to this possibility.

4.7 USING ZEBRAFISH TO INVESTIGATE WHETHER A HEMOGENIC ENDOTHELIUM IS FORMED IN THE FISH HEART AFTER INJURY

Establishing whether EHT occurs in the fish heart after injury required reliable marking of cells with a dual HSC/endothelial identity, so that these cells could be followed across the injury timeline and their nature defined more faithfully. Labelling cells with fluorescent proteins allows the cells to be isolated, for example by Fluorescence Activated Cell Sorting (FACS), based on this expression for further experimentation. It was therefore necessary to use fluorescently-labelled transgenic fish, as the expression of the fluorescent label should faithfully recapitulate endogenous expression of the promoter region that controls the transgene expression. As mentioned previously, creating transgenic *A. mexicanus* is still very difficult due to the long generational time and generating the line would take longer than the duration of the project. Fortunately, a zebrafish line that has labelled Runx1-positive cells is in existence, tg(*runx1-P2:citrine)* (henceforth known as r*unx1:citrine)*, that has been generated by and made available to the laboratory by Professor Roger Patient, Dr Florian Bonkhofer and Dr Jana Koth. This line has a fluorescent protein, Citrine, under the control of the P2 region of the *runx1* promoter. The P2 promoter is one of 2 Runx1 promoter regions controlling expression of 2 different isoforms. The P2 promoter is known to drive expression

in definitive HSCs in the dorsal aorta during development (Yi Ni Lam et al. 2009). In this line all cells expressing *runx1* from the P2 promoter should have Citrine present in their cytoplasm. In the uninjured heart, the only Citrine-positive cells seen are in the blood, suggesting circulating hematopoietic cells. The laboratory is also in possession of an endothelial line, tg(*kdrl:Has.HRAS-mCherry*) (henceforth known as *kdrl:mCherry*), where a membrane-trapped mCherry is under the control of the *kdrl* promoter, meaning the membranes of all endothelial cells are labelled with mCherry. The availability of these lines means that double positive cells are easy to identify, track and isolate for further experimentation. Therefore, this line was used to check for double cells like that seen in *A mexicanus* and then for further characterisation and analysis.

4.8 THE RUNX1-P2:CITRINE TRANSGENE RECAPITULATES RUNX1 MRNA EXPRESSION AND IS FOUND IN MULTIPLE CELL TYPES AFTER INJURY

To ensure that the Runx1 transgenic line faithfully recapitulates Runx1 mRNA expression, RNAscope was performed in injured zebrafish hearts. Visual analysis of transgene expression in the zebrafish heart 3 days after cryoinjury shows that the transgene is expressed extensively in the wound area and in the regenerating tissue around the wound (Fig. 4.8 A). In contrast to the antibody staining seen in *A. mexicanus*, the transgene appears to be expressed in endothelial-type cells only within and in very close approximation to the wound site, whereas with the antibody expression all endothelial cells in the whole heart are positive (Fig. 4.8 A, C). Also in contrast to *A. mexicanus*, where antibody staining is limited to endothelial and HSC-type cells, staining in other cell types is seen, with strong staining seen in what appears to be the regenerating myocardium in the border zone of the wound and in

the epicardium (Fig 4.8 B, C arrowheads). These are interesting findings, as these are all tissues that are known to play key roles in successful heart regeneration.

Importantly, Runx1 mRNA, as indicated by the punctate RNA staining, is found in Citrine-positive cells (Fig. 4.8). Most cells positive for the transgene contain 3 or more points of staining, with the myocardial cells often having many more. Cells that are not Citrine-positive can be seen to contain RNAscope staining, however, these are at low levels, often only 1 dot, and may represent low basal expression or cells that are beginning to upregulate Runx1 expression, before they have formed the Citrine protein.

The conclusion is that the transgene incorporated to create *runx1:citrine* fish recreates endogenous *runx1* expression faithfully enough for further experimentation. However, it has also highlighted that the expression pattern of Runx1 in the transgenic zebrafish after injury varies in some ways from that shown by the antibody staining in *A. mexicanus*. The staining is similar, in that it is found in HSC-like and endothelial-like cells in the wound, but differs in the extent of endothelial staining, and the appearance of staining in myocardial and epicardial cells. This could be due to the differences between antibody staining and true endogenous expression, as where the antibody binds in *A. mexicanus* is not known, whereas the RNAscope probe has been specifically designed and targeted toward *runx1* expression in zebrafish. There is a possibility that it could be due to fundamental differences in expression pattern between the two fish species.

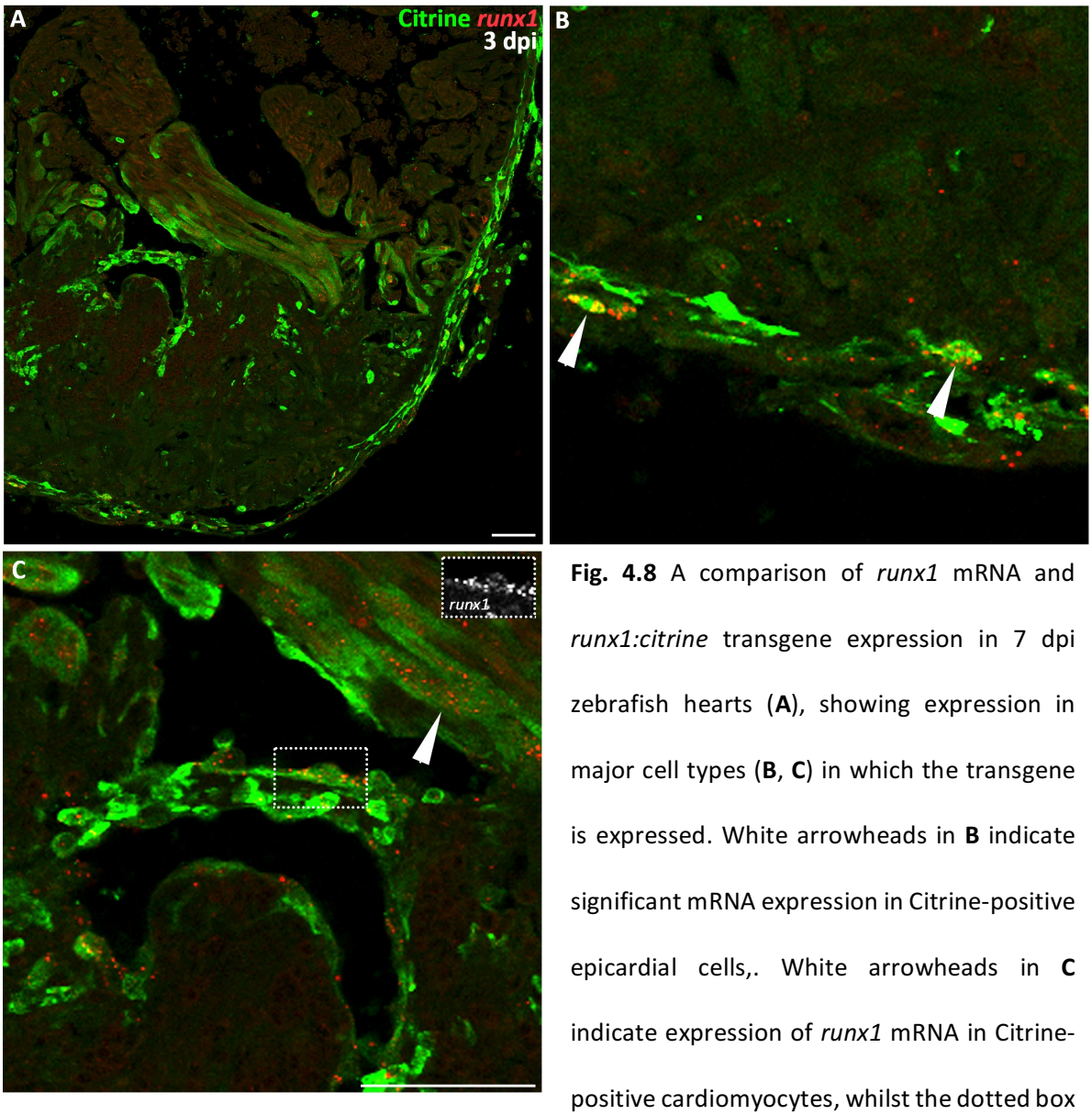


Fig. 4.8 A comparison of *runx1* mRNA and *runx1:citrine* transgene expression in 7 dpi zebrafish hearts (**A**), showing expression in major cell types (**B**, **C**) in which the transgene is expressed. White arrowheads in **B** indicate significant mRNA expression in Citrine-positive epicardial cells,. White arrowheads in **C** indicate expression of *runx1* mRNA in Citrine-positive cardiomyocytes, whilst the dotted box indicates expression in endocardial cells, shown with the red panel in the top right hand corner. N=3. Scale bars indicate 100 µm.

4.9 THE ZEBRAFISH HEART ALSO CONTAINS PDGFRα-POSITIVE RUNX1-POSITIVE AND ERG1-POSITIVE RUNX1-POSITIVE CELLS AFTER INJURY

In order to use the transgenic zebrafish to investigate the novel endothelial/hematopoietic cell found in the cavefish heart, it was important to establish whether the same type of cell,

namely a Pdgfrα/Runx1 and Runx1/Erg1 positive cell, is present in the zebrafish. This was especially important as the expression pattern of Runx1 appears to differ slightly between the two species, whether due to the techniques involved or underlying species differences.

Antibody staining for Pdgfrα was performed in transgenic fish hearts 7 days after cryoinjury. The staining indicates that Pdgfrα/Runx1 double positive cells are present in what appears to be the endothelium within, and in close apposition to, the wound site (Fig. 4.9 arrowheads). It also appears that there are double positive cells within the epicardium surrounding the wounded area. The staining of the endothelial-type cells looks very similar to that seen previously in both the surface fish and the cavefish.

Co-staining with Erg1, the endothelial marker, shows that, like in *A. mexicanus* ecotypes, Runx1 expression overlaps with expression of the endothelial marker in the zebrafish wound site (Fig. 4.9, arrowheads). These cells appear to be mostly deep in the wound in the dead tissue, rather than in the regenerating myocardium, though some are present there also. Double-positive cells are found away from the wound, in the rest of the ventricle also, but they are extremely rare.

Therefore, it appears that the novel cell types identified in *A. mexicanus* are present also in the zebrafish, and successfully demarcated by the Runx1 transgene. The presence again of Runx1/ERG1 hematopoietic/endothelial dual-identity cells indicates that EHT may also occur in the zebrafish heart and could be common to teleost fish. However, ERG1 has limitations as an endothelial marker and can also delineate certain blood cells, therefore, use of a transgenic fish line with an endothelial-specific marker is essential. Therefore, double transgenic *runx1:citrine*; *kdrl:mCherry* fish were generated, where endothelial cells have red fluorescently-labelled membranes.

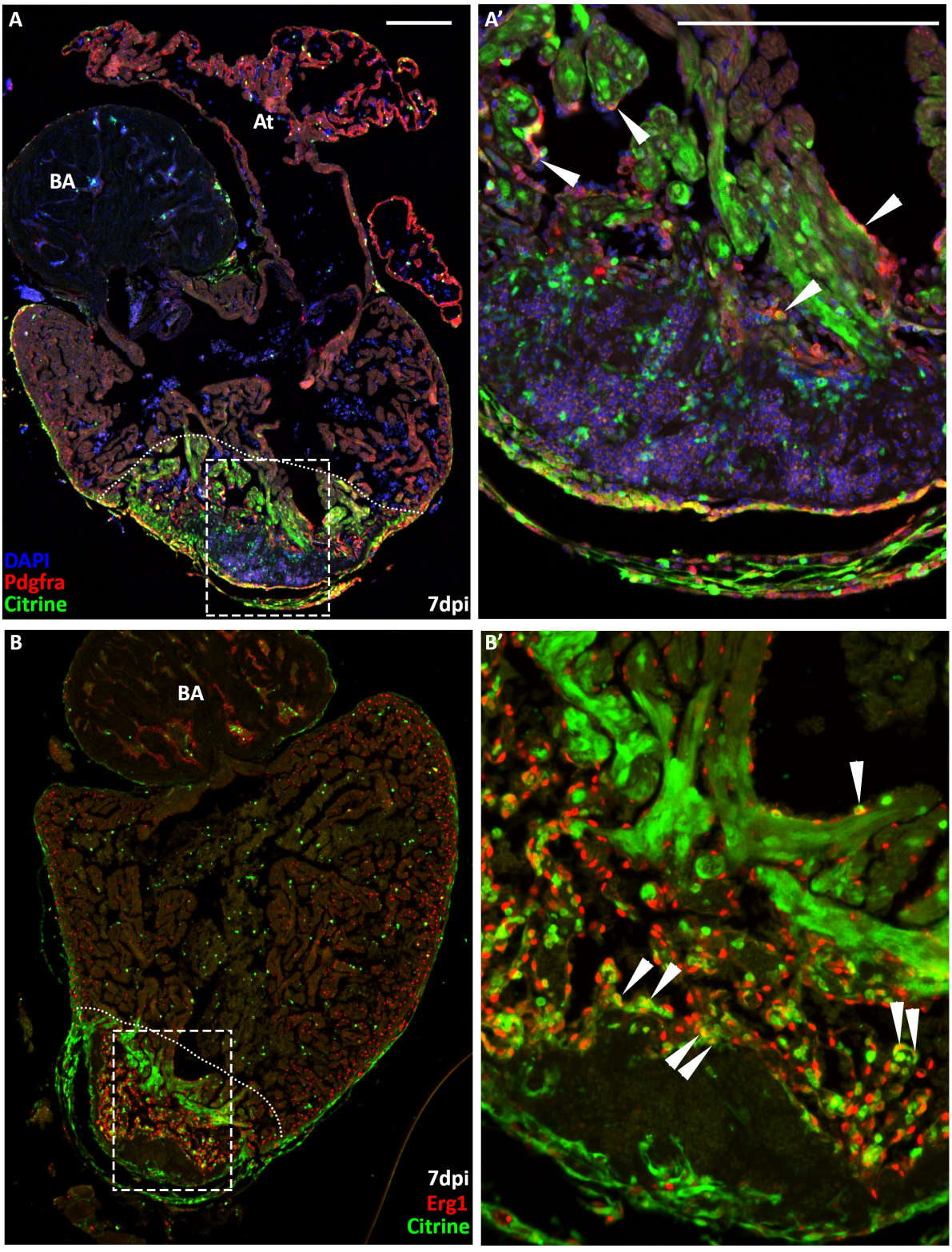


Fig. 4.9 Immunohistochemistry showing co-expression of Citrine from the *runx1* transgene with Pdgfrα (**A**, **A'**) and erg1 (**B**, **B'**) in the injured zebrafish heart, similar to that seen previously in *A. mexicanus*. Arrowheads indicate co-expression of markers. Dotted lines show approximate apical injury region; dashed boxes indicate magnified regions. N=3. Scale bar shows 100 μm.

4.10 RUNX1 KDRL DOUBLE POSITIVE CELLS APPEAR IN RESPONSE TO WOUNDING

To understand the nature of the Runx1 Kdrl double positive cell production in fish hearts, expression was analysed in hearts isolated from uninjured fish, fish that had undergone a sham procedure and fish at 1, 3, 7 and 14 days after cryoinjury.

Uninjured fish show little to no Runx1 expression in anything other than the occasional cell present in the blood, presumably a circulating HSC or, potentially, the progeny of an HSC in which Citrine has not yet been degraded (the maturation and degradation times of Citrine are not known, or could not be found). These cells tend to have extremely bright Citrine staining (Fig. 4.10 A, A'). There are very few double positive cells in uninjured fish hearts. Surprisingly, sham operated fish show some response, with Runx1 expression seen in the epicardium and compact myocardium (Fig. 4.10 B, B'). Again, the only other cells that have Citrine expression are circulating blood cells that are very bright and there are few double positive cells present.

At 1 dpi, there appear to be many round, bright Runx1-positive cells in the wound site, present in clusters (Fig. 4.10 C, C'). These resemble more the circulating blood cells seen in the uninjured and sham hearts in terms of morphology and levels of Citrine present, and they are also predominantly Kdrl negative. There are some double positive cells present in the wound, some of which look to be bright (magenta arrowhead) and some with greatly reduced levels of Citrine (white arrowheads). These cells with low levels of Citrine shall be called 'dim' from here further. The bright Citrine positive cells are presumably involved in the initial immune response to the injury in some capacity. The dim ones could represent transitioning cells, in which the fluorescent proteins are degrading or beginning to be switched on. Interestingly, the entire epicardium appears to express Runx1 at this stage, as Citrine expression is not limited to the peri-wound area and covers the ventricle.

At 3 dpi, there are drastically fewer bright, round Citrine-positive cells in the wound site, though they are still present (Fig. 4.10 D, D'). There now appear to be many double positive 'dim' cells in the wound area, that show a more endothelial morphology (white arrowheads). However, there are very few of the bright double positive cells seen at 1 dpi. Epicardial expression is becoming more limited to the area covering the wound and its immediate surroundings. Interestingly, there also appear to be high numbers of 'dim' double positive cells in the wound site at 7dpi (Fig. 4.10 E, E'), showing that this process takes place across a long period of early injury resolution. Runx1 expression appears to be more widespread in the myocardium, whilst epicardial expression appears more limited, compared to 3 dpi. By 14 dpi, it appears that only myocardial Runx1 expression is remaining, with endothelial and epicardial Runx1 expression greatly reduced (Fig. 4.10 F, F'). There are very few double-positive cells and myocardial Citrine expression is also reduced, indicating a return to basal pre-injury levels.

Counts were performed looking at the numbers of bright and dim double positive cells in the wound and the rest of the ventricle. These results show an interesting pattern, with an initial wave of bright double positive cells that resemble more blood-like cells than endothelial cells seen in the wound site at 1 dpi and a small rise in the number of dim, more endothelial-like double positive cells. At 3dpi, the bright double positive cells are no longer present, but a huge number of dim cells are. This number is roughly maintained at 7dpi, dropping drastically by 14dpi.

Therefore, it would appear that the formation of double positive cells is part of the early injury response before scar resolution, with the 'dim' endothelial type cells being the greatest in number in the period of scar deposition and cardiomyocyte proliferation induction. The

formation of such large numbers of these cells over such a long period of injury resolution is suggestive of a key role of injury response.

Fig. 4.10

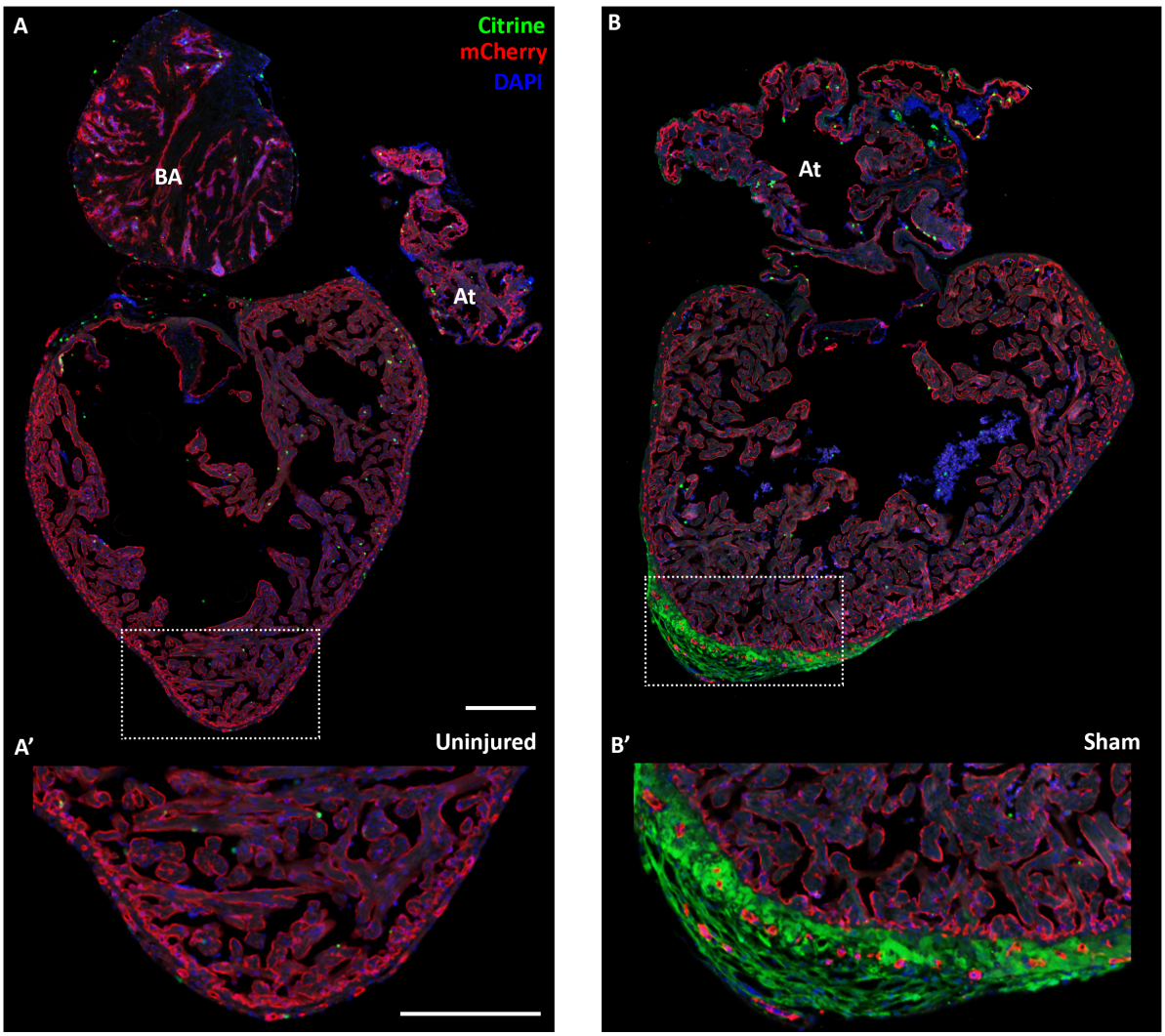
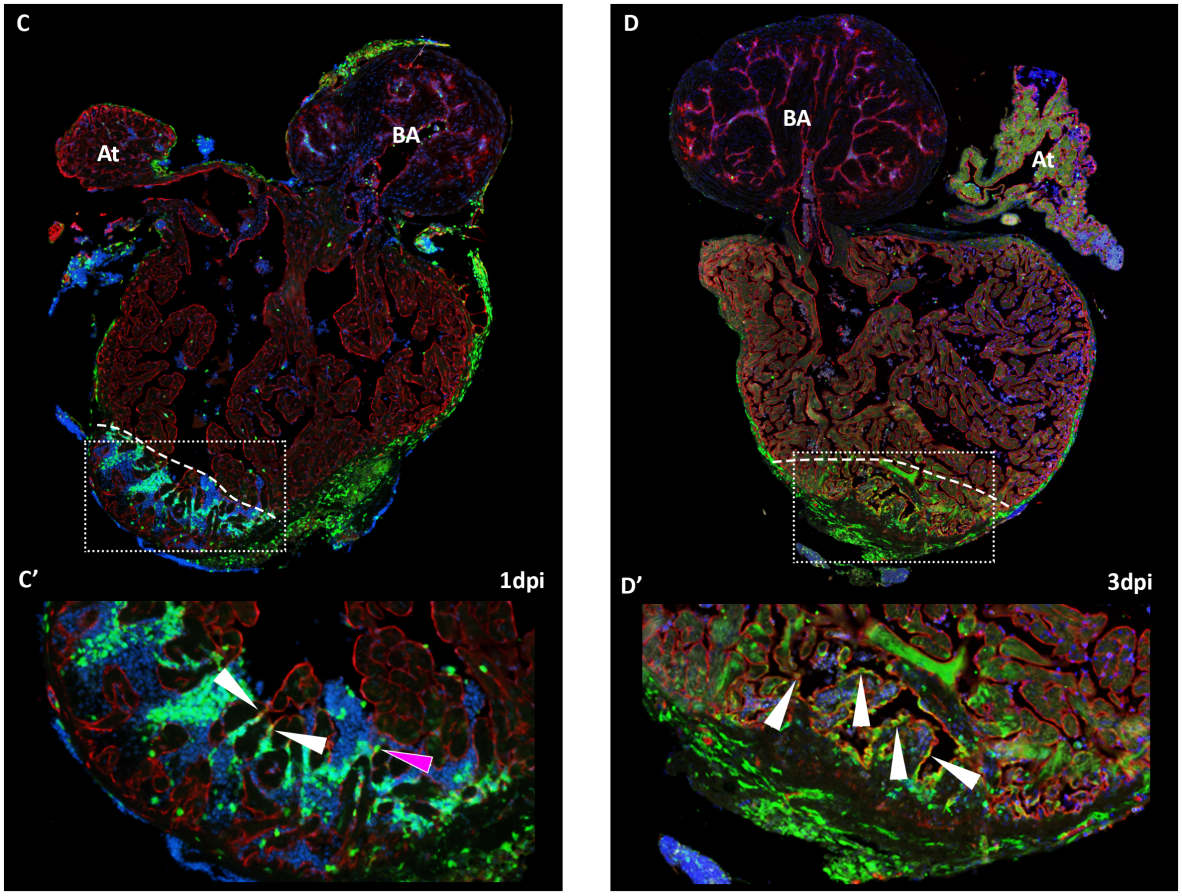
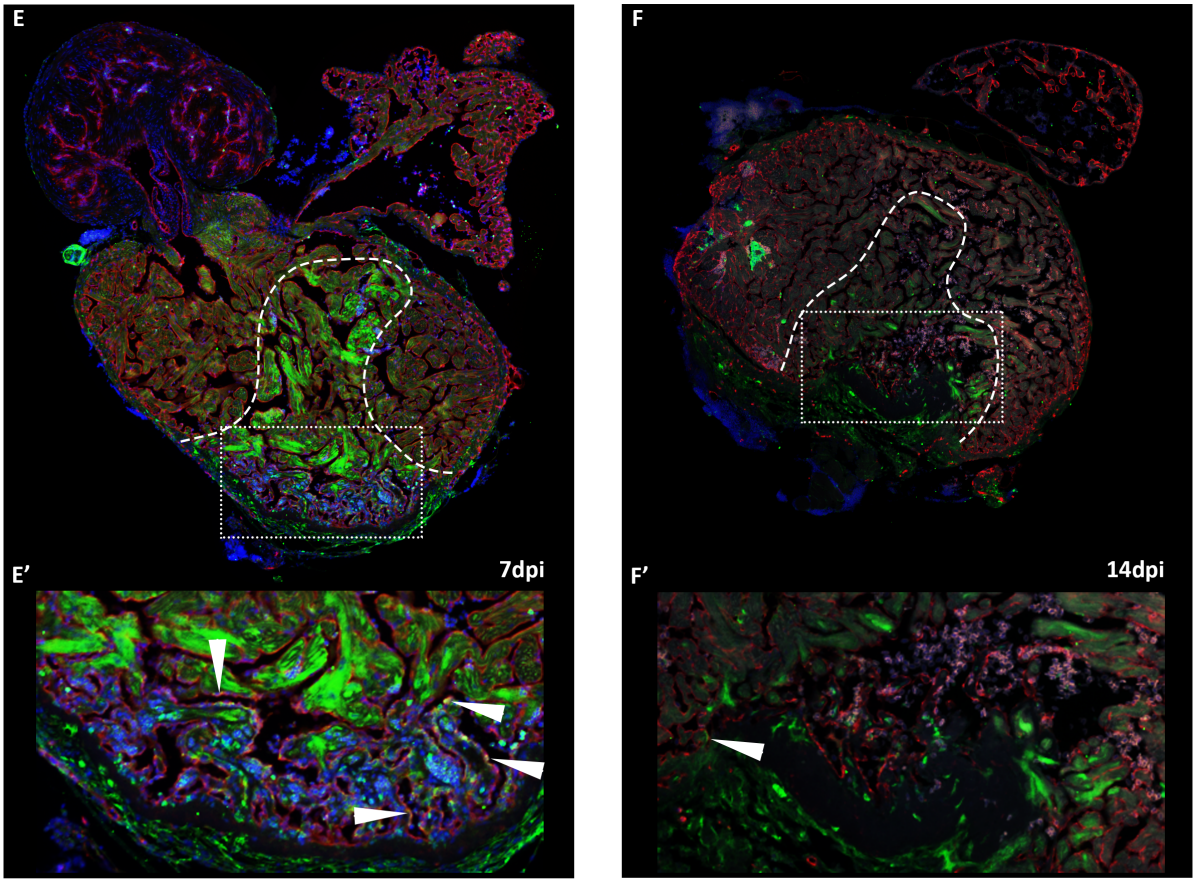


Fig. 4.10





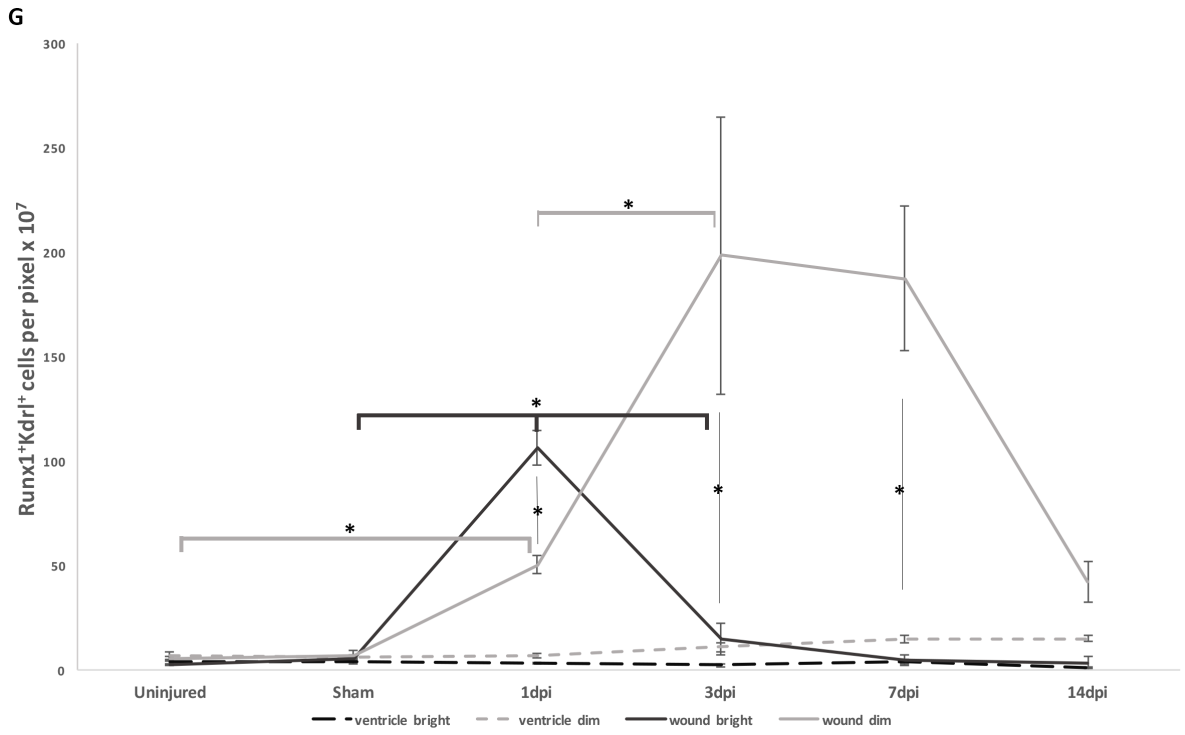


Fig. 4.10 Immunohistochemistry for Citrine and mCherry in sections from *runx1:citrine*; *kdrl:mCherry* fish that are uninjured (**A**, **A'**), sham injured (**B**, **B'**) and 1 (**C**, **C'**), 3 (**D**, **D'**), 7 (**E**, **E'**) and 14 (**F**, **F'**) dpi and

quantitative analysis of double cell numbers across the injury timeline (**G**). White arrowheads indicate endothelial type double-positive cells with dim expression of fluorescent proteins. The magenta arrowhead indicates a bright double positive cell, resembling more a blood cell. The lines indicate the approximate injury area, whilst the boxes indicate the magnified area. N=4 per timepoint. Statistics performed by two-way ANOVA, $p<0.05$ *, $p<0.001$ ** for comparisons between ventricle dim and ventricle bright cells and between time-points. Vertical bars indicate differences between wound bright and dim cells at that timpoint and horizontal bars indicate differences between wound bright (dark grey) and dim (light grey) between timpoints. Comparison of wound bright and dim cells at 3 dpi performed by unpaired t-test. Scale bars are 100 μm.

4.11 RUNX1 KDRL DOUBLE POSITIVE CELLS APPEAR TO HAVE MULTIPLE MORPHOLOGIES THAT REPRESENT THE STAGES OF EHT

Sections of hearts isolated from *runx1:citrine*; *kdrl:mCherry* fish at 3 days post cryoinjury show the presence of many double positive cells within the wound site. These cells have many different shapes; some are quite flat and some look like they are nearly detached from the rest of the endothelium. The endothelial cells that are most flat seem to have only a little Citrine, perhaps representing the switching on of *runx1* (Fig. 4.11, 1). There are others that look like a small bump in the endothelial surface that are a little rounder and have considerably more Runx1 expression throughout the cell (Fig. 4.11, 2). There are then many cells that appear to be rounder still and full of diffuse Citrine expression (Fig. 4.11, 3). Some of these very rounded cells are not in considerable contact with the surrounding endothelium, as shown by them being very nearly completely enclosed in mCherry (Fig. 4.11, 4). They look as though they are about to detach.

Past papers looking at visualisation of EHT, as mentioned above, show that hemogenic endothelial cells start off flat, then begin to round-up and bring their neighbours into close apposition with each other. When its neighbours meet, the cell is then extruded into the lumen. The different cell morphologies seen in the wound could be snapshots of cells at different points in this process, as shown in Fig. 4.9.

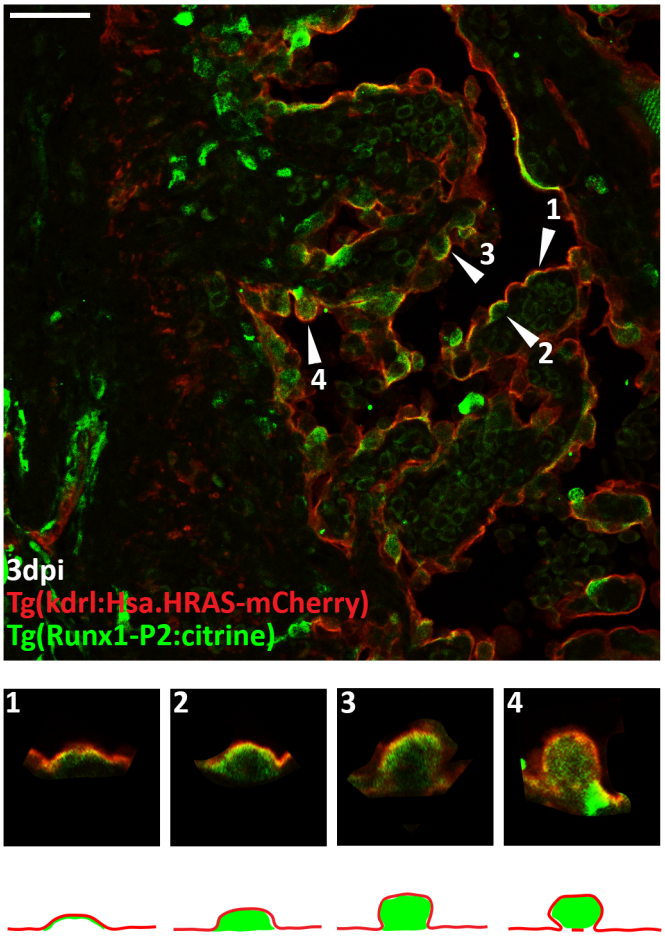


Fig. 4.11 A demonstration of the potential stages of EHT within the 3 dpi *runx1:citrine*; *kdrl:mCherry* heart. **1** represents the first stage, with initial *runx1* expression within a flattened endothelial cell. **2** and **3** represent the cell becoming increasingly rounded and **4** shows the cell beginning to detach, with a complete endothelium forming below. Arrowheads and numbers in the large panel indicate the cells in the boxes below. Scale bar is 50 μm.

4.12 DISCUSSION

This work shows that blood and endothelial cells that are Pdgfrα-positive in the *A mexicanus* heart fluctuate in number in response to injury and that similar populations in the wound also appear in great number. The changes in cell number follows the same trend in both ecotypes, but there are subtle differences that might allude to altered function or response. Further

identification of these cells with other markers shows that these cells express stem cell markers, as well as an unexpected expression of blood cell markers in the endocardial-type Pdgfrα-positive cells and blood borne Runx1-positive cells. Further analysis of the intriguing Pdgfrα and blood marker-positive endocardial cells in *A mexicanus* and zebrafish shows that cells of a dual Runx1/endothelial identity are formed in the fish heart after injury in great numbers and for a sustained period, in a manner that is conserved amongst both species of teleost fish. The fact that these cells express both an endothelial marker and Runx1, a key regulator of hematopoiesis, indicates the possibility that a hemogenic endothelium is formed in the wound site after injury. During development the hemogenic endothelium forms HSCs through prescribed cell movements and these look to be reproduced in the cell morphologies seen in the double positive Runx1/Kdrl fish hearts imaged at both 3 and 7dpi. It is therefore possible that a hemogenic endothelium formed after injury might be undergoing EHT, extruding HSCs into the wound area.

The expression of Pdgfrα in hemogenic endothelium is, on the face of it, surprising. It is mostly seen as a marker of mesenchymal lineages at varying states of differentiation. However, the finding of Pdgfrα in the developing endocardium in zebrafish (El-Rass et al. 2017) indicates that expression of Pdgfrα in adult endocardial cells might demarcate endothelial cells that have retained some of their developmental potential, especially as these cells are also positive for some progenitor markers. The appearance of these cells within the wound suggests that wound endothelial cells resemble their developmental counterparts. Knowing that the endocardium has been seen to undergo EHT during development (Nakano et al. 2013), it is easy to speculate that these developmental endocardial cells that undergo this process still express Pdgfrα.

Given the exciting possibility of a hemogenic endothelium after injury, the blood-borne Pdgfrα-positive cells were not investigated further due to the limited time and material constraints. However, the data showing that blood-borne Pdgfrα-positive cells increase in number at 3 dpa and then decrease after suggests that they might play a role in the initial wound response. The differences between the two fish, where the cavefish possess an initial higher number than the surface fish, suggests that cavefish have increased numbers of circulating progenitors at baseline. It is interesting to speculate how this difference could affect injury response. Investigating the nature of these cells and whether they are indeed circulating progenitors could provide an interesting new insight into regenerative capacity. It is also possible that these cells are the progeny of Pdgfrα-positive hemogenic endothelial cells that have undergone EHT and have still detectable Pdgfrα expression.

Whilst this chapter provides evidence that EHT occurs after injury, this data is limited by the fact that these images are only a snapshot in time in one focal plane and it would be hard to conclude that these are not cells all in the same state sectioned in different orientations, or, whether the cells that look like they are detaching are, in fact, invading. The work is further limited by the fact that it only uses 2 markers, one for each cell type. Kdrl is a well-established endothelial cell marker, but the specificity of Runx1 to HSCs in the context of the heart is unknown. Indeed, Runx1, as shown in this data, is expressed in cell types other than blood-borne cells and prospective hemogenic endothelium in the heart after injury. It is also expressed in cardiomyocytes and epicardial cells; these cells have in common the fact that they are engaging in known developmental pathways. Runx1 is found in multiple organ systems and its activity is not limited to regulation of hematopoiesis; it seems to generally play a role in regulation of the differential and proliferative state of a cell (Bao et al. 2018;

Sarper et al. 2018; Zhou et al. 2018; Umansky et al. 2015; Murthy et al. 2014). Therefore, it could be that its expression is linked to the endothelium reaching a less differentiated state, that is not linked to an acquisition of hematopoietic potential.

If it is true that the Pdgfrα-positive endocardium becomes hemogenic after injury, it is interesting to speculate about the subtle differences in cell numbers of endocardial cells between the ecotypes of *A. mexicanus*. Before injury, Surface fish have more endocardial Pdgfrα-positive cells than cavefish and this number decreases after injury. The cavefish endocardial cells appear to increase in number after injury initially and it has many more than surface fish at 0 dpa, before numbers decrease similarly to the surface fish. This could mean that more cells are available to undergo EHT after injury in the cavefish, indicating that EHT levels might differ between the two fish.

Taking the current findings and their limitations into account, the decision was made to perform further experiments to image the process of EHT in real time and analyse the genetic identity of double positive cells in-depth. These experiments were designed to look for expression of other genes found in the developing hemogenic endothelium and show that individual endothelial cells can undergo the cell morphology changes associated with developmental EHT. These experiments are described in the next chapter.

4.13 CONCLUSION

The work in this chapter indicates that the activated wound endothelium in teleost fish may become a hemogenic endothelium, that undergoes EHT after injury and forms HSCs *de novo*. The potential formation of a hemogenic endothelium from injury-area endocardium after

injury has never been proposed before, in fish or mammals, and is an exciting finding that requires further exploration. Further work will aim to investigate more deeply whether this is occurring and try to investigate the effect of Runx1-positive cells in heart regeneration.

CHAPTER 5 – INVESTIGATING INJURY INDUCED HEMOGENIC ENDOTHELIUM

CHAPTER 5 – INTRODUCTION

5.1.1 SUMMARY OF THE CHAPTER

The identification of Pdgfrα-positive populations in the blood and on the endocardium after injury as putative hematopoietic progenitor cells, which are potentially formed from the endothelium via recapitulation of a developmental cell-transition process, endothelial-to-hematopoietic transition (EHT), is a novel and intriguing finding that requires further investigation. The following chapter describes work done to examine whether this process does indeed occur after injury and what role it might play in regenerative capacity, by attempting to visualise this process occurring in the heart in real time, capturing these cells based on transgene expression and then looking at their gene expression profile. Attempts at functional analysis to evaluate the effect of the loss of Runx1, a key regulator of hematopoiesis, on this population are also described.

After development of a novel experimental technique to allow imaging of the inside of the heart after injury, it is shown that individual endocardial cells can undergo the same cell movements as that seen during developmental EHT, suggesting hematopoiesis from the endocardium after injury. Isolation of cells that express both Kdrl, the endothelial marker, and Runx1, the HSC marker, shows that endothelial/hematopoietic cells are found in increased numbers in single cell digestions of injured hearts over uninjured hearts. Furthermore, analysis of the expression of key markers of endothelium, hemogenic endothelium and mature HSCs in isolated Runx1/Kdrl-positive cells marks them further as a hemogenic endothelium.

Analysis of the Runx1 mutant shows that loss of Runx1 function is cardio-protective, but also enhances proliferation in cardiomyocytes after injury. In addition, the mutants show potentially delayed scar deposition that clears at a slower pace relative to myocardial regeneration than in the wildtype. Analysis of sections shows that a HE appears to still be specified in the mutant. Single cell sequencing analysis of cells doubly or singly positive for Runx1 and Kdrl transgenes from uninjured and injured WT fish and injured Runx1 mutant fish indicates that mutant fish lack thrombocytes and have additional, or increased numbers, of hematopoietic progenitor populations than WT fish. Their cardiomyocytes appear to have increased expression of hemoglobins, which may protect them from apoptosis induced by the cryoinjury as they are less likely to become starved of oxygen. There is also evidence that they have an altered metabolism and increased calcium signalling capacity. Cells that are positive for both Runx1 and Kdrl transgenes are shown to have similar gene expression profile to developmental hemogenic endothelium, suggesting that the injured endocardium does indeed become a hemogenic endothelium after injury. Further analysis of the data set in comparison to developmental single cell data could indicate if these cells have lineage-restricted potential that would suggest a function. For example, they could be more limited to leukocyte fate than erythropoietic.

In summary, the following chapter describes further evidence for the presence of a hemogenic endothelium after injury in the fish heart, through visualisation of the process occurring in living tissue and through transcriptomic analysis of isolated cells. It also describes attempts to ascribe a function to the HE in regeneration and shows that loss of *runx1* has a positive net effect on regeneration through increased speed of cardiomyocyte renewal, but with some deficiencies in scar removal.

5.1.2 BACKGROUND INFORMATION

The identification of a potential hemogenic endothelium formed in the wound raised the questions: what is the nature of the hemogenic endothelium; what cell types does it produce; and what effect does EHT in the wound have on injury outcome? The work in this chapter aimed to address these questions.

Single cell sequencing has been used extensively to characterise gene expression during hematopoietic differentiation from before HE specification, through to HE, HSCs and their lineages (Baron et al. 2018; Athanasiadis et al. 2017; Guibentif et al. 2017; Angelos et al. 2017; Macaulay et al. 2016; Zhou et al. 2016; Drissen et al. 2016; Carmona et al. 2017). These studies on the whole indicate that hematopoietic differentiation is a gradual process, with gradual transcriptional changes denoting differentiation down certain lineages. However, they demonstrate that the transcriptional state of hematopoietic stem cells can be quite distinct, with prediction of their subsequent lineage on expression of just a few genes possible, even before endothelial genes are down-regulated (Athanasiadis et al. 2017; Guibentif et al. 2017; Macaulay et al. 2016).

Due to the increasing use of this experimental method for investigation of hematopoiesis, single cell sequencing was used as it was thought that it could provide valuable insights into the nature and function of the wound hemogenic endothelium.

5.2 DEVELOPING A NOVEL SLICE CULTURE TECHNIQUE TO IMAGE EHT AFTER INJURY IN REAL TIME

To investigate if EHT is occurring in the endocardium after injury, it was important to try and watch it happening, as has been done in the work that first identified the EHT process in the mouse and zebrafish during development. The experiments performed in developing zebrafish larvae looking at EHT benefited from the fact that zebrafish larvae are transparent; so by immobilising the fish and imaging under a confocal microscope, *in vivo* processes can be seen in real-time. Sadly, the same cannot be said for the adult zebrafish heart, where the chest wall and the heart itself are opaque, making it very difficult to watch endothelial cells round-up and detach from the underlying cardiomyocytes. Some imaging methods that can observe the inside of hearts in live adult fish have been developed, but lack the resolution to follow single cells (Koth et al. 2017; Merrifield et al. 2017; Hein et al. 2015). In addition, following a single cell in a rapidly moving environment such as the beating zebrafish heart would likely prove extremely difficult. In order to see the process of EHT occurring in the heart after injury, it is vital that a way to look inside a living adult heart in enough detail to track a single cell be found.

In other fields of research, particularly in the neuroscience field, cultures of thin slices of tissue are commonplace and used for studies of various cellular processes taking place within a tissue. For example, slices of brain can be kept alive, in a tissue-specific culture medium, and imaged over time to study brain development and neurogenesis (Humpel, 2015). These cultures maintain their structure and many cell functions for extended periods and have contributed much to the study of brain development, through allowing analysis of cell

survival, proliferation and migration. Organotypic cultures of fish heart tissue have thus far been limited to whole heart, or myocardial/epicardial explant cultures (Kim et al. 2012; Cao & Kenneth D Poss 2016; Münch et al. 2017). The former is useful for real-time study of processes on the outside or most superficial layers of the heart, but not the inside, whilst the latter of these does little to maintain the structure of the original tissue that would be required to watch EHT occur. Culturing slices of injured heart tissue could be highly beneficial for scrutinising multiple regenerative processes, particularly here, where viewing the activity of individual cells on the inside of the heart is crucial to investigating EHT. Though not an *in vivo* approach, it offers the ability to see cells within the structures of the heart. Under optimal conditions, the slice of heart tissue may be true enough to *in vivo* conditions to recapitulate cellular processes that occur within living fish, including EHT. Therefore, it is highly beneficial to develop this approach in the fish heart to investigate whether EHT occurs after injury, and as a tool that could be useful for multiple other avenues of research in heart biology.

To develop this method as an experimental tool there are three main techniques to adapt to fish heart tissue. The first is the sectioning of the live fish heart into slices that maintain tissue structure. To see EHT occurring, it would be beneficial to be able to identify the structures of the heart, namely have visible trabeculae, lumen and, ideally, wound tissue. Therefore, any technique used to section the heart must be clean enough and create thick enough slices to maintain tissue integrity. Secondly, the culture of these slices must be optimised. Experiments in the cultured mouse HE and developing zebrafish show that EHT is a process that takes 15h or more (Lam et al. 2010; Bertrand, Chi, et al. 2010) and so it is possible that cultures will be required to remain live, and in a good state of health, for up to 24h or more after isolation from the fish. Fortunately, as mentioned above, culturing of primary cells and tissue from the

fish heart has been performed previously and culture methods can be adapted from these protocols (Cao & Kenneth D. Poss 2016). Lastly is the imaging technique. The images must be of high resolution, as single cells are the focus of the experiment, whilst still being able to show a larger area of the heart to allow appreciation of the tissue structure. The slices will be thicker than regular histology sections, so the microscope must be of a type that can more easily exclude extraneous light from levels of the slice outside the focal plane. Additionally, it is required that an image be taken of the slice in the same position at frequent intervals for many hours, so a method to hold the slice still must be developed. The following work shows how these three areas were optimised for the fish heart, resulting in a protocol for live culture and imaging of live fish heart slices over the course of up to 15h, with slices that are not being imaged kept living for up to 48h in culture conditions.

5.2.1 OPTIMISATION OF THE SECTIONING PROCESS

To obtain even, clean and live slices of a heart to culture and image, the heart must be kept healthy and perfectly still whilst being sectioned. Commonly, those who section live tissues mount them into blocks of gelatin or low-melting point agarose to immobilise the tissue (Humpel, 2015). The process of this embedding may be harsh on the tissue, causing damage by starving the tissue of oxygen, exposure to abnormal osmotic pressures and also potential damage from the heat of the molten embedding media. To minimise these potentially harmful effects, the agarose/gelatin is generally dissolved into PBS and low-melting point versions are used, so that they remain molten at low enough temperatures to not be harmful to the tissue. Once the media is added to the tissue, to aid preservation it is placed immediately onto ice to solidify.

Mounting using both gelatin and low-melting point agarose was attempted in the development of a protocol for fish heart slice culture. The advantages of gelatin are that it remains liquid at lower temperatures than the agarose, however, the co-effect of this is that it takes longer to solidify. 12% gelatin was tried, as it had previously been used in tissue roughly equivalent in size to the fish heart (Gurusinghe & Ehrlich 1986) but it took around half an hour for the blocks to become solid. This means the hearts are in the blocks for extended periods, out of culture medium and starved of nutrients, likely having a negative impact on cell survival. 2% and 4% low-melting point agarose were also tried, 4% is commonly used in heart slice cultures in adult and embryonic mice, whilst a lower percentage was also tried because of the smaller heart size (Peinkofer et al. 2017; Pillekamp et al. 2005). Both percentages solidified very quickly, however, the 2% agarose was too soft for the block to remain solid whilst handling. 4% agarose therefore presented as the best option for mounting the heart. If kept in a water bath at 42C, the agarose can be prepared in advance and remains molten for extended periods, ready for use when required and solidifies in 2-3 minutes on ice. This means sectioning of the heart can begin very rapidly after isolation, minimising the amount of time the heart is cut-off from nutrients.

To ensure the heart is held well in the block, all excess blood that has stuck to the outside of the heart during the isolation process must be removed. This can be done gently with forceps under a dissecting microscope, so the heart tissue is not damaged. The removal ensures the agarose is in direct contact with the heart tissue and helps keep the heart in place. For the same reason, the heart should also be dried as far as possible before being mounted using tissue paper. The hearts normally stop beating before they are embedded into the block or whilst they are embedded, some hearts remained beating even after sectioning, with no

deleterious effect on the embedding and sectioning process. If cessation of beating is required, 2,3-butanedione monoxime, a myosin inhibitor, can be added (Peinkofer et al. 2017).

The previous papers (Peinkofer et al. 2017; Pillekamp et al. 2005) that show heart slice cultures in mice use a vibratome as the method for the slicing of the heart. Vibratomes consist of a sharp blade attached to a moving part that causes the blade to both move across a plane in a slicing motion and also oscillate from side-to-side as it moves across the slice. The side-to-side motion prevents compression of the slice by the blade, allowing the creation of a slice of even thickness. The sectioning is done in a bath of a medium of choice, in this case PBS, to help keep the tissue alive. The exact speed of the blade movement and the oscillations can be controlled and optimal conditions vary between tissues. For the heart, the best quality slices were produced under the following conditions on the Leica VT 1000S vibratome: speed 1.1mm/s and vibration frequency 600 Hz. Other conditions caused a variety of issues, including ragged edges and pushing the heart out of the block of agarose when the blade comes into contact.

As mentioned previously, for imaging purposes it is necessary to have as thin a slice as possible whilst maintaining endogenous structures of the heart. Hearts were sliced into a range of thicknesses, from 50-200 µm to find the optimal value that fits these criteria. It was found that the smallest slice thickness with clean edges and structures still visible is 75 µm (Figure 5.1 A, A').

By following the conditions above, it is possible to obtain 5-15 slices of living tissue from each isolated fish heart that still possess visible structures such as trabeculae and lumen.

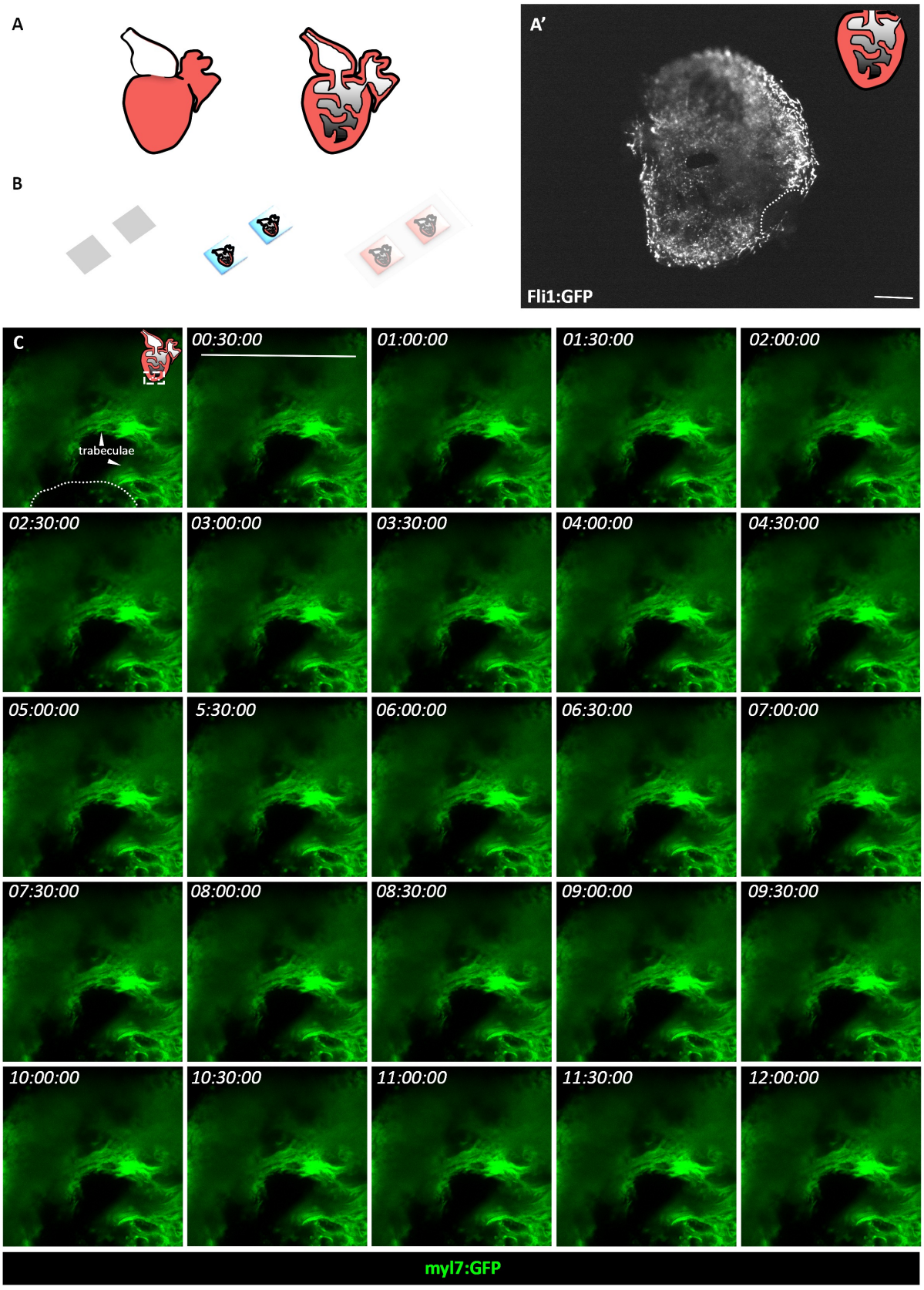


Fig. 5.1 Overview of zebrafish heart slice culture method. **A** shows a schematic of a heart after being sliced, showing the structures expected to be present inside. **A'** is an example slice from a *fli1:GFP*

fish, where endothelial cells have nuclear GFP. Note the presence of a lumen maintained in the heart and absence of GFP at site of injury (2 dpi). **B** shows a schematic of the process of mounting in a coverslip. The blue represents the 1% LMP agarose, pink is culture medium. **C** shows imaging of a slice culture from a *myl7:GFP* fish, where cardiomyocytes express GFP, over 12 hours with imaging every 30 minutes. Arrowheads indicate trabeculae and note the presence of luminal structures. N=3.

5.2.2 CULTURE CONDITIONS FOR FISH HEART SLICES

Once the slices have been cut, they must be transferred into culture medium that will maintain viability and growth for the duration of the culture period. Additionally, as these are primary cultures and therefore obtained from a non-sterile environment, the medium must contain antibiotics and fungicides to prevent contamination.

As mentioned previously, cultures of zebrafish heart primary tissue have been done before. Perhaps the culture most similar to the conditions desired for a slice culture experiment are the whole heart explant cultures performed by Cao and Poss (Cao & Kenneth D Poss 2016). These cultures are similar in that all cell types in the zebrafish heart are present, as in slice cultures, tissue structure is maintained and similar amounts of contamination are expected. Additionally, they look to culture the hearts for extended periods, as with the slice culture experiments. Therefore, the culture conditions presented by Cao and Poss are ideal for adaptation to this experimental method. The medium contains Non-Essential Amino Acids (NEAAs) that are commonly supplemented into media to aid cell growth and viability. Beta-mercaptoethanol is also added to reduce the levels of free oxygen radicals. To prevent contamination penicillin and streptavidin are added, as is primocin. Contamination of the slice cultures has never been seen using this culture medium, over culture periods of 48h. After

48h, the slices still appear healthy, however beating, if it does still remain after sectioning, ceases after 24h.

5.2.3 OPTIMISATION OF THE IMAGING PROCESS

To capture the cell movements involved in the whole EHT process in developing zebrafish larvae requires regular periodic imaging over 15h or more (Kissa & Herbomel 2010; Lam et al. 2010). For these experiments dealing with adult tissue under *in vitro* conditions, it can be expected that the process would take at least as long, if not longer. In addition, the slices present a greater challenge to image as there are many more fluorescent cells in multiple planes, making it more difficult to capture identify regions of interest. Further obstacles include immobilisation of the slices: zebrafish larvae can be kept alive and immobilised, after being anaesthetised, in PBS/agar or similar (Kaufmann et al. 2012; Godinho 2011; Renaud et al. 2011), however, using the same immobilisation techniques for slice cultures may starve the slice of necessary nutrients that maintain viability for the culture period, or be insufficient to keep such low density, fragile tissue still.

To keep the slices alive during imaging, they are placed into coverslips that have a silicon layer on one side. There are wells cut into the silicon that create miniature culture wells the slices can be placed in and then the well can be filled with culture medium (Grace Bio-Labs CultureWell chambered cover-glass (Sigma) 3 wells, thickness 1 mm volume 300-500 µL). Unfortunately, the slice does not adhere to any part of the well, therefore to keep it still during imaging the slice is immobilised in a thin layer of 1% agarose. The process of mounting the slice onto the coverslip to keep it immobile is as follows: the coverslip is placed on a hot plate at 42°C and molten low melting point agarose is added to the wells. With a pair of

forceps, the slice is carefully floated on top of the agarose, such that a small part of the bottom of the section is under the surface. The excess agarose is then removed from the well, leaving only a thin layer on the bottom to keep the slice in place once solidified. This method allows sufficient adhesion, whilst still allowing enough of the tissue to remain in contact with the culture medium.

Initially, images were taken under a standard upright fluorescence microscope. However, it was impossible to follow the dynamics of individual cells due to noise from other fluorescent cells outside the focal plane and view. Confocal microscopes exclude light from outside the desired focal plane and are used in the published developmental study. The authors use the spinning disc confocal, as this has a much faster scanning time than an airy scan confocal, with the trade-off being an increase in noise. Unfortunately, this increase in noise means that images of adult heart slices aren't of sufficient quality to allow tracking of single cells (microscope used was a PE Ultraview spinning disk). The airy scan confocal (Zeiss LSM 880 Airy Scan), however, gave images of good enough quality that single cells could be seen and could scan 8-10 images in 2.5 mins. This frequency of imaging should be ample to capture the cell movements associated with EHT.

Using this method of microscopy and culture, slice cultures can be kept alive and imaged for at least 15 – 24 hours.

5.2.4 EXPLORING THE USES OF ZEBRAFISH HEART SLICE CULTURE EXPERIMENTS

Successful slice cultures created using the method outlined above allow imaging of the interior of the heart after injury, presenting an exciting new way to investigate multiple injury

responses in the heart. However, *ex vivo* conditions do not completely replicate the conditions *in vivo* and, consequently, it is possible that some processes known to occur during the injury response in living fish do not do so in culture.

Slice cultures from 7 dpi transgenic fish with GFP-expressing cardiomyocytes show that cardiac muscle remains relatively inactive in these conditions, with very little movement seen in images of the slices taken every 30 mins for 12 hours (figure 5.1 C). Slice cultures, unless further refined, are therefore of limited use for studying the activities of cardiomyocytes after injury, though perhaps further study with fish that contain live markers of proliferation might be of use to show cardiomyocyte proliferation. This lack of cardiomyocyte movement could be due to the tissue undergoing being sectioned and cultured, suboptimal culture conditions, or the loss of various paracrine signals required for proliferation of cardiomyocytes into the culture medium. However, cardiomyocytes are not the only cell type that respond to injury. Blood cells and the immune response have been shown to have multiple important effects on response to injury, being able to both promote and inhibit regeneration. Slice cultures of injured hearts from fish expressing GFP in macrophages show that macrophages in the heart remain present in the slices after the sectioning and culturing processes and, in contrast to cardiomyocytes, are extremely active (Fig. 5.2). They appear to be undergoing dramatic cell movements, seeming to either send out pseudopodia to phagocytose debris, or attempt to move around the tissue. With the importance of the immune response in wound healing and heart regeneration becoming increasingly apparent, slice cultures could be a very useful tool to aid in the study of this field.

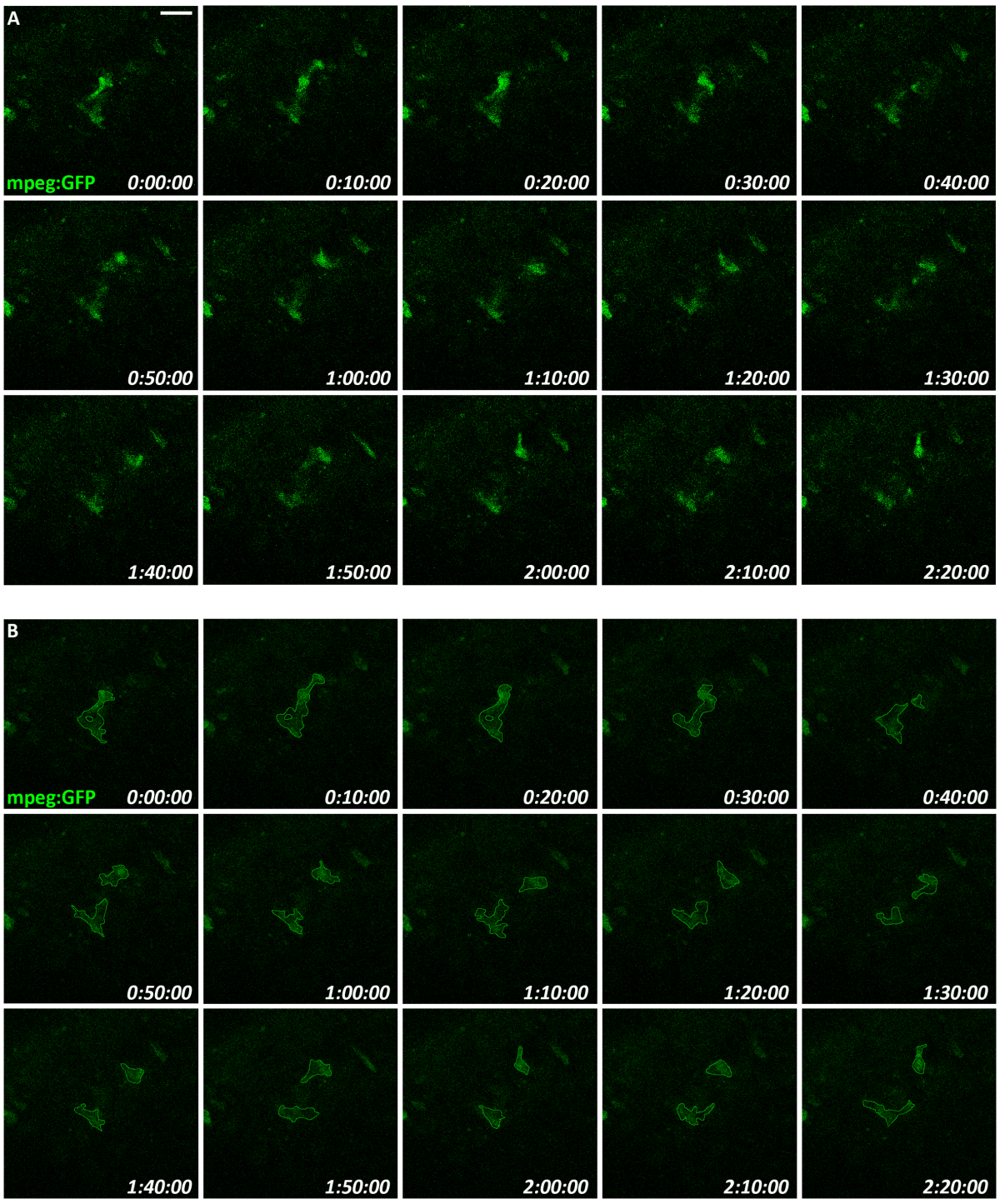


Fig. 5.2 Movements of a macrophage over 2h 20 min in a slice culture from an *mpeg:GFP* fish, where macrophages express GFP. **A** shows the original images, **B** has the macrophage(s) outlined in green to aid tracking. N=3. Scale bar is approximately 10 μm and applies to both A and B.

5.2.5 ADAPTING THE PROTOCOL SPECIFICALLY FOR INVESTIGATING EHT

As the aim of this experiment in this study was to investigate whether EHT is occurring after injury in the transgenic fish heart, the generalised protocol outlined above was tailored. In this instance, imaging should take place over at least 15h and use transgenic fish lines that mark endothelial cells and/or HSCs. The lines used were tg(*kdrl:GFP*), tg(*kdrl:GFP;myl7:dsRed*), *runx1:citrine* and *runx1:citrine*; *kdrl:mCherry*. Additionally, the cell counts performed previously show that 3 dpi is an ideal time to look for EHT occurring, as it appears to be at a peak at this time-point in living fish.

5.3 RUNX1 POSITIVE CELLS ARE HIGHLY ACTIVE AFTER INJURY

As EHT is a process where the endothelium transitions into a Runx1-positive HSC, the ideal zebrafish line to watch this process would be one where the endothelium and Runx1 expressing cells are fluorescently labelled. Therefore, initial slice culture experiments were done using *runx1:citrine*; *kdrl:mCherry* fish.

Initial imaging was performed with 1 image taken every 10 minutes, however, very bright Runx1-positive cells, presumably blood-borne cells, appear in and out of the focal plane in between image capture. Reducing the capture interval to 2 minutes allowed tracking of individual cells more easily, as their journey could be followed. Imaging at this frequency shows that lots of bright Runx1-positive cells are highly mobile and change shape rapidly, altering their morphology and position constantly within 2 minutes (Fig. 5.3). Given their shape changes, it seems likely that the majority of these cells are leukocytes, though they could also be circulating progenitor cells. The brightness, frequency and mobility of these cells makes it very difficult to spot Runx1 expression in hemogenic endothelium, where Citrine expression would be expected to be low, and to watch for EHT occurring in endothelial cells.

Therefore, double positive cells were hard to detect and not identifiable. It would be hard to say if the movements seen were EHT, or a Citrine-positive cell moving into the focal plane or changing shape.

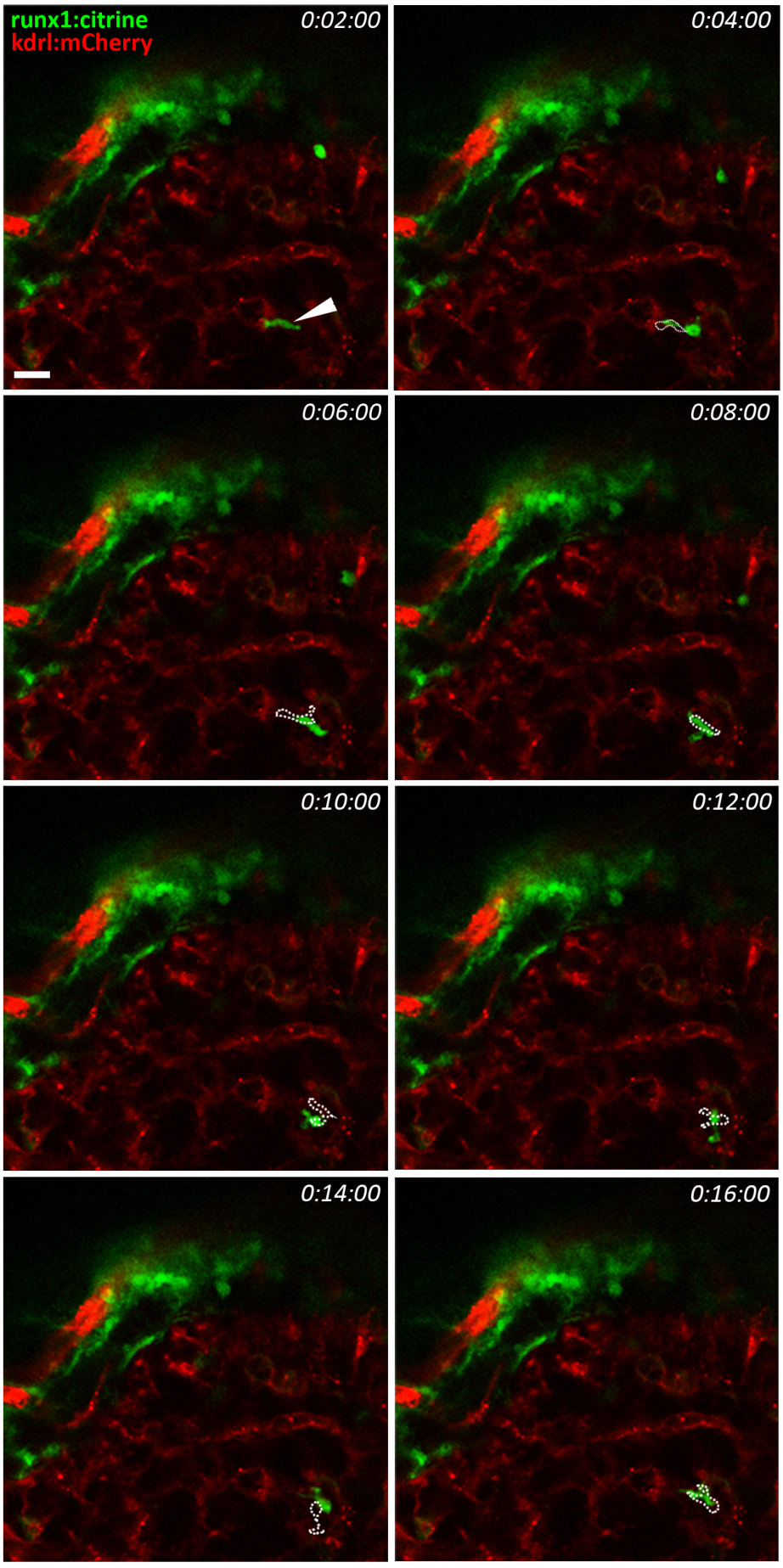


Fig. 5.3 Following a runx1-positive cell over 16 minutes in a slice culture. The arrowhead indicates the cells whilst the dotted line represents the cell outline in the previous picture, to emphasise cell movement. The image area is at the edge of a slice from a 3 dpi heart. The two lines of relatively flat green cells in the mid to the top left of the image represent cells in the epicardium and a layer between the trabecular and compact myocardium. Red endothelial/cardial cells in the trabecular myocardium indicate edges of trabeculae. Scale bar indicates approximately 10µm.

The developmental work in the zebrafish that followed EHT was done using *kdrl* expression as a marker, therefore further slice culture work looking at EHT was done in *kdrl:GFP* fish.

5.4 ENDOTHELIAL CELLS APPEAR TO ROUND AND DETATCH AFTER INJURY

Slice culture experiments in *kdrl:GFP* fish were undertaken to see if GFP-positive cells near the injury site undergo the same cell movements associated with EHT in the developing zebrafish. Images were taken every 10 minutes over 15h on a confocal microscope on slices isolated from hearts 3-7 days after injury, when EHT is indicated to occur in the fixed sections.

Examples of endothelial cells beginning to round up, then fully round and detach from the surface can be seen in these images in a manner similar to that seen during EHT in development (Fig. 5.4). The endothelium is uninterrupted after the cell detaches, indicating that the departing cell draws surrounding cells into close apposition as it contracts, allowing the formation of new cell junctions. This is also similar to that seen in development. The detached cell appears to disappear into the culture medium in the well and disappears out of focal view immediately after detaching (Fig. 5.4).

The cell movements seen in some endothelial cells in slice cultures from injured hearts mimic closely those seen in the hemogenic endothelium of the dorsal aorta in developing zebrafish larvae. During the course of these experiments, these events were relatively rare, but witnessed on more than 3 occasions. The rarity is likely due to *in vitro* conditions being sub-optimal for this process compared to those in living fish, as it is likely that lots of injury related signals are lost into the culture medium and extra stress is placed on all cells, both of which likely increase the rarity of this event.

The slice culture experiments show that endocardial cells can become rounded, HSC-like cells after injury that detach, in a manner closely mirroring EHT from the hemogenic endothelium after development. In concert with the immunohistochemistry data indicating Runx1 expression in rounded cells, it is possible that the wound endocardium is a hemogenic endothelium that can undergo EHT after injury.

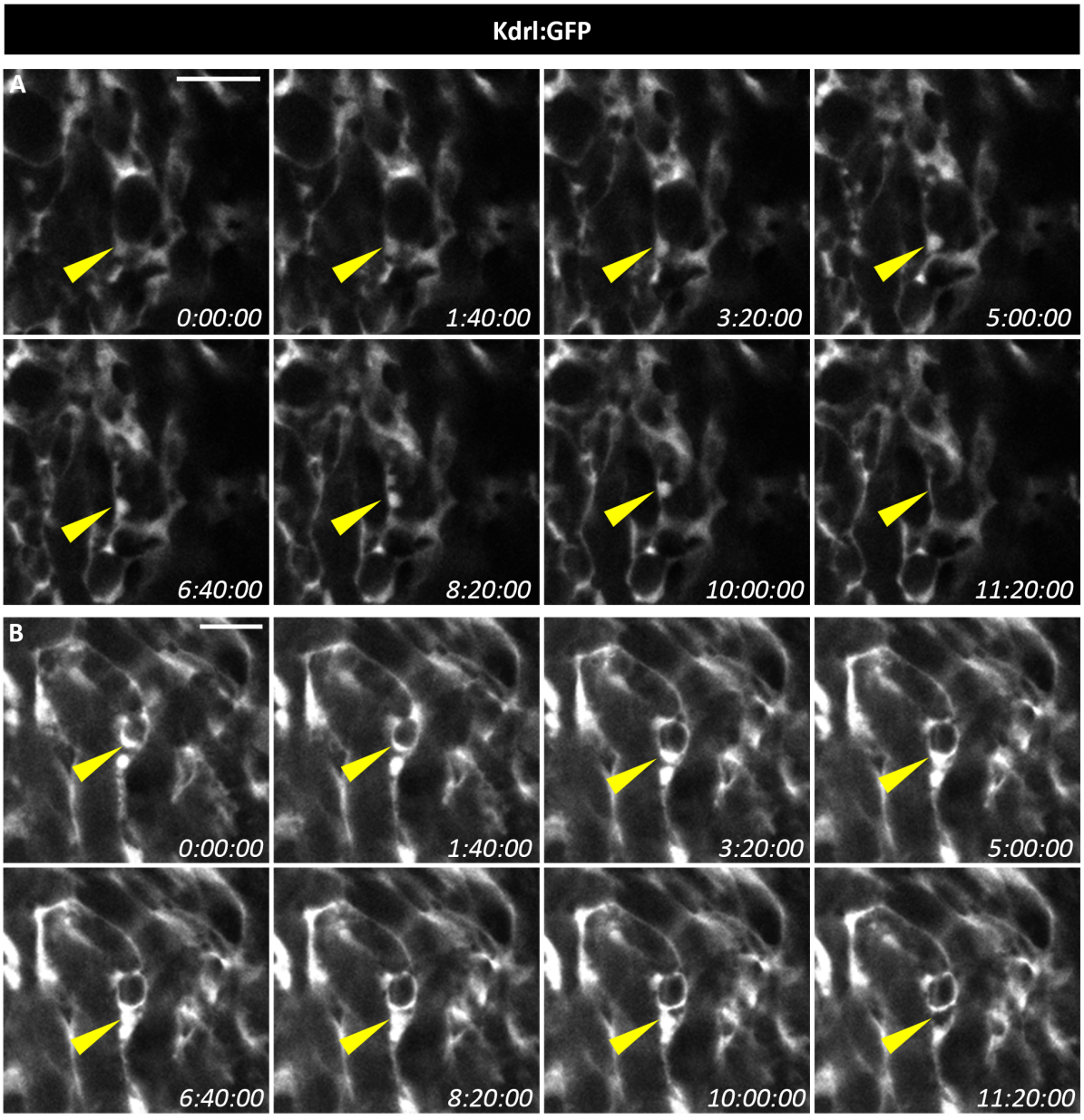


Fig. 5.4 Observing potential EHT in endothelial cells in *kdrl:GFP* fish. **A** shows one example of an endothelial cell becoming increasingly round, then detaching. **B** is another example, note how flat the

cell is at the start. The process occurs across roughly 12 hours. Yellow arrowheads indicate the cell undergoing suspected EHT. Scale bars are approximately 10 μm.

5.5 ANALYSING CELLS WITH ENDOTHELIAL AND HEMATOPOIETIC IDENTITY

Whilst endothelial cells undergoing the same type of movements seen in developmental EHT are seen in the injured fish heart, this fact is not proof that these cells are indeed hemogenic. They could be detaching as part of other cell transitions, as their hematopoietic nature is not confirmed. To further investigate the presence of a hemogenic endothelium in the fish, it was necessary to look deeper at the nature of cells that are hematopoietic and endothelial.

Thus far, identification of proposed hemogenic endothelial cells has relied on *runx1* expression as a marker of hematopoietic identity. *Runx1* expression, however, is not limited to hematopoietic cells after injury. Therefore, experiments were performed to isolate and investigate the transcriptomic identity of presumptive HE, to determine if *runx1* expression is indeed indicative of a hematopoietic identity.

5.5.1 FLUORESCENCE ACTIVATED CELL SORTING CAN ISOLATE RUNX1/KDRL DOUBLE POSITIVE CELLS FROM ZEBRAFISH HEARTS

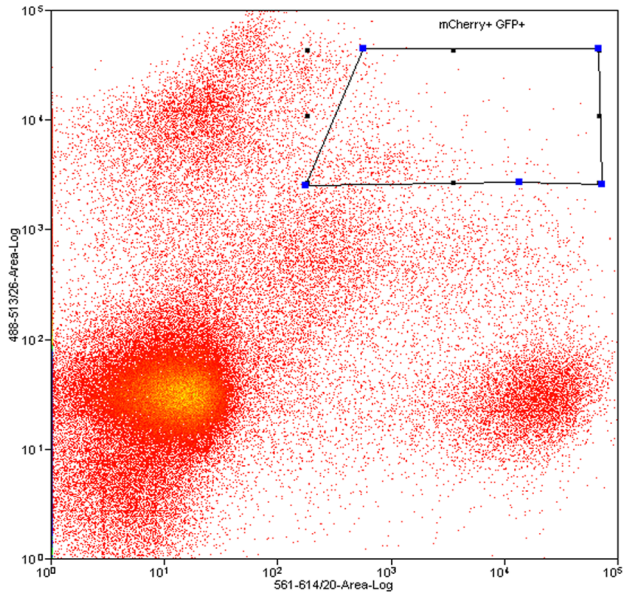
Fluorescence activated cell sorting (FACS) was used to investigate the proportion of Runx/Kdrl double positive cells from digests of whole hearts of *runx1:citrine*; *kdrl:mCherry* fish, to see if these cells can be isolated. Single cell suspensions from uninjured and injured hearts were compared to see if these cells are more numerous after injury, as suggested by the previous immunohistochemistry data.

4 separate FACS experiments were run and the results show that double positive cells can be isolated from whole heart digests (Fig. 5.5). They are a very rare population that increases drastically after injury, with numbers being so low as to be almost negligible in uninjured

hearts unless large numbers of hearts (>15) are pooled. This increase in numbers of positive cells after injury is in line with the previous immunohistochemistry data as is the almost negligible numbers of these cells before injury.

The FACS data suggests that cells of a dual endothelial/hematopoietic nature are present in living tissue and corroborate the immunohistochemistry data. It also shows that these cells can be isolated from whole heart digests for further analysis.

A



B

Sort	% double positive
1	0.64
2	0.53
3	1.2
4	0.82

Fig. 5.5 Example FACS plot and table of double-positive cell proportions indicated by FACS. **A** shows a FACS plot of single cells from digested *runx1:citrine*; *kdrl:mCherry* 3 dpi injured hearts. Each dot represents a single cell, with levels of GFP/Citrine expression (the same wavelength is used for both) on the Y axis and mCherry expression on the X axis. The box labelled mCherry/GFP double-positive marks out double positive cells. **B** is a table showing percentages of double positive cells in FACS sorts.

5.5.2 GENE EXPRESSION ANALYSIS OF ENDOTHELIAL AND HEMATOPOIETIC CELLS BY QPCR

RNA isolation from FAC sorted cells from *Runx1:citrine;kdrl:mCherry* fish allowed qPCR to be performed on generated cDNA. This permitted analysis of gene expression levels of marker genes for the endothelium, hemogenic endothelium and mature HSCs in single and double positive cells. The marker genes used were *kdrl, fli1a, lmo2, gata2b, gfi1aa* and *myb*. The first two are commonly used endothelial markers, *lmo2* can demarcate hemogenic endothelium and HSCs, *gata2b* is switched on during hemogenic endothelium specification and *gfi1aa* and *myb* mark more mature HSCs (Sood & Liu 2012; Tober et al. 2016; Jankowska-Steifer et al. 2015; Lempereur et al. 2018; Yzaguirre et al. 2017; Angelos et al. 2017; Macaulay et al. 2016; Athanasiadis et al. 2017).

Comparisons of Citrine and mCherry single positive cells show that single mCherry-positive cells express much more endothelial early hemogenic endothelium genes (*kdrl, fli1a1* and *lmo2)* in comparison to Citrine single-positive cells (Fig. 5.6 N.B. N=1). Intriguingly, they also express roughly the same levels of *gata2b*, a later marker of specified hematopoietic endothelium. This could suggest that the endocardium has latent hematopoietic potential, arrested before Runx1 expression, which is switched on when HSCs are specified within in the HE (reviewed in Yzaguirre et al. 2017). Expression of mature HSC markers are markedly reduced in mCherry-positive cells relative to Citrine-positive cells. In brief summary, these relative expression profiles suggest that mCherry-positive cells are more endothelial than Citrine-positive cells and Citrine-positive cells are more HSC-like than mCherry-positive cells, which is to be expected.

Double positive cells are broadly more endothelial and hemogenic endothelium-marker positive than single Citrine-positive cells (Fig. 5.6 B). They have lower expression of mature

HSC markers, which is anticipated if the double positive cells are a hemogenic endothelium. When compared to single-positive mCherry cells, they are roughly as endothelial, but have higher expression of hematopoietic endothelium genes and HSC genes (Fig. 5.6 C). These relative expression levels of marker genes, whilst only an n of 1, is suggestive of a hemogenic endothelium.

Further gene expression analysis and functional analysis was required to explore the possibility of a hemogenic endothelium. What other genes do double-positive cells express? How different are they to pure endothelial cells? Does the hemogenic endothelium produce HSCs that are distinct from circulating HSCs? What happens if endocardial EHT is prevented? To answer these questions, experiments examining a mutant fish line with loss of Runx1 function was analysed and single cell sequencing was performed on samples from uninjured and injured WT fish and injured Runx1 KO fish. Runx1 is required for the emergence of HSCs from the hemogenic endothelium (Kissa & Herbomel 2010; Zhen et al. 2013), thus if the injured endocardium is a HE, it should still be specified as such but successful HSC emergence will not occur.

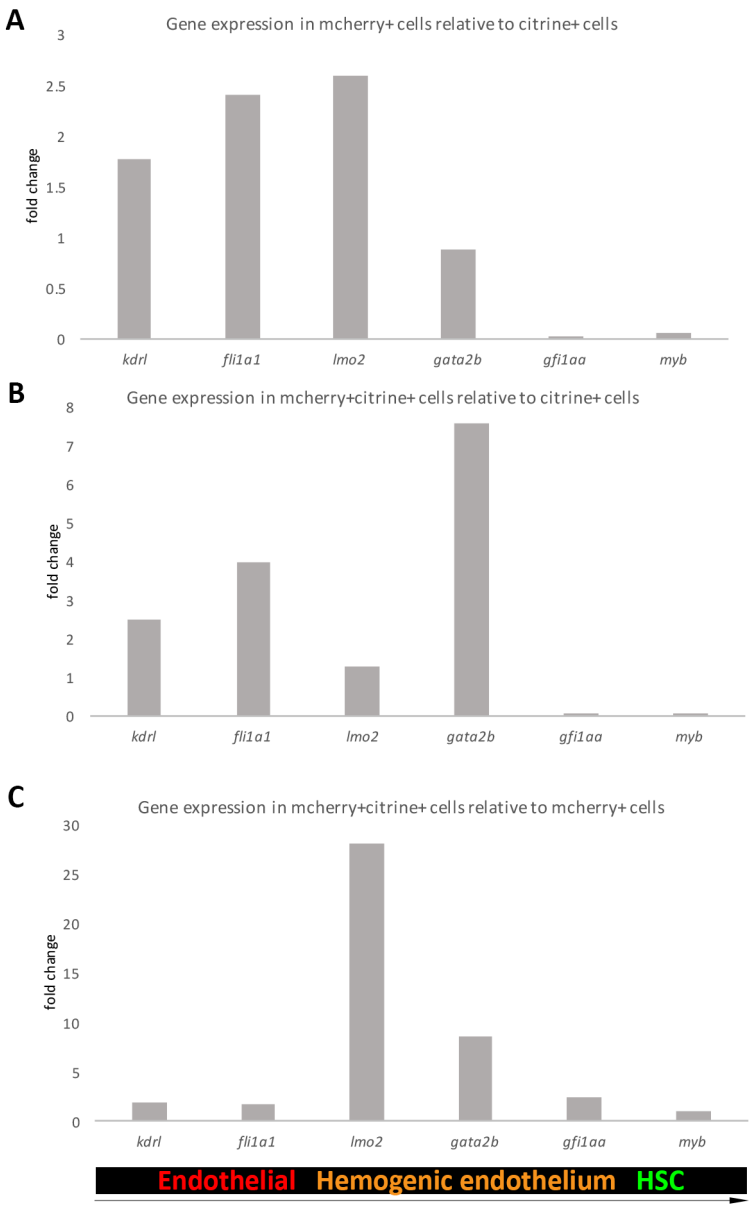


Fig. 5.6 relative expression of mRNA for endothelial, hemogenic endothelial and HSC genes in FAC sorted cells from *runx1:*citrine; *kdrl:mCherry* 3dpi hearts assessed by qPCR. **A** shows expression of single mCherry-positive cells relative to single Citrine-positive cells. **B** shows double-positive cells relative to single Citrine-positive cells and **C** is relative to single positive mCherry cells. N=1.

5.6 REMOVING RUNX1 FUNCTION IMPROVES REGENERATION

Before single cell sequencing could be performed on the mutant hearts, the mutant heart injury phenotype needed to be analysed. To this end AFOG staining was performed on WT and mutant sections, to analyse regeneration and scarring.

The *runx1* mutant has been previously described in zebrafish as a truncation of the Runx1 protein, leading to loss of function (Sood et al. 2010). These fish lack definitive hematopoiesis,

but some survive and recover hematopoiesis later through an unknown Runx1-independent mechanism. However, it is not a full recovery and some blood cell types are not produced, or are present in altered proportions to WT fish. In the mouse, loss of Runx1 has been found to be cardio-protective, protecting against adverse remodelling through altering calcium handling within cardiomyocytes (McCarroll et al. 2018).

The loss of full-length *runx1* in the hemogenic endothelium of developing zebrafish causes the hemogenic endothelial cells to fragment as they bend away from the rest of the endothelium (Kissa & Herbomel 2010; Zhen et al. 2013). As Runx1 is required for developmental EHT, it was hypothesised that any phenotype observed in these mutant fish could be due to the loss of post-injury EHT. Analysis of the regenerative capacity of Runx1 loss of function mutants was performed using AFOG staining, to highlight the scar (Fig. 5.7 A). Measurements were taken of the compact myocardium scar size, showing how long it takes for the compact myocardium to re-form a contiguous wall and restore myocardial integrity. This is a common measurement of regeneration time.

Comparison of these measurements with WT fish indicated that regeneration of the compact myocardium occurs much more rapidly in the loss of function mutant, with regeneration being mostly complete by 7 to 14 dpi (Fig. 5.7 A B). By contrast, some WT fish still had a small amount of scar left by 70 dpi, though were statistically indistinguishable from Runx1 mutants from 30 dpi.

When analysing the scar staining in WT and Runx1 mutant hearts, scar levels in the trabecular myocardium, directly in contact with the compact myocardium, were seen to be following a different pattern to the compact myocardium. Measurements show that there is little difference in this scar size between the fish, except for at 7 dpi, where the *runx1* mutant has

significantly less and at 3 dpi, when the mutant has significantly more (Fig. 5.7 C). Closer observation of the AFOG staining suggests that initial fibrin deposition (pink staining) is delayed and/or reduced in the mutant. In the WT, it is clearly visible at 3 dpi, whilst in the mutant, it is visible in 1 heart at 7 dpi and in most hearts at 14 dpi, along with collagen. In the mutant at 3 dpi, the measured 'scar' is more a measurement of injured myocardium than actual scar deposition.

At 14 dpi, collagenous scar tissue is present in both fish, along with fibrin. From observations, at 30 dpi the WT appears to have more densely packed collagen fibres, whereas the mutant has a less dense scar. Measurements of the scar areas show that there are no significant differences in scar size between the fish from 14 dpi onwards. The mutant does appear to have slightly less scar tissue, but not sufficiently for statistical significance. These results suggest that the scarring response is altered in the mutant compared to WT, in that the mutant scar seems to appear later and also has a slightly different composition to the WT. The myocardial measurements suggest almost complete myocardial regrowth of the compact layer by 7 dpi in the mutant, with the levels of regeneration at 7, 14, 30 and 70 dpi not differing significantly from each other (Fig. 5.7 B). The WT does not catch up until 30 dpi, suggesting that scar area should similarly be significantly different before this stage. It is surprising, then, that the mutant does not have a significantly reduced scar size at 14 dpi. This suggests that scar clearance might be slower relative to myocardial regeneration speed, than in the WT. Another explanation is that the scar is laid down later than in the WT, as suggested by the lack of fibrin at 3 dpi and this means that as deposition occurs later, resolution subsequently occurs later. Both cases could negatively affect regeneration, later scar deposition increases risk of cardiac rupture, whilst delayed clearance would mean non-

contractile scar tissue would remain in the heart, potentially reducing function. Longer term monitoring would be interesting to see if scar does remain in the heart longer in the mutant than in the WT, but unfortunately time for this experiment ran out.

The increase in speed of compact myocardium regeneration in the mutant could suggests that the myocardium is better at surviving the initial injury insult, or has increased proliferative capacity. A myocardial phenotype in the mutant is perhaps expected, as *runx1* expression is seen in the WT myocardium after injury, suggesting that *runx1* is otherwise active in the injured myocardium. The alterations in scar deposition and scar clearance could be due to loss or reduction of scar depositing and clearing cell types, due to the effect of *runx1* loss on definitive hematopoiesis. It could also be due to uncoupling of myocardial regeneration and scar clearance, through disruption of an unknown mechanism.

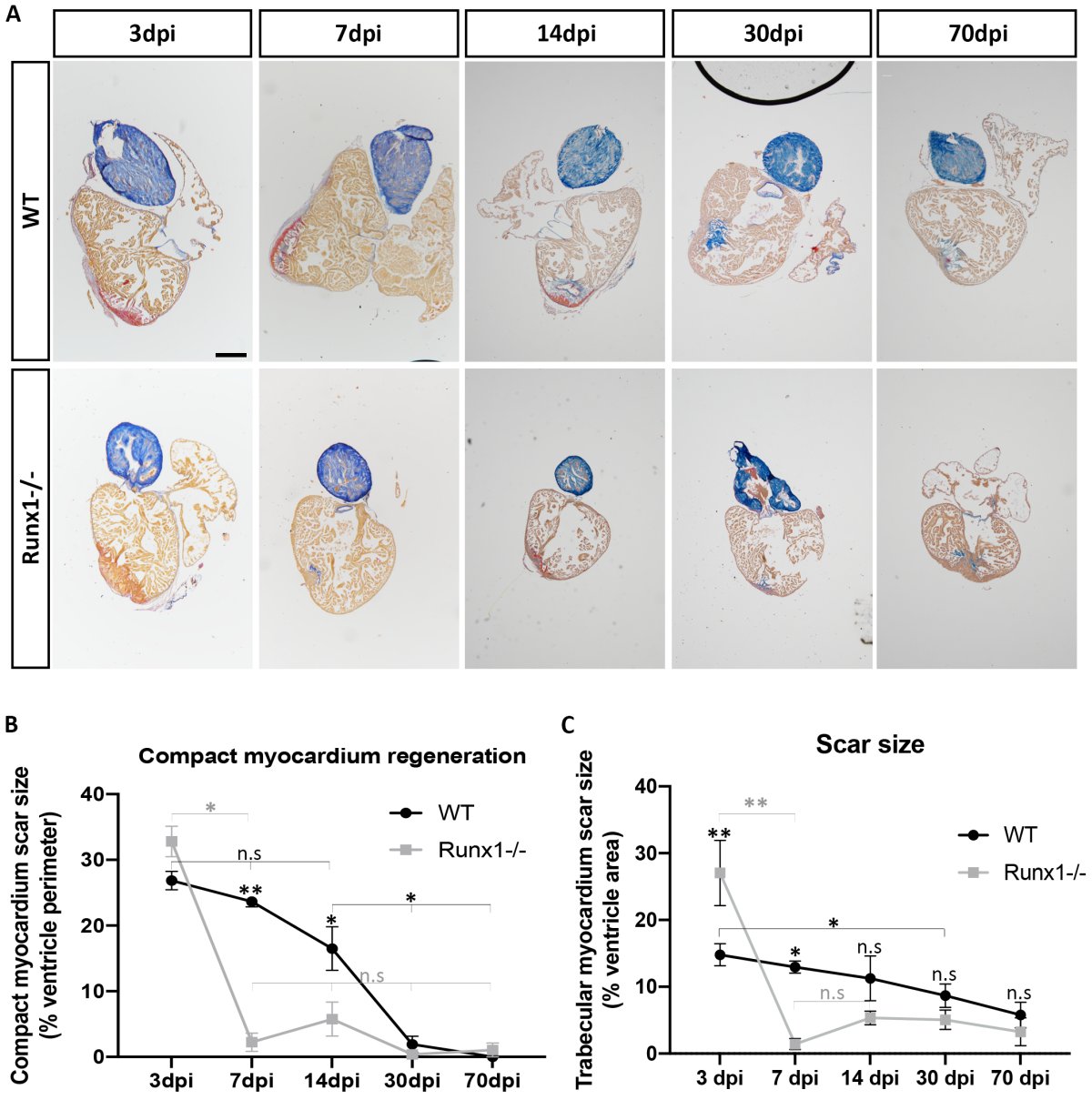
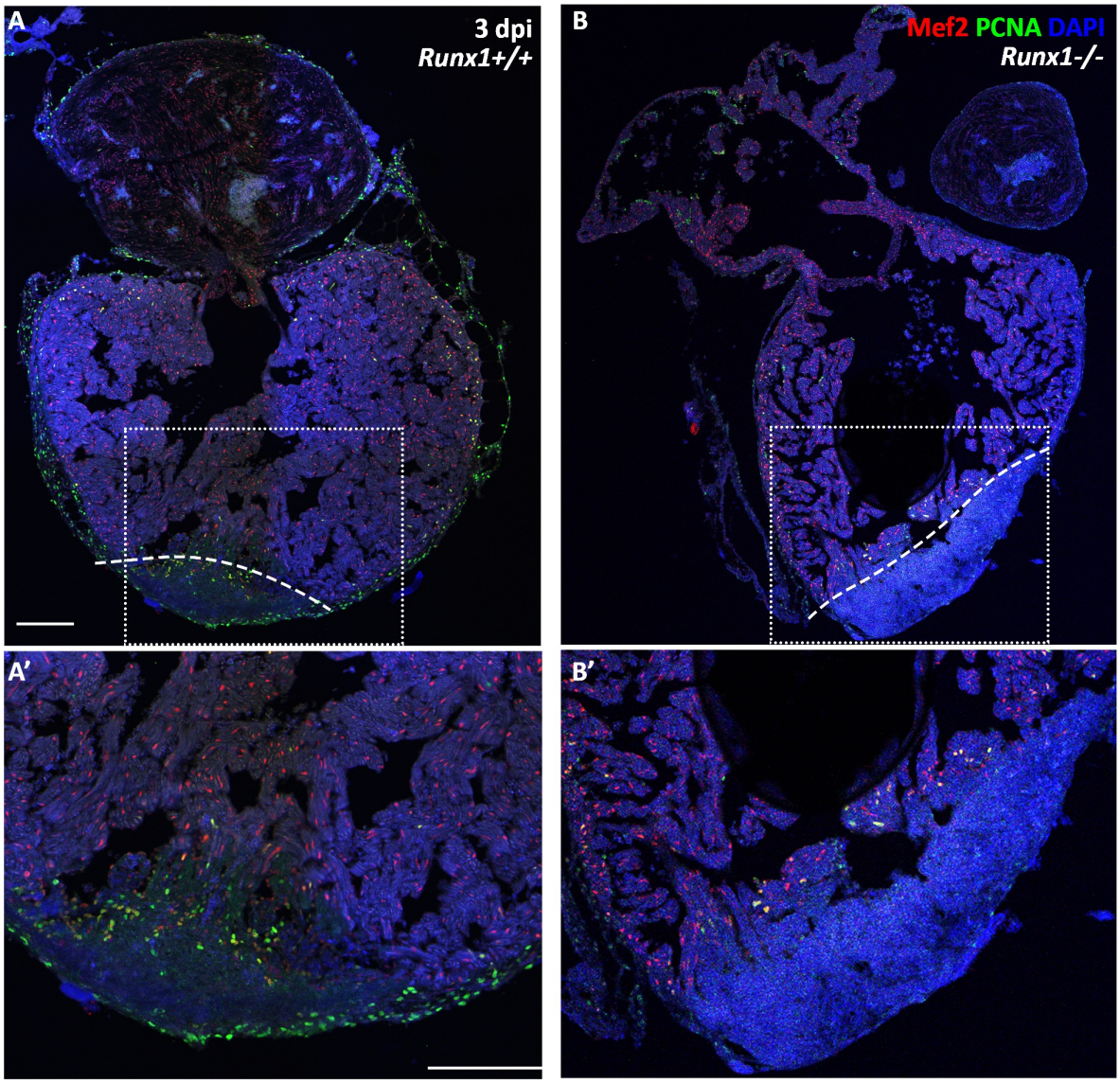


Fig. 5.7 Comparing the regenerative response in runx1 mutant and WT fish. **A** shows AFOG staining in sections from injured hearts. Myocardium is orange, fibrin is pink and collagen is blue. **B** shows a chart of scar length in the compact myocardium relative to the perimeter of the heart in the two fish. **C** is a chart of scar length in the trabecular myocardium relative to ventricle perimeter. * denotes p≤0.05 ** denotes p≤0.001. Grey bars indicate comparison between time points for mutant fish, black bars for the WT. N=5 for both fish at each time-point. Error bars indicate SEM. Statistics performed by two-way ANOVA. Scale bar is 100 μm.

5.7 LOSS OF RUNX1 HAS A PROTECTIVE AND PRO-PROLIFERATIVE EFFECT ON INJURED MYOCARDIUM

The analysis of scar size and myocardial regeneration in the *runx1* mutant and WT fish shows enhanced myocardial regeneration in the mutant by 7 dpi. Therefore, myocardial proliferation and survival were compared between the WT and mutant fish at an earlier time-point, 3 dpi.

The comparison of myocardial proliferation was performed by staining paraffin sections from WT and KO fish with PCNA, a nuclear marker of proliferating cells, and Mef2, a nuclear marker of cardiomyocytes. The number of Mef2-positive nuclei in the border zone of the wound was then counted and the percentage of those nuclei that were also positive for PCNA was calculated. This comparison reveals a statistically significant increase in the percentage of proliferating cardiomyocytes in the KO compared to the WT, with more than a 100% increase (Fig. 5.8 $p<0.05$). This suggests that the increased myocardial regeneration by 7 dpi is at least in part due to increased production of new cardiomyocytes in the mutant myocardium.



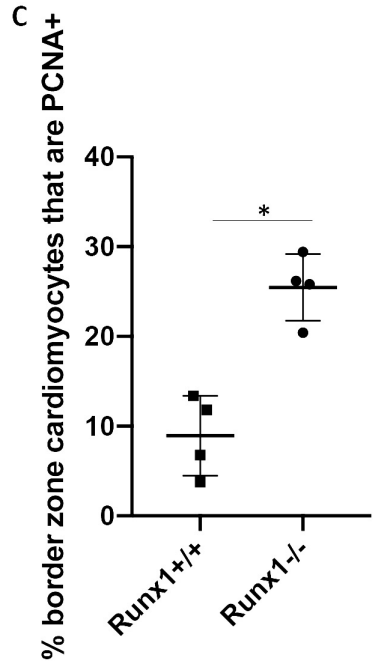


Fig. 5.8 Comparison of myocardial proliferation at 3 dpi between Runx1 mutant and WT fish. **A**, **A'** show immunohistochemistry for PCNA and Mef2 in WT fish and **B**, **B'** shows KO fish. **C** is a graph showing the percentage of Mef2+ nuclei that were also PCNA-positive in the border zone of the wound. Each dot represents the average percentage for 1 fish. N=4, P≤0.05 unpaired t-test. Dashed lines show approximate injury region and dotted boxes show areas magnified in A' and B'. Scale bars = 100 µm.

The investigation of cell survival was performed by observations of MF20 myocardial marker staining within the injury region in KO and WT fish at 3 dpi (Fig. 5.9). It is evident that cardiomyocytes were present in the wound region in KO fish but not WT fish, as MF20 staining persists in the wound area in the KO but not in the WT fish (Fig. 5.9 C, D). Staining levels are reduced in intensity in the KO wound area, but readily visible. This indicates that cardiomyocytes within the wound area survive better in the *runx1* KO than in the WT.

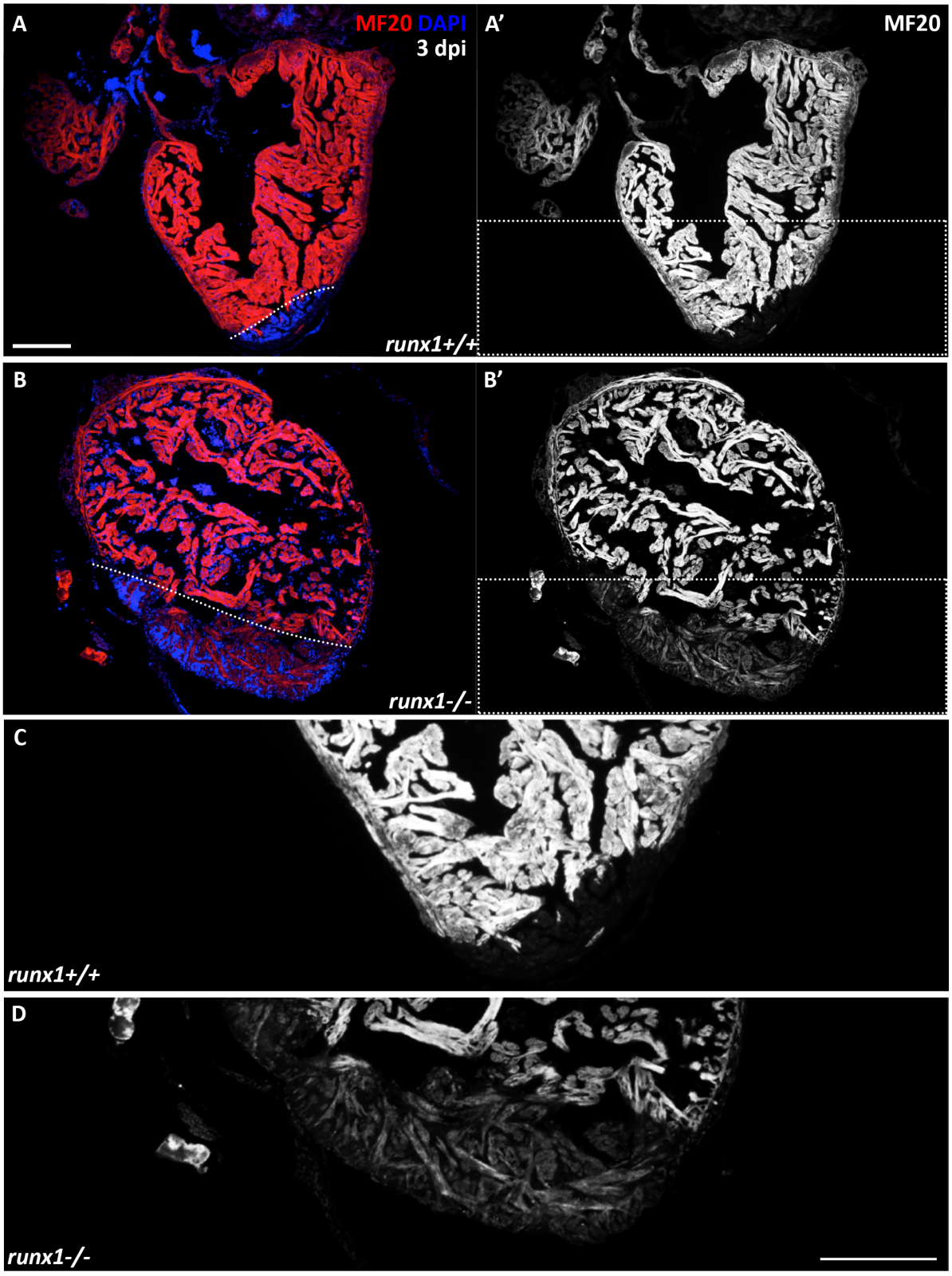


Fig. 5.9 A comparison of myocardial survival in *runx1* mutant and wildtype fish at 3 dpi. **A** and **A'** show immunohistochemistry for MF20 (myocardium) and DAPI staining in a *runx1* WT fish at 3 dpi. **B** and **B'**

show the KO fish. **C** and **D** are magnified images of the injury region shown in the dotted boxes in A' and B' for side by side comparison. N=4. Scale bars = 100 µm.

These results suggest that the enhanced myocardial regeneration seen in the *runx1* mutant fish is due to a combination of increased cardiomyocyte survival and proliferation. However, these results do not explain the alterations seen in scar handling.

5.8 LOSS OF RUNX1 DOES NOT APPEAR TO AFFECT THE APPEARANCE OF RUNX1-POSITIVE ENDOCARDIUM

The aim of analysing the regenerative capacity of the *runx1* mutant was to investigate the effect of the loss of post-injury EHT on regeneration. However, as *runx1* is also expressed in the myocardium, it is difficult to un-pick what aspects of the mutant phenotype are due to loss of Runx1 function in cardiomyocytes to those from loss of function in other cells, including the putative hemogenic endocardium. To help, EHT in the mutant was analysed in sections.

In the literature, loss of Runx1 function during development was seen to have no effect on the specification of HE and initial stages of EHT in the zebrafish, only when HSCs were about to detach did they fragment (Kissa & Herbomel 2010; Zhen et al. 2013). Therefore, 3 dpi mutant zebrafish were analysed for the appearance of hemogenic endothelial-like cells.

Images of Citrine and *runx1* (*runx1* mRNA is truncated, but present in enough length for RNAscope to detect) expression in sections from 3 dpi *runx1:citrine;runx1-/-* fish show double-positive cells that look to be endocardial within the injured area of the myocardium (Fig. 5.10 A-D arrowheads). These look very similar to the WT, as seen in the previous chapter and Fig. 5.10 E, F. This suggests that a HE is specified in the mutant, as endocardial cells switch

on expression of the Runx1 transgene and truncated endogenous *runx1*. It could not be determined whether EHT was abortive in the mutant, as it would be hard to capture a fragmenting cell in time. However, very rounded dimly citrine positive cells and ones that looked to be detaching were not seen in the mutant, suggesting that EHT might not progress beyond a certain point.

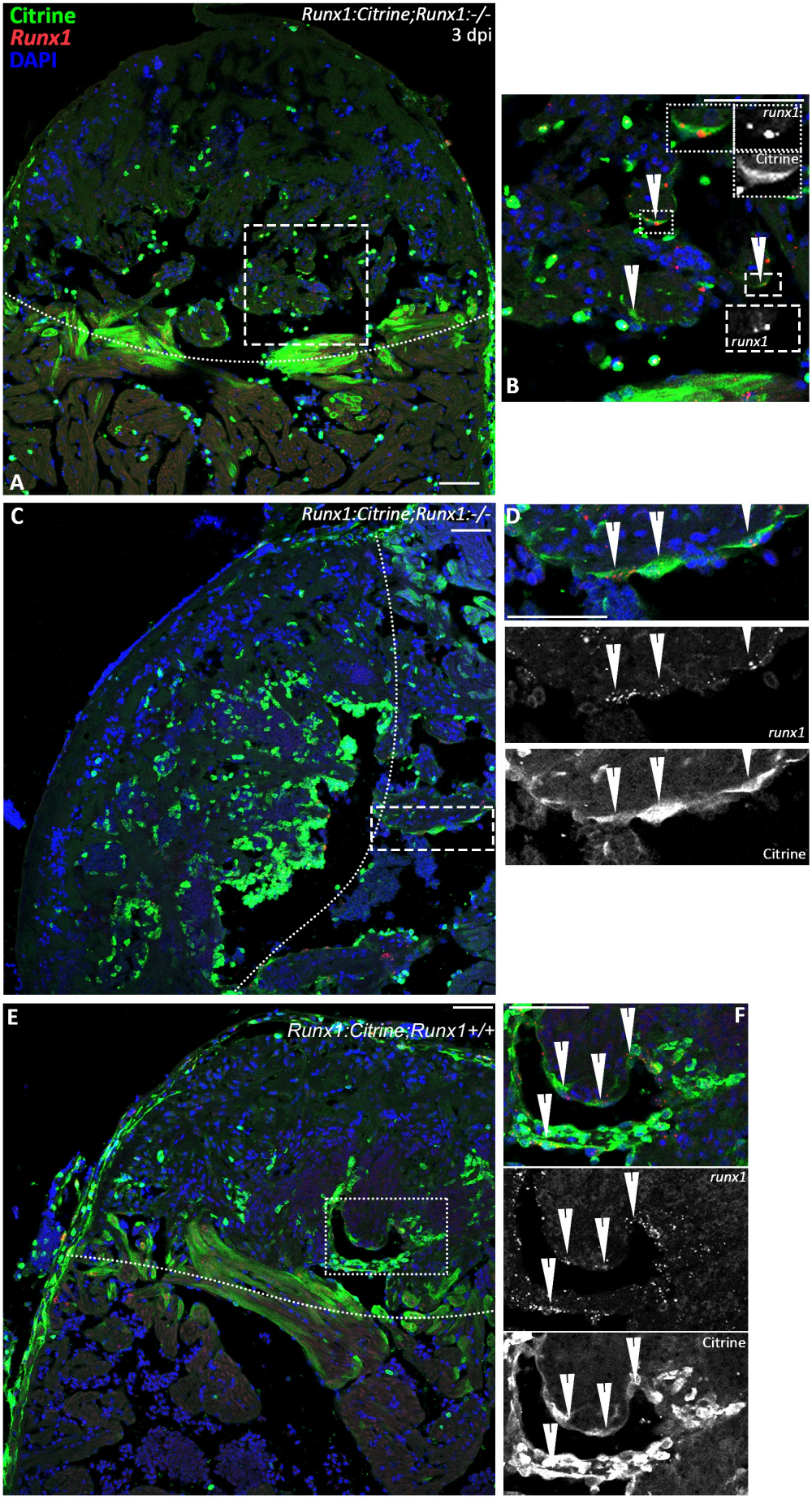

Citrine
Runx1
DAPI
Runx1:Citrine;Runx1:-/-
3 dpi
A
runx1
Citrine
runx1
B
C
Runx1:Citrine;Runx1:-/-
D
runx1
Citrine
E
Runx1:Citrine;Runx1+/+
F
runx1
Citrine

Fig. 5.10 Demonstrating EHT-like cells in the Runx1 loss-of-function mutant. **A** shows an overview of the injury area at 3 dpi, **B** shows the region denoted by the box in A magnified. The boxes in B show areas of further magnification of separate channels for clarity. **C** shows another mutant at 3 dpi as a further example. **D** are separate channel panels magnified from C. **E** shows a WT heart for comparison and **F** shows magnified separate channel panels of the boxed region in E. White arrowheads indicate cells that resemble the hemogenic endothelium. Scale bar shows 50 µm.

Attempting to investigate defects in EHT in sections is unlikely to be fruitful, as it would be hard to capture the fragmentation in a snapshot. Additionally, it would be impossible to say if any defects seen during a slice culture are due to loss of *runx1* function or damage due to slicing and culturing. Therefore, it was decided to capture single cells from the putative HE of mutant fish and analyse their transcriptomes for any differences to those in WT fish. In addition, single cell sequencing of putative HE from WT and mutant fish would allow further analysis of their gene expression and confirmation of their identity.

5.9 GENE EXPRESSION ANALYSIS OF ENDOTHELIAL AND HEMATOPOIETIC CELLS BY SINGLE CELL SEQUENCING

Whilst the previous data is indicative of a hemogenic endothelium, it is based on the expression of only two markers. To further interrogate whether a hemogenic endothelium is formed after injury, it was necessary to isolate the presumptive HE and look further at the gene expression profile of these cells. Do they express other markers of the hemogenic endothelium and hematopoiesis, such as other endothelial markers, HSC markers downstream of Runx1 and very early hemogenic genes seen in development? How does the expression profile of these cells change after injury? Additionally, analysis of mutant and wild-

type cells for comparison might indicate the effect of loss of Runx1 function on post-injury EHT.

To do this, single and double positive cells from double transgenic Runx1 WT and mutant fish were isolated from whole ventricle digests from uninjured WT fish and injured WT and KO fish at 3 dpi (N=20 for each sample). The hearts were then digested enzymatically to create single cell suspensions, which were then sorted by FACs. Single Citrine and mCherry positive cells and double positive cells were separately extracted for each sample and non-positive cells were removed. The positive cells were then recombined so that 1/3 of the total cell number was formed of each cell type, namely single mCherry-positive, Citrine-positive and double-positive. The end result was 3 single cell suspensions, 1 for each sample (WT uninjured, WT injured and KO injured).

These suspensions were then processed using the 10X Chromium Single Cell 3' Solution (10X Genomics) using the Single Cell 3' Reagent Kits v2 (Single Cell Library & Gel Bead Kit, Single Cell A Chip Kit, i7 Multiplex Kit). In this system, the cells are captured by individual gel microbeads, 1 cell per bead, and then are lysed before undergoing reverse transcription. The RT primers are anchored to the beads and contain an OligodT to recognise the 3' poly A sequence of mRNAs, a unique molecule identifier and a unique barcode, which is individual to each bead. Reverse transcription then proceeds from the 3' end of the mRNA, leaving the 3' end of the cDNA tagged with the unique molecule identifier and barcode. This cDNA from all the cells is then pooled for library prep. Library preparation involves the PCR amplification of the cDNA followed by enzyme fragmentation. Only tagged fragments are processed further, meaning that only the 3' end of the cDNA is kept for sequencing. Full length cDNA is too long, but some fragments will be too short to give sufficient detail, so fragments of the

correct size are then selected for further steps. Further ligation and PCR steps ensure all sequences, such as the Illumina P5 and P7 sequence, are then present in the fragment for Illumina bridge amplification and sequencing. The library fragments thus contain a partial 3' cDNA sequence, the 10X barcode, the unique molecule identifier and the Illumina sequences. Sequencing length was 75 bp. The library is then sequenced using Illumina Sequencing Technology (Illumina) and the reads are compared to a reference genome, in 2 lanes of approximately 5000 cells each (though reads were achieved for more like 7500 cells per lane). In this case the reference genome was the *Danio rerio* (zebrafish) GRCz11 genome assembly. By reading the cDNA sequences, along with the unique molecule identifiers and the barcode, it is possible to see how many transcripts of sequenced genes were present in each cell before sequencing.

The sequencing data was subsequently analysed by Xiaonan Wang, of Professor Göttgen's research group in Cambridge. Quality control was performed, excluding cells with more than 4000 genes to remove potential doublets, where two cells were caught by the same bead, and also excluding cells with more than 0.4% of their genes being mitochondrial. High numbers of mitochondrial transcripts can indicate cell stress and could influence subsequent analysis, causing group sorting to be done by cell stress levels rather than identity. After Quality control, 4077 cells from the WT uninjured sample, 4058 cells from the injured WT sample and 5741 cells from the KO injured sample could be used for further analysis.

The amplification of cDNA step and variability in the library preparation process means that each cell should be normalised by total counts over all genes. After normalisation, each cell has a total count equal to the median of total counts per cell before the normalisation. This means that the relative levels of expression of each gene can be compared between cells.

Following normalisation, highly variable genes were selected using the Seurat method (Satija et al. 2015). After this, 2070 highly variable genes were selected. Uninteresting cell-cell variation driven by the number of detected reads and mitochondrial gene expression is then regressed out.

The cells were then grouped into clusters, representing different cell types, and gave us gene expression level data for the cluster. This clustering was done using the Louvain clustering method. This data could be further subdivided into expression levels in cells from before and after injury and from WT and mutant fish, to indicate if there are any differences due to the injury environment. In addition, analysis could be further restricted to cells expressing both mCherry and Citrine transcripts.

Once the data had been prepared by Xiaonan Wang and returned, further analysis of this data took place. The clusters were analysed for identity and compared to known cell types in the WT and mutant fish. Additionally, levels of gene expression for certain cell groups were compared to detect populations with high levels of hemogenic endothelium gene expression.

5.9.1 SOME CELL TYPES ARE ONLY PRESENT IN INJURED HEARTS OR ARE DRASTICALLY INCREASED IN INJURED FISH

After cluster analysis, 15 cell types were identified that are mCherry and/or Citrine positive in the zebrafish uninjured and injured ventricle (Fig. 5.11 A). These were labelled clusters 0 – 14 and given suggested cell type identities based on marker gene expression. A table containing the cluster number, differentially expressed genes in that cluster and the proposed identity of cells in that cluster can be found in table A.5, in the appendix. Analysis of the percentage

of cells from each cluster from each sample, WT injured, WT uninjured and KO injured, allowed identification of injury-related mCherry and/or Citrine positive cells (Fig. 5.11 B).

Clusters 3, 4, 7, 10 and 11 are predominantly composed of cells from injured fish. Identification of these clusters from expression of biological markers shows that these cells are early heart cells, epicardial cells/ myofibroblasts, monocytes, leukocytes, smooth muscle cells and epithelial cells respectively. The finding of epicardial cells, monocytes and leukocytes in predominantly/only injured samples is unsurprising. Runx1 positive epicardium is only seen after injury, whilst there is a drastic increase in monocytes and leukocytes into the heart after injury.

Clusters 3, 10 and 11 are harder to discern. Cluster 3 is ill-defined and does not fit an easy cell type label. It is formed of both mCherry and Citrine single and double positive cells (Fig. 5.11 C) that express markers associated with early heart cells (*hand2* and *foxc1a*) (Conway et al. 2010; Yue et al. 2018), as well as epithelial (*krt8* and *18*) (Gong et al. 2002; Wang et al. 2006) and epicardial and endocardial injury response markers (*serpine1* and *aldh1a2*) (Münch et al. 2017; Kikuchi et al. 2011). Cluster 10, smooth muscle cells, are composed mostly of Citrine-positive cells. Citrine expression is extensive in the wound, as shown in this and previous chapters and likely encapsulates injury-responsive smooth muscle. Cluster 11, the epithelial cells, are vaguely similar in expression to cluster 4, with expression of collagens and epithelial cytoskeletal markers.

In summary, the cluster analysis indicates the presence of injury predominant/only populations within Citrine and/or mCherry positive cells in the fish heart. These are epicardial cells, leukocytes and monocytes.

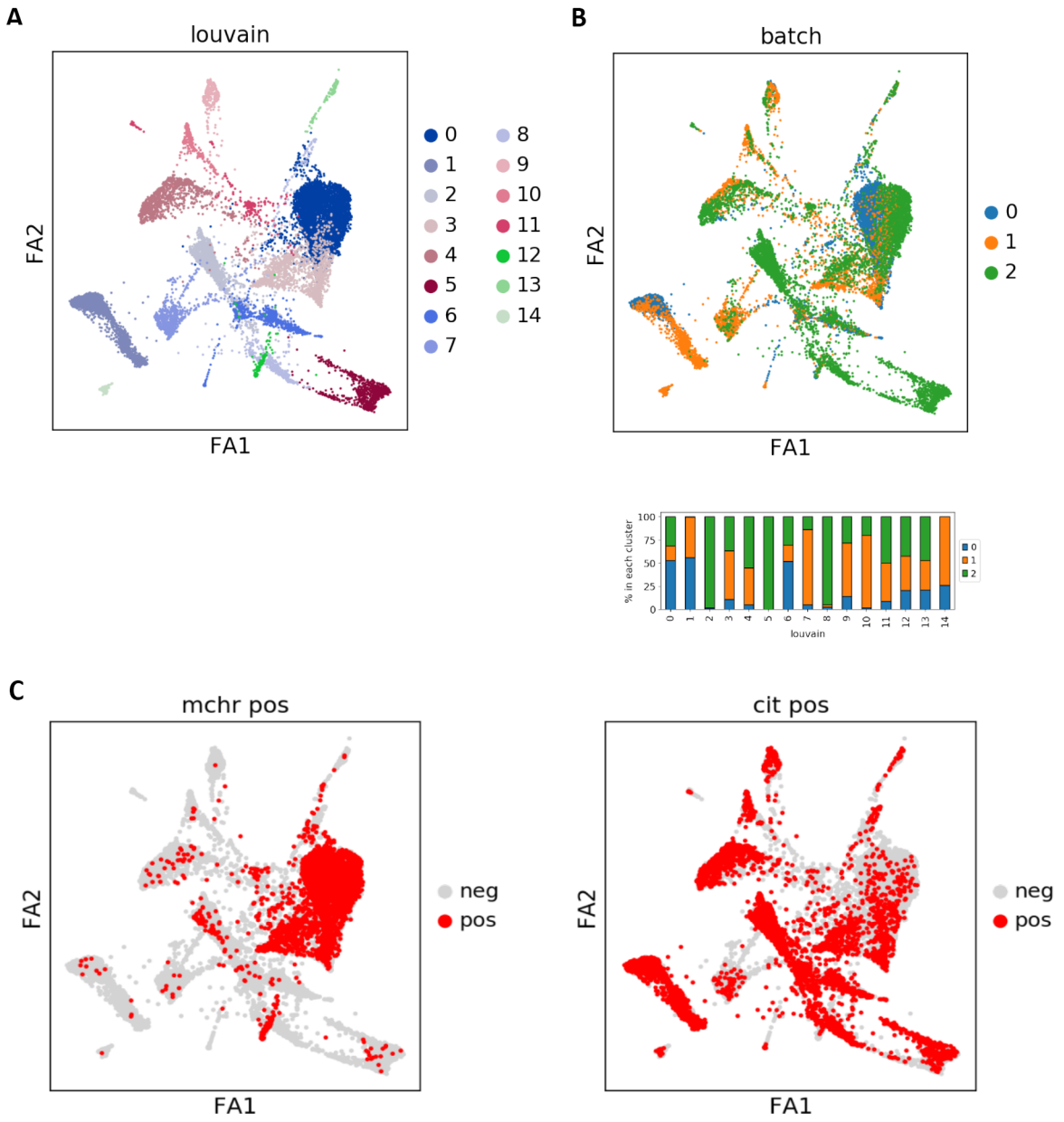


Fig. 5.11 Overview of single cell cluster analysis for single and double positive cells isolated from uninjured and 3 dpi injured *runx1:citrine; kdrl:mCherry* and injured *runx1-/-; runx1:citrine: kdrl:mCherry* hearts. **A** shows the arrangements of the 15 identified clusters from the samples. **B** shows what proportion of cells in each cluster come from each sample. 0 is the WT uninjured sample, 1 is the injured WT sample and 2 is the mutant injured sample. **C** indicates which cells in the clusters were positive for mCherry (LHS) and Citrine (RHS). Each dot represents 1 cell. All data compiled and graphed by Xiaonan Wang.

5.9.2 THE RUNX1 MUTANT HAS A DIFFERENT CELL COMPLEMENT TO WT FISH

Of the 15 identified clusters, the Runx1 mutant lacked clusters 1 and 14. The mutant also had cell populations that the WT hearts did not, or had drastically increased numbers. These were clusters 2, 5 and 8 (Fig. 5.11 B).

The absence of cells from mutant fish in cluster 1 is not unexpected, as this cluster represents thrombocytes through the expression of thrombospondins, platelet glycoproteins and platelet-derived growth factors, as well as *mpl* and *nfe2* (Lin et al. 2005; Rost et al. 2018; Kopp et al. 2006), markers of thrombocyte precursors. Arrested thrombocyte development has been previously noted in the fish mutant, so their absence here indicates correct clustering in this respect (Sood et al. 2010).

Cluster 14 was labelled as another monocyte population or at least a myeloid precursor, due to expression of *spi1a* and *spi1b* and *mpeg1.1* (Athanasiadis et al. 2017; Rissone & Burgess 2018; Ellett et al. 2011). Runx1 mutant fish have been shown to have a broadly normal complement of myeloid-lineage cells (excluding thrombocytes), with mostly the full range of cell types produced still, but some in reduced numbers (Sood et al. 2010). The finding of a myeloid-lineage cell, potentially of monocyte/macrophage lineage, that is absent in the Runx1 mutant here is an unexpected and novel finding.

Cluster 2 look to be mature, circulating HSCs due to their high expression of *myb*, *tal1* and *lmo2* (Bertrand et al. 2008; Lancrin et al. 2009; Nottingham et al. 2007). In the Runx mutant, definitive hematopoiesis as recognised in wild-type animals does not occur and the fish initially survives on primitive hematopoiesis alone, gradually becoming bloodless. However, approximately 20% of these larvae survive, through development of late Runx1-independent definitive hematopoiesis. It could be that these cluster 2 cells are the HSCs that are produced

from this process and would thus be distinct from those produced in WT fish. Cluster 8 is another circulating HSC population, that is found in all three samples, but predominantly in the mutant sample. It appears to show expression of markers of erythroid, neutrophil, macrophage and thrombocyte lineages and could represent a population of HSCs that are differentiating into multiple hematopoietic cell types *in situ* or a population that has defective differentiation and stuck in a half-way state.

Cluster 5 are erythroid cells, based on high levels of hemoglobin expression. Cluster 5 is formed from predominantly single Citrine positive cells from only the *runx1* mutant fish. The expression of Citrine in *runx1* mutant red blood cells is somewhat surprising and unexpected. Red blood cells are also undoubtedly present in the WT fish ventricle, but they are not Citrine positive. Runx1 normally inhibits the erythroid gene program in Megakaryocyte-erythrocyte progenitors. In the mutant, Runx1 is non-functional, allowing the erythroid gene program to proceed without *runx1* inhibition. Therefore, *runx1* transgene expression may still be switched on in some RBCs as it was never inhibited during their differentiation.

Overall the cluster analysis indicates and identifies many of the cells expressing *runx1* and/or *kdrl* before and after injury in the fish heart and identifies cell-types that are absent or present only in the KO fish. This is important to the understanding of cell types that express Runx1 after injury and the effect of Runx1 loss on the cell complement that responds to injury. However, the cluster analysis is of less use when it comes to identifying and investigating the hemogenic endothelium. Some of the clusters are of undetermined identity and there are multiple clusters with a hematopoietic identity. Therefore, identifying a single cluster containing the hemogenic endothelium was difficult, and, indeed, the hemogenic endothelium may itself be highly heterogeneous and not limited to one cluster. Therefore,

focus was put on comparing all isolated double-positive (Citrine and mCherry positive) cells to the others, to look at their expression of hemogenic endothelial genes.

5.9.3 COMPARING CARDIOMYOCYTES FROM INJURED WT AND KO FISH

As the analysis of the KO and WT thus far indicated that KO cardiomyocytes appear to show increased proliferation and better survival after injury, the single cell data was analysed to look at differences between cardiomyocytes.

Cluster 13 (Fig. 5.11 A) was determined to be cardiomyocytes and comprised cells from all three samples. The overall number of cells in this cluster was 106, with more cells coming from the KO injured sample than the WT samples. The number of cells is small, reducing the certainty of conclusions drawn, but statistically significant variance in gene expression was seen. The transcriptomes of the mutant injured and WT injured cells were compared and genes that were significantly differently expressed were identified. The top 20 most differentially regulated genes were then investigated further for the gene ontology (GO) terms associated with them (Fig. 5.12). Amongst the most upregulated in the mutant cardiomyocytes genes are hemoglobins *hbba1-1, hbba2, hbaa1* and *hbaa2.* Genes controlling Ca^{2+} sensing and handling are differentially regulated as well, according to GO terms associated with the genes *rrad*, *smdt1b* and *calm2b*. Genes associated with metabolism are also amongst the most differentially regulated, *trib3* and *pisd*. Interestingly cytoskeletal genes *acta2* and *actc1a-1* are differentially regulated, with one being down-regulated and the other upregulated in the mutant. A gene relating to cell cycle activity *pa2g4a* is upregulated in the mutant, hinting at the increased proliferation seen in the PCNA analysis of mutant and WT sections at the same time-point.

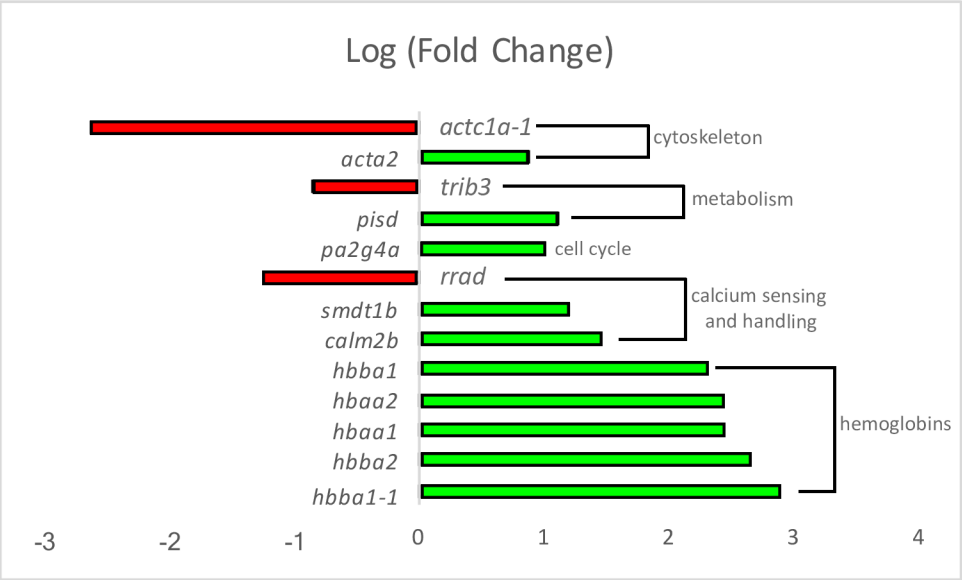


Fig. 5.12 Largest Log(Fold Changes) in gene expression in Runx1 KO cardiomyocytes compared to wild-type, with their associated GO terms labelled. P<0.05.

The changes in calcium sensing and handling is an indication that the same changes that occur in the *Runx1* conditional mouse mutant after cardiac injury might occur in the zebrafish as well. McCarroll and colleagues found that calcium uptake and dependent functions in the sarcoplasmic reticulum were altered in the mutant after injury (McCarroll et al. 2018). The increased expression of hemoglobins is interesting. Hemoglobins have been found to be expressed in cardiomyocytes after dosing with a potent erythropoietin (EPO) inducer and is thought to give some protection against ischemic injury (Hsu et al. 2013). Could it be possible that it also improves cardiomyocyte survival after injury by cryo-probe, through increasing availability of oxygen to injured cardiomyocyte mitochondria?

The expression differences highlighted by this analysis hint at the mechanisms underlying the improved survival and proliferation seen in the AFOG analysis and suggest that a similar calcium-handling phenotype might be present in the fish as seen in the mouse. However, the

main focus of this work is progenitor populations, so the rest of this chapter concentrates on further characterisation of the hemogenic endothelium.

5.9.4 ANALYSING DOUBLE POSITIVE CELLS

The hemogenic endothelium is by definition both endothelial and hematopoietic, with overlapping expression of marker genes for each. The work done in histological sections shows that it can be expected to be greater in number, or more hematopoietic in nature, in the WT injured sample relative to the uninjured sample. It may or may not be present in the mutant sample.

Of the sequenced cells, 627 were positive for both citrine and mCherry transcripts. This number, approximately 5% of the total cell number, appears low. It should be roughly 33% of the total cell number as 1/3 of the input cells were FAC sorted as double-positive cells. However, sequencing depth – or the number of reads per cell, is relatively shallow using the 10X genomics method and transcripts are not always detected. Identification of differentially expressed genes shows that these cells express more *kdrl*, *cdh5*, *lmo2*, *runx1*, *gata2b* and *gfi1aa* than non-double positive cells, but express less *myb*. This suggests that they broadly represent a hemogenic endothelial-like population, rather than a mature HSC population in terms of gene expression.

To investigate this population further, the double-positive population was analysed to see if it contained distinct populations within itself. Cluster analysis shows that there are approximately 10 populations of double positive cells, so it appears to be a highly heterogeneous population (Fig. 5.13 A). Analysis looking at which fish sample contributed to each cluster shows that WT uninjured hearts lack double-positive clusters 4, 7, 8 and 9. Injured WT hearts contain all clusters except 8, which is limited to KO hearts only. KO injured

hearts have cells from all clusters, but the number of cells in each cluster varies compared to the WT injured heart. For example, the WT injured heart has greater numbers of cluster 1, 3 and 7 and much fewer cells in cluster 2, compared to the KO. This suggests that Citrine/mCherry double-positive cells have slightly different identities between the two fish. The lack of clusters 4, 7, 8 and 9 and low levels of cluster 2 in the uninjured heart suggests that these are the injury-derived populations for further investigation in future experiments, once further analysis of their identity has been performed. This is currently on-going.

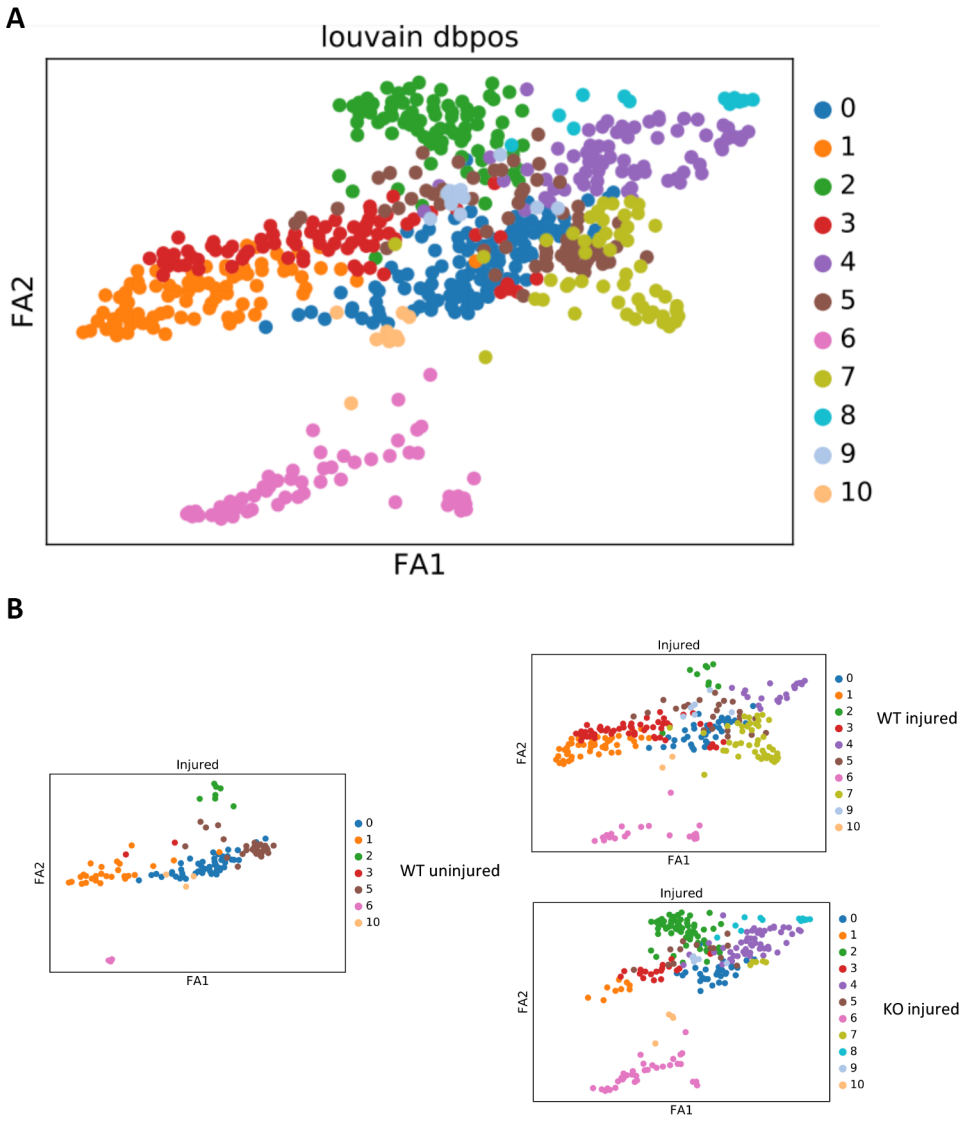

A
louvain dbpos
FA2
FA1
0
1
2
3
4
5
6
7
8
9
10
B
Injured
FA2
FA1
WT uninjured
WT injured
KO injured
C
louvain
FA2
FA1
0
1
2
3
4
5
6
7
8
9
10
11
12
13
14

Fig. 5.13 Cluster analysis of double positive cells. **A** shows the double positive cell clusters **B** shows the sample origin of the cell clusters in A. **C** is the same plot, but with cells labelled with their original cluster identity from Fig. 5.11. Each dot represents 1 cell. Data compiled and graphed by Xiaonan Wang.

To try to determine which of the original clusters of the total cells could contain the hemogenic endothelium, the double-positive cell clusters were labelled with which of the original 15 clusters they arise from (Fig. 5.13 C). Table A5 in the appendix shows how the double-positive clusters map onto the original clusters and the identities of the original clusters based on differential gene expression. This graph shows that the original clusters 0 and 3 are the major contributors to the double positive population. Original cluster 0 gives rise to the majority of cells in the double-positive clusters 0 and 1. Double-positive cells from original cluster 3 form double-positive clusters 3, 4 and 7. Cells from original cluster 1 compose the major part of double-positive cluster 5, original cluster 4 forms double-positive cluster 6, original clusters 2, 6, 7 and 8 form double-positive cluster 2 and original cluster 5 gives rise to the majority of double-positive cluster 8. Another example is original cluster 9 giving rise to double-positive cluster 10.

Double-positive cells are found in original clusters that were labelled as not endothelial or hematopoietic lineage cells. The majority of these are in original clusters labelled as epithelial or epicardial, such as cluster 4. In the double-positive cluster analysis these cells are very separate from the others, for example cells from original cluster 4 form double-positive cluster 6, which is separated from the other double-positive cells.

Original clusters 0 and 3 were originally labelled as ‘heart’ cells. On closer inspection, the double-positive cells in both clusters express higher levels of the majority of hemogenic

endothelium genes than other double positive cells. It could be that clusters 0 and 3 represent hemogenic endothelium at different levels of differentiation, or HE with distinct potential. For example, one could be hemogenic endothelium immediately after specification and the other further down the differentiation pathway towards becoming a HSC. Or one could be cells

The double-positive clusters not covered by cells from original clusters 0 and 3 likely represent HSCs that have arisen from the HE and are embarking on distinct lineage differentiation pathways. An example is double-positive cluster 8 being in original cluster 5, which are erythrocytes, and double-positive cluster 2 comprising originally labelled hematopoietic progenitors, T cells and monocytes. Cluster 10 is composed mostly of cells from original cluster 9, which are leukocytes.

To summarise, the double-positive cells in original clusters 0 and 3 likely comprise distinct stages of the hemogenic endothelium or perhaps HE cells of distinct potential. The other double-positive cells are likely HSCs that have emerged from the HE and are embarking down distinct differentiation pathways and their progeny, that still contain Citrine and mCherry mRNA. Analysis comparing the double-positive cell clusters and assigning them an identity is under-way.

5.10 RNASCOPE MARKER GENES

The single cell sequencing results indicated that the mutant injured heart contains more mature HSCs than the WT injured fish and that there is a population of hemogenic endothelium positive for markers such as *gata2b*, *runx1*, *tal1* and lower levels of *myb*. The next step was to look at expression of these markers in sections of injured mutant and WT

hearts, to see if the cells identified in the single cell data can be found in heart sections and, if so, where they are located within the heart.

To this end, RNAscope was performed in sections of WT and mutant 1 dpi and 3 dpi hearts for *myb*, *runx1*, *tal1* and *gata2b*. 3 dpi is when the single cell sequencing was performed and by this time-point distinct differences in injury response between the WT and KO fish are already evident. As such, looking at a time-point before this one was determined to be additionally useful.

Images of *runx1* and *tal1* expression in 1 dpi mutant and WT *runx1:citrine* fish show infiltration of bright, round Citrine positive cells in both fish (Fig. 5.14). These cells appear to be positive for *runx1* and *tal1* (Fig. 5.14 A', B', arrowheads, A", B")). *Tal1* expression is seen extensively in erythrocytes and other unidentified blood-borne cells, so perhaps can be seen as more a pan-blood cell marker, than a specific HSC marker. This expression pattern is in line with reported expression of *Tal1* in mammalian HSCs, myeloid progenitors and mature myeloid cells (e.g. erythrocytes, megakaryocytes). It is also expressed at low levels in eosinophils, macrophages and neutrophils, but not in mature lymphoid cells (Porcher et al. 2017). Analysis of *gata2b* and *myb* expression at 1 dpi however, indicates expression of *myb* in the Citrine positive cells of both WT and KO fish, however, *gata2b* expression was restricted to the rounded cells of KO fish only (Fig. 5.15 arrowheads). Combined expression of *runx1, myb*, *tal1* and also *gata2b* in the mutant is certainly suggestive that hematopoietic progenitors infiltrate the wound site at 1 dpi of both fish.

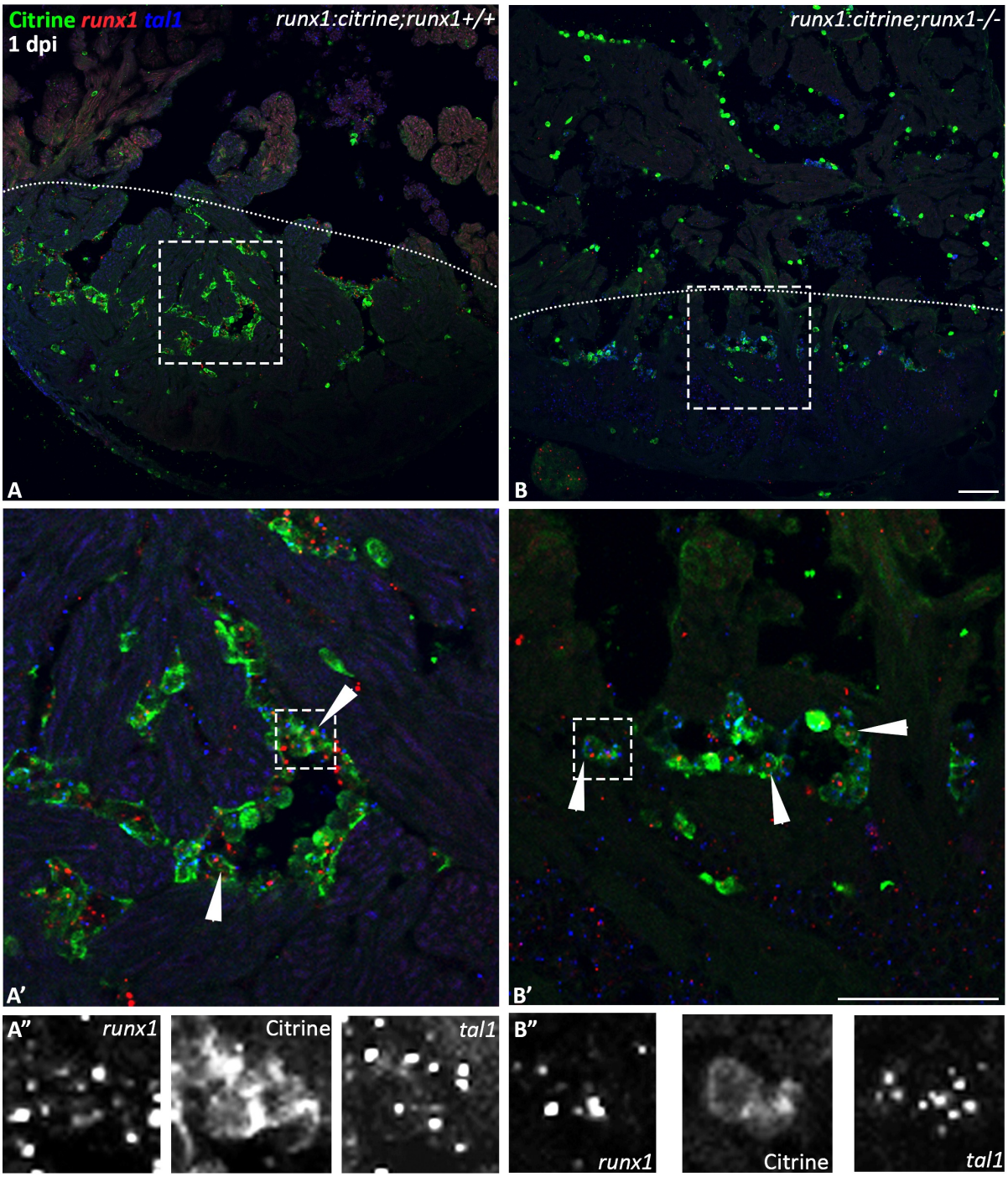


Fig. 5.14 Comparison of *runx1* and *tal1* expression in *runx1* mutant and wild-type *runx1:citrine* fish at 1 dpi. **A** and **A'** show the wild-type fish, where A' is a magnification of the region indicated by the box in A. **A"** is the magnification of the box in A'. **B**, **B'** and B" show the same for the *runx1* loss of function

mutant. Arrowheads indicate cells that show expression of Citrine and both *runx1* and *tal1*. Scale bar indicates 50 µm. N=3.

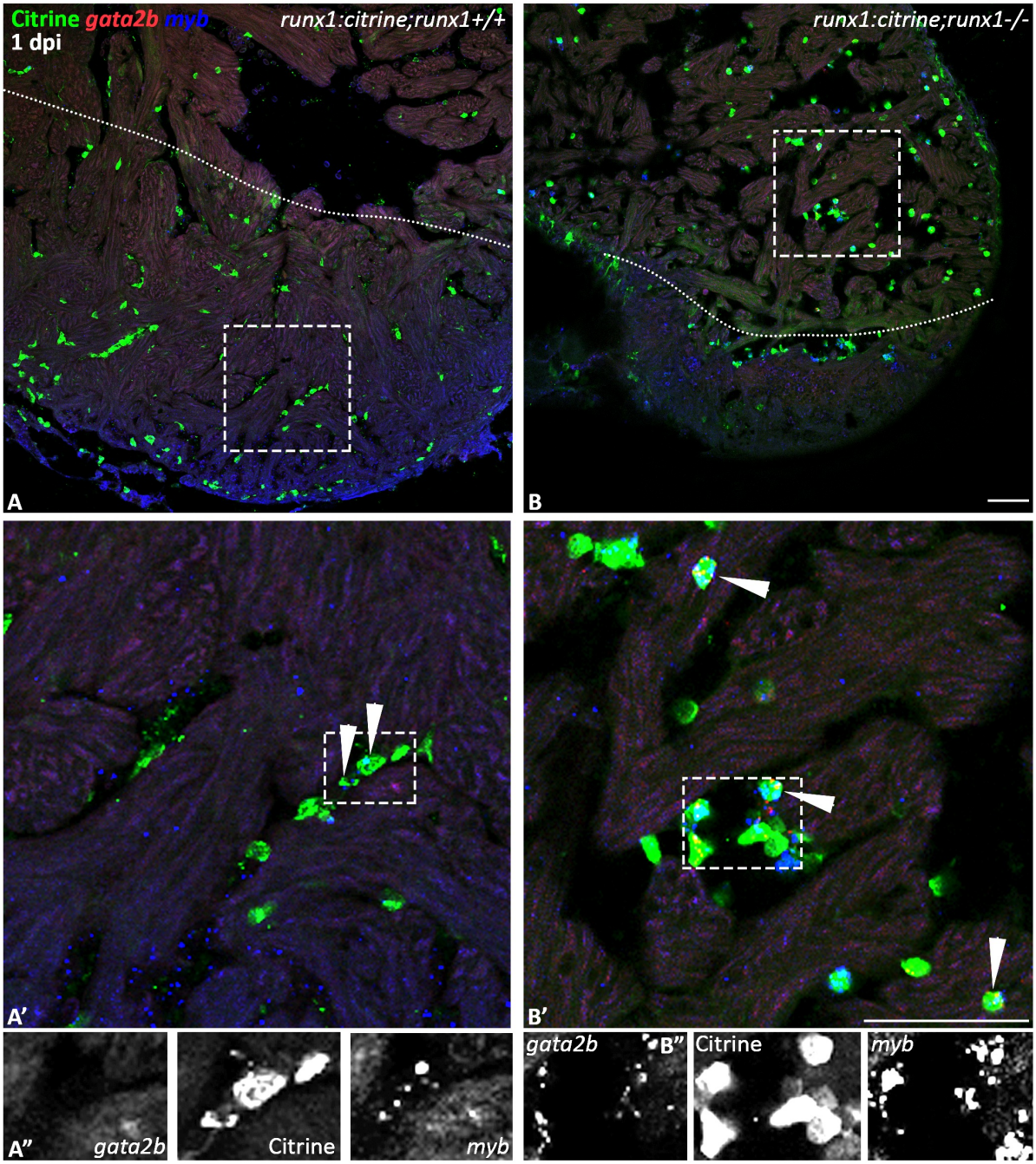


Fig. 5.15 Comparison of *myb* and *gata2b* expression in *runx1* mutant and wild-type *runx1:citrine* fish at 1 dpi. **A** and **A'** show the wild-type fish, where A' is a magnification of the region indicated by the box in A. **A"** is the magnification of the box in A'. **B**, **B'** and **B"** show the same for the *runx1* loss of

function mutant. Arrowheads indicate cells that show expression of Citrine and both *myb* and *gata2b* in the mutant and *myb* and Citrine only in the WT. Scale bar indicates 50 μm. N=3.

Analysing expression of these markers at 3 dpi shows interesting contrasts between the mutant and the WT fish. In both the mutant and the WT fish, endocardial Citrine-positive cells are positive for *tal1* and *runx1* (Fig. 5.16 arrowheads). These are the cells identified previously as putative hemogenic endothelium. However, looking at *gata2b* and *myb* expression in these cells gives some surprising results. In the WT, these endocardial Citrine-positive cells are also *gata2b* positive and sometimes *myb* positive, though predominantly they are solely *gata2b* positive (Fig. 5.17 A, A'). The KO, on the other hand, lacks *gata2b* staining in these cells, whilst some are *myb* positive (Fig. 5.17 B' white arrowheads are *myb* positive, pink arrowheads are *myb* negative). The cells found in the KO that are positive for both of these markers are, in fact, bright Citrine-positive round cells, that appear to be strongly positive for both *gata2b* and *myb* (Fig. 5.17 B''). In the wild-type, the bright, round cells appear to be *gata2b*-negative and occasionally *myb* positive (Fig. 5.17 A"). Therefore, expression of *gata2b* and *myb* appears to mark a different population in the WT and KO hearts. In the WT, the injured endocardium is positive for *runx1*, *myb*, *tal1* and *gata2b*, whilst in the KO these markers combined delineate only circulating cells, according to RNAscope experiments.

Overall, these results show that hematopoietic progenitors, delineated by their expression of *runx1, tal1* and *myb* appear to be circulating and infiltrating the wound at 1 dpi in both the mutant and WT. The mutant cells differ in that they also express the marker *gata2b*, a marker of hemogenic endothelium. At 3 dpi, cells that resemble a hemogenic endothelium emerge in both fish, where endocardial cells express *runx1* and *tal1.* In the mutant, these cells are

seen to express *myb* as well, but do not express *gata2b*. In the wild-type, these cells do express *gata2b* and occasionally express *myb* too, though relatively rarely.

These results corroborate the single cell sequencing findings that showed many HSC like cells in the mutant fish that were not present in the wild-type, with the circulating *myb* and *gata2b* positive cells seen in this staining. The staining also shows subtle differences in the gene expression in the putative hemogenic endothelium between mutant and WT cells, which may indicate some difference in EHT between the fish.

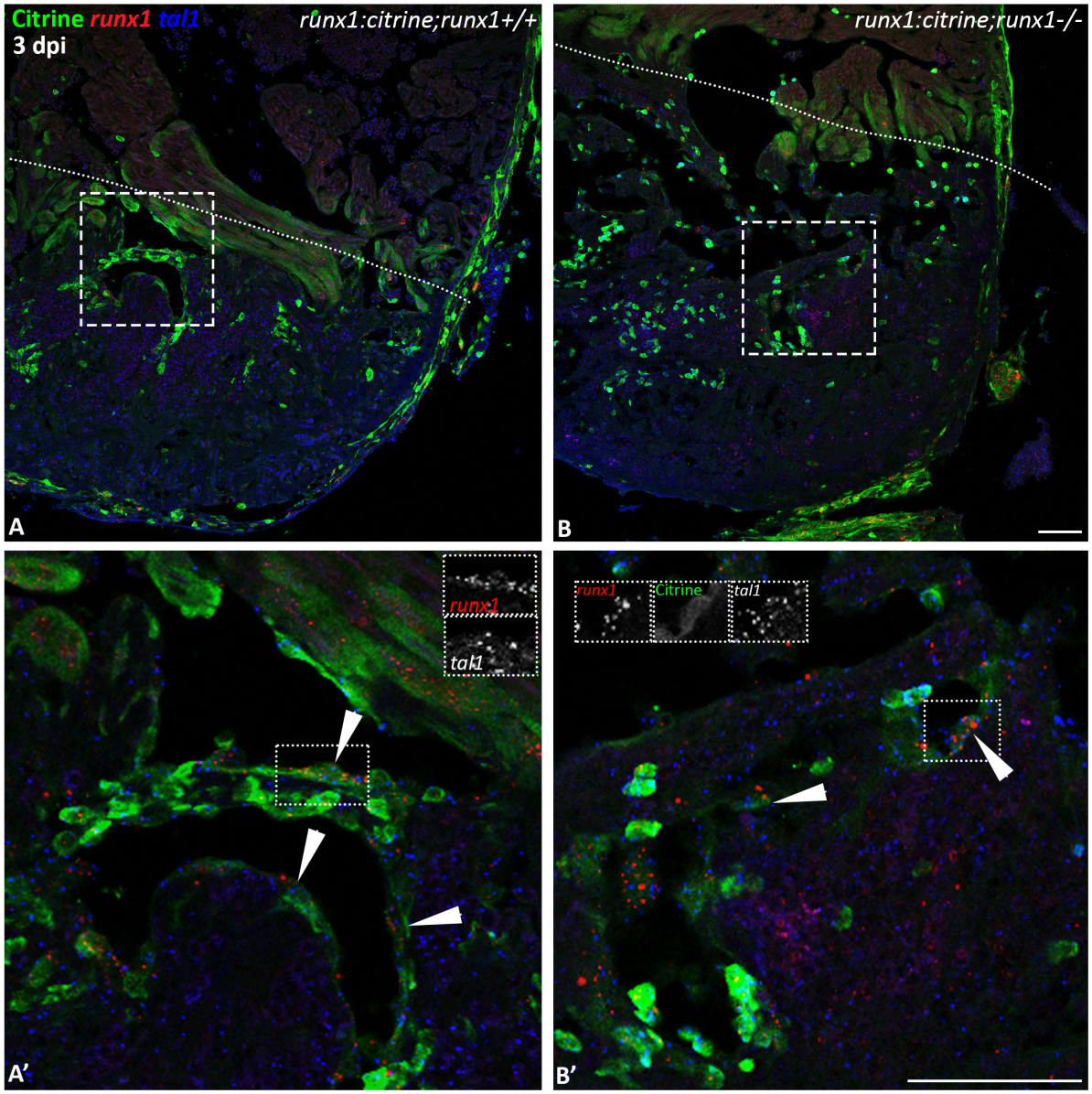


Fig. 5.16 Comparison of *runx1* and *tal1* expression in *runx1* mutant and wild-type *runx1:citrine* fish at 3dpi. **A** and **A'** show the wild-type fish, where A' is a magnification of the region indicated by the box in A. **B** and **B'** show the same for the *runx1* loss of function mutant. Arrowheads indicate cells that show expression of Citrine and both *runx1* and *tal1*. Scale bar indicates 50 µm. N=3.

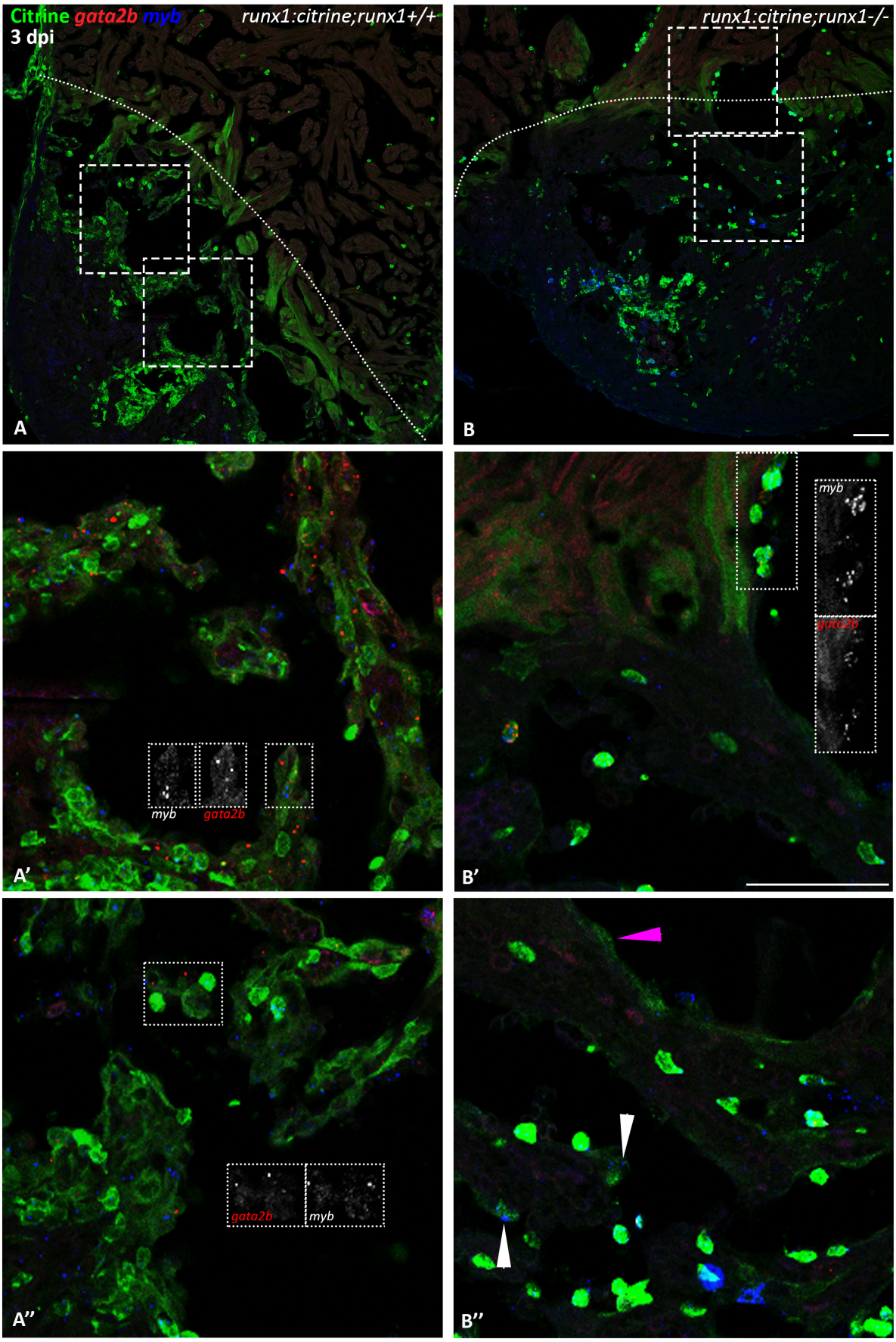

Citrine gata2b myb
3 dpi
runx1:citrine;runx1+/+
runx1:citrine;runx1-/-
A
B
myb
gata2b
A'
myb
gata2b
B'
gata2b
myb
A''
B''

Fig. 5.17 Comparison of *myb* and *gata2b* expression in *runx1* mutant and wild-type *runx1:citrine* fish at 1 dpi. **A**, **A'** and **A"** show the wild-type fish, where A' and A" are magnifications of the regions indicated by the boxes in A. **B, B' B** and **B''** show the same for the *runx1* loss of function mutant. White arrowheads in B' indicate HE-like cells with *myb* expression and the pink arrow indicates one without *myb* expression. The dotted boxes containing greyscale images in A', A", B' and B" are single channel images of the RGB region enclosed by a dotted box in the same image. A' shows an endocardial cell, A" shows blood-borne cells, as do the boxes in B". Scale bar indicates 50 μm. N=3.

5.11 DISCUSSION

The work in this chapter gives further evidence that a hemogenic endothelium is formed in the fish heart after injury and that this endothelium undergoes endothelial-to-hematopoietic transition. This is shown through live-imaging of cultured heart slices, where it was seen that endocardial cells in the wound can undergo the same cell movements as those undertaken by hemogenic endothelial cells during EHT in development. Additional evidence is given by analysis of gene expression in isolated cells by qPCR and single cell sequencing, that shows that cells from *runx1:citrine;kdrl:mCherry* fish that express mCherry and Citrine express high levels of hemogenic endothelial genes in comparison to other cells, and to endothelial and pure HSCs. RNAscope experiments show expression of these genes spatially within the putative hemogenic endothelium.

The single cell data indicates that a hemogenic endocardium that resembles the developmental hemogenic endothelium arises after injury, based on published data on developmental hemogenic endothelium gene expression. It was initially conceived to provide a sample from developing zebrafish as well for comparison, as there is some evidence that

developmental hemogenic endocardium has a different signature to that from the dorsal aorta (Zamir et al. 2017), but unfortunately the sequencing in this sample was unsuccessful. However, published and emerging data sets, for example from (Athanasiadis et al. 2017) can be compared to the data in this thesis in future.

During development, Notch signalling turns on expression of *gata2b* in the hemogenic endothelium in the dorsal aorta and this then turns on *Runx1* expression (Butko et al. 2015). This Notch signalling is in turn regulated by TGFß through regulation of ligand expression in endothelial cells (Monteiro et al. 2016). There is evidence that retinoic acid signalling is necessary within endothelial cells for hemogenic endothelium function and EHT itself requires additional Notch signalling as well as hypoxia and inflammatory signalling mediated by TLR4-NF-κB signalling (reviewed in Gritz & Hirschi 2016). It is known that the endocardium expresses Notch receptors after injury and takes part in Notch signalling (Zhao et al. 2014). In addition, cardiac damage induces TLR signalling and TGFβ, NF-κB and retinoic acid signalling (Chablais & Jaźwińska 2012; Karra et al. 2015; Kikuchi et al. 2011). Therefore, the cocktail required for developmental hematopoiesis and HE specification appears to be largely recapitulated after injury. Furthermore, observations show that the endocardium forms a dense network in the injury area through intense proliferation until 3 dpi that is greater than in the heart in general and that this network matures and remodels from 7-9 dpi (Münch et al. 2017). There is, therefore, a surplus of endocardial cells after wounding that resolves during regeneration and it is interesting to speculate about what happens to these excess cells. Some probably are devoted to angiogenesis (Kobayashi et al. 2017), but this timeline also neatly fits with the timeline of HE specification and EHT presented here and it seems possible that some of this excess is due to endothelial cells undergoing EHT.

This chapter also demonstrates some functional analysis into the hemogenic endothelium after injury through analysis of regenerative capacity in the *runx1* mutant, where truncation leads to a loss of function. Loss of *runx1* in development abrogates EHT, so it was theorised that it should do the same in post-injury EHT and the effect of the absence of this process could be analysed. The mutant showed enhanced myocardial regeneration, with increased myocardial survival and proliferation seen at 3 dpi, leading to regeneration of a contiguous compact myocardium by as early as 7 dpi. The single cell analysis indicated that the myocardial cells show increased hemoglobin expression, calcium signalling and energy release compared to WT cardiomyocytes.

Besides this myocardial phenotype, the mutant shows some potential defects in scar deposition and clearance. Fibrin deposition appears to be later than in the WT and, whilst the myocardium appears to regenerate faster, scar clearance does not show a concurrent increase. Attempts to investigate whether EHT was affected in the mutant were inconclusive: there was evidence that the hemogenic endothelium is still specified in the mutant and RNAscope suggested that it is subtly different in gene expression to the WT. The single cell sequencing data suggested some difference in the putative hemogenic endothelium between mutant and wild-type fish and there was some indication of a non-myocardial phenotype in the *runx1* mutant heart after injury, suggesting further functional analysis might show a role for EHT in injury outcome.

It is interesting to speculate about the potential role of EHT in the wound site: it could be a by-product of the intense number of signals that are produced after injury and the activation of the injured endocardium, but it could also play an active role in the ability to regenerate. Where these HSCs go after being extruded from the endocardium is unknown, they could

disappear into the blood as they do into the culture medium of the slice cultures, or they could be caught by the stickiness of the surrounding wound tissue. It has been seen in murine models that hematopoietic stem cells can be recruited to injury sites by the expression of chemokines from injured endothelium. The injured endothelium also expresses cellular adhesion molecules that 'catch' HSCs, such as Selectins and Integrins (Rennert et al. 2012). Whether the cells initially enter circulation, or are caught straight away by injured tissue, it seems likely that EHT within the wound increases the number of HSCs present in wound tissue as they are captured by injured cells. Here, they can aid regeneration through the generation and recruitment of macrophages and neutrophils to clear debris and scar tissue, or generate anti-fibrotic signals, as has recently been seen in HSCs that home to the fibrotic mouse liver (King et al. 2017). It has been shown in mice that HSCs can interpret wound signals to generate more cells of a certain lineage; after cardiac injury, a hematopoietic stem progenitor cell with a myeloid bias is seen (Dutta et al. 2015). Therefore, it seems likely that production of HSCs benefits regeneration, likely through generation and modulation of immune cells in scar handling and resolution.

Overall, this chapter provides strong evidence that endothelial cells within the wound area of the hearts of zebrafish become a hemogenic endothelium and undergo endothelial-to-hematopoietic transition. This is a phenomenon that has not been found before in fish or any other vertebrate and is an exciting finding, that continues the notion that injury causes developmental pathways to re-emerge. Analysis of the function of these cells should be possible in the near future and the data presented here shows many avenues for further work to take place. As mentioned previously, analysis of the single cell transcriptomics data is ongoing and analysis of the Runx1/Kdrl double positive cells should shed some insight into

the function of these cells. It has been found in *in vitro* hematopoiesis from human embryonic stem cells that their lineage was determined before they had fully become true hematopoietic cells and downregulated their endothelial genes (Guibentif et al. 2017). Therefore, hemogenic endothelial cells can have their subsequent lineage identified whilst they can still be identified as hemogenic endothelium. For example, this may indicate that injury-induced EHT produces predominantly leukocytic cells, though in the mutant they are predominantly erythrocytic or express high levels of apoptotic genes.

5.12 CONCLUSION

This chapter gives further evidence that the fish heart forms a hemogenic endothelium after injury, through live-imaging of EHT occurring in living heart tissue and transcriptomic analysis demonstrating expression of developmental hemogenic endothelial genes in these cells. It also demonstrates that the loss of Runx1 function is cardio-proliferative and protective, but that scar resolution and potentially deposition is negatively affected. This phenotype is in part due to phenotypic changes in cardiomyocytes alone.

CHAPTER 6 – DISCUSSION AND CONCLUSION OF THE TOTAL WORK

6.1 A SUMMARY OF THE FINDINGS OF THE STUDY

This thesis demonstrates the work undertaken to identify two novel progenitor populations in the fish heart. Evidence is given demonstrating that the epicardium can form fat during development and after injury, likely through the epicardial-mesenchymal-transition identified by previous studies. Through analysis of fish models with varying regenerative capacity, it seems that fat production after wounding is linked to scar deposition, which would be an interesting avenue to explore further.

The second identified progenitor population found is the wound endothelium, which can produce hematopoietic stem cells through endothelial-to-hematopoietic transition. This is another example of a recapitulation of a developmental process in the post-injury environment. The hemogenic endothelium population appears in zebrafish and both ecotypes of *A mexicanus* and has never before been identified in fish or mammals.

These progenitor populations could play profound roles in the ability to regenerate. The fat progenitor can certainly sense the wound environment, and its response in deciding whether to produce fat or not could aid or diminish regeneration. As discussed previously, heart fat and mesenchymal progenitors can have a beneficial effect after injury, yet fat in wounds is often found in non-regenerative environments. Given the important roles of immune cells to multiple areas of the injury response, the creation of HSCs *in situ* is an exciting finding.

The importance of the identification of novel progenitor populations cannot be underestimated and functional analysis of these populations in the future could give important insights into regenerative capacity and give rise to new therapeutic targets.

6.2 LIMITATIONS OF THE STUDY

6.2.1 IDENTIFICATION OF THE EPICARDIAL FAT PROGENITOR

The epicardial progenitor was identified through initial investigation of the expression pattern of Pdgfrα, a mesenchymal stem cell marker, within *A mexicanus* hearts that identified expression in cells of the epicardium. The epicardium gives rise to epicardial fat during development and after injury in the mouse (Liu et al. 2014), suggesting this Pdgfrα-positive epicardial population might be responsible for fat formation in the fish. After the *pdgfrα* lineage tracing lines in the zebrafish and *A mexicanus* could not be created, lineage tracing was performed in the zebrafish using an epicardial marker, *tcf21*. This lineage tracing indicated that the epicardium gives rise to fat both during development and after injury in the zebrafish.

The expression of Pdgfrα in cells of the epicardium was demonstrated by immunohistochemistry, but it should be taken into account that the specificity of the Pdgfrα antibody in fish is unknown. According to the manufacturer, it was designed against human and mouse Pdgfrα and the region of the protein it targets is unknown. It is therefore possible that a different protein is recognised in the fish and this issue is the case for the majority of antibodies used in this work, as specificity in the fish is unknown for most. Generation of a transgenic *pdgfrα* marker line, or use of the recently described line in El-Rass et al. 2017 would confirm if this expression pattern is correct in this instance.

The lineage tracing evidence is presented as whole-mount images and, for the post injury tracing, also immunohistochemistry for the lineage-labelling fluorescent protein in paraffin sections, where large round holes were presumed to be fat in the scar tissue. This evidence demonstrates expression of mCherry, denoting lineage from a *tcf21*-expressing cell, in small

cells within the fat tissue assumed to be the adipocyte cell bodies outside of lipid-storage, which is indicative of fat tissue arising from epicardial cells. However, a direct link between mCherry-positive cells and fat cells could not be shown, for example by co-expression of mCherry and fat-related markers. Antibodies against fat-related transcription factors and other fat-related markers that worked in the fish could not be found, that would allow demonstration of mCherry within the adipocytes in sections. In addition, a fluorescent basic lipid stain, Nile red, is, unfortunately also red and could not be used with our lineage labelling system. In addition, the lineage labelling uses one marker only, for confirmation, another epicardial Cre-line should be used but one was not available here.

To conclude, whilst the data presented here is indicative that the epicardium can produce fat after injury and during development, further work is required once the tools are available to increase the certainty that this conclusion is valid.

6.2.2 IDENTIFICATION OF A HEMOGENIC ENDOTHELIUM AFTER INJURY

It was shown that immunohistochemistry for Runx1 and Erg, hematopoietic progenitor and endothelial cell markers respectively, marks cells that resemble endothelial cells in the wound site in *A mexicanus*. To avoid issues with antibody specificity in the fish, transgenic zebrafish lines where Citrine is expressed under the control of the Runx1 promoter and mCherry is expressed under the control of the Kdrl promoter were used. The expression pattern of the fluorescent markers recapitulated the immunohistochemistry patterns seen in *A mexicanus*, where cells positive for both markers resembling endothelial cells were found in the wound.

The use of kdrl as a promoter for transgene expression in endothelial cells is long established and commonly used. The *runx1:citrine* line is new, however, and is generated using the P2 region of the *runx1* promoter. Work that shows the specificity and correct recapitulation of

endogenous *runx1* expression is due to be published soon by the generator of the line, Dr Florian Bonkhofer, and the laboratory of Professor Roger Patient.

Following analysis of double-positive cell activity after injury, a novel method was developed to show EHT occurring in live heart tissue. Evidence was shown that indicates endothelial cells undergoing the same cell movements as those seen during developmental EHT. Whilst convincing, it is possible that the cell movements seen are an artefact of the imaging process. It could be that a cell moving around just outside the focal plane appears to show EHT occurring. The slice culture method, however, represents the best method that could be devised to image this process occurring live. Alone, it is not sufficient to conclude EHT occurs, but in concert with the data from fixed sections and the transcriptomics data it is convincing.

The qPCR data demonstrates expression of hemogenic endothelial genes in double positive cells, where the putative hemogenic endothelial cells expressed increased levels of endothelial genes than pure Citrine-single positive cells (assumed mature HSCs) and increased levels of hematopoietic genes than single mCherry positive cells (non-hemogenic endothelial cells) from *runx1:citrine;kdrl:mCherry* FAC sorted hearts. However, it must be noted that due to running out of time, this experiment was performed only once using a pool of 10 hearts. Single-cell sequencing offered the same type of data but with much more power, so resources were saved in favour of pursuing it over repetition of qPCR data.

The single cell transcriptomics data indicates that cells positive for both Runx1 and Kdrl express increased levels of hemogenic endothelial genes compared to other cells. Cells were analysed from uninjured wild-type fish, and injured wild-type and *runx1* mutant fish. Cluster analysis of double-positive cells indicates that they are a heterogeneous population and that

to a certain extent cells from uninjured, injured WT and injured KO fish can be distinguished by cluster analysis.

The single cell analysis suggests that a hemogenic endothelium exists within the fish heart, but cannot show spatially where this population is located. To link the single cell data to the population shown in the fixed sections, RNAscope for the genes highlighted by the single cell analysis showed that the hemogenic endothelium identified in fixed sections expresses these genes. Comparisons of expression in mutant and wild-type fish suggested that expression of these genes might pick out different cells in the two fish, with round Citrine positive cells, rather than the hemogenic endothelium, expressing *gata2b* in the mutant. It could be that the *gata2b* probe failed to work effectively in all three mutant fish, but regardless it suggests care must be taken when drawing further conclusions from the single cell transcriptomics data.

The analysis of the post-injury phenotype used AFOG analysis, PCNA proliferation analysis and analysed survival of the myocardium. The AFOG data at 7 dpi is currently being repeated, as the lack of scar at this time point was highly surprising, especially when one heart did show scarring. It could be that injury was performed unsuccessfully on the majority of fish harvested at this time-point, so this is being repeated. This means that the idea that the mutant deposits scar later than the mutant is under debate, however, the early myocardial regeneration and scar persistence are demonstrated at other time points so these conclusions remain valid. The survival analysis shows clearly increased myocardium in the wound at 3 dpi in the mutant compared to the wild-type by increased myocardial antibody staining. However, to ensure that this is not an experimental artefact, staining for a marker of apoptosis or cell death should be performed. Unfortunately, immunohistochemistry for

cleaved-caspase 3 (CC3) was unsuccessful and attempts to use TUNEL staining are ongoing in the laboratory group.

Overall, there are limitations to the methods used to identify the hemogenic endothelium, but the combination of work is such that a conclusion can be drawn, with the above-mentioned caveats.

6.3 WHAT DO THESE PROGENITORS TELL US ABOUT REGENERATIVE CAPACITY?

The current therapies aimed at replenishing lost cardiomyocytes involve complete organ transplantation or transplantation of cells. Both of these options are imperfect; the former primarily due to lack of availability, the latter due to issues with arrhythmias and incomplete grafting in animal tests (Lin & Pu 2014; Shiba et al. 2016; Chong et al. 2014; Tzahor & Poss 2017; Laflamme & Murry 2011). The ability to regrow heart tissue *in situ* offers an ideal solution, as no donors are required and endogenous signals can correctly pattern the growth and incorporation of the new tissue, as seen in the zebrafish and other regenerative models. It is during development and growth that the organ was originally patterned. Therefore, to successfully re-grow lost tissue, these developmental pathways should be reactivated.

Whilst this sounds simple, it can be seen in the mouse and human that some developmental pathways are reactivated, yet regeneration is still incomplete. Both the endocardium and epicardium enter developmental type states and some cardiomyocytes do undergo limited de-differentiation and proliferation (Wang et al. 2017; Senyo et al. 2013; Simoes & Riley 2018; Münch et al. 2017). In adult mammals, however, these responses are slightly different or insufficient and regeneration is not complete. Something about the nature of the adult mammal is different to the neonate and to other animal models where regeneration is possible. It is perhaps interesting to note that most of those animals in which re-activation of

developmental pathways contributes to successful regeneration are those that are in the process of growing, or demonstrate indeterminate growth. Zebrafish continue growing, at a decreasing rate, until they reach senescence (Tsai et al. 2007), axolotls, another animal model that can regenerate, also show indeterminate growth (Seifert et al. 2012) and neonatal mice are evidently growing rapidly. Humans and mice have determinate growth and once they reach adulthood, they do not grow further. Recent evidence suggests that the cavefish is more limited in the size it can reach compared to the surface fish, likely to limit excess energy expenditure and food requirements in the nutrient-poor cave environment (Simon et al. 2017). in the cavefish the heart also appears to grow less relative to body size increases, compared to surface fish (Tang et al. 2018).

There is evidence in the mouse that great epigenetic changes occur in the heart at P7, at the end of the neo-natal regenerative window (Górnikiewicz et al. 2016). These changes, along with an increase in blood pressure, a switch in metabolism, altered ECM components and the choice of cell growth rather than proliferation for further heart growth suggest that the heart environment is very different in neonatal animals than that in adults (Le et al. 2012; Puente et al. 2014; Lalowski et al. 2018; Bassat et al. 2017). In addition to the heart environment, the immune system is also different, with the immune complement in mouse neonatal cardiac injury very different to that in adults (Sattler & Rosenthal 2016). Therefore, simply re-activating the signalling pathways involved in heart development will likely have a different effect in these adults and could even be deleterious.

It seems probable that the heart cannot pick and choose which developmental processes reappear, due to the abundance of overlapping signals involved in each process. For example retinoic acid signalling acts in the endocardium and epicardium whilst Notch signalling is at

play in angiogenesis and EHT (Kikuchi et al. 2011; Guadix et al. 2011; Kanz et al. 2016; MacGrogan et al. 2018). Therefore, these signalling pathways could represent blunt tools that are deployed after injury, causing all cells that come into contact with them and that can process these, to respond in the ways they did during development as far as possible in the current environment. The expression pattern of *runx1* and the effect of its loss on regeneration could be a good example of this. Here it is shown that *runx1* is expressed in many of the cells that have been identified to revert to a developmental-type state or process after injury: the myocardium, epicardium and endocardium, and the loss of its function is both helpful and potentially harmful to regeneration, with a demonstrable cardio-protective and pro-proliferative effect but some alterations in scar handling.

To overcome these difficulties and be able to regenerate human heart muscle, it is necessary to understand the developmental processes that take place during the initial growth of the heart, how these developmental processes re-activate after injury and their effect, and how these processes differ after injury between regenerative and non-regenerative models based on the heart environment.

The discovery that the fish epicardium forms fat in the same way that mice do during development and after injury is important to our understanding of developmental processes that are re-started after injury. In mice, the epicardium forms cells that contribute to the coronary vasculature, fibroblasts and fat during development (Simoes & Riley 2018; Yamaguchi et al. 2015). After injury, the mouse epicardium also produces fibroblasts, contributes cells to the coronary vasculature and produces epicardial adipose tissue (Liu et al. 2014) yet despite what, on the face of it, looks to be successful recapitulation of developmental potential, regeneration fails to progress and instead the activated epicardium

contributes to excess fibrosis and fat deposition. The work presented here shows that this progenitor is able to sense the regenerative environment, explaining why the same process can be part of healthy growth during development and scarring after injury. Fish hearts of different regenerative potential show varying levels of scar formation and fat deposition from the epicardium after injury. The zebrafish forms less fat on its heart relative to the non-regenerative cavefish, showing that this progenitor is sensitive to the regenerative environment. Work has been done in mice to understand the signals involved in fat production from the mouse epicardium and has highlighted signals from the underlying myocardium, such as prokineticin-2, IGF-1 and its receptor and expression of PPARγ in the epicardium as important controls regulating adipogenic differentiation (Yamaguchi et al. 2015; Qureshi et al. 2017; Zangi et al. 2017). Comparing these pathways in regenerative and non-regenerative fish could give important insights into how this progenitor can sense the regenerative environment.

The finding that EHT occurs from injured endocardium is a previously unknown reactivation of a developmental pathway in any organism, and investigations comparing the process in regenerative and non-regenerative models could provide important insights into regenerative capacity. In mouse development, EHT can occur from Nkx2-5-positive endocardium as a contribution to definitive hematopoiesis, through the formation of transient progenitors that generate erythroid and non-erythroid lineages (Nakano et al. 2013). From work in mice and chicks, it is believed that a common hemogenic angioblast population migrates and forms clusters in the dorsal aorta and endocardium, and that these form the hemogenic endothelium/endocardium at these sites (Zamir et al. 2017). In the zebrafish, hematopoiesis from the endocardium during development has not been explored,

but work done previously has found that the endocardium arises from a region of the lateral plate mesoderm that will later form part of the dorsal aorta, where definitive hematopoiesis takes place (Bussmann et al. 2007). This is very similar to the common progenitor that forms the dorsal aorta and hemogenic endocardium in the mouse, suggesting that the hemogenic endocardium is conserved during development amongst species. Comparing the EHT injury response between species could give interesting insights into the role of this progenitor in injury response.

If regeneration is to be achieved by successful reactivation of developmental pathways, then understanding what processes are reactivated in successful injury responses and how these developmental reactivations change in non-regenerative settings is crucial. This thesis contributes 2 new pieces to the picture by demonstrating a novel reactivation of a developmental process, EHT, which occurs in a regenerative model and showing, through the identification and different activities of the epicardial fat progenitor in separate fish models, how a reactivated developmental process can change depending on the regenerative environment.

6.4 FURTHER WORK

6.4.1 FURTHER IDENTIFICATION OF THE EPICARDIAL FAT PROGENITOR AND ITS FUNCTION

This study demonstrates that the epicardium contains a progenitor that produces fat and that this progenitor might be the epicardial Pdgfrα-positive population. However, exactly which epicardial cells produce fat is unknown, and only when they are specifically identified can they be isolated and manipulated. It has been discovered recently that the epicardium is highly heterogeneous, with at least three distinct subpopulations that express different

combinations of the epicardial marker genes *tcf21*, *tbx18* and *wt1* ((Cao et al. 2015) and work awaiting publication from Dr Michael Weinberger of the Riley and Sauka-Spengler laboratories). The epicardial progenitors produced by the epicardium are likewise heterogeneous (Bollini et al. 2014). Therefore, one single marker alone is certainly insufficient for identification of this progenitor.

Further identification through analysis of expression of other marker genes is possible. To avoid difficulties of antibody specificity and availability in the fish, RNAscope for known markers of adipogenic progenitors could be performed in fixed sections of hearts after injury and during development, to find more specific markers. Once this has been achieved, lines can be generated that target this cell for destruction, for example through conditional Cre-mediated expression of Diphtheria Toxin A in these cells and knockouts of key regulatory genes can be generated. The effect of their absence on regeneration can be analysed, which should be especially useful to compare between the non-regenerative cavefish and the regenerative surface fish.

6.4.2 FUNCTIONAL ANALYSIS OF POST-INJURY EHT

The function of EHT in injury response is currently unknown, but the production of hematopoietic cells within the site of injury could have profound effects, due to the known importance of blood-borne cells in regenerative capacity. To investigate this, further experiments should focus on the effect of EHT loss on regenerative capacity, the investigation of hematopoietic cell types formed by EHT after injury and EHT in other non-regenerative models, such as the cavefish and adult mouse should be investigated further.

Investigating the progeny of the HE after injury might be possible from the ongoing analysis of the single cell sequencing data, as has been possible in human IPSCs and the mouse (Zhou

et al. 2016; Guibentif et al. 2017). However, if this is not possible, isolation and culture of hemogenic endothelial cells, to allow analysis of their differentiation potential might prove enlightening. HE could be isolated by FACs using the *runx1:citrine;kdrl:mCherry* fish and a culturing method established to allow the progeny of these cells to be assessed for identity. Alternatively, a method for Cre-mediated lineage labelling of these cells could be derived, with tamoxifen-controlled expression of Cre under the *gata2b* promoter, for example, allowing lineage labelling of injury-related HE. An endothelial CreER^{T2}-line could also be crossed with a floxed *gata2b* line, for example, to prevent EHT from occurring after injury. If the same lines are generated in the surface fish and cavefish, differences in EHT progeny in regenerative and non-regenerative settings can be compared.

6.5 FINAL CONCLUSION

Overall, this thesis fulfils the aim of finding novel progenitors in the fish heart by identifying an epicardial progenitor that forms fat in the fish heart and presents compelling evidence that the endocardium produces hematopoietic stem cells in the wound after injury. Both of these processes have not been described in the fish before and the endothelial-to-hematopoietic transition of the wound endothelium has never been reported in any model animal at all previously. These represent exciting findings that present new avenues for research and functional analysis of these cells might provide fruitful future avenues for therapeutic intervention.

APPENDIX

PUBLICATIONS

PUBLICATIONS FROM WORK PERFORMED DURING THE DPHIL

1 or possibly 2 publications looking at the injury-induced hemogenic endothelium and the role of Runx1 (Joint with Dr Jana Koth) *In progress*.

Stockdale, W.T., Lemieux, M.E., Killen, A.C., Zhao, J., Hu, Z., Riepsaame, J., Hamilton, N., Kudoh, T., Riley, P.R., van Aerle, R., Yamamoto, Y. and Mommersteeg, M.T.M., 2018. Heart Regeneration in the Mexican Cavefish. *Cell reports*, 25(8), p.1997–2007.e7.

Tang, J.L.Y., Guo, Y., Stockdale, W.T., Rana, K., Killen, A.C., Mommersteeg, M.T.M. and Yamamoto, Y., 2018. The developmental origin of heart size and shape differences in Astyanax mexicanus populations. *Developmental biology*, 441(2), pp.272–284.

PREVIOUS PUBLICATIONS

Killen, A.C., Barber, M., Paulin, J.J.W., Ranscht, B., Parnavelas, J.G. and Andrews, W.D., 2017. Protective role of Cadherin 13 in interneuron development. *Brain structure & function*, 222(8), pp.3567–3585.

Memi, F., Killen, A.C., Barber, M., Parnavelas, J.G. and Andrews, W.D., 2018. Cadherin 8 regulates proliferation of cortical interneuron progenitors. *Brain structure & function*.

TABLE A.1 – ANTIBODIES

Target	Concentration/Species	Company	Catalogue no.
Arg1 E	1:200/Goat	Santa Cruz	Sc18351
C-Kit	1:200/Goat	R&D systems	AF1356
Col1	1:200/Rabbit	Abcam	Ab34710
GFP	1:200/Chicken	Aves labs, inc.	GFP-1020
Isl1	1:200/Goat	Neuromics	GT15051
mCherry E	1:200/Mouse	Abcam	Ab125096
MF20	1:100/Mouse	DSHB	AB_2147781
Pdgfrα E	1:350/Rabbit	Millipore	07-276
Pdgfrβ	1:200/Rabbit	Abcam	Ab32570
Runx1 E	1:200/Goat	Santa Cruz	Sc8563

Wt1	1:200/Rabbit	Cabiochem	CA1026

TABLE A.2 – PRIMERS

Gene	Sequence	Type
Kdrl-F	CTCCTGTACAGCAAGGAATG	qPCR (Bertrand, Cisson, et al. 2010)
Kdrl-R	ATCTTTGGGCACCTTATAGC	qPCR
Fli1a-F	TATTAGGACCCACCAGCAGTC	qPCR
Fli1a-R	CTGGGTCCGTCATCTTGAAC	qPCR
Lmo2-F	AAATGAGGAGCCGGTGGAT	qPCR (Bertrand et al. 2008)
Lmo2-R	GCTCGATGGCCTTCAGAAA	qPCR
Gata2b - F	ATCTGCTCGGAAACATGACG	qPCR – Dr Florian Bonkhofer
Gata2b - R	ATGACCTGTGCCATCTCTCC	qPCR
Gfi1aa -F	AGCGGGTCCTACAAATGCAT	qPCR – Dr Florian Bonkhofer
GFi1aa - R	ACAGATTTCGCAGGCAAAGG	qPCR
Myb - F	AGAGGGTGAAAGAAATCGAG	qPCR
Myb - R	ACTGAAACAACAATGCCAAC	qPCR

TABLE A.3 – SGRNAS

Target	Sequence
Zebrafish *Pdgfrα* 5' UTR	GGAATAAAGGGATCTTTTTGCGG
Zebrafish *Pdgfrα* 5' UTR	TGGGAATGCACAATTACATTCGG
Zebrafish *Pdgfrα* 5' UTR	GAATAAAGGGATCTTTTTGCGGG
Zebrafish *Pdgfrα* 5' UTR	AGGGGCCCTTTTGGAATAAAGGG
Cavefish *Pdgfrα* 5' UTR	TTCCTATACTTGTCACAGTATGG
Cavefish *Pdgfrα* 5' UTR	ATCTAGCTTTGACACAGTTAAGG
Cavefish *Pdgfrα* 5' UTR	CTATACTTGTCACAGTATGGTGG
Cavefish *Pdgfrα* 5' UTR	CACCATACTGTGACAAGTATAGG

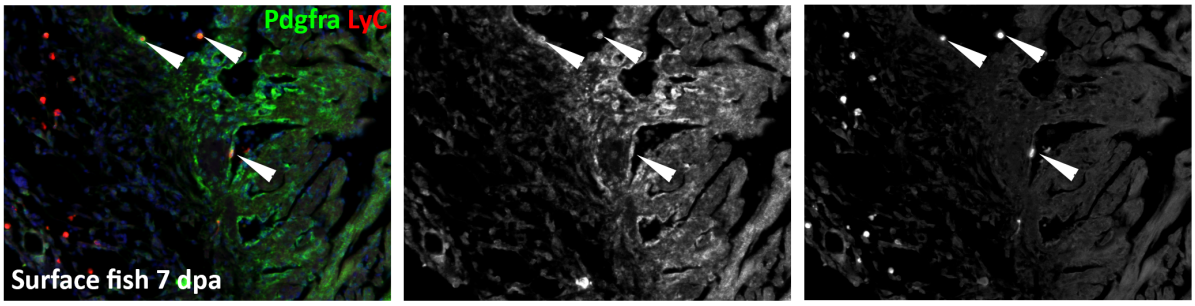
TABLE A.4 – RNASCOPE PROBES

mRNA target name	Target region (bp)	Channel
Runx1	242-1213	1
Tcf21	2-1061	2
Myb	557-1466	3
Tal1	357-1380	3
Gata2b	94-1335	2

TABLE A.5 – Gene lists for cluster analysis

Original Cluster – number and identity	Differentially expressed genes	Double positive cluster
0 - heart	*Hand2, foxc1a, mb, spock3, fabp11a, ramp2, fosab*	0,1
1 - thrombocytes	*Itga2b, mpl, nfe2, pdgfbb, hbegfb, admb, fgl2a*	5
2 - HSPCs	*Tal1, lmo2, myb, gata2b, fgfrl1a, pfn1*	2
3 - heart	*Hand2, foxc1a, krt18, krt8, serpine1, aldh1a2*	3, 4, 7
4 - epicardial	*Tcf21, col1a2, fn1b, col1a1b, mmp2, col1a1a*	6
5 - erythroid	*Hbaa1, hbba1, hbba1-1, hemgn*	8
6 – T-cells/NK cells	*Lck, il7r, cxcr4b, sla2, cebpb, coro1a*	2
7 - monocytes	*Cd74a, lygl1, ctsba, c1qb, grn1*	2
8 - HSPCs	*Tal1, lmo2, creg1, pfn1, grap2b, hdr*	2
9 - leukocytes	*Lect2l, scinlb, pnp5a, scpp8, ncf1*	10
10 - smooth muscle cells	*Tagln, pdgfrb, sparc, rgs5a, rgs5b*	
11 - epithelial	*Epcam, npb, and2, krt8, cfl1l, cldnb*	
12 – endothelial/hematopoietic	*Sox7, etv2, pecam1, krt18, hopx*	
13 - cardiomyocytes	*Myl7,cmlc1, tnnt2a, actc1a, tnni1b*	
14 - monocytes	*Cd74a, spi1a, spi1b, mpeg1.1, cxcr4b*	

SUPPLEMENTARY INFORMATION



REFERENCES

Alié, A. et al., 2018. Developmental evolution of the forebrain in cavefish, from natural variations in neuropeptides to behavior. *eLife*, 7, p.e32808. Available at: https://www.ncbi.nlm.nih.gov/pubmed/29405116.

Angelos, M.G. et al., 2017. Single Cell Resolution of Human Hematoendothelial Cells Defines Transcriptional Signatures of Hemogenic Endothelium. *STEM CELLS*, 36(2), pp.206–217. Available at: https://doi.org/10.1002/stem.2739.

Anversa, P. & Nadal-Ginard, B., 2002. Myocyte renewal and ventricular remodelling. *Nature*, 415, p.240. Available at: https://doi.org/10.1038/415240a.

Aspiras, A.C. et al., 2015. Melanocortin 4 receptor mutations contribute to the adaptation of cavefish to nutrient-poor conditions. *Proceedings of the National Academy of Sciences* , 112(31), pp.9668–9673. Available at: http://www.pnas.org/content/112/31/9668.abstract.

Athanasiadis, E.I. et al., 2017. Single-cell RNA-sequencing uncovers transcriptional states and fate decisions in haematopoiesis. *Nature Communications*, 8(1), p.2045. Available at: https://doi.org/10.1038/s41467-017-02305-6.

Auer, T.O. et al., 2014. CRISPR/Cas9-mediated conversion of eGFP- into Gal4-transgenic lines in zebrafish. *Nat. Protocols*, 9(12), pp.2823–2840. Available at: http://dx.doi.org/10.1038/nprot.2014.187.

Aurora, A.B. et al., 2014. Macrophages are required for neonatal heart regeneration. *The Journal of clinical investigation*, 124(3), pp.1382–1392. Available at: https://www.ncbi.nlm.nih.gov/pubmed/24569380.

Balsam, L.B. et al., 2004. Haematopoietic stem cells adopt mature haematopoietic fates in ischaemic myocardium. *Nature*, 428(6983), pp.668–673.

Bao, M. et al., 2018. Runx1 promotes satellite cell proliferation during ischemia - Induced muscle regeneration. *Biochemical and Biophysical Research Communications*, 503(4), pp.2993–2997. Available at: http://www.sciencedirect.com/science/article/pii/S0006291X18317674.

Baron, C.S. et al., 2018. Single-cell transcriptomics reveal the dynamic of haematopoietic stem cell production in the aorta. *Nature communications*, 9(1), p.2517. Available at: https://www.ncbi.nlm.nih.gov/pubmed/29955049.

Bassat, E. et al., 2017. The extracellular matrix protein agrin promotes heart regeneration in mice. *Nature*, 547(7662), pp.179–184. Available at: https://www.ncbi.nlm.nih.gov/pubmed/28581497.

Bax, N.A.M. et al., 2010. Cardiac malformations in Pdgfrα mutant embryos are associated with increased expression of WT1 and Nkx2.5 in the second heart field. *Developmental dynamics : an official publication of the American Association of Anatomists*, 239(8), pp.2307–2317. Available at: http://www.ncbi.nlm.nih.gov/pmc/articles/PMC2911638/.

Bax, N.A.M. et al., 2011. In vitro epithelial-to-mesenchymal transformation in human adult epicardial cells is regulated by TGFβ-signaling and WT1. *Basic Research in Cardiology*, 106(5), pp.829–847. Available at: http://www.ncbi.nlm.nih.gov/pmc/articles/PMC3149675/.

Bayes-Genis, A. et al., 2013. Cardiac adipose tissue: A new frontier for cardiac regeneration? *International Journal of Cardiology*, 167(1), pp.22–25. Available at: http://www.sciencedirect.com/science/article/pii/S0167527312007292.

Beale, A. et al., 2013. Circadian rhythms in Mexican blind cavefish Astyanax mexicanus in the lab and in the field. *Nat Commun*, 4. Available at: http://dx.doi.org/10.1038/ncomms3769.

Bedell, V.M. et al., 2012. In vivo Genome Editing Using High Efficiency TALENs. *Nature*, 491(7422), pp.114–118. Available at: http://www.ncbi.nlm.nih.gov/pmc/articles/PMC3491146/.

Beltrami, A.P. et al., 2003. Adult cardiac stem cells are multipotent and support myocardial regeneration. *Cell*, 114. Available at: http://dx.doi.org/10.1016/S0092-8674(03)00687-1.

Bergmann, O. et al., 2009. Evidence for cardiomyocyte renewal in humans. *Science (New York, N.Y.)*, 324(5923), pp.98–102. Available at: https://www.ncbi.nlm.nih.gov/pubmed/19342590.

van Berlo, J.H. et al., 2014. c-kit+ cells minimally contribute cardiomyocytes to the heart. *Nature*, 509(7500), pp.337–341. Available at: https://www.ncbi.nlm.nih.gov/pubmed/24805242.

Bersell, K. et al., 2009. Neuregulin1/ErbB4 signaling induces cardiomyocyte proliferation and repair of heart injury. *Cell*, 138(2), pp.257–270.

Bertrand, J.Y. et al., 2008. CD41+ cmyb+ precursors colonize the zebrafish pronephros by a novel migration route to initiate adult hematopoiesis. *Development (Cambridge, England)*, 135(10), pp.1853–1862.

Bertrand, J.Y., Chi, N.C., et al., 2010. Hematopoietic stem cells derive directly from aortic endothelium during development. *Nature*, 464(7285), pp.108–111. Available at: http://www.ncbi.nlm.nih.gov/pmc/articles/PMC2858358/.

Bertrand, J.Y., Cisson, J.L., et al., 2010. Notch signaling distinguishes 2 waves of definitive hematopoiesis in the zebrafish embryo. *Blood*, 115(14), pp.2777–2783.

Biere, L. et al., 2017. Relation of Quantity of Subepicardial Adipose Tissue to Infarct Size in Patients With ST-Elevation Myocardial Infarction. *The American journal of cardiology*, 119(12), pp.1972–1978.

Bilandzija, H. et al., 2013. A potential benefit of albinism in Astyanax cavefish: downregulation of the oca2 gene increases tyrosine and catecholamine levels as an alternative to melanin synthesis. *PloS one*, 8(11), p.e80823.

Bilandzija, H. et al., 2018. Behavioural changes controlled by catecholaminergic systems explain recurrent loss of pigmentation in cavefish. *Proceedings. Biological sciences*, 285(1878).

Birbrair, A. et al., 2013. Role of pericytes in skeletal muscle regeneration and fat accumulation. *Stem cells and development*, 22(16), pp.2298–2314.

Bitinaite, J. et al., 1998. FokI dimerization is required for DNA cleavage. *Proceedings of the National Academy of Sciences of the United States of America*, 95(18), pp.10570–10575. Available at: http://www.ncbi.nlm.nih.gov/pmc/articles/PMC27935/.

Blin, M. et al., 2018. Developmental evolution and developmental plasticity of the olfactory epithelium and olfactory skills in Mexican cavefish. *Developmental biology*, 441(2), pp.242–251.

Boch, J. et al., 2009. Breaking the code of DNA binding specificity of TAL-type III effectors. *Science (New York, N.Y.)*, 326(5959), pp.1509–1512.

Boisset, J.-C. et al., 2010. In vivo imaging of haematopoietic cells emerging from the mouse aortic endothelium. *Nature*, 464, p.116. Available at: http://dx.doi.org/10.1038/nature08764.

Bollini, S. et al., 2014. Re-activated adult epicardial progenitor cells are a heterogeneous population molecularly distinct from their embryonic counterparts. *Stem cells and development*, 23(15), pp.1719–1730.

Burns, C.E. et al., 2009. A genetic screen in zebrafish defines a hierarchical network of pathways required for hematopoietic stem cell emergence. *Blood*, 113(23), pp.5776–5782. Available at: http://www.ncbi.nlm.nih.gov/pmc/articles/PMC2700318/.

Burns, C.E. et al., 2005. Hematopoietic stem cell fate is established by the Notch–Runx pathway. *Genes & Development*, 19(19), pp.2331–2342. Available at: http://www.ncbi.nlm.nih.gov/pmc/articles/PMC1240042/.

Bussmann, J., Bakkers, J. & Schulte-Merker, S., 2007. Early Endocardial Morphogenesis Requires Scl/Tal1. *PLOS Genetics*, 3(8), p.e140. Available at: https://doi.org/10.1371/journal.pgen.0030140.

Butko, E. et al., 2015. Gata2b is a restricted early regulator of hemogenic endothelium in the zebrafish embryo. *Development (Cambridge, England)*, 142(6), pp.1050–1061. Available at: http://www.ncbi.nlm.nih.gov/pmc/articles/PMC4360177/.

Cao, J. et al., 2015. Single epicardial cell transcriptome sequencing identifies Caveolin-1 as

an essential factor in zebrafish heart regeneration. *Development*. Available at: http://dev.biologists.org/content/early/2015/12/07/dev.130534.abstract.

Cao, J. & Poss, K.D., 2016. Explant culture of adult zebrafish hearts for epicardial regeneration studies. *Nat. Protocols*, 11(5), pp.872–881. Available at: http://dx.doi.org/10.1038/nprot.2016.049.

Cao, J. & Poss, K.D., 2016. Explant culture of adult zebrafish hearts for epicardial regeneration studies. *Nature protocols*, 11(5), pp.872–881.

Cao, J. & Poss, K.D., 2018. The epicardium as a hub for heart regeneration. *Nature Reviews Cardiology*, 15(10), pp.631–647. Available at: https://doi.org/10.1038/s41569-018-0046-4.

Carmona, S.J. et al., 2017. Single-cell transcriptome analysis of fish immune cells provides insight into the evolution of vertebrate immune cell types. *Genome research*, 27(3), pp.451–461. Available at: https://www.ncbi.nlm.nih.gov/pubmed/28087841.

Ceci, M. et al., 2018. Micro RNAs are involved in activation of epicardium during zebrafish heart regeneration. *Cell Death Discovery*, 4, p.41. Available at: http://www.ncbi.nlm.nih.gov/pmc/articles/PMC5849881/.

Chablais, F. et al., 2011. The zebrafish heart regenerates after cryoinjury-induced myocardial infarction. *BMC Developmental Biology*, 11, p.21. Available at: http://www.ncbi.nlm.nih.gov/pmc/articles/PMC3078894/.

Chablais, F. & Jaźwińska, A., 2012. The regenerative capacity of the zebrafish heart is dependent on TGFβ signaling. *Development*, 139(11), pp.1921–1930. Available at: http://dev.biologists.org/content/139/11/1921.abstract.

Chen, M.J. et al., 2009. Runx1 is required for the endothelial to hematopoietic cell transition but not thereafter. *Nature*, 457(7231), pp.887–891. Available at: http://www.ncbi.nlm.nih.gov/pmc/articles/PMC2744041/.

Chen, W.C.W. et al., 2016. Decellularized zebrafish cardiac extracellular matrix induces mammalian heart regeneration. *Science advances*, 2(11), pp.e1600844–e1600844. Available at: https://www.ncbi.nlm.nih.gov/pubmed/28138518.

Chen, W.C.W. et al., 2015. Human Myocardial Pericytes: Multipotent Mesodermal Precursors Exhibiting Cardiac Specificity. *Stem cells (Dayton, Ohio)*, 33(2), pp.557–573. Available at: http://www.ncbi.nlm.nih.gov/pmc/articles/PMC4762368/.

Chien, K.R., 2004. Lost in translation. *Nature*, 428, p.607. Available at: https://doi.org/10.1038/nature02500.

Chistiakov, D.A., Orekhov, A.N. & Bobryshev, Y. V, 2016. The role of cardiac fibroblasts in post-myocardial heart tissue repair. *Experimental and Molecular Pathology*, 101(2), pp.231–240. Available at: http://www.sciencedirect.com/science/article/pii/S0014480016302532.

Cho, S.W. et al., 2013. Targeted genome engineering in human cells with the Cas9 RNA-

guided endonuclease. *Nature Biotechnology*, 31, p.230. Available at: http://dx.doi.org/10.1038/nbt.2507.

Choi, W.-Y. et al., 2013. In vivo monitoring of cardiomyocyte proliferation to identify chemical modifiers of heart regeneration. *Development (Cambridge, England)*, 140(3), pp.660–666. Available at: http://www.ncbi.nlm.nih.gov/pmc/articles/PMC3561784/.

Chong, J.J.H. et al., 2011. Adult Cardiac-Resident MSC-like Stem Cells with a Proepicardial Origin. *Cell stem cell*, 9(6), pp.527–540. Available at: http://www.ncbi.nlm.nih.gov/pmc/articles/PMC3652240/.

Chong, J.J.H. et al., 2014. Human embryonic-stem-cell-derived cardiomyocytes regenerate non-human primate hearts. *Nature*, 510(7504), pp.273–277.

Chong, J.J.H. et al., 2013. Progenitor Cells Identified by PDGFR-Alpha Expression in the Developing and Diseased Human Heart. *Stem Cells and Development*, 22(13), pp.1932–1943. Available at: http://www.ncbi.nlm.nih.gov/pmc/articles/PMC3685392/.

Cong, L. et al., 2013. Multiplex Genome Engineering Using CRISPR/Cas Systems. *Science (New York, N.Y.)*, 339(6121), pp.819–823. Available at: http://www.ncbi.nlm.nih.gov/pmc/articles/PMC3795411/.

Conway, S.J., Firulli, B. & Firulli, A.B., 2010. A bHLH code for cardiac morphogenesis. *Pediatric cardiology*, 31(3), pp.318–324. Available at: https://www.ncbi.nlm.nih.gov/pubmed/20033146.

Drissen, R. et al., 2016. Distinct myeloid progenitor-differentiation pathways identified through single-cell RNA sequencing. *Nature immunology*, 17(6), pp.666–676. Available at: https://www.ncbi.nlm.nih.gov/pubmed/27043410.

Duboué, E.R., Keene, A.C. & Borowsky, R.L., 2011. Evolutionary Convergence on Sleep Loss in Cavefish Populations. *Current Biology*, 21(8), pp.671–676. Available at: http://www.sciencedirect.com/science/article/pii/S0960982211002922.

Dutta, P. et al., 2015. Myocardial Infarction Activates CCR2(+) Hematopoietic Stem and Progenitor Cells. *Cell stem cell*, 16(5), pp.477–487.

Dzierzak, E. & Speck, N.A., 2008. Of lineage and legacy: the development of mammalian hematopoietic stem cells. *Nature immunology*, 9(2), pp.129–136. Available at: https://www.ncbi.nlm.nih.gov/pubmed/18204427.

Eilken, H.M., Nishikawa, S.-I. & Schroeder, T., 2009. Continuous single-cell imaging of blood generation from haemogenic endothelium. *Nature*, 457, p.896. Available at: http://dx.doi.org/10.1038/nature07760.

El-Rass, S. et al., 2017. Disruption of pdgfra alters endocardial and myocardial fusion during zebrafish cardiac assembly. *Biology open*, 6(3), pp.348–357. Available at: https://www.ncbi.nlm.nih.gov/pubmed/28167492.

Elipot, Y. et al., 2014. A mutation in the enzyme monoamine oxidase explains part of the Astyanax cavefish behavioural syndrome. *Nat Commun*, 5. Available at:

http://dx.doi.org/10.1038/ncomms4647.

Elipot, Y. et al., 2013. Evolutionary Shift from Fighting to Foraging in Blind Cavefish through Changes in the Serotonin Network. *Current Biology*, 23(1), pp.1–10. Available at: http://www.sciencedirect.com/science/article/pii/S0960982212012651.

Ellett, F. et al., 2011. mpeg1 promoter transgenes direct macrophage-lineage expression in zebrafish. *Blood*, 117(4), pp.e49-56.

Ellison, G.M. et al., 2013. Adult c-kit(pos) cardiac stem cells are necessary and sufficient for functional cardiac regeneration and repair. *Cell*, 154(4), pp.827–842.

Espín-Palazón, R. et al., 2014. Proinflammatory signaling regulates hematopoietic stem cell emergence. *Cell*, 159(5), pp.1070–1085. Available at: http://www.ncbi.nlm.nih.gov/pmc/articles/PMC4243083/.

Farahani, R.M. & Xaymardan, M., 2015a. Platelet-Derived Growth Factor Receptor Alpha as a Marker of Mesenchymal Stem Cells in Development and Stem Cell Biology. *Stem Cells International*, 2015, p.362753. Available at: http://www.ncbi.nlm.nih.gov/pmc/articles/PMC4519552/.

Farahani, R.M. & Xaymardan, M., 2015b. Platelet-Derived Growth Factor Receptor Alpha as a Marker of Mesenchymal Stem Cells in Development and Stem Cell Biology. *Stem Cells International*, 2015, p.362753.

Farkas, J.E. & Monaghan, J.R., 2017. A brief history of the study of nerve dependent regeneration. *Neurogenesis (Austin, Tex.)*, 4(1), pp.e1302216–e1302216. Available at: https://www.ncbi.nlm.nih.gov/pubmed/28459075.

Farup, J. et al., 2015. Interactions between muscle stem cells, mesenchymal-derived cells and immune cells in muscle homeostasis, regeneration and disease. *Cell Death Dis*, 6, p.e1830. Available at: http://dx.doi.org/10.1038/cddis.2015.198.

Fiore, D. et al., 2016. Pharmacological blockage of fibro/adipogenic progenitor expansion and suppression of regenerative fibrogenesis is associated with impaired skeletal muscle regeneration. *Stem Cell Research*, 17(1), pp.161–169. Available at: http://www.sciencedirect.com/science/article/pii/S1873506116300708.

Forte, E., Furtado, M.B. & Rosenthal, N., 2018. The interstitium in cardiac repair: role of the immune–stromal cell interplay. *Nature Reviews Cardiology*, 15(10), pp.601–616. Available at: https://doi.org/10.1038/s41569-018-0077-x.

Friedland, A.E. et al., 2013. Heritable genome editing in C. elegans via a CRISPR-Cas9 system. *Nature methods*, 10(8), pp.741–743. Available at: http://www.ncbi.nlm.nih.gov/pmc/articles/PMC3822328/.

Frøland Steindal, I.A. et al., 2018. Development of the Astyanax mexicanus circadian clock and non-visual light responses. *Developmental biology*, 441(2), pp.345–354. Available at: https://www.ncbi.nlm.nih.gov/pubmed/29909064.

Fu, X. et al., 2018. Specialized fibroblast differentiated states underlie scar formation in the

infarcted mouse heart. *The Journal of clinical investigation*, 128(5), pp.2127–2143. Available at: https://www.ncbi.nlm.nih.gov/pubmed/29664017.

Fumey, J. et al., 2018. Evidence for late Pleistocene origin of Astyanax mexicanus cavefish. *BMC evolutionary biology*, 18(1), p.43. Available at: https://www.ncbi.nlm.nih.gov/pubmed/29665771.

Gamba, L. et al., 2017. Collagenolytic Activity Is Associated with Scar Resolution in Zebrafish Hearts after Cryoinjury S. M. Wu & N. C. Chi, eds. *Journal of Cardiovascular Development and Disease*, 4(1), p.2. Available at: http://www.ncbi.nlm.nih.gov/pmc/articles/PMC5715691/.

Gao, Z. et al., 2018. PDGFRalpha/PDGFRbeta signaling balance modulates progenitor cell differentiation into white and beige adipocytes. *Development (Cambridge, England)*, 145(1).

Gemberling, M. et al., 2015. Nrg1 is an injury-induced cardiomyocyte mitogen for the endogenous heart regeneration program in zebrafish M. E. Bronner, ed. *eLife*, 4, p.e05871. Available at: http://www.ncbi.nlm.nih.gov/pmc/articles/PMC4379493/.

Gering, M. & Patient, R., 2005. Hedgehog Signaling Is Required for Adult Blood Stem Cell Formation in Zebrafish Embryos. *Developmental Cell*, 8(3), pp.389–400. Available at: https://doi.org/10.1016/j.devcel.2005.01.010.

Godinho, L., 2011. Live imaging of zebrafish development. *Cold Spring Harbor protocols*, 2011(7), pp.770–777.

Gohbara, M. et al., 2016. Association between epicardial adipose tissue volume and myocardial salvage in patients with a first ST-segment elevation myocardial infarction: An epicardial adipose tissue paradox. *Journal of Cardiology*.

Goldfarb, J.W., Roth, M. & Han, J., 2009. Myocardial fat deposition after left ventricular myocardial infarction: assessment by using MR water-fat separation imaging. *Radiology*, 253(1), pp.65–73.

Goldstein, S. et al., 1984. Timing, mechanism and clinical setting of witnessed deaths in postmyocardial infarction patients. *Journal of the American College of Cardiology*, 3(5), pp.1111–1117. Available at: http://www.sciencedirect.com/science/article/pii/S0735109784801679.

Gong, Z. et al., 2002. Green fluorescent protein expression in germ-line transmitted transgenic zebrafish under a stratified epithelial promoter from keratin8. *Developmental dynamics : an official publication of the American Association of Anatomists*, 223(2), pp.204–215.

González-Rosa, J.M. et al., 2011. Extensive scar formation and regression during heart regeneration after cryoinjury in zebrafish. *Development*, 138(9), p.1663 LP-1674. Available at: http://dev.biologists.org/content/138/9/1663.abstract.

Gonzalez-Rosa, J.M., Peralta, M. & Mercader, N., 2012. Pan-epicardial lineage tracing reveals that epicardium derived cells give rise to myofibroblasts and perivascular cells

during zebrafish heart regeneration. *Developmental biology*, 370(2), pp.173–186.

Górnikiewicz, B. et al., 2016. Changes in gene methylation patterns in neonatal murine hearts: Implications for the regenerative potential. *BMC Genomics*, 17, p.231. Available at: http://www.ncbi.nlm.nih.gov/pmc/articles/PMC4791959/.

Gratz, S.J. et al., 2013. Genome Engineering of Drosophila with the CRISPR RNA-Guided Cas9 Nuclease. *Genetics*, 194(4), pp.1029–1035. Available at: http://www.ncbi.nlm.nih.gov/pmc/articles/PMC3730909/.

Gritz, E. & Hirschi, K.K., 2016. Specification and function of hemogenic endothelium during embryogenesis. *Cellular and molecular life sciences : CMLS*, 73(8), pp.1547–1567. Available at: https://www.ncbi.nlm.nih.gov/pubmed/26849156.

Gross, J.B. et al., 2016. A pleiotropic interaction between vision loss and hypermelanism in Astyanax mexicanus cave x surface hybrids. *BMC evolutionary biology*, 16(1), p.145. Available at: https://www.ncbi.nlm.nih.gov/pubmed/27363593.

Gross, J.B., 2012. The complex origin of Astyanax cavefish. *BMC Evolutionary Biology*, 12, p.105. Available at: http://www.ncbi.nlm.nih.gov/pmc/articles/PMC3464594/.

Guadix, J.A. et al., 2011. Wt1 controls retinoic acid signalling in embryonic epicardium through transcriptional activation of Raldh2. *Development (Cambridge, England)*, 138(6), pp.1093–1097. Available at: http://www.ncbi.nlm.nih.gov/pmc/articles/PMC3042868/.

Guibentif, C. et al., 2017. Single-Cell Analysis Identifies Distinct Stages of Human Endothelial-to-Hematopoietic Transition. *Cell Reports*.

Gupta, V. et al., 2013. An Injury-Responsive Gata4 Program Shapes the Zebrafish Cardiac Ventricle. *Current biology : CB*, 23(13), pp.1221–1227. Available at: http://www.ncbi.nlm.nih.gov/pmc/articles/PMC3759223/.

Gurusinghe, C.J. & Ehrlich, D., 1986. Gelatin embedding of central nervous system tissue improves the quality of vibratome sections. *Stain technology*, 61(5), pp.324–326.

Hamilton, C.A., 1997. Low-density lipoprotein and oxidised low-density lipoprotein: Their role in the development of atherosclerosis. *Pharmacology & Therapeutics*, 74(1), pp.55–72. Available at: http://www.sciencedirect.com/science/article/pii/S0163725896002021.

Han, C. et al., 2015. Acute inflammation stimulates a regenerative response in the neonatal mouse heart. *Cell research*, 25(10), pp.1137–1151. Available at: https://www.ncbi.nlm.nih.gov/pubmed/26358185.

Harrison, M.R.M. et al., 2015. Chemokine-guided angiogenesis directs coronary vasculature formation in zebrafish. *Developmental cell*, 33(4), pp.442–454. Available at: https://www.ncbi.nlm.nih.gov/pubmed/26017769.

He, L. et al., 2017. Preexisting endothelial cells mediate cardiac neovascularization after injury. *The Journal of clinical investigation*, 127(8), pp.2968–2981. Available at:

https://www.ncbi.nlm.nih.gov/pubmed/28650345.

Hein, S.J. et al., 2015. Advanced Echocardiography in Adult Zebrafish Reveals Delayed Recovery of Heart Function after Myocardial Cryoinjury. *PLOS ONE*, 10(4), p.e0122665. Available at: https://doi.org/10.1371/journal.pone.0122665.

Herman, A. et al., 2018. The role of gene flow in rapid and repeated evolution of cave-related traits in Mexican tetra, Astyanax mexicanus. *Molecular Ecology*, 0(0). Available at: https://doi.org/10.1111/mec.14877.

Hille, F. & Charpentier, E., 2016. CRISPR-Cas: biology, mechanisms and relevance. *Philosophical Transactions of the Royal Society B: Biological Sciences*, 371(1707), p.20150496. Available at: http://www.ncbi.nlm.nih.gov/pmc/articles/PMC5052741/.

Hisano, Y. et al., 2015. Precise in-frame integration of exogenous DNA mediated by CRISPR/Cas9 system in zebrafish. *Scientific Reports*, 5, p.8841. Available at: http://www.ncbi.nlm.nih.gov/pmc/articles/PMC4350073/.

Horckmans, M. et al., 2017. Neutrophils orchestrate post-myocardial infarction healing by polarizing macrophages towards a reparative phenotype. *European Heart Journal*, 38(3), pp.187–197. Available at: http://dx.doi.org/10.1093/eurheartj/ehw002.

Hsieh, P.C.H. et al., 2007. Evidence from a genetic fate-mapping study that stem cells refresh adult mammalian cardiomyocytes after injury. *Nature medicine*, 13(8), pp.970–974. Available at: https://www.ncbi.nlm.nih.gov/pubmed/17660827.

Hsu, P.-L. et al., 2013. Activation of mitochondrial function and Hb expression in non-haematopoietic cells by an EPO inducer ameliorates ischaemic diseases in mice. *British journal of pharmacology*, 169(7), pp.1461–1476. Available at: https://www.ncbi.nlm.nih.gov/pubmed/23530756.

Huang, W.-C. et al., 2013. Treatment of Glucocorticoids Inhibited Early Immune Responses and Impaired Cardiac Repair in Adult Zebrafish P. C. H. Hsieh, ed. *PLoS ONE*, 8(6), p.e66613. Available at: http://www.ncbi.nlm.nih.gov/pmc/articles/PMC3689762/.

Huang, Y. et al., 2013. Igf Signaling is Required for Cardiomyocyte Proliferation during Zebrafish Heart Development and Regeneration. *PLoS ONE*, 8(6).

HUMPEL, C., 2015. ORGANOTYPIC BRAIN SLICE CULTURES: A REVIEW. *Neuroscience*, 305, pp.86–98. Available at: http://www.ncbi.nlm.nih.gov/pmc/articles/PMC4699268/.

Hwang, W.Y. et al., 2013. Efficient genome editing in zebrafish using a CRISPR-Cas system. *Nat Biotechnol*, 31(3), pp.227–229.

Ichikawa, Y. et al., 2009. Adipose tissue detected by multislice computed tomography in patients after myocardial infarction. *JACC. Cardiovascular imaging*, 2(5), pp.548–555.

Irion, U., Krauss, J. & Nüsslein-Volhard, C., 2014. Precise and efficient genome editing in zebrafish using the CRISPR/Cas9 system. *Development (Cambridge, England)*, 141(24), pp.4827–4830. Available at: http://www.ncbi.nlm.nih.gov/pmc/articles/PMC4299274/.

Jablonski, K.A. et al., 2015. Novel Markers to Delineate Murine M1 and M2 Macrophages.

PloS one, 10(12), pp.e0145342–e0145342. Available at: https://www.ncbi.nlm.nih.gov/pubmed/26699615.

Jaffredo, T. et al., 1998. Intraaortic hemopoietic cells are derived from endothelial cells during ontogeny. *Development*, 125(22), p.4575 LP-4583. Available at: http://dev.biologists.org/content/125/22/4575.abstract.

Jaggard, J. et al., 2017. The lateral line confers evolutionarily derived sleep loss in the Mexican cavefish. *The Journal of Experimental Biology*, 220(2), p.284 LP-293. Available at: http://jeb.biologists.org/content/220/2/284.abstract.

Jaggard, J.B. et al., 2018. Hypocretin underlies the evolution of sleep loss in the Mexican cavefish. *eLife*, 7, p.e32637. Available at: https://www.ncbi.nlm.nih.gov/pubmed/29405117.

Jankowska-Steifer, E. et al., 2015. Vasculogenic and hematopoietic cellular progenitors are scattered within the prenatal mouse heart. *Histochemistry and Cell Biology*, 143, pp.153–169. Available at: http://www.ncbi.nlm.nih.gov/pmc/articles/PMC4298664/.

Jeffery, W.R., 2009. Regressive evolution in Astyanax cavefish. *Annual review of genetics*, 43, pp.25–47. Available at: https://www.ncbi.nlm.nih.gov/pubmed/19640230.

Jesty, S.A. et al., 2012. c-kit+ precursors support postinfarction myogenesis in the neonatal, but not adult, heart. *Proceedings of the National Academy of Sciences of the United States of America*, 109(33), pp.13380–13385. Available at: https://www.ncbi.nlm.nih.gov/pubmed/22847442.

Jinek, M. et al., 2012. A Programmable Dual-RNA–Guided DNA Endonuclease in Adaptive Bacterial Immunity. *Science*, 337(6096), p.816 LP-821. Available at: http://science.sciencemag.org/content/337/6096/816.abstract.

Joe, A.W.B. et al., 2010. Muscle injury activates resident fibro/adipogenic progenitors that facilitate myogenesis. *Nature cell biology*, 12(2), pp.153–163. Available at: http://www.ncbi.nlm.nih.gov/pmc/articles/PMC4580288/.

Johansen, M.D. et al., 2018. Mycobacterium marinum infection drives foam cell differentiation in zebrafish infection models. *Developmental and comparative immunology*, 88, pp.169–172.

Jopling, C. et al., 2010. Zebrafish heart regeneration occurs by cardiomyocyte dedifferentiation and proliferation. *Nature*, 464. Available at: http://dx.doi.org/10.1038/nature08899.

Kanz, D. et al., 2016. Endothelial-to-hematopoietic transition: Notch-ing vessels into blood. *Annals of the New York Academy of Sciences*, 1370(1), pp.97–108. Available at: https://doi.org/10.1111/nyas.13030.

Karra, R. et al., 2015. Myocardial NF-κB activation is essential for zebrafish heart regeneration. *Proceedings of the National Academy of Sciences* , 112(43), pp.13255–13260. Available at: http://www.pnas.org/content/112/43/13255.abstract.

Kaufmann, A. et al., 2012. Multilayer mounting enables long-term imaging of zebrafish development in a light sheet microscope. *Development (Cambridge, England)*, 139(17), pp.3242–3247.

Keith, M.C.L. & Bolli, R., 2015. "String theory" of c-kit(pos) cardiac cells: a new paradigm regarding the nature of these cells that may reconcile apparently discrepant results. *Circulation research*, 116(7), pp.1216–1230. Available at: https://www.ncbi.nlm.nih.gov/pubmed/25814683.

Kikuchi, K. et al., 2011. Retinoic acid production by endocardium and epicardium is an injury response essential for zebrafish heart regeneration. *Developmental cell*, 20(3), pp.397–404. Available at: http://www.ncbi.nlm.nih.gov/pmc/articles/PMC3071981/.

Kim, E.J. et al., 2017. Platelet-Derived Growth Factor Receptor-Positive Pericytic Cells of White Adipose Tissue from Critical Limb Ischemia Patients Display Mesenchymal Stem Cell-Like Properties. *Clinics in orthopedic surgery*, 9(2), pp.239–248.

Kim, J.-H. et al., 2016. Transplantation of Immortalized CD34+ and CD34- Adipose-Derived Stem Cells Improve Cardiac Function and Mitigate Systemic Pro-Inflammatory Responses Z. Ivanovic, ed. *PLoS ONE*, 11(2), p.e0147853. Available at: http://www.ncbi.nlm.nih.gov/pmc/articles/PMC4740491/.

Kim, J. et al., 2012. In vitro culture of epicardial cells from adult zebrafish heart on a fibrin matrix. *Nature protocols*, 7(2), pp.247–255. Available at: http://www.ncbi.nlm.nih.gov/pmc/articles/PMC3541820/.

Kim, J. et al., 2010. PDGF signaling is required for epicardial function and blood vessel formation in regenerating zebrafish hearts. *Proceedings of the National Academy of Sciences* , 107(40), pp.17206–17210. Available at: http://www.pnas.org/content/107/40/17206.abstract.

Kim, P.G. et al., 2013. Signaling axis involving Hedgehog, Notch, and Scl promotes the embryonic endothelial-to-hematopoietic transition. *Proceedings of the National Academy of Sciences of the United States of America*, 110(2), pp.E141–E150. Available at: http://www.ncbi.nlm.nih.gov/pmc/articles/PMC3545793/.

Kim, S.-H. et al., 2015. A post-developmental genetic screen for zebrafish models of inherited liver disease. *PloS one*, 10(5), pp.e0125980–e0125980. Available at: https://www.ncbi.nlm.nih.gov/pubmed/25950913.

Kimura, Y. et al., 2014. Efficient generation of knock-in transgenic zebrafish carrying reporter/driver genes by CRISPR/Cas9-mediated genome engineering. *Scientific Reports*, 4, p.6545. Available at: http://www.nature.com/doifinder/10.1038/srep06545.

King, A. et al., 2017. Sphingosine-1-Phosphate Prevents Egress of Hematopoietic Stem Cells From Liver to Reduce Fibrosis. *Gastroenterology*, 153(1), p.233–248.e16.

Kissa, K. & Herbomel, P., 2010. Blood stem cells emerge from aortic endothelium by a novel type of cell transition. *Nature*, 464, p.112. Available at: http://dx.doi.org/10.1038/nature08761.

Klaassen, H. et al., 2018. CRISPR mutagenesis confirms the role of oca2 in melanin pigmentation in Astyanax mexicanus. *Developmental Biology*, 441(2), pp.313–318. Available at: http://www.sciencedirect.com/science/article/pii/S0012160618300988.

Klotz, L. et al., 2015. Cardiac lymphatics are heterogeneous in origin and respond to injury. *Nature*, 522(7554), pp.62–67. Available at: https://www.ncbi.nlm.nih.gov/pubmed/25992544.

Knudsen, K.J. et al., 2015. ERG promotes the maintenance of hematopoietic stem cells by restricting their differentiation. *Genes & development*, 29(18), pp.1915–1929. Available at: https://www.ncbi.nlm.nih.gov/pubmed/26385962.

Kobayashi, K. et al., 2017. Dynamics of angiogenesis in ischemic areas of the infarcted heart. *Scientific reports*, 7(1), p.7156. Available at: https://www.ncbi.nlm.nih.gov/pubmed/28769049.

Kopp, H.-G. et al., 2006. Thrombospondins deployed by thrombopoietic cells determine angiogenic switch and extent of revascularization. *The Journal of clinical investigation*, 116(12), pp.3277–3291. Available at: https://www.ncbi.nlm.nih.gov/pubmed/17143334.

Koth, J. et al., 2017. High-Resolution Magnetic Resonance Imaging of the Regenerating Adult Zebrafish Heart. *Scientific Reports*, 7(1), p.2917. Available at: https://doi.org/10.1038/s41598-017-03050-y.

Kowalko, J.E. et al., 2013. Convergence in feeding posture occurs through different genetic loci in independently evolved cave populations of Astyanax mexicanus. *Proceedings of the National Academy of Sciences* , 110(42), pp.16933–16938. Available at: http://www.pnas.org/content/110/42/16933.abstract.

Lacaud, G. et al., 2002. Runx1 is essential for hematopoietic commitment at the hemangioblast stage of development in vitro. *Blood*, 100(2), p.458 LP-466. Available at: http://www.bloodjournal.org/content/100/2/458.abstract.

Laflamme, M.A. & Murry, C.E., 2011. Heart regeneration. *Nature*, 473. Available at: http://dx.doi.org/10.1038/nature10147.

Lai, S.-L. et al., 2017. Reciprocal analyses in zebrafish and medaka reveal that harnessing the immune response promotes cardiac regeneration. *eLife*, 6, p.e25605. Available at: https://www.ncbi.nlm.nih.gov/pubmed/28632131.

Lalowski, M.M. et al., 2018. Characterizing the Key Metabolic Pathways of the Neonatal Mouse Heart Using a Quantitative Combinatorial Omics Approach. *Frontiers in physiology*, 9, p.365. Available at: https://www.ncbi.nlm.nih.gov/pubmed/29695975.

Lam, E.Y.N. et al., 2010. Live imaging of Runx1 expression in the dorsal aorta tracks the emergence of blood progenitors from endothelial cells. *Blood*, 116(6), p.909 LP-914. Available at: http://www.bloodjournal.org/content/116/6/909.abstract.

Lancrin, C. et al., 2012. GFI1 and GFI1B control the loss of endothelial identity of hemogenic endothelium during hematopoietic commitment. *Blood*.

Lancrin, C. et al., 2009. The haemangioblast generates haematopoietic cells through a haemogenic endothelium stage. *Nature*, 457(7231), pp.892–895. Available at: http://www.ncbi.nlm.nih.gov/pmc/articles/PMC2661201/.

Lavine, K.J. et al., 2014. Distinct macrophage lineages contribute to disparate patterns of cardiac recovery and remodeling in the neonatal and adult heart. *Proceedings of the National Academy of Sciences of the United States of America*, 111(45), pp.16029–16034. Available at: https://www.ncbi.nlm.nih.gov/pubmed/25349429.

Le, T.Y.L. & Chong, J.J.H., 2016. Cardiac progenitor cells for heart repair. *Cell Death Discovery*, 2, p.16052. Available at: http://dx.doi.org/10.1038/cddiscovery.2016.52.

Le, V.P., Kovacs, A. & Wagenseil, J.E., 2012. Measuring left ventricular pressure in late embryonic and neonatal mice. *Journal of visualized experiments : JoVE*, (60), p.3756. Available at: https://www.ncbi.nlm.nih.gov/pubmed/22395602.

Lemos, D.R. et al., 2015. Nilotinib reduces muscle fibrosis in chronic muscle injury by promoting TNF-mediated apoptosis of fibro/adipogenic progenitors. *Nature medicine*, 21(7), pp.786–794. Available at: http://www.nature.com.go.libproxy.wakehealth.edu/nm/journal/v21/n7/full/nm.3869.html#affil-auth.

Lempereur, A. et al., 2018. The TGFβ pathway is a key player for the endothelial-to-hematopoietic transition in the embryonic aorta. *Developmental Biology*, 434(2), pp.292–303. Available at: http://www.sciencedirect.com/science/article/pii/S0012160617307200.

Li, Z. et al., 2012. Mouse Embryonic Head as a Site for Hematopoietic Stem Cell Development. *Cell Stem Cell*, 11(5), pp.663–675. Available at: https://doi.org/10.1016/j.stem.2012.07.004.

Liang, O.D. et al., 2017. Endothelial to haematopoietic transition contributes to pulmonary arterial hypertension. *Cardiovascular Research*.

Lie-A-Ling, M. et al., 2014. RUNX1 positively regulates a cell adhesion and migration program in murine hemogenic endothelium prior to blood emergence. *Blood*, 124(11), p.e11 LP-e20. Available at: http://www.bloodjournal.org/content/124/11/e11.abstract.

Lin, H.-F. et al., 2005. Analysis of thrombocyte development in CD41-GFP transgenic zebrafish. *Blood*, 106(12), pp.3803–3810. Available at: https://www.ncbi.nlm.nih.gov/pubmed/16099879.

Lin, Z. & Pu, W.T., 2014. Strategies for cardiac regeneration and repair. *Science translational medicine*, 6(239), p.239rv1-239rv1. Available at: https://www.ncbi.nlm.nih.gov/pubmed/24898748.

Lis, R. et al., 2017. Conversion of adult endothelium to immunocompetent haematopoietic stem cells. *Nature*, 545(7655), pp.439–445. Available at: http://www.ncbi.nlm.nih.gov/pmc/articles/PMC5794215/.

Liu, Q. et al., 2014. Epicardium-to-fat transition in injured heart. *Cell Research*, 24(11),

pp.1367–1369. Available at: http://www.nature.com/articles/cr2014125.

Liu, Q. et al., 2015. Genetic lineage tracing identifies in situ Kit-expressing cardiomyocytes. *Cell Research*, 26, p.119. Available at: https://doi.org/10.1038/cr.2015.143.

Livak, K.J. & Schmittgen, T.D., 2001. Analysis of relative gene expression data using real-time quantitative PCR and the 2(-Delta Delta C(T)) Method. *Methods (San Diego, Calif.)*, 25(4), pp.402–408.

Lloyd, E. et al., 2018. Evolutionary shift towards lateral line dependent prey capture behavior in the blind Mexican cavefish. *Developmental Biology*, 441(2), pp.328–337. Available at: http://www.sciencedirect.com/science/article/pii/S0012160618301192.

Ma, L. et al., 2015. Genome Editing Using TALENs in Blind Mexican Cavefish, <italic>Astyanax mexicanus</italic>. *PLoS ONE*, 10(3), p.e0119370. Available at: http://dx.doi.org/10.1371%252Fjournal.pone.0119370.

Macaulay, I.C. et al., 2016. Single-Cell RNA-Sequencing Reveals a Continuous Spectrum of Differentiation in Hematopoietic Cells. *Cell Reports*, 14(4), pp.966–977. Available at: https://doi.org/10.1016/j.celrep.2015.12.082.

MacGrogan, D., Münch, J. & de la Pompa, J.L., 2018. Notch and interacting signalling pathways in cardiac development, disease, and regeneration. *Nature Reviews Cardiology*. Available at: https://doi.org/10.1038/s41569-018-0100-2.

Maguire, E.M., Pearce, S.W.A. & Xiao, Q., 2018. Foam cell formation: A new target for fighting atherosclerosis and cardiovascular disease. *Vascular Pharmacology*. Available at: http://www.sciencedirect.com/science/article/pii/S1537189118301083.

Mahmoud, A.I. et al., 2015. Nerves Regulate Cardiomyocyte Proliferation and Heart Regeneration. *Developmental Cell*, 34(4), pp.387–399. Available at: http://www.sciencedirect.com/science/article/pii/S1534580715004244.

Malek Mohammadi, M. et al., 2017. The transcription factor GATA4 promotes myocardial regeneration in neonatal mice. *EMBO molecular medicine*, 9(2), pp.265–279. Available at: https://www.ncbi.nlm.nih.gov/pubmed/28053183.

Mali, P. et al., 2013. RNA-Guided Human Genome Engineering via Cas9. *Science (New York, N.Y.)*, 339(6121), pp.823–826. Available at: http://www.ncbi.nlm.nih.gov/pmc/articles/PMC3712628/.

Maliken, B.D. et al., 2018. Gata4-Dependent Differentiation of c-Kit(+)-Derived Endothelial Cells Underlies Artefactual Cardiomyocyte Regeneration in the Heart. *Circulation*, 138(10), pp.1012–1024. Available at: https://www.ncbi.nlm.nih.gov/pubmed/29666070.

Marín-Juez, R. et al., 2016. Fast revascularization of the injured area is essential to support zebrafish heart regeneration. *Proceedings of the National Academy of Sciences of the United States of America*, 113(40), pp.11237–11242. Available at: https://www.ncbi.nlm.nih.gov/pubmed/27647901.

Marinkovic, M. et al., 2017. Skeletal muscle fibro-adipogenic progenitors of dystrophic mice are insensitive to NOTCH-dependent regulation of adipogenesis. *bioRxiv*, p.223370. Available at: http://biorxiv.org/content/early/2017/11/22/223370.abstract.

Masters, M. & Riley, P.R., 2014. The epicardium signals the way towards heart regeneration. *Stem Cell Research*, 13(3), pp.683–692. Available at: http://www.ncbi.nlm.nih.gov/pmc/articles/PMC4241487/.

McCarroll, C.S. et al., 2018. Runx1 Deficiency Protects Against Adverse Cardiac Remodeling After Myocardial Infarction. *Circulation*, 137(1), pp.57–70. Available at: http://www.ncbi.nlm.nih.gov/pmc/articles/PMC5757664/.

Mercer, S.E., Odelberg, S.J. & Simon, H.-G., 2013. A dynamic spatiotemporal extracellular matrix facilitates epicardial-mediated vertebrate heart regeneration. *Developmental biology*, 382(2), pp.457–469. Available at: https://www.ncbi.nlm.nih.gov/pubmed/23939298.

Merrifield, G.D. et al., 2017. Rapid and recoverable in vivo magnetic resonance imaging of the adult zebrafish at 7T. *Magnetic resonance imaging*, 37, pp.9–15. Available at: https://www.ncbi.nlm.nih.gov/pubmed/27751860.

Miller, Y.I. et al., 2009. Toll-like receptor-4 and lipoprotein accumulation in macrophages. *Trends in cardiovascular medicine*, 19(7), pp.227–232. Available at: https://www.ncbi.nlm.nih.gov/pubmed/20382346.

Minicucci, M.F. et al., 2011. Heart failure after myocardial infarction: clinical implications and treatment. *Clinical cardiology*, 34(7), pp.410–414.

Monteiro, R. et al., 2016. Transforming Growth Factor β Drives Hemogenic Endothelium Programming and the Transition to Hematopoietic Stem Cells. *Developmental Cell*, 38(4), pp.358–370. Available at: http://www.ncbi.nlm.nih.gov/pmc/articles/PMC4998007/.

Moran, D., Softley, R. & Warrant, E.J., 2014. Eyeless Mexican Cavefish Save Energy by Eliminating the Circadian Rhythm in Metabolism. *PLoS ONE*, 9(9), p.e107877. Available at: http://dx.plos.org/10.1371/journal.pone.0107877.

Moran, D., Softley, R. & Warrant, E.J., 2015. The energetic cost of vision and the evolution of eyeless Mexican cavefish. *Science Advances*, 1(8), p.e1500363. Available at: http://www.ncbi.nlm.nih.gov/pmc/articles/PMC4643782/.

Morita, H. et al., 2017. Exogenous gene integration mediated by genome editing technologies in zebrafish. *Bioengineered*, 8(3), pp.287–295. Available at: http://www.ncbi.nlm.nih.gov/pmc/articles/PMC5470516/.

Moscou, M.J. & Bogdanove, A.J., 2009. A simple cipher governs DNA recognition by TAL effectors. *Science (New York, N.Y.)*, 326(5959), p.1501.

Mouton, A.J. et al., 2018. Mapping macrophage polarization over the myocardial infarction time continuum. *Basic research in cardiology*, 113(4), p.26. Available at: https://www.ncbi.nlm.nih.gov/pubmed/29868933.

Münch, J. et al., 2017. Notch signalling restricts inflammation and serpine1 expression in the dynamic endocardium of the regenerating zebrafish heart. *Development*, 144(8), p.1425 LP-1440. Available at: http://dev.biologists.org/content/144/8/1425.abstract.

Muñoz-Cánoves, P. & Serrano, A.L., 2015. Macrophages decide between regeneration and fibrosis in muscle. *Trends in endocrinology and metabolism: TEM*, 26(9), pp.449–50. Available at: http://www.sciencedirect.com/science/article/pii/S1043276015001381 [Accessed November 4, 2015].

Murphy, D.T. et al., 2010. Cardiac MRI in arrhythmogenic right ventricular cardiomyopathy. *AJR. American journal of roentgenology*, 194(4), pp.W299–W306.

Murry, C.E. et al., 2004. Haematopoietic stem cells do not transdifferentiate into cardiac myocytes in myocardial infarcts. *Nature*, 428(6983), pp.664–668.

Murthy, M. et al., 2014. Transcription factor Runx1 inhibits proliferation and promotes developmental maturation in a selected population of inner olfactory nerve layer olfactory ensheathing cells. *Gene*, 540(2), pp.191–200. Available at: http://www.sciencedirect.com/science/article/pii/S0378111914002273.

Nagata, H. et al., 2016. Cardiac Adipose-Derived Stem Cells Exhibit High Differentiation Potential to Cardiovascular Cells in C57BL/6 Mice. *Stem Cells Translational Medicine* , 5(2), pp.141–151. Available at: http://stemcellstm.alphamedpress.org/content/5/2/141.abstract.

Nakada, Y. et al., 2017. Hypoxia induces heart regeneration in adult mice. *Nature*, 541(7636), pp.222–227.

Nakada, Y. et al., 2016. Hypoxia induces heart regeneration in adult mice. *Nature*, 541, p.222. Available at: https://doi.org/10.1038/nature20173.

Nakade, S. et al., 2014. Microhomology-mediated end-joining-dependent integration of donor DNA in cells and animals using TALENs and CRISPR/Cas9. *Nature Communications*, 5, p.5560. Available at: http://www.ncbi.nlm.nih.gov/pmc/articles/PMC4263139/.

Nakagawa, M. et al., 2006. AML1/Runx1 rescues Notch1-null mutation-induced deficiency of para-aortic splanchnopleural hematopoiesis. *Blood*, 108(10), p.3329 LP-3334. Available at: http://www.bloodjournal.org/content/108/10/3329.abstract.

Nakano, H. et al., 2013. Haemogenic endocardium contributes to transient definitive haematopoiesis. *Nature communications*, 4, p.1564. Available at: http://www.pubmedcentral.nih.gov/articlerender.fcgi?artid=3612528&tool=pmcentrez&rendertype=abstract.

Noseda, M. et al., 2015. PDGFRα demarcates the cardiogenic clonogenic Sca1(+) stem/progenitor cell in adult murine myocardium. *Nature Communications*, 6, p.6930. Available at: http://www.ncbi.nlm.nih.gov/pmc/articles/PMC4479024/.

Notari, M. et al., 2018. The local microenvironment limits the regenerative potential of the

mouse neonatal heart. *Science Advances*, 4(5). Available at: http://advances.sciencemag.org/content/4/5/eaao5553.abstract.

Nottingham, W.T. et al., 2007. Runx1-mediated hematopoietic stem-cell emergence is controlled by a Gata/Ets/SCL-regulated enhancer. *Blood*, 110(13), pp.4188–4197. Available at: http://www.ncbi.nlm.nih.gov/pmc/articles/PMC2234795/.

Orlic, D. et al., 2001. Bone marrow cells regenerate infarcted myocardium. *Nature*, 410, p.701. Available at: https://doi.org/10.1038/35070587.

Owlarn, S. et al., 2017. Generic wound signals initiate regeneration in missing-tissue contexts. *Nature Communications*, 8, p.2282. Available at: http://www.ncbi.nlm.nih.gov/pmc/articles/PMC5741630/.

Patra, C. et al., 2017. The zebrafish ventricle: A hub of cardiac endothelial cells for in vitro cell behavior studies. *Scientific Reports*, 7(1), p.2687. Available at: https://doi.org/10.1038/s41598-017-02461-1.

Paylor, B. et al., 2014. In vivo characterization of neural crest-derived fibro/adipogenic progenitor cells as a likely cellular substrate for craniofacial fibrofatty infiltrating disorders. *Biochemical and Biophysical Research Communications*, 451(1), pp.148–151. Available at: http://www.sciencedirect.com/science/article/pii/S0006291X1401331X.

Peinkofer, G., Hescheler, J. & Halbach, M., 2017. Murine Short Axis Ventricular Heart Slices for Electrophysiological Studies. *Journal of visualized experiments : JoVE*, (124).

Peng, R., Lin, G. & Li, J., 2015. Potential pitfalls of CRISPR/Cas9-mediated genome editing. *FEBS Journal*, p.n/a-n/a. Available at: http://dx.doi.org/10.1111/febs.13586.

Peralta, M. et al., 2014. The Epicardium in the Embryonic and Adult Zebrafish. *Journal of developmental biology*, 2(2), pp.101–116. Available at: https://www.ncbi.nlm.nih.gov/pubmed/24926432.

Pfeffer, M.A. & Braunwald, E., 1990. Ventricular remodeling after myocardial infarction. Experimental observations and clinical implications. *Circulation* , 81(4), pp.1161–1172.

Pillekamp, F. et al., 2005. Establishment and characterization of a mouse embryonic heart slice preparation. *Cellular physiology and biochemistry : international journal of experimental cellular physiology, biochemistry, and pharmacology*, 16(1–3), pp.127–132.

Pinto, A.R. et al., 2016. Revisiting Cardiac Cellular Composition. *Circulation research*, 118(3), pp.400–409. Available at: https://www.ncbi.nlm.nih.gov/pubmed/26635390.

Poling, J. et al., 2012. The Janus face of OSM-mediated cardiomyocyte dedifferentiation during cardiac repair and disease. *Cell cycle (Georgetown, Tex.)*, 11(3), pp.439–445.

Porcher, C., Chagraoui, H. & Kristiansen, M.S., 2017. SCL/TAL1: a multifaceted regulator from blood development to disease. *Blood*, 129(15), p.2051 LP-2060. Available at: http://www.bloodjournal.org/content/129/15/2051.abstract.

Porrello, E.R. et al., 2011. Transient regenerative potential of the neonatal mouse heart.

Science (New York, N.Y.), 331(6020), pp.1078–80.

Porrello, E.R. & Olson, E.N., 2014. A neonatal blueprint for cardiac regeneration. *Stem cell research*, 13(3 0 0), pp.556–570. Available at: http://www.ncbi.nlm.nih.gov/pmc/articles/PMC4316722/.

Poss, K.D., Wilson, L.G. & Keating, M.T., 2002. Heart regeneration in zebrafish. *Science (New York, N.Y.)*, 298(5601), pp.2188–2190.

de Preux Charles, A.-S. et al., 2016. Distinct effects of inflammation on preconditioning and regeneration of the adult zebrafish heart. *Open Biology*, 6(7), p.160102. Available at: http://www.ncbi.nlm.nih.gov/pmc/articles/PMC4967830/.

Puente, B.N. et al., 2014. The oxygen-rich postnatal environment induces cardiomyocyte cell-cycle arrest through DNA damage response. *Cell*, 157(3), pp.565–579. Available at: https://www.ncbi.nlm.nih.gov/pubmed/24766806.

Qureshi, R. et al., 2017. Prokineticin receptor-1-dependent paracrine and autocrine pathways control cardiac tcf21(+) fibroblast progenitor cell transformation into adipocytes and vascular cells. *Scientific reports*, 7(1), p.12804.

Rafferty, S.A. & Quinn, T.A., 2018. A beginner's guide to understanding and implementing the genetic modification of zebrafish. *Progress in Biophysics and Molecular Biology*. Available at: http://www.sciencedirect.com/science/article/pii/S007961071830124X.

Ratajska, A. et al., 2009. New morphological aspects of blood islands formation in the embryonic mouse hearts. *Histochemistry and cell biology*, 131(3), pp.297–311.

Raya, Á. et al., 2003. Activation of Notch signaling pathway precedes heart regeneration in zebrafish. *Proceedings of the National Academy of Sciences of the United States of America*, 100(Suppl 1), pp.11889–11895. Available at: http://www.ncbi.nlm.nih.gov/pmc/articles/PMC304103/.

Renaud, O., Herbomel, P. & Kissa, K., 2011. Studying cell behavior in whole zebrafish embryos by confocal live imaging: application to hematopoietic stem cells. *Nature Protocols*, 6, p.1897. Available at: https://doi.org/10.1038/nprot.2011.408.

Rennert, R.C. et al., 2012. Stem cell recruitment after injury: lessons for regenerative medicine. *Regenerative medicine*, 7(6), pp.833–850. Available at: https://www.ncbi.nlm.nih.gov/pubmed/23164083.

Riddle, M.R. et al., 2018. Insulin resistance in cavefish as an adaptation to a nutrient-limited environment. *Nature*, 555(7698), pp.647–651. Available at: https://www.ncbi.nlm.nih.gov/pubmed/29562229.

Rissone, A. & Burgess, S.M., 2018. Rare Genetic Blood Disease Modeling in Zebrafish. *Frontiers in genetics*, 9, p.348. Available at: https://www.ncbi.nlm.nih.gov/pubmed/30233640.

Rost, M.S. et al., 2018. Nfe2 is dispensable for early but required for adult thrombocyte formation and function in zebrafish. *Blood advances*, 2(23), pp.3418–3427. Available at:

https://www.ncbi.nlm.nih.gov/pubmed/30504234.

Rudat, C. et al., 2013. Epicardial function of canonical Wnt-, Hedgehog-, Fgfr1/2-, and Pdgfra-signalling. *Cardiovascular Research*, 100(3), pp.411–421. Available at: http://cardiovascres.oxfordjournals.org/content/100/3/411.abstract.

Sacks, H.S. & Fain, J.N., 2007. Human epicardial adipose tissue: A review. *American Heart Journal*, 153(6), pp.907–917. Available at: http://www.sciencedirect.com/science/article/pii/S0002870307002414.

Sallin, P. & Jaźwińska, A., 2016. Acute stress is detrimental to heart regeneration in zebrafish. *Open Biology*, 6(3). Available at: http://rsob.royalsocietypublishing.org/content/6/3/160012.abstract.

Sánchez-Iranzo, H. et al., 2018. Transient fibrosis resolves via fibroblast inactivation in the regenerating zebrafish heart. *Proceedings of the National Academy of Sciences of the United States of America*, 115(16), pp.4188–4193. Available at: http://www.ncbi.nlm.nih.gov/pmc/articles/PMC5910827/.

Sarper, S.E. et al., 2018. Runx1-Stat3 signaling regulates the epithelial stem cells in continuously growing incisors. *Scientific Reports*, 8, p.10906. Available at: http://www.ncbi.nlm.nih.gov/pmc/articles/PMC6053438/.

Satija, R. et al., 2015. Spatial reconstruction of single-cell gene expression data. *Nature biotechnology*, 33(5), pp.495–502.

Satoh, A., Mitogawa, K. & Makanae, A., 2018. Nerve roles in blastema induction and pattern formation in limb regeneration. *The International journal of developmental biology*, 62(9–10), pp.605–612.

Sattler, S. & Rosenthal, N., The neonate versus adult mammalian immune system in cardiac repair and regeneration. *Biochimica et Biophysica Acta (BBA) - Molecular Cell Research*. Available at: http://www.sciencedirect.com/science/article/pii/S0167488916300015.

Seifert, A.W. et al., 2012. The influence of fundamental traits on mechanisms controlling appendage regeneration. *Biological reviews of the Cambridge Philosophical Society*, 87(2), pp.330–345.

Senyo, S.E. et al., 2013. Mammalian heart renewal by pre-existing cardiomyocytes. *Nature*, 493(7432), pp.433–436. Available at: https://www.ncbi.nlm.nih.gov/pubmed/23222518.

Sharma, A. & Wu, S.M., 2015. Members Only: Hypoxia-Induced Cell-Cycle Activation in Cardiomyocytes. *Cell Metabolism*, 22(3), pp.365–366. Available at: https://doi.org/10.1016/j.cmet.2015.08.004.

Shen, B. et al., 2013. Generation of gene-modified mice via Cas9/RNA-mediated gene targeting. *Cell Research*, 23(5), pp.720–723. Available at: http://www.ncbi.nlm.nih.gov/pmc/articles/PMC3641603/.

Shiba, Y. et al., 2016. Allogeneic transplantation of iPS cell-derived cardiomyocytes

regenerates primate hearts. *Nature*, 538(7625), pp.388–391.

Shin, J., Chen, J. & Solnica-Krezel, L., 2014. Efficient homologous recombination-mediated genome engineering in zebrafish using TALE nucleases. *Development (Cambridge, England)*, 141(19), pp.3807–3818. Available at: http://www.ncbi.nlm.nih.gov/pmc/articles/PMC4197590/.

Simoes, F.C. & Riley, P.R., 2018. The ontogeny, activation and function of the epicardium during heart development and regeneration. *Development (Cambridge, England)*, 145(7).

Simon, V. et al., 2017. Comparing growth in surface and cave morphs of the species Astyanax mexicanus: insights from scales. *EvoDevo*, 8, p.23. Available at: https://www.ncbi.nlm.nih.gov/pubmed/29214008.

Smart, N. et al., 2007. Thymosin beta-4 is essential for coronary vessel development and promotes neovascularization via adult epicardium. *Annals of the New York Academy of Sciences*, 1112, pp.171–188.

Smart, N. & Riley, P.R., 2012. The epicardium as a candidate for heart regeneration. *Future cardiology*, 8(1), pp.53–69. Available at: http://www.ncbi.nlm.nih.gov/pmc/articles/PMC3977139/.

Smith, C.L. et al., 2011. Epicardial derived cell epithelial to mesenchymal transition and fate specification require PDGF receptor signaling. *Circulation research*, 108(12), pp.e15–e26. Available at: http://www.ncbi.nlm.nih.gov/pmc/articles/PMC3134964/.

Soares, D. et al., 2004. The Lens Has a Specific Influence on Optic Nerve and Tectum Development in the Blind Cavefish *Astyanax*. *Developmental Neuroscience*, 26(5–6), pp.308–317. Available at: http://www.karger.com/DOI/10.1159/000082272.

Sood, R. et al., 2010. Development of multilineage adult hematopoiesis in the zebrafish with a runx1 truncation mutation. *Blood*, 115(14), pp.2806–2809. Available at: https://www.ncbi.nlm.nih.gov/pubmed/20154212.

Sood, R. & Liu, P., 2012. Novel insights into the genetic controls of primitive and definitive hematopoiesis from zebrafish models. *Advances in hematology*, 2012, p.830703. Available at: https://www.ncbi.nlm.nih.gov/pubmed/22888355.

Stockdale, W.T. et al., 2018. Heart Regeneration in the Mexican Cavefish. *Cell reports*, 25(8), p.1997–2007.e7.

Stuelsatz, P., Shearer, A. & Yablonka-Reuveni, Z., 2014. Ancestral Myf5 gene activity in periocular connective tissue identifies a subset of fibro/adipogenic progenitors but does not connote a myogenic origin. *Developmental Biology*, 385(2), pp.366–379. Available at: http://dx.doi.org/10.1016/j.ydbio.2013.08.010%5Cnhttp://ac.els-cdn.com/S0012160613004223/1-s2.0-S0012160613004223-main.pdf?_tid=29ea5d3a-d73c-11e4-9844-00000aacb362&acdnat=1427761592_3c934f9d2e600fc242f8b57b4250665b.

Sultana, N. et al., 2015. Resident c-kit(+) cells in the heart are not cardiac stem cells. *Nature*

communications, 6, p.8701. Available at: https://www.ncbi.nlm.nih.gov/pubmed/26515110.

Suster, M.L. et al., 2011. Transposon-mediated BAC transgenesis in zebrafish. *Nature Protocols*, 6, p.1998. Available at: http://dx.doi.org/10.1038/nprot.2011.416.

Svedberg, H., Richter, J. & Gullberg, U., 2001. Forced expression of the Wilms tumor 1 (WT1) gene inhibits proliferation of human hematopoietic CD34(+) progenitor cells. *Leukemia*, 15(12), pp.1914–1922.

Swiers, G. et al., 2013. Early dynamic fate changes in haemogenic endothelium characterized at the single-cell level. *Nature communications*, 4, p.2924. Available at: http://www.ncbi.nlm.nih.gov/pmc/articles/PMC4362711/.

T., L.R., 2018. Adult Cardiac Stem Cell Concept and the Process of Science. *Circulation*, 138(25), pp.2940–2942. Available at: https://doi.org/10.1161/CIRCULATIONAHA.118.036407.

Talbot, J.C. & Amacher, S.L., 2014. A streamlined CRISPR pipeline to reliably generate zebrafish frameshifting alleles. *Zebrafish*, 11(6), pp.583–585. Available at: https://www.ncbi.nlm.nih.gov/pubmed/25470533.

Talman, V. & Ruskoaho, H., 2016. Cardiac fibrosis in myocardial infarction-from repair and remodeling to regeneration. *Cell and tissue research*, 365(3), pp.563–581.

Tanaka, Y. et al., 2012. The transcriptional programme controlled by Runx1 during early embryonic blood development. *Developmental Biology*, 366(2), pp.404–419. Available at: http://www.ncbi.nlm.nih.gov/pmc/articles/PMC3430866/.

Tang, J.L.Y. et al., 2018. The developmental origin of heart size and shape differences in Astyanax mexicanus populations. *Developmental biology*, 441(2), pp.272–284.

Tatin, F. et al., 2017. Apelin modulates pathological remodeling of lymphatic endothelium after myocardial infarction. *JCI insight*, 2(12), p.e93887. Available at: https://www.ncbi.nlm.nih.gov/pubmed/28614788.

Thambyrajah, R. et al., 2016. GFI1 proteins orchestrate the emergence of haematopoietic stem cells through recruitment of LSD1. *Nature Cell Biology*.

Theodore, L.N. et al., 2017. Distinct Roles for Matrix Metalloproteinases 2 and 9 in Embryonic Hematopoietic Stem Cell Emergence, Migration, and Niche Colonization. *Stem Cell Reports*, 8(5), pp.1226–1241. Available at: http://www.ncbi.nlm.nih.gov/pmc/articles/PMC5425629/.

Thijssen, V.L., Ausma, J. & Borgers, M., 2001. Structural remodelling during chronic atrial fibrillation: act of programmed cell survival. *Cardiovascular research*, 52(1), pp.14–24.

Tian, Y. et al., 2015. A microRNA-Hippo pathway that promotes cardiomyocyte proliferation and cardiac regeneration in mice. *Science translational medicine*, 7(279), p.279ra38.

Tober, J., Maijenburg, M.W. & Speck, N.A., 2016. Chapter Five - Taking the Leap: Runx1 in the Formation of Blood from Endothelium. In E. H. B. T.-C. T. in D. B. Bresnick, ed.

Hematopoiesis. Academic Press, pp. 113–162. Available at: http://www.sciencedirect.com/science/article/pii/S0070215316000090.

Toyoda, Y., Guy, T.S. & Kashem, A., 2013. Present Status and Future Perspectives of Heart Transplantation. *Circulation Journal*, 77(5), pp.1097–1110.

Tsai, S.B. et al., 2007. Differential effects of genotoxic stress on both concurrent body growth and gradual senescence in the adult zebrafish. *Aging cell*, 6(2), pp.209–224.

Turner, N.A., 2016. Inflammatory and fibrotic responses of cardiac fibroblasts to myocardial damage associated molecular patterns (DAMPs). *Journal of Molecular and Cellular Cardiology*, 94, pp.189–200. Available at: http://www.sciencedirect.com/science/article/pii/S0022282815301073.

Tzahor, E. & Poss, K.D., 2017. Cardiac regeneration strategies: Staying young at heart. *Science (New York, N.Y.)*, 356(6342), pp.1035–1039. Available at: http://www.ncbi.nlm.nih.gov/pmc/articles/PMC5614484/.

Uezumi, A. et al., 2010. Mesenchymal progenitors distinct from satellite cells contribute to ectopic fat cell formation in skeletal muscle. *Nat Cell Biol*, 12(2), pp.143–152. Available at: http://dx.doi.org/10.1038/ncb2014.

Umansky, K.B. et al., 2015. Runx1 Transcription Factor Is Required for Myoblasts Proliferation during Muscle Regeneration G. A. Cox, ed. *PLoS Genetics*, 11(8), p.e1005457. Available at: http://www.ncbi.nlm.nih.gov/pmc/articles/PMC4537234/.

Valiente-Alandi, I., Schafer, A.E. & Blaxall, B.C., 2016. Extracellular matrix-mediated cellular communication in the heart. *Journal of molecular and cellular cardiology*, 91, pp.228–237. Available at: https://www.ncbi.nlm.nih.gov/pubmed/26778458.

Vieira, J.M. et al., 2018. The cardiac lymphatic system stimulates resolution of inflammation following myocardial infarction. *The Journal of clinical investigation*, 128(8), pp.3402–3412. Available at: https://www.ncbi.nlm.nih.gov/pubmed/29985167.

Vishvanath, L. et al., 2016. Pdgfrbeta+ Mural Preadipocytes Contribute to Adipocyte Hyperplasia Induced by High-Fat-Diet Feeding and Prolonged Cold Exposure in Adult Mice. *Cell metabolism*, 23(2), pp.350–359.

Wang, H. et al., 2013. One-Step Generation of Mice Carrying Mutations in Multiple Genes by CRISPR/Cas-Mediated Genome Engineering. *Cell*, 153(4), pp.910–918. Available at: http://www.ncbi.nlm.nih.gov/pmc/articles/PMC3969854/.

Wang, J. et al., 2015. Epicardial regeneration is guided by cardiac outflow tract and Hh signaling. *Nature*, 522(7555), pp.226–230. Available at: http://www.ncbi.nlm.nih.gov/pmc/articles/PMC4494087/.

Wang, W.E. et al., 2017. Dedifferentiation, Proliferation, and Redifferentiation of Adult Mammalian Cardiomyocytes After Ischemic Injury. *Circulation*, 136(9), pp.834–848. Available at: https://www.ncbi.nlm.nih.gov/pubmed/28642276.

Wang, Y.-H. et al., 2006. Spatiotemporal expression of zebrafish keratin 18 during early

embryogenesis and the establishment of a keratin 18:RFP transgenic line. *Gene expression patterns : GEP*, 6(4), pp.335–339.

White, I.A. et al., 2015. Sympathetic Reinnervation Is Required for Mammalian Cardiac Regeneration. *Circulation research*, 117(12), pp.990–994. Available at: https://www.ncbi.nlm.nih.gov/pubmed/26371181.

Wu, C.-C. et al., Spatially Resolved Genome-wide Transcriptional Profiling Identifies BMP Signaling as Essential Regulator of Zebrafish Cardiomyocyte Regeneration. *Developmental Cell*. Available at: http://www.sciencedirect.com/science/article/pii/S1534580715007959.

Wu, Y. et al., 2017. Epicardial Fat in the Maintenance of Cardiovascular Health. *Methodist DeBakey cardiovascular journal*, 13(1), pp.20–24. Available at: https://www.ncbi.nlm.nih.gov/pubmed/28413578.

Xiong, S. et al., 2018. Early adipogenesis contributes to excess fat accumulation in cave populations of Astyanax mexicanus. *Developmental Biology*, 441(2), pp.297–304. Available at: http://www.sciencedirect.com/science/article/pii/S0012160618301921.

Xu, S. et al., 2018. Matrix metalloproteinases (MMPs) mediate leukocyte recruitment during the inflammatory phase of zebrafish heart regeneration. *Scientific reports*, 8(1), p.7199. Available at: https://www.ncbi.nlm.nih.gov/pubmed/29740050.

Yahalom-Ronen, Y. et al., 2015. Reduced matrix rigidity promotes neonatal cardiomyocyte dedifferentiation, proliferation and clonal expansion. *eLife*, 4, p.e07455. Available at: https://www.ncbi.nlm.nih.gov/pubmed/26267307.

Yamaguchi, Y. et al., 2015. Adipogenesis and epicardial adipose tissue: A novel fate of the epicardium induced by mesenchymal transformation and PPARγ activation. *Proceedings of the National Academy of Sciences*, 112(7), pp.2070–2075. Available at: http://www.pnas.org/lookup/doi/10.1073/pnas.1417232112.

Yamamoto, Y. et al., 2003. Development and evolution of craniofacial patterning is mediated by eye-dependent and -independent processes in the cavefish Astyanax. *Evolution & Development*, 5(5), pp.435–446. Available at: http://dx.doi.org/10.1046/j.1525-142X.2003.03050.x.

Yamamoto, Y. et al., 2009. Pleiotropic functions of embryonic sonic hedgehog expression link jaw and taste bud amplification with eye loss during cavefish evolution. *Developmental Biology*, 330(1), pp.200–211. Available at: http://www.sciencedirect.com/science/article/pii/S0012160609001705.

Yan, L. et al., 2018. Genetic Lineage Tracing of Nonmyocyte Population by Dual Recombinases. *Circulation*, 138(8), pp.793–805. Available at: https://doi.org/10.1161/CIRCULATIONAHA.118.034250.

Yi Ni Lam, E. et al., 2009. Zebrafish runx1 promoter-EGFP transgenics mark discrete sites of definitive blood progenitors. *Blood*, 113(6), p.1241 LP-1249. Available at: http://www.bloodjournal.org/content/113/6/1241.abstract.

Yoshizawa, M. et al., 2015. Distinct genetic architecture underlies the emergence of sleep loss and prey-seeking behavior in the Mexican cavefish. *BMC Biology*, 13(1), pp.1–12. Available at: http://dx.doi.org/10.1186/s12915-015-0119-3.

Yoshizawa, M. et al., 2012. Evolution of an adaptive behavior and its sensory receptors promotes eye regression in blind cavefish. *BMC Biology*, 10, p.108. Available at: http://www.ncbi.nlm.nih.gov/pmc/articles/PMC3565949/.

Yoshizawa, M. et al., 2018. The evolution of a series of behavioral traits is associated with autism-risk genes in cavefish. *BMC evolutionary biology*, 18(1), p.89. Available at: https://www.ncbi.nlm.nih.gov/pubmed/29909776.

Yue, Y. et al., 2018. The transcription factor Foxc1a in zebrafish directly regulates expression of nkx2.5, encoding a transcriptional regulator of cardiac progenitor cells. *The Journal of biological chemistry*, 293(2), pp.638–650.

Yzaguirre, A.D., de Bruijn, M.F.T.R. & Speck, N.A., 2017. The role of Runx1 in embryonic blood cell formation. *Advances in experimental medicine and biology*, 962, pp.47–64. Available at: http://www.ncbi.nlm.nih.gov/pmc/articles/PMC5813695/.

Yzaguirre, A.D. & Speck, N.A., 2016. Insights into blood cell formation from hemogenic endothelium in lesser-known anatomic sites. *Developmental dynamics : an official publication of the American Association of Anatomists*, 245(10), pp.1011–1028. Available at: http://www.ncbi.nlm.nih.gov/pmc/articles/PMC5801748/.

Zamir, L. et al., 2017. Nkx2.5 marks angioblasts that contribute to hemogenic endothelium of the endocardium and dorsal aorta. *eLife*, 6.

Zangi, L. et al., 2017. Insulin-Like Growth Factor 1 Receptor-Dependent Pathway Drives Epicardial Adipose Tissue Formation After Myocardial Injury. *Circulation*, 135(1), pp.59–72. Available at: https://www.ncbi.nlm.nih.gov/pubmed/27803039.

Zaruba, M.-M. et al., 2010. Cardiomyogenic potential of C-kit(+)-expressing cells derived from neonatal and adult mouse hearts. *Circulation*, 121(18), pp.1992–2000. Available at: https://www.ncbi.nlm.nih.gov/pubmed/20421520.

Zeng, W.R. et al., 2017. Production of zebrafish cardiospheres and cardiac progenitor cells in vitro and three-dimensional culture of adult zebrafish cardiac tissue in scaffolds. *Biotechnology and Bioengineering*, 114(9), pp.2142–2148. Available at: https://doi.org/10.1002/bit.26331.

Zhang, M. & Huang, B., 2012. The multi-differentiation potential of peripheral blood mononuclear cells. *Stem cell research & therapy*, 3(6), p.48. Available at: https://www.ncbi.nlm.nih.gov/pubmed/23200034.

Zhao, L. et al., 2014. Notch signaling regulates cardiomyocyte proliferation during zebrafish heart regeneration. *Proceedings of the National Academy of Sciences of the United States of America*, 111(4), pp.1403–1408. Available at: http://www.ncbi.nlm.nih.gov/pmc/articles/PMC3910613/.

Zhen, F. et al., 2013. Hemogenic endothelium specification and hematopoietic stem cell

maintenance employ distinct Scl isoforms. *Development*, 140(19), p.3977 LP-3985. Available at: http://dev.biologists.org/content/140/19/3977.abstract.

Zhou, B. et al., 2011. Adult mouse epicardium modulates myocardial injury by secreting paracrine factors. *The Journal of Clinical Investigation*, 121(5), pp.1894–1904. Available at: https://doi.org/10.1172/JCI45529.

Zhou, F. et al., 2016. Tracing haematopoietic stem cell formation at single-cell resolution. *Nature*, 533, p.487. Available at: https://doi.org/10.1038/nature17997.

Zhou, P. & Pu, W.T., 2016. Recounting Cardiac Cellular Composition. *Circulation research*, 118(3), pp.368–370.

Zhou, Q. et al., 2015. Cardiac telocytes are double positive for CD34/PDGFR-α. *Journal of Cellular and Molecular Medicine*, 19(8), pp.2036–2042. Available at: http://www.ncbi.nlm.nih.gov/pmc/articles/PMC4549054/.

Zhou, T. et al., 2018. Runt-Related Transcription Factor 1 (RUNX1) Promotes TGF-β-Induced Renal Tubular Epithelial-to-Mesenchymal Transition (EMT) and Renal Fibrosis through the PI3K Subunit p110δ. *EBioMedicine*, 31, pp.217–225. Available at: http://www.ncbi.nlm.nih.gov/pmc/articles/PMC6013935/.

Zlatanova, I., Pinto, C. & Silvestre, J.-S., 2016. Immune Modulation of Cardiac Repair and Regeneration: The Art of Mending Broken Hearts. *Frontiers in cardiovascular medicine*, 3, p.40. Available at: https://www.ncbi.nlm.nih.gov/pubmed/27790620.

Zovein, A.C. et al., 2008. Fate tracing reveals the endothelial origin of hematopoietic stem cells. *Cell stem cell*, 3(6), pp.625–636. Available at: http://www.ncbi.nlm.nih.gov/pmc/articles/PMC2631552/.